Journal of Robotics

Rehabilitation Robotics

Guest Editors: Haruhisa Kawasaki, Daniel Cox, Doyoung Jeon, Ludovic Saint-Bauzel, and Tetuya Mouri

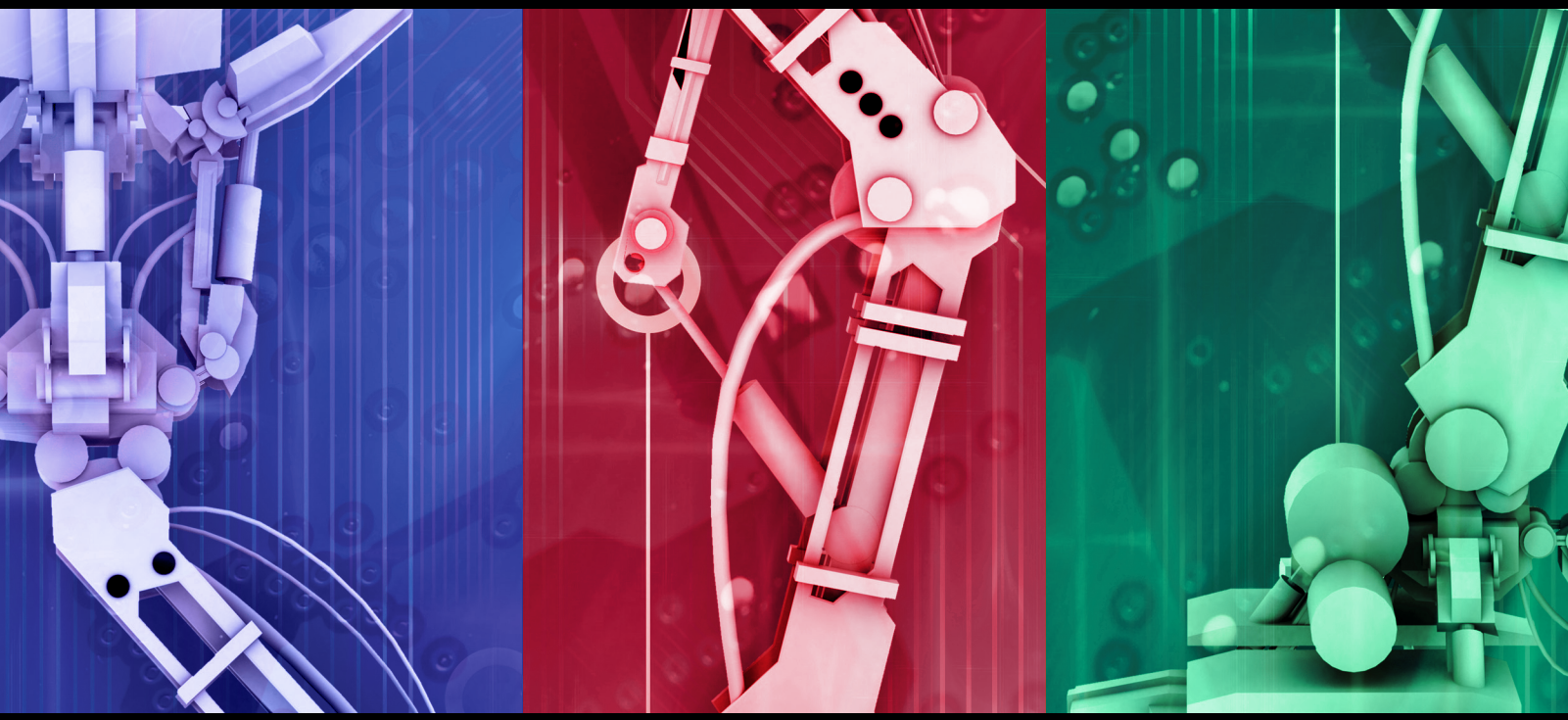

Rehabilitation Robotics

Journal of Robotics

Rehabilitation Robotics

Guest Editors: Haruhisa Kawasaki, Daniel Cox, Doyoung Jeon, Ludovic Saint-Bauzel, and Tetuya Mouri

Editorial Board

Contents

Hindawi Publishing Corporation
Journal of Robotics
Volume 2011, Article ID 937875, 2 pages
doi:10.1155/2011/937875

Editorial
Rehabilitation Robotics

Haruhisa Kawasaki,[1] Daniel Cox,[2] Doyoung Jeon,[3] Ludovic Saint-Bauzel,[4] and Tetuya Mouri[1]

[1] *Department of Human and Information Systems, Faculty of Engineering, Gifu University, 1-1 Yanagido, Gifu 501-1193, Japan*
[2] *Mechanical Engineering, School of Engineering, University of North Florida, 1 UNF Drive, Jacksonville, FL 32224, USA*
[3] *Department of Mechanical Engineering, Sogang University, Mapoku, Seoul 121-742, Republic of Korea*
[4] *Institut des Systèmes Intelligents et de Robotique, Université Pierre et Marie Curie, 75005 Paris, France*

Correspondence should be addressed to Haruhisa Kawasaki, h_kawasa@gifu-u.ac.jp

Received 29 November 2011; Accepted 29 November 2011

Rehabilitation robotics has produced exciting new ideas and novel human assistive devices in the growing field of biomedical robotics. The successful research and development of such rehabilitation robotics requires a thorough understanding of not only mechanical, electrical, and software components, but also the related physiology, biology, neuroscience, and brain science. The science and technology of rehabilitation robotics will progress through the collaboration among robotic researchers, medical doctors, and patients. This special issue focuses on the most recent advances in modeling, design, analysis, implementation, and therapeutic testing of the human assistive rehabilitation robotics.

The paper entitled "*Lower-limb robotic rehabilitation: literature review and challenges*" of this special issue presents a survey of existing robotic systems for lower-limb rehabilitation. This paper presents an overview of all lower-limb robotic rehabilitation systems to date, including information about their commercialization as well as their clinical use, but only presenting a short description of each system. The paper entitled "*Gait rehabilitation device in central nervous system disease: a review*" presents outlines of spinal cord injury and cerebrovascular disease as two of the major causes of gait disturbance and introduces gait rehabilitation for central nervous system disorders as well as the gait rehabilitation orthoses currently being studied. These two papers will be a very valuable source of information on lower-limb and gait robotic rehabilitation systems. The paper entitled "*Mina: a sensorimotor robotic orthosis for mobility assistance*" describes the initial concept, design goals, and methods of a wearable over-ground robotic mobility device called Paralyzed, which uses compliant actuation to power the hip and knee joints. An initiated sensory substitution feedback mechanism is used to augment the user's sensory perception of his or her lower extremities.

The paper entitled "*Mechanical performance of actuators in an active orthosis for the upper extremities*" presents a lightweight, portable, active orthosis for the upper limbs. This paper focuses on the actuators for the support of the elbow function and the internal rotation, adduction, and anteversion of the shoulder and the inflatable shell structure. The paper entitled "*Stroke rehabilitation in frail elderly with the robotic training device ACRE: a randomized controlled trial and cost-effectiveness study*" reports an active rehabilitation robotic device called ACRE that was developed to enhance therapeutic treatment of upper limbs after stroke. The aim of this study was to assess the effects and costs of ACRE training for frail elderly patients and to establish whether ACRE can be a valuable addition to standard therapy in nursing home rehabilitation. The paper entitled "*Two-fingered haptic device for robot hand teleoperation*" presents a two-fingered haptic device called ExoPhalanx for robot hand teleoperation. The device provides reaction force on the distal phalange and proximal phalange to the remote operator. The effectiveness of the proposed system for teleoperation applications was verified through preliminary experiments. The paper entitled "*Finger rehabilitation support system using a multifingered haptic interface controlled by a surface electromyogram*" presents a new type of finger rehabilitation system using a multifingered haptic interface that is controlled by the patient though a surface electromyogram. The multi-fingered haptic interface robot called HIRO III can give 3-directional forces to 5 fingertips. The proposed system provides active hand rehabilitation using the surface electromyogram.

The paper entitled "*Single-switch user interface for robot arm to help disabled people using RT-middleware*" presents the construction of the user interface system using RT-Middleware. To support disabled people, especially those with less muscle strength such as muscular dystrophy patients, a single switch and scanning menu panel are introduced as the input device for the manual control of the robot arm. Patients with muscular dystrophy tested and evaluated the user interface. The paper entitled "*Toward monitoring and increasing exercise adherence in older adults by robotic intervention: a proof of concept study*" presents a proof of concept study aimed at increasing adherence for elderly adults using a small humanoid robot. The robot physically demonstrates exercises for the user to follow and monitors the user's progress using a vision-processing unit that detects face and hand movements. Socially assistive robots have the potential to improve the quality of life of elderly adults by encouraging and guiding their performance of rehabilitation exercises while offering cognitive stimulation and companionship.

Haruhisa Kawasaki
Daniel Cox
Doyoung Jeon
Ludovic Saint-Bauzel
Tetuya Mouri

Hindawi Publishing Corporation
Journal of Robotics
Volume 2011, Article ID 528425, 13 pages
doi:10.1155/2011/528425

Research Article

Single-Switch User Interface for Robot Arm to Help Disabled People Using RT-Middleware

Yujin Wakita,[1] Natsuki Yamanobe,[1] Kazuyuki Nagata,[1] and Eiichi Ono[2]

[1] *Intelligent Systems Research Institute, National Institute of Advanced Industrial Science and Technology (AIST), Ibaraki, Tsukuba 305-8568, Japan*
[2] *Department of Rehabilitation Engineering, Research Institute of National Rehabilitation Center for Persons with Disabilities, Saitama, Tokorozawa, 359-8555, Japan*

Correspondence should be addressed to Yujin Wakita, wakita.y@aist.go.jp

Received 1 June 2011; Revised 16 September 2011; Accepted 30 September 2011

Academic Editor: Tetsuya Mouri

We are developing a manipulator system in order to support disabled people with less muscle strength such as muscular dystrophy patients. Such a manipulator should have an easy user interface for the users to control it. But the supporting manipulator for disabled people cannot make large industry, so we should offer inexpensive manufacturing way. These type products are called "orphan products." We report on the construction of the user interface system using RT-Middleware which is an open software platform for robot systems. Therefore other user interface components or robot components which are adapted to other symptoms can be replaced with the user interface without any change of the contents. A single switch and scanning menu panel are introduced as the input device for the manual control of the robot arm. The scanning menu panel is designed to perform various actions of the robot arm with the single switch. A manipulator simulation system was constructed to evaluate the input performance. Two muscular dystrophy patients tried our user interface to control the robot simulator and made comments. According to the comments by them, we made several improvements on the user interface. This improvements examples prepare inexpensive manufacturing way for orphan products.

1. Introduction

The use of assistive technologies by persons with disabilities to pursue self-care, educational, vocational, and recreational activities continues to increase in both quantity and quality [1]. The number of academic programs, clinical centers, schools, hospitals, and research institutes applying these assistive technologies has increased dramatically. The assistive technology device is defined as an item, piece of equipment, or product system that is used to increase, maintain, or improve functional capabilities of individuals with disabilities. As described in [1], the assistive technology system is consisting of an assistive technology device, a human operator who has a disability and an environment in which the functional activity is to be carried out.

The human activity assistive technology (HAAT) model is proposed as a framework for understanding the place of assistive technology in the lives of persons with disabilities, guiding both clinical applications and research investigations [1]. The model has four components, the human, the activity, the assistive technology, and the context in which these three integrated factors exist. The assistive technology includes human/technology interface, environmental interface, and activity output component to contribute to functional performance. One of the important activity outputs is manipulation.

To establish the manipulation as an activity output, service robots which can support disabled people in their daily life are expected to appear in the real market. The robotic arms which can support disabled people with muscular dystrophy, spinal cord injuries, ALS, and cerebral paralysis are under development [2–6]. The manipulator should be portable for use on a bed or wheel chair and be easy for the user to control. The symptoms of the patients are varied, and the input methods to control the robot should be adapted to them individually.

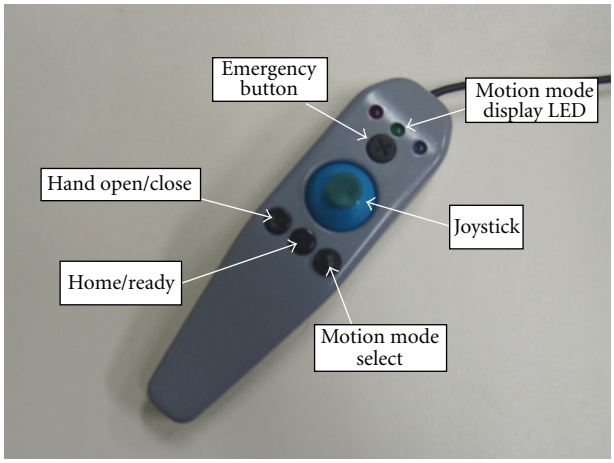

Figure 1: A joystick to control a manipulator.

For example, the iARM (Assistive Robotic Manipulator) [6] was developed to be attached to the side of wheel chairs or bed in order to perform its user's task. The iARM includes several user interfaces: keypad, joystick, and single-switch. The patients with muscular dystrophy can operate the manipulator with these user interfaces according to their conditions. However the information display device of the iARM is only a 7×5 matrix type indicator which is placed on the robot arm shoulder. Before using the manipulator, the single switch user must know all the presented characters shown on the indicator and also the state transitions for the control mode of the manipulator.

Now we are developing a portable manipulator system for patients with less muscle power such as muscular dystrophy patients. The authors are developing some types of user interface for the system. One of them is a single switch with a scanning menu panel. The single switch with a scanning menu panel is an important method for disabled people [1, 7].

The single switch with autoscan panel is remarkably important for the upper-limb disability people. In [1], the indirect selection interfaces have importance for the disabled people. There are some selection modes of the auto-scan menu, and the row-column scanning is most general way. We adopt this row-column scanning way.

These products for the minority users (e.g., upper-limb disabled patients) are called the "orphan products [8]." The orphan products are severely desirable for the specific users with specific symptoms but it is difficult to make industry products because the turnover is not expected. Because the symptoms of the patients are varied, the variation of the user interface should be large. The interface should be configured and reconstructed independently to each user. We will introduce our user interfaces and its improvements for the support robot. To offer the support robot to the market, we consider standard software components of the robotic system, RT-Middleware.

In this paper, we report on the development of the single-switch user interface with RT-Middleware [9]. The conditions of patients, whose behavior is restricted, are varied. Therefore the operational input for the robot should have many types and grades. These multiple types of input method can be adopted simply through RT-Middleware because RT-Middleware is a common software platform for robot systems. We developed some types of user interface, such as a keypad, a joystick (Figure 1), and a single-switch with autoscan panel (Figure 2).

Two patients tried the single-switch user interface and made comments about it. Then we report the improvement of the single-switch user interface according to the comments. Our user interface is constructed with a single switch and input button panel on the computer console. This button panel is an autoscan type and adopts a row-column scanning way [10]. The input panel was rigid, and the user could not change its configuration as he/she likes. The first improvement enables a user to customize the input panel configuration. For the user's convenience, we added a new function to replace the buttons' location in the panel by the user him/herself only with the single switch. Furthermore, we add alternative scanning way of the button panel. Through a new scanning way, the user can put the scanned button forward by a single click of the single switch. And the user can select the button by double click of the single switch.

The precise evaluations of the robot system are reported on [11]. In this paper, we discuss the basic evaluation of the system and the improvements' examples of the user interface to offer our "orphan products" to the real users' daily life.

In the following section, we discuss RT-Middleware and the OpenRTM-aist implementation of it. In Section 3, we introduce the user interface system constructed with RT-Middleware. In Section 4, we describe the operation and evaluation by the patients for the user interface. In Section 5, we describe the improvement of the user interface according to the evaluation by the patients for the user interface and finally conclude this paper.

2. RT-Middleware

RT-Middleware is developed by AIST as an open robot software platform. "RT" means "Robot Technology," which is applied not only to the industrial field but also to the nonindustrial field such as human daily life support systems. RT-Middleware is a software platform for RT systems. RT-Middleware aims at establishing a common platform based on distributed object technology that supports the construction of various networked robotic systems by the integration of various network-enabled robotic elements called RT-Components. If the communication protocol between RT-Components is unified, any other RT-Components can be replaced with them. Modularization of RT elements and RT-Middleware has been studied and developed at AIST, which promotes the application of RT in various fields. RT-Middleware may raise the efficiency of robotic study and development, expand the RT target field, and make a new robot market [12].

2.1. RT-Component Architecture. An RT-Component is the basic functional unit of RT-Middleware-based systems.

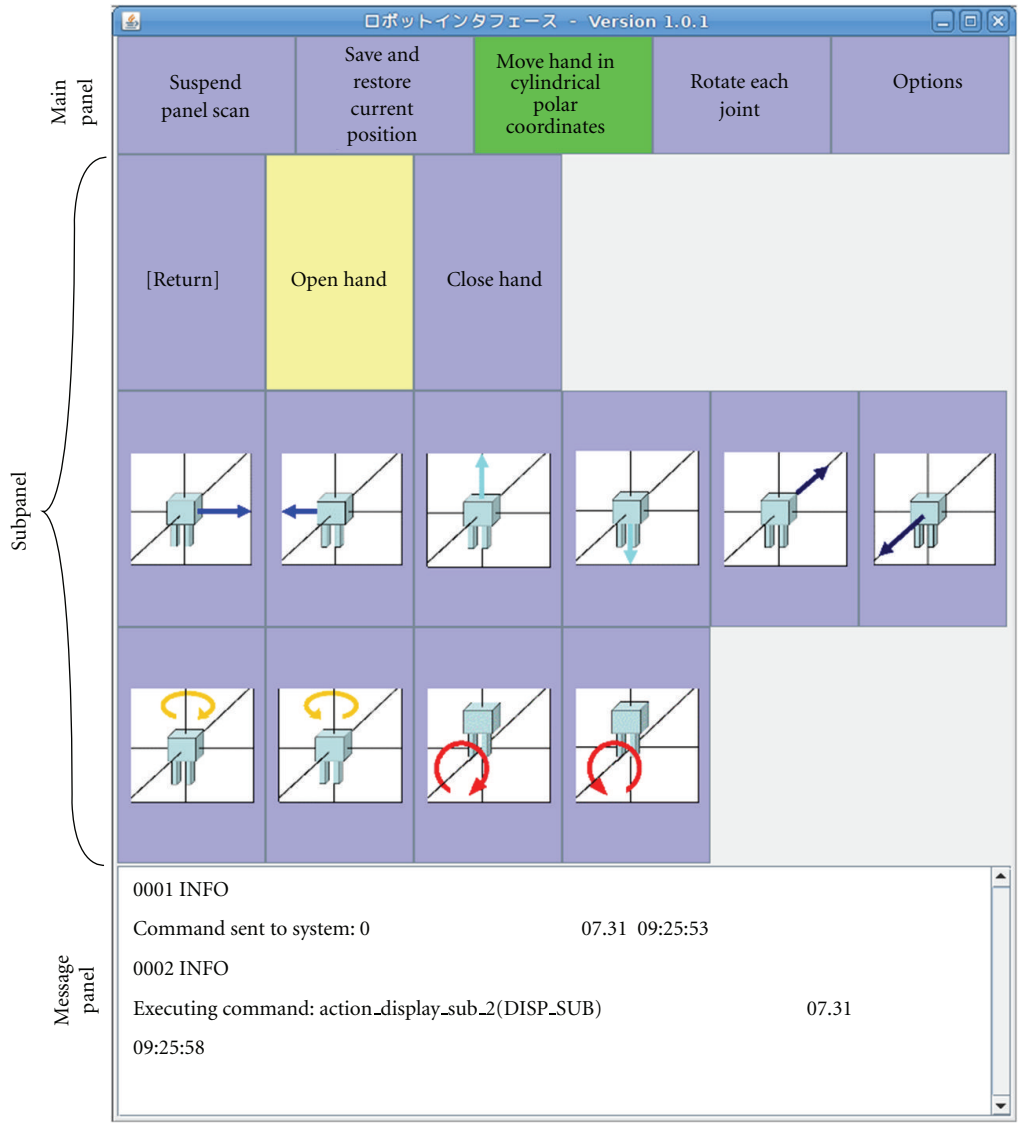

Figure 2: An autoscan panel for a single-switch to control a manipulator.

Figure 3 shows the architecture block diagram of an RT-Component.

For platform independencies, CORBA (common object request broker architecture) is adopted as the distributed object middleware and is used for modeling RT-Components. An RT-Component consists of the following objects and interfaces:

(i) component object,

(ii) activity,

(iii) inPort as input port object,

(iv) outPort as output port object,

(v) servicePort as service interface,

(vi) configuration interfaces.

The general distributed object model can be described as some interfaces that contain operations with parameters and a return value, for example, a torque command and an encoder value. On the other hand, the RT-Component model has a component object as the main body, activity as the main process unit and input ports (InPort), and output ports (OutPort) as data stream ports.

2.2. OpenRTM-aist. "OpenRTM-aist" is developed and distributed by AIST as an implementation of the RT-Middleware interface specification and RT-Component object model [13, 14]. "OpenRTM-aist" consists of an RT-Component development frame work, manager, and a set of tools.

Because RT-Middleware aims to improve the reuse of software, our single-switch interface component and robotic simulator component can be replaced with the joystick component and real manipulator control component, respectively.

Furthermore, when many types of user interfaces are developed to correspond to the patient's symptoms, these

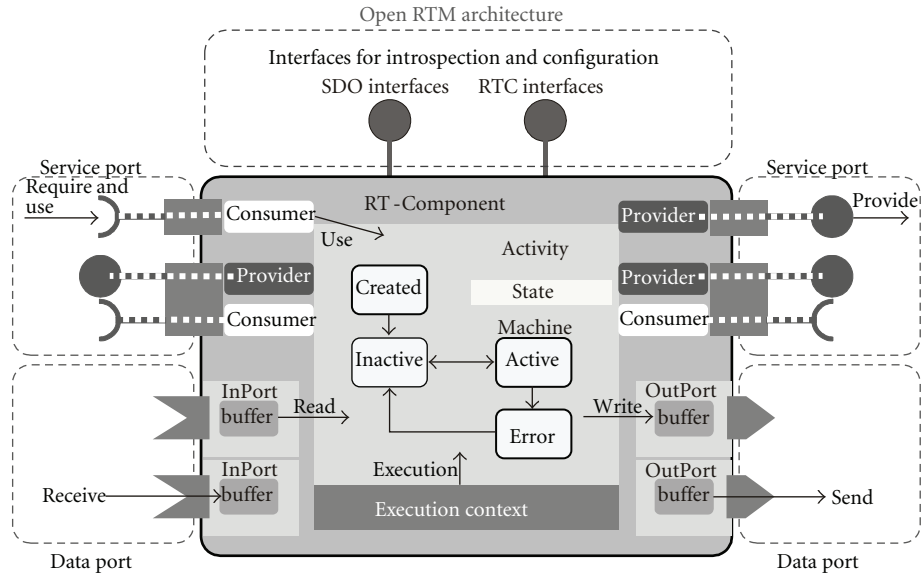

Figure 3: Architecture of RT-Component. RT-Component has a component object, command interface, an activity, InPorts, OutPorts, and service ports.

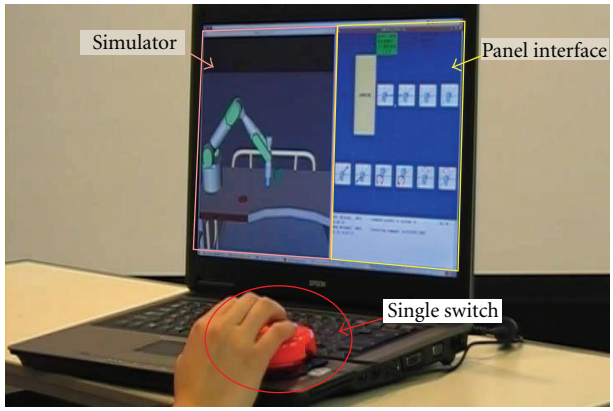

Figure 4: Overview of user interface and robot components with a single-switch.

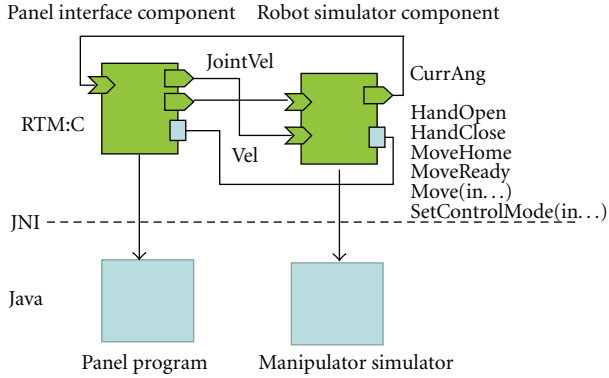

Figure 5: Connection of components.

new components can be connected to the original components without any change in them and used, if the communication protocol of the components is the same.

3. User Interface System

3.1. An Example of Single-Switch Interface. Single-switch user interfaces are used by disabled people to control computers [8]. There are several commercial software packages [15, 16] for the single-switch. For example, "Den-no-shin" is one application. In den-no-shin, the computer shows a panel of buttons on the console. The buttons' color changes in order (scanning), and the user can select the highlighted button to push the single-switch. This software enables the disabled people to input literals, to speak the input sentences, to start Windows applications, to control the mouse cursor with the cross-cursor on the console, and to click the mouse cursor.

However there are few single-switch user interface systems to control a robot. Control of a robotic wheelchair by single-switch scanning has been reported in [16]. But the user can only give commands to change the direction of the wheelchair. We developed a single-switch scanning user interface component to control a robot arm.

3.2. An Outline of the System. User interfaces for disabled people have many variations because their symptoms are varied and the input methods available to them are restricted. Even if the user interfaces are varied, the communication protocol of the user interface and the robot components can be decided in advance. Under the protocol, many kinds of user interfaces and robot components can be connected uniformly as RT-Components [9].

The overview of the user interface and the robot simulator on the computer console with the single-switch is shown

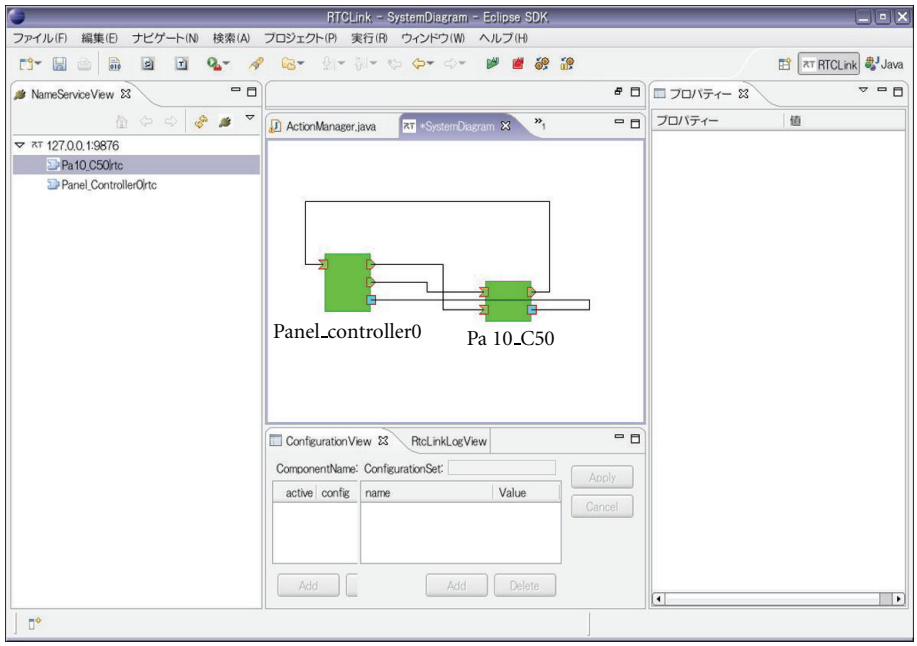

Figure 6: Components on rtc-link.

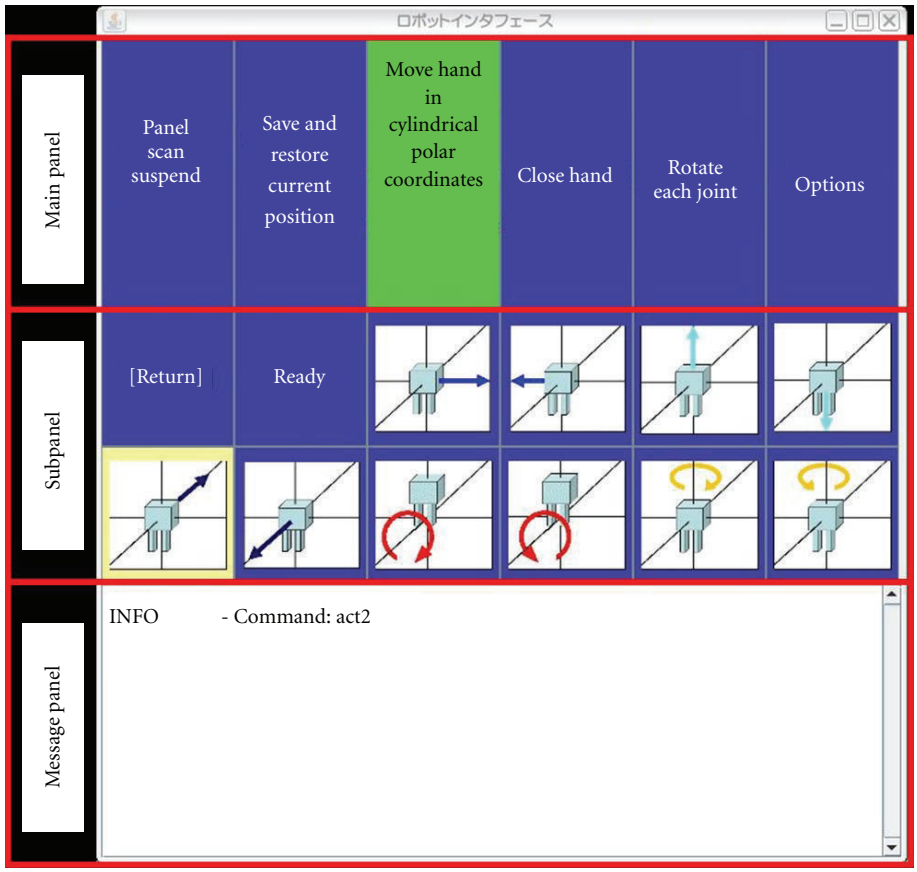

Figure 7: Input panel for single-switch scanning and 5 DOF arm.

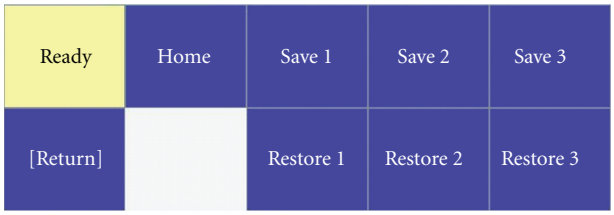

Figure 8: Subpanel for save and restore functions.

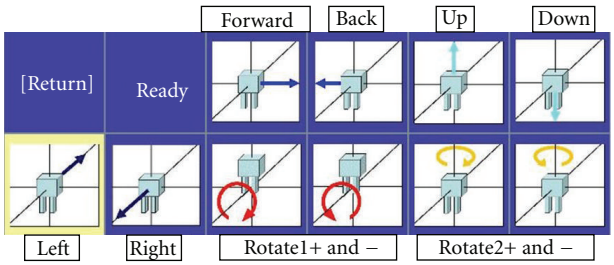

Figure 9: Subpanel for move command buttons.

in Figure 4. The user interface consists of a single-switch and scanning menu panel interface. A manipulator simulator controlled by the user interface is shown on the left of the panel interface.

The panel interface and the robot simulator are created from the interface component and the simulator component, respectively.

3.3. Robot Component. The communication protocol of the user interface and robot components depends on the input/output data of the robot component. The robot component should have the following functions:

(1) manual control of robot motion,

(2) move to home position,

(3) move to ready position,

(4) hand open/close,

(5) servo on/off.

The robot arm has two control modes. One of them is a coordinate control mode. In this mode, the coordinates of the robot hand can be controlled. Another control mode is a joint mode. Joints of the robot arm can be controlled.

The home position is the closing configuration of the robot arm. The ready position is the initial position of the robot arm to start to move.

The robot hand can open and close to grasp an object.

The robot arm can suspend and restart with the servo on/off function.

In this paper, the robot arm has 5 or 6 degrees of freedom. The coordinate commands are given as cylindrical polar and Cartesian coordinates.

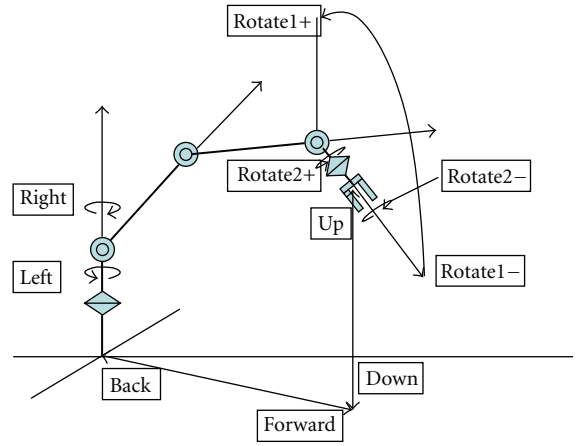

Figure 10: Directions of hand in the simulation.

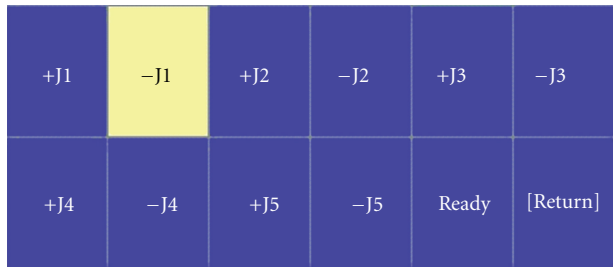

Figure 11: Subpanel for joint command buttons.

3.4. Communication Protocol. To realize the above mentioned functions in the robot component, we decide the communication protocol between the robot component and the user interface component as follows. The data of the output ports of the user interface component are as follows:

(1) the reference velocity of the robot hand,

(2) the reference joint angles.

The robot component receives the above data and moves along with them. The data of the input port of the user interface component is as follows:

(1) the current joint angles of the robot arm.

The user interface component can record the configuration of the robot with the data.

The service port is used for asynchronous commands. The service port commands from the user interface component to the robot component are as follows:

(1) servo on-off,

(2) set of the control mode,

(3) move to target joint angles,

(4) move to home position,

(5) move to ready position

(6) hand open-close.

A precise diagram of component connections is shown in Figure 5.

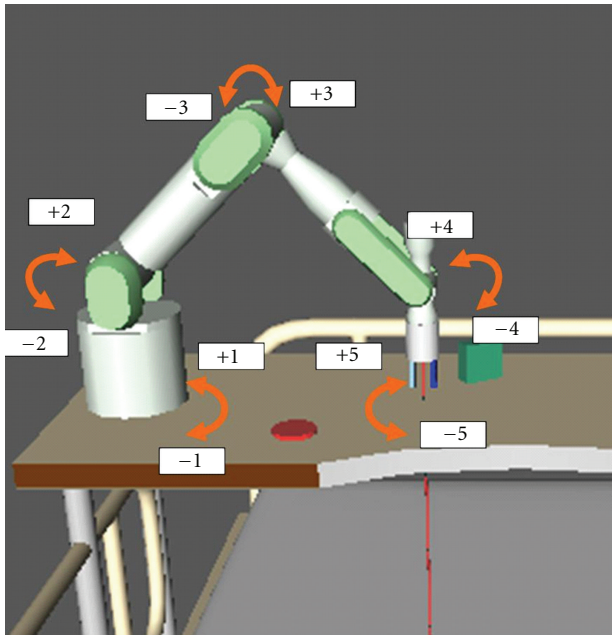

Figure 12: Rotations of joints in the simulation.

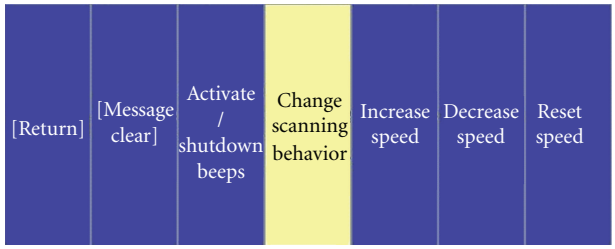

Figure 13: Subpanel for option buttons.

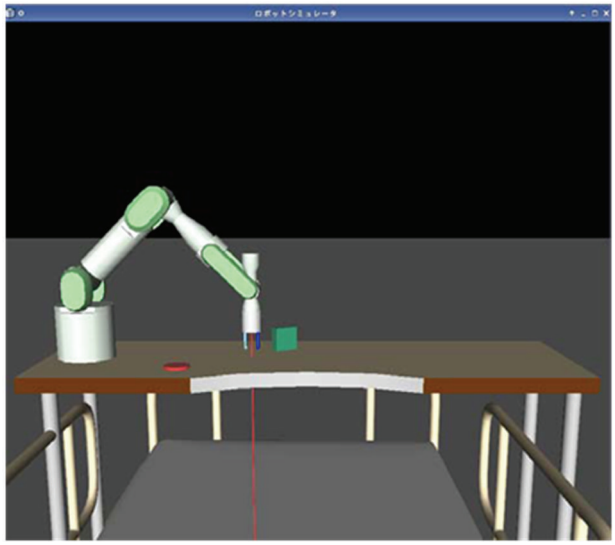

Figure 14: Moving robot arm in simulation.

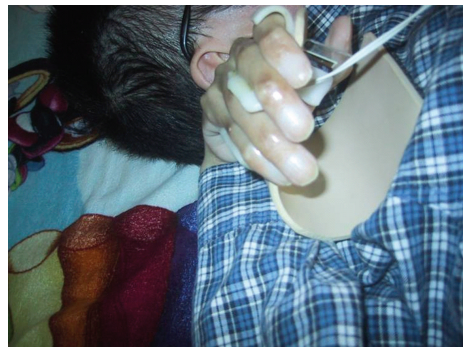

(a)

(b)

Figure 15: Tester's single switches.

RT-Components are connected with "rtc-link." The rtc-link is a GUI tool that manages connections of InPort/OutPort and Service Ports between RT-Components and performs activation/deactivation of an RT-Component. Rtc-link is a powerful tool which can be used when development and debugging of RT-Components is performed. Moreover, it can also be used in verification and experimentation with a robot system, performing the low level integration of components. The rtc-link is shown in Figure 6.

Each component is described and executed in Linux, and both components can be executed on Windows with VMware.

3.5. Panel Interface. Our operational user interface includes a button panel shown on the computer monitor. The buttons on the panel change their color in order (scanning in order). When the target button is highlighted, the user can select it with single-switch pushing and control the robot arm (Figure 7).

The panel includes three parts. They are a main panel, a subpanel, and a message panel. The user can command the robot by selecting the button on a main panel and on a subpanel. The message panel shows the executed actions result and the errors.

The main panel has six buttons. The first button is to start and suspend panel scanning. The second button is to save and restore the robot hand's current position. The third button is the move command using the robot hand coordinates.

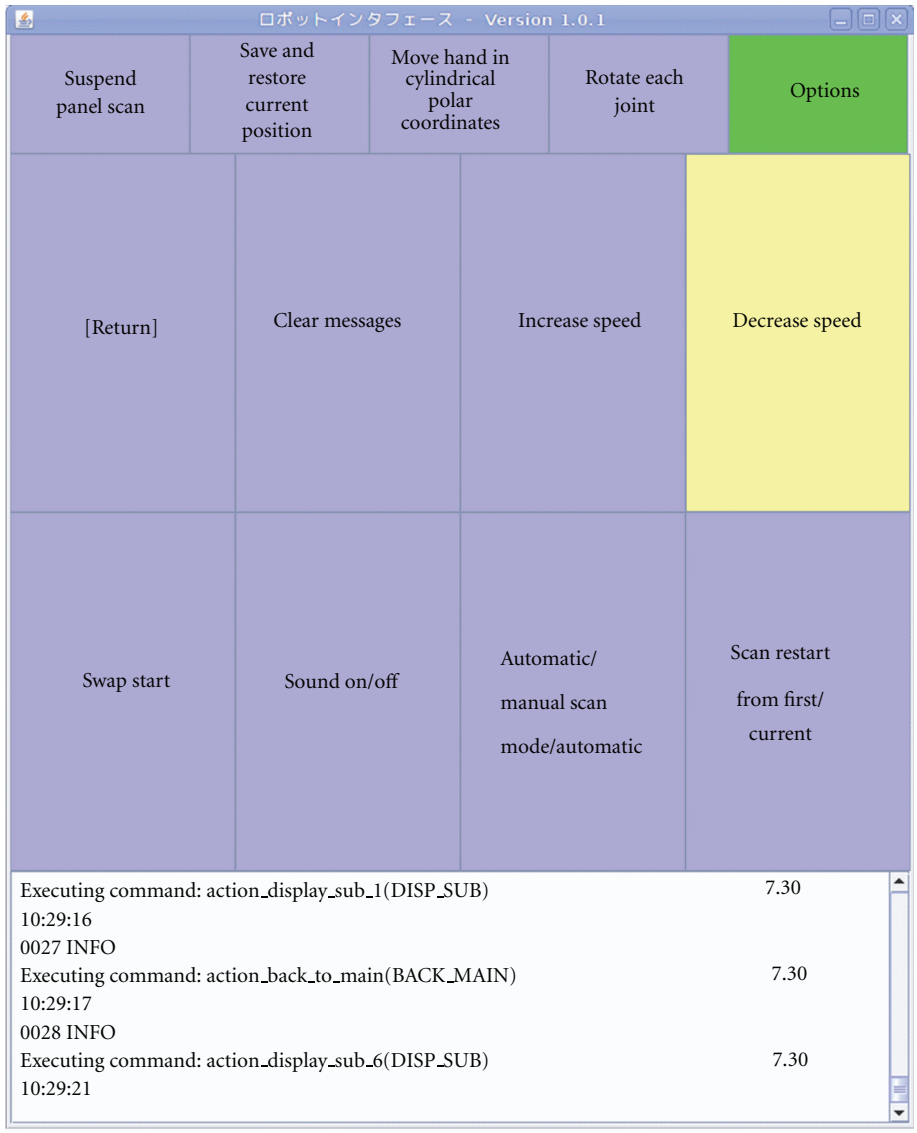

Figure 16: Option panel.

The fourth button is open-close of the finger of the robot arm. The fifth button is move command of the robot's joints' angle. The sixth button corresponds to options.

(1) Scan/Suspend Button. When this button is selected, scanning of the panel is suspended. If the single-switch is pressed again, scanning restarts.

(2) Save/Restore Button. This button opens a subpanel to save the current arm position and restore the position. The subpanel is shown in Figure 8. The subpanel contains buttons to move to ready position and home position.

(3) Coordinate Move Command Button. This button opens a subpanel for the command button of the robot's hand coordinates (Figure 9). In the beginning of our project, the target manipulator was taken to have 5 degrees of freedom. There are 10 commands. The user can select a button among these 10 buttons to indicate the direction of the robot hand's motion.

The selected buttons control the robot hand to move in the directions in Figure 10. The directions and rotations of the robot hand motions are the same in the appearance of the simulation and the buttons' characters in the panel.

These buttons are toggle buttons. When the single-switch is pressed and the button is selected, the robot starts to move. Then the single-switch is pressed again, and the robot stops.

(4) Hand Open/Close Button. When this button is selected, the hand closes if the hand already is open. When this button is selected again, the hand opens.

(5) Joint Command Button. This button opens a subpanel of the joints' angle command of the robot arm (Figure 11).

Figure 17: Button swap in panel.

The user can command 5 joints' rotations in plus and minus directions. In Figure 12, the rotations of all the joints of the manipulator are shown.

These buttons are toggle buttons. When the single-switch is pressed and the button is selected, the robot starts to move. Then the single switch is pressed again, and the robot stops.

(6) Options Button. This button opens a subpanel for options to change the panel settings (Figure 13). Buttons to clear the literals in message panel, to set the on/off of the beep sound of panel scanning, to set the scanning order when the scanning restarts, and to change the scanning speed of the buttons are shown in this panel.

All the button actions can be recorded in a log file with their executed time.

Our panel user interface is written in Java. The C++ program calls the panel user interface program through JNI as shown in Figure 4. Our system is developed with OpenRTM-aist-0.4.0.

3.6. Robot Arm Simulator. We constructed a robot simulator to evaluate the single-switch scanning user interface (Figure 14). The robot arm moves in the simulator window according to the commands from the operation of the single-switch scanning interface.

We developed a simple task in the simulator. The task is to let the robot grasp the green box and place it on the red circle. The initial position of the green box and the red circle are alterable with a configuration file for the simulator.

In our simulator, the contact between the robot hand and the grasping object or the environment is not calculated. When the hand closes near enough to the target object, the simulator decides that the robot has grasped the object and

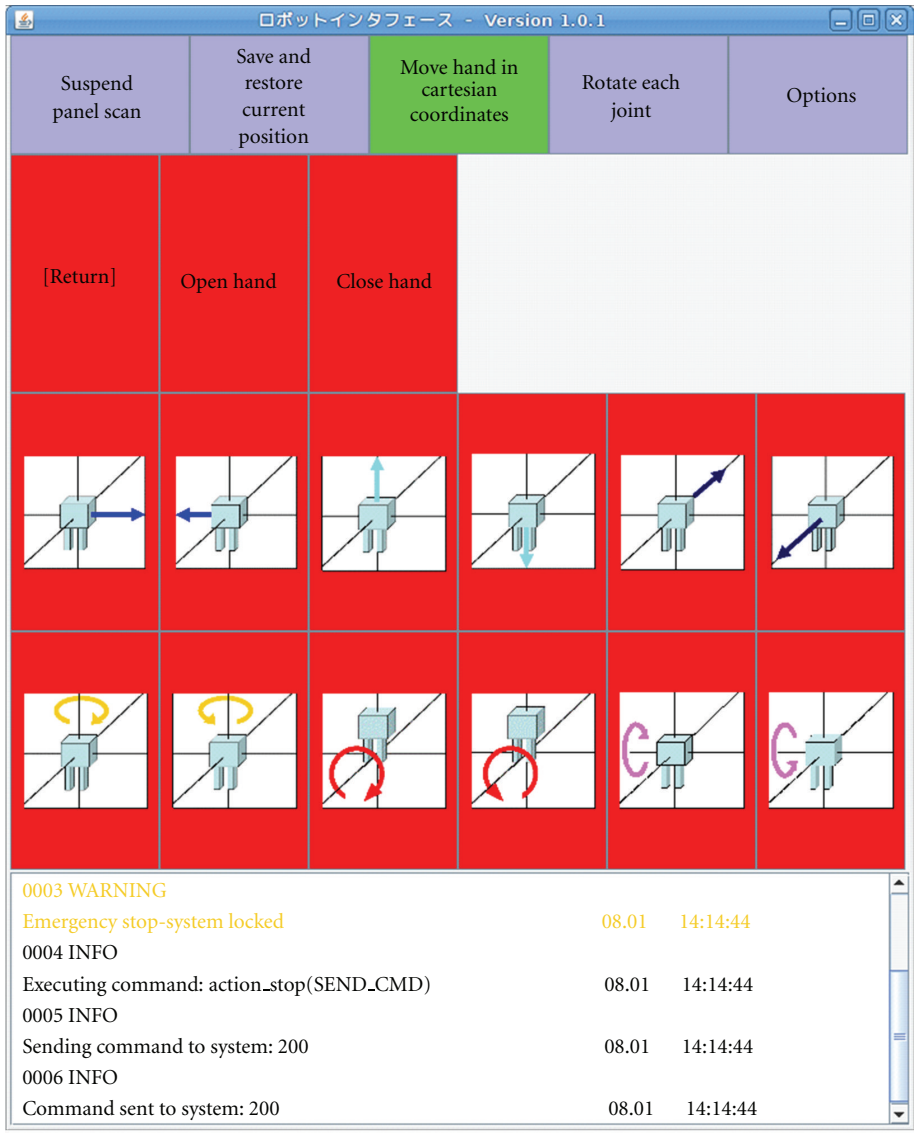

Figure 18: Input panel at emergency stop.

draws the object between the fingers of the robot as the grasping is completed.

The image of the simulator is drawn on a plane. Therefore the user cannot understand the robot hand position precisely in the depth direction. A red line like a laser pointer is drawn from the center of the hand on the vertical line of the hand to show the relative position of the hand in the task environment.

The simulator is written in Java similar to the user interface panel and the C++ program calls it through JNI.

4. Operation and Evaluation by Users

We cooperated with the Shimoshizu national hospital, Japan. The hospital has a special ward for muscular dystrophy patients. Two patients made trials of our user interface and simulator for 30 minutes. Before the trials, we investigated about human ergonomic experiment and applied for the ethics committee in the AIST. Both of them usually used single-switch scanning user interface to control computers so they are accustomed to the single-switch scanning user interface. Their own single switches were connected to the user interface computer through a USB connection (Figure 15).

First, examiners simply explained about the user interface and the simulator and demonstrated the task. Then each subject separately performed the task of taking the box and placing it on the target position in the simulator. During the task execution and after the task, the examiners asked subjects about general impressions, contents of buttons, scanning speed of buttons, safety issues, and their desire to control robot arms with this user interface. Their comments are shown in Table 1.

Table 1: Comments by subjects.

	Subject A	Subject B
Evaluations of easiness of operations	At first I was afraid that it may be difficult to control the robot. I feel easier to use it.	When the new robot will appear with this interface, I want to use them very much. This robot will be much better than to call a helper.
Evaluations and desire about the panel	Configuration of the button on the panel seems good, but the contents of the button are difficult to understand.	I want to configure the scanning speed. The scanning can be continued anytime.
	Scanning of the button should start at the beginning of the list when the scanning restarts.	The number of the buttons on the panel seems to be necessary and sufficient. If I can select one of the many types of the panels, it seems preferable.
	The scanning should be stopped unless the user wants to use this interface.	Beep sound at scanning of button is preferable.
Request about safety	I want the emergency stopping button to push the single switch for a long time or in the panel	It is better for me if the single switch involves emergency stopping function. If the system can find the freezing of the computer and let the robot stop, I can feel safer.

Both subjects stated that this user interface is mainly good to use and they want to control a real robot with this user interface by all means. They also commented on safety functions for the user interface.

In this evaluation, only the move command of hand subpanel is used by the examiner and subjects to simplify the evaluation. Subpanels described in the previous section have been refined using the patients' comments [17].

This evaluation is basic to improve our user interface. Precise human ergonomic evaluations with real manipulator "RAPUDA" are reported in [11]. The examinees responses are generally good. The evaluations by real users are the Pegboard task in [11]. The test and evaluation in their daily life should be performed for the next step.

5. Improvements of User Interface

5.1. Request from Patients of Muscle Dystrophy. As stated in the above section, we let 2 patients of the muscle dystrophy test our user interface. One of the patients gave us a following comment as "If I can select one of the many types of the panels, it seems preferable." (Table 1).

The previous input panel is rigid as shown in Figure 7. The panel configuration is described in the initial configuration file.

The programmer of the system can rewrite it and reconfigure the panel configuration. But the user of the user interface is not supposed to reconfigure the panel by him/herself alone.

Reconfigurable function of the input panel can be more convenient than other types of the input panel for the user.

Another patient told us "If scanning of buttons does not continue automatically and is commanded by myself, it seems preferable." (Table 1).

Both of the patients expressed the necessity of the emergency stop function. Besides, patients' comments are as follows, "Scanning of the button should start at the beginning of the list when the scanning restarts" and "The scanning should be stopped unless the user wants to use this user interface." (Table 1).

5.2. Button Replacement Function. Therefore we made new function so the user can replace the location of the buttons in the input panel freely and made the replace button in the option panel (Figure 16).

When the user selects the button, the user interface will enter to the button replace mode. The next selected button with the single switch click and the following selected button are replaced in the panel (Figure 17). This panel is utilized for the manipulator with the 6 degrees of freedom motion.

To escape from the replace mode, the long click of the single switch is utilized.

The result of the replacement of the buttons by this function can be stored in the initial configuration file of the input panel.

This function allows the user to change freely the location of the button which he/she use usually.

5.3. Alternative Mode for Scanning and Selection of Buttons. We made alternative scanning mode for the user to control the button scanning according to his/her will. The user can command one button scanning with single click and can select the button with double click. The alternative scanning mode button is prepared in the option panel (Figure 16).

The user can let the buttons scan by him/herself with this function. The options which the user can select become rich.

5.4. Emergency Stop with Long Click. The emergency stop function is prepared with a long click of the single switch.

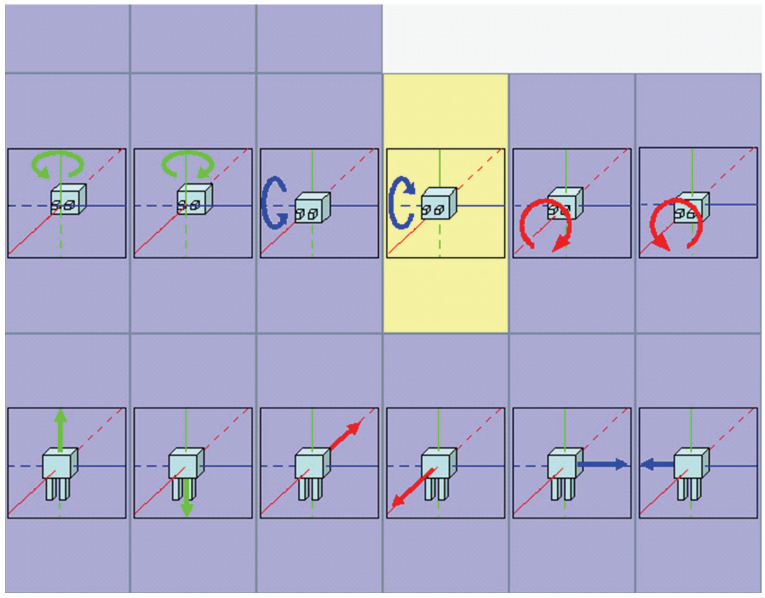

Figure 19: Scanning button replacement according to the previous input.

The long click makes the color of all the panel red and sends a stop command to the robot component (Figure 18).

The long click is used to escape from the replace mode too. During the replace mode, the robot does not move anyway. Therefore the user will not be confused [15].

The long click time can be changed. In this system, 1 second is indicated. The time should be decided according to the robot speed and autoscan speed.

5.5. Changing Position of Scanning Restart. The restart position of the scanning can be set at the first in the button list or the current button. The toggle button of this option is set in the options panel (Figure 16).

5.6. Suspend Button of Scanning. The suspend panel scan button is set on the top of the main panel. This button was added because of the patients' request (Figure 7).

5.7. Scanning Button Replacement according to the Previous Input. The order of the panel buttons are exchanged automatically according to the user's previous operation. The order is exchanged in 2 steps. At first the parallel motion low and rotation motion low are exchanged. In the low, previous command set (+ and −) are located on the top of the low. Figure 19 shows the replaced low and position of button sets in the scanning panel (Figure 19).

With this improvement, the user can easily repeat a desirable command's + and −. 2 trained operators have performed pick and place task with this user interface. The average total time of the task is decreased 6%.

6. Conclusion

The supporting robot for disabled people cannot make large industry, so we should offer inexpensive manufacturing way. These type products are called as "orphan products." In order to support disabled people especially with less muscle strength such as muscular dystrophy patients, we developed a single-switch scanning user interface to control a manipulator system. The input menu panel is designed to perform various actions of the robot arm with the single switch and to be easy for users to understand. All the components of the user interface and the robot simulator are constructed with RT-Middleware. Therefore other new user interface components can be reconnected to our system without any change in them and utilized if the communication protocol of the components is the same.

Patients with muscular dystrophy tested the user interface and made evaluations. Both patients stated that this user interface is mainly good to use, and they want to control a real robot with this user interface by all means.

According to the testers' comments, we improved a single-switch scanning user interface to control a manipulator system. The first improvement enables a user to customize the input panel configuration. We added the function to replace the buttons' location in the panel by the user him/herself only with the single switch.

Furthermore, we have added an alternative way of scanning the button panel. Through the new scanning, the user can put the scanned button forward by a single click of the single switch. And the user can select the button by double clicking of the single switch.

Besides, we added an emergency stop function, an option for changing position at scanning restart and a scanning suspend function.

Finally, we made an optional improvement that the order of the panel buttons are exchanged automatically according to the user's previous operation.

These new input functions which involve user configuration can make our user interface system more user friendly.

In this project, we will synthesize the user interface and the real manipulator for the result. Moreover, this simulator can be a training kit to control a service robot for use in daily life.

Acknowledgments

The authors appreciate the cooperation of the patients and staff of the Shimoshizu National Hospital, Japan in this research. Also we would like to thank the staff of the AIST project for the personal robot. This research was carried out as one of UCROA (User Centered Robot Open Architecture) project at AIST [12].

References

[1] A. Cook and J. Polgar, *Assistive Technologies, Princeples and Practice*, Mosby Elsevier, Baltimore, Md, USA, 3rd edition, 2008.

[2] J. Sijs, F. Liefhebber, and G. W. R. B. E. Römer, "Combined position & force control for a robotic manipulator," in *Proceedings of the 10th IEEE International Conference on Rehabilitation Robotics (ICORR '07)*, pp. 106–111, Noordwijk, The Netherlands, June 2007.

[3] M. J. Johnson, G. A. Di Lauro, M. C. Carrozza, E. Guglielmelli, and P. Dario, "GIVING-A-HAND: early development of a small, countertop, mobile robot kitchen assistant for elderly and mudium- to high-disabled persons," in *Proceedings of the 8th International Conference on Rehabilitation Robotics (ICORR '03)*, pp. 120–123, April, 2003.

[4] M. Nokhtari, B. Abdulzarak, M. A. Fki, R. Rodriguez, and B. Grandjean, "Integration of rehabilitation robotics in the context of smart homes: application to assistive robotics," in *Proceedings of the 8th International Conference on Rehabilitation Robotics (ICORR '03)*, pp. 5–8, April, 2003.

[5] G. Verburg, M. Milner, S. Naumann, J. Bishop, and O. Sas, "An evaluation of the MANUS wheelchair-mounted manipulator," in *Proceedings of the RESNA International '92*, pp. 602–604, 1992.

[6] http://www.exactdynamics.com/.

[7] J. Angelo, "Factors affecting the use of a single switch with assistive technology devices," *Journal of Rehabilitation Research and Development*, vol. 37, no. 5, pp. 591–598, 2000.

[8] http://www.rehab.go.jp/ri/event/html/english.html.

[9] K. Nagata, Y. Wakita, N. Yamanobe, and N. Ando, "Development of assistive robotic arm system with Robot Technology Middleware (RTM)," in *Proceedings 19th IEEE International Workshop on Robot and Human Interactive Communication (Ro-man '10)*, pp. 737–742, 2010.

[10] Y. Wakita, N. Yamanobe, K. Nagata, N. Ando, and M. Clerc, "Development of user interface with single switch scanning for robot arm to help disabled people using RT-middleware," in *Proceedings of the 10th International Conference on Control, Automation, Robotics and Vision (ICARCV '08)*, pp. 1515–1520, Hanoi, Vietnam, December 2008.

[11] N. Yamanobe, Y. Wakita, K. Nagata, M. Clerc, T. Kinose, and E. Ono, "Robotic arm operation training system for persons with disabled upper limbs," in *Proceedings 19th IEEE International Workshop on Robot and Human Interactive Communication (Ro-man '10)*, pp. 749–754, 2010.

[12] AIST 2005/2006 Annual Report.

[13] N. Ando, T. Suehiro, K. Kitagaki, T. Kotoku, and W. -K. Yoon, "RT-Middleware: distributed component middleware for RT (Robot Technology)," in *Proceedings of the IEEE/RSJ International Conference on Intelligent Robots and Systems (IROS '05)*, pp. 3555–3560, Edmonton, Canada, 2005.

[14] http://www.openrtm.org/openrtm/en.

[15] K. Ozawa, "Barrier free and accessibility of information processing equipment," *The Journal of the Institute of Electronics, Information, and Communication Engineers*, vol. 81, no. 2, pp. 166–169, 1998 (Japanese).

[16] H. A. Yanco and J. Gips, "Driver performance using single switch scanning with a powered wheelchair: robotic assisted control versus traditional control," in *Proceedings of the Annual Conference of the Rehabilitation Engineering and Assistive Technology Society of North America*, pp. 298–300, RESNA Press, Minneapolis, Minnesota, June 1998.

[17] Y. Wakita, N. Yamanobe, K. Nagata, and M. Clerc, "Customize function of single switch user interface for robot arm to help a daily life," in *Proceedings of the 10th IEEE International Conference on Robotics and Biomimetics (ROBIO '08)*, pp. 945–950, Bangkok, Thailand, 2009.

Hindawi Publishing Corporation
Journal of Robotics
Volume 2011, Article ID 348207, 14 pages
doi:10.1155/2011/348207

Review Article

Gait Rehabilitation Device in Central Nervous System Disease: A Review

Kazuya Kubo,[1] Takanori Miyoshi,[1] Akira Kanai,[2] and Kazuhiko Terashima[1]

[1] *Toyohashi University of Technology, Hibarigaoka 1-1, Tempaku-Cho, Toyohashi, Aichi 441-8580, Japan*
[2] *Department of Physical Therapy, Toyohashi Sozo University School of Health Sciences, 20-1 Matsushita, Ushikawa-Cho, Toyohashi, Aichi 440-8511, Japan*

Correspondence should be addressed to Kazuya Kubo, kubo@syscon.me.tut.ac.jp

Received 1 June 2011; Accepted 8 August 2011

Academic Editor: Haruhisa Kawasaki

Central nervous system diseases cause the gait disorder. Early rehabilitation of a patient with central nervous system disease is shown to be benefit. However, early gait training is difficult because of muscular weakness and those elderly patients who lose of leg muscular power. In the patient's walking training, therapists assist the movement of patient's lower limbs and control the movement of patient's lower limbs. However the assistance for the movement of the lower limbs is a serious hard labor for therapists. Therefore, research into and development of various gait rehabilitation devices is currently underway to identify methods to alleviate the physical burden on therapists. In this paper, we introduced the about gait rehabilitation devices in central nervous system disease.

1. Introduction

Walking is one of the most basic forms of locomotion. Factors obstructing the ability to walk include aging, orthopedic disease (e.g., fracture), and central nervous system (CNS) disease (e.g., cerebrovascular disease (CVD) and spinal cord injury (SCI)). Decreased power of the lower limb muscles, decreased range of motion, and pain can all contribute to gait disorder due to aging and orthopedic disease. Causes of gait disorder with CNS disease likewise include decreased power of the lower limb muscles and decreased range of motion, along with effects on the locomotion center. Rehabilitation is achieved as shown in Figure 1. The method of learning gait involves passive gait exercise by two therapists. To teach a patient how to walk again, therapists must guide the leg movements of the patient, and this task usually requires one therapist for each leg [1–4]. Hospital-based rehabilitation is generally carried out 4-5 times a week for about 10–20 min per session and is very physically taxing, so prolonged sessions often prove to be difficult. Research into and development of various gait rehabilitation orthoses is currently underway to identify methods to alleviate the physical burden on therapists. This paper outlines SCI and CVD as two of the major causes of gait disturbance and introduces gait rehabilitation for CNS disorders as well as the gait rehabilitation orthoses currently being studied. Muscle strengthening is not addressed in this study, as that issue encompasses areas other than CNS disorders. Moreover, functional electrical stimulation (FES) can be used as a method of learning gait. However, the purpose of FES is to achieve motion assistance and to facilitate learning gait. As distinguishing these two functions is difficult, this method was excluded from the present paper.

2. Spinal Cord Injuries

Spinal cord injuries (SCIs) occur when the spinal cord is damaged by trauma to the vertebral column. Similar disabilities can also occur due to internal factors such as spinal cord tumors and herniation. Unlike peripheral nerves, the CNS including the spinal cord is largely unable to repair or regenerate itself after injury. Major causes of CNS injury include motor vehicle and sporting accidents. SCIs are classified as "complete" and "incomplete," with the former referring to transection of the spinal cord resulting in total

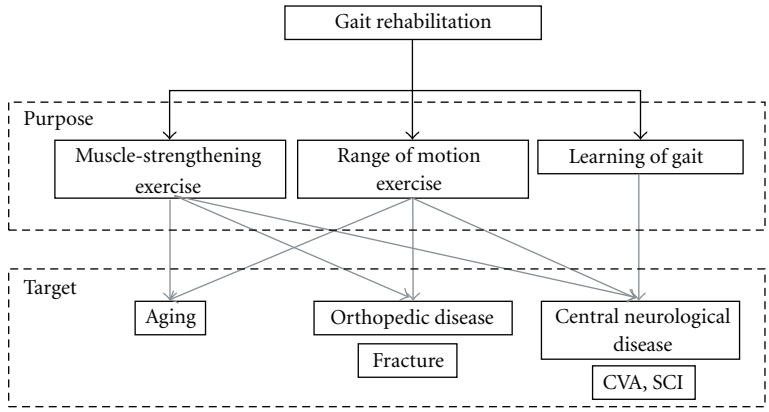

Figure 1: Purpose and target of gait rehabilitation.

interruption of neurotransmission function, and the latter implying partial injury or compression of the spinal cord with only partial loss of function. In complete SCI, control of the area below the injury by the upper CNS is lost along with motor function as signals from the brain fail to reach the injured region. Sensory perception is also lost due to the interruption of sensory pathways carrying information back to the upper CNS. The human vertebral column is divisible into the cervical vertebrae (C1-7), thoracic vertebrae (Th1-12), lumbar vertebrae (L1-5), sacral vertebrae (S1-5), and coccygeal vertebrae (coccyx). The higher an injury is located on the spinal column, the greater the associated area of paralysis. Complete lower thoracic spinal injuries cause paraplegia, while complete upper thoracic spinal injuries cause quadriplegia and respiratory paralysis. A damaged spinal cord does not recover, so the paralyzed area does not change over time. Rehabilitation therefore targets the area above the injury instead of the paralyzed area below. However, prolonged recumbency causes muscle weakness, so it is preferable to commence the rehabilitation program as soon as possible after sustaining the injury. Although lower thoracic spinal injuries cause paraplegia, central pattern generators (CPGs) present in the spinal cord below the injured area are capable of moving the legs even when motor outputs from the brain do not reach the legs. Accordingly, some gait rehabilitation programs seek to reteach motor activities to CPGs in conjunction with trunk- and arm-muscle strengthening and wheelchair training. Patients with upper thoracic spinal injuries involving paralysis of the legs and trunk, but not affecting movement of the arms, often undergo rehabilitation focusing on arm-muscle strengthening and wheelchair training. Gait rehabilitation is performed to prevent orthostatic hypotension and increase physical strength. Some movements of vertebrate animals are thought to be controlled by the neural networks in the spine known as CPGs. These include periodic motions such as walking or swimming. Graham Brown [5] conducted research on CPGs in which decerebrate cats exhibited natural gait when placed in a harness suspended over a moving treadmill and even ambulated when electric stimulus was applied to the area of the brain known as the mesencephalic locomotor region (MLR), leading to the hypothesis that CPGs are present as gait pattern-forming areas in the spine and that walking is the result of interactions between the mesencephalon and the spinal cord. A study verifying the presence of CPGs in swimming was carried out on lamprey eels as primitive vertebrates [6, 7], followed by an experiment eliciting treadmill locomotion in monkeys [8]. Research on CPGs in humans [9–12] is also being undertaken in an attempt to achieve ambulation in patients with upper SCIs. Elicitation of ambulatory patterns has been identified as likely to occur with slow gait speed and small load or normal gait speed and large load [13, 14]. Afferent stimuli from proprioceptive sensory organs such as muscle and neurotendinous spindles in the leg muscle groups induce ambulatory patterns via CPGs. Electrical output from CPGs is enhanced by repetitive gait rehabilitation and reduced by the lack of such training [15, 16].

3. Cerebrovascular Disease

CVD occurs when an anomaly in the intracranial blood vessels nourishing the brain triggers a hemorrhage that eventually damages the brain tissue due to inflammation/displacement or ischemia. CVD is generally classified into cerebral infarction, cerebral hemorrhage, or subarachnoid hemorrhage according to the form of injury. Cerebral infarction occurs when the supply of blood to the brain is interrupted due to stenosis or occlusion of cerebral arteries as a result of events such as thrombosis. Cerebral hemorrhage refers to the formation of a mass known as an intracerebral hematoma caused by the rupture and subsequent hemorrhaging of brain capillaries. Subarachnoid hemorrhage is a condition in which an aneurysm formed in the subarachnoid space ruptures and the subsequent bleeding places pressure on the brain. Symptoms vary according to the site of the damage, with injuries to the left hemisphere of the brain generally associated with language disorders and injuries in the right hemisphere causing unilateral spatial neglect (USN). However, a common symptom is motor/sensory paralysis on the side contralateral to the injury. Like SCI,

functions in areas that are damaged by CVD do not recover, but are instead taken over by peripheral and other areas of the body and resumed by reconfiguration of neural networks [17–19]. Beginning rehabilitation as soon as possible after sustaining the injury is recommended to prevent the onset of disuse syndrome. CVD rehabilitation focuses on strengthening the muscles on the unaffected side as well as performing repetitive motor training on the paralyzed side to reteach motor activities to the brain. Rehabilitation programs are designed according to the symptoms of the patient, such as higher brain dysfunction. CVD patients with USN, for example, may undergo symmetrical gait rehabilitation using a mirror.

4. Gait Rehabilitation in CNS Disease

Gait rehabilitation is implemented in a variety of ways, according to the condition of the patient. Some examples include the use of walking sticks, lower limb orthoses, parallel bars, walking frames, and treadmills. Aims of rehabilitation include teaching gait action, strengthening muscles, and building endurance. When teaching gait action, the therapist usually holds on to the legs and waist of the patient and provides guidance. This approach may involve the use of a treadmill and suspension device known as a bodyweight support (BWS) system to prevent the patient from falling and to enable the therapist to hold the patient more easily. BWS systems may employ springs, weights, or winches and can be used to preclude the onset of disuse syndrome by enabling gait rehabilitation in patients who cannot assume a standing posture while preventing them from falling [20–24]. Gait retraining targets reticulospinal tract CPGs [25] in SCI patients, and healthy areas of the cerebrum in CVD patients. Input stimuli for the purpose of retraining consist of changes in muscle length detected by muscle spindles and changes in muscle strength detected by neurotendinous spindle. Moving the legs during gait rehabilitation while applying a load is believed to produce input to the CNS regarding changes in muscle length and muscle strength, whereas moving the legs without application of a load only generates inputs for changes in muscle length. Research is therefore being undertaken into ways of automatically controlling load and leg joint movements in order to send stimuli to the CNS during gait rehabilitation in a safe and suitable manner. Gait rehabilitation immediately after injury places a considerable burden on the therapist, making extended sessions difficult. Furthermore, therapist instruction is lacking in terms of reproducibility and is therefore considered unsuitable for certain gait patterns. Accordingly, the following gait rehabilitation devices are being researched and developed to mitigate the physical burden on therapists, enable extended rehabilitation sessions, and provide appropriate stimuli to the CNS. These devices can be broadly classified into four types: those with functions of supporting the body and guiding the legs (lifting device with lower limb orthosis); those with a function of supporting the body only (lifting device); those with a function of guiding the legs only (lower limb orthosis); those resembling wheeled walkers or rollators (Walker) as shown in Tables 1 and 2 and Figure 2. The rehabilitation orthoses discussed in this paper are tabulated according to the target user, description of conducted experiments, and system configuration. Rollator-style devices [26–29] are used by individuals with muscle weakness as well as CNS disorder patients and are utilized in daily living as well as in rehabilitation. This broad range of users and applications makes comparison difficult, so these devices have been excluded from the scope of this paper. And FES (Functional Electrical Stimulation) is researched as a gait ability acquisition method [30–33]. In FES, there are two purposes of assistance and rehabilitation of gait. Because these distinctions are difficult, we exclude it in this paper.

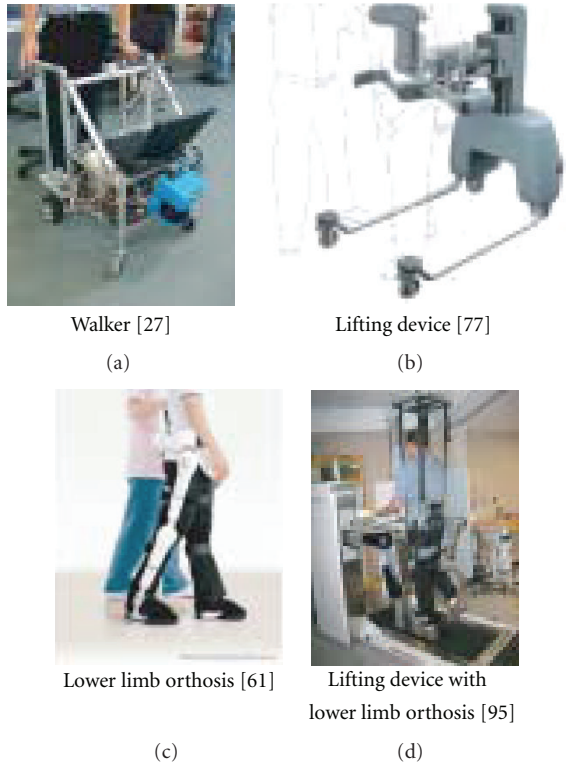

Figure 2: Type of gait rehabilitation.

5. Gait Rehabilitation Device

In a study by Hesse et al. [34] on the feasibility of restoring gait function in CNS disorder patients through repetitive training, comparison of walking cycle and electromyographic (EMG) signals in hemiparetic patients who underwent gait rehabilitation using a BWS system and treadmill or bed-based gait rehabilitation revealed that cyclical walking patterns were induced in patients using the BWS system and treadmill rehabilitation. Hesse et al. also conducted a study in which cerebral palsy patients underwent regular ambulatory rehabilitation using a BWS system and treadmill for 3 months, revealing that gross motor function measure (GMFM) and functional ambulatory category (FAC) scores

Table 1: Reference about gait rehabilitation device number 1.

Type	Device name	Target	Rehabilitation method	Subject	Evaluation item	Reference
Lower limb orthosis	HAL	Other	Active gait	—		[61]
	GBO	CVD	Active gait	—		[62]
				Healthy CVD	Knee and hip angle Knee and hip torque EMG of lower limbs Foot trajectory	[63]
				Healthy CVD	Knee and hip angle	[64]
	ALEX	SCI, CVD	Passive gait	Healthy	Foot trajectory	[65]
				CVD	Knee and hip angle foot trajectory	[66]
	LOPES	SCI, CVD	Passive gait Active gait	Healthy	Step height	[49]
				Healthy	Knee and hip angle Step height	[50]
				Healthy	Knee and hip angle EMG of lower limbs	[51]
				Healthy	Knee and hip angle EMG of lower limbs	[52]
	Nango's research		Passive gait	—		[67]
				—		[68]
				—		[69]
Lifting device	WARD	CVD	Active gait	Healthy	Gait velocity, stride	[70]
	RGR Trainer	CVD	Active gait	Healthy	Pelvic obliquity	[57]
	STRING-MAN	CVD	Active gait	Healthy	ZMP position	[71]
	Lokolift	CVD	Active gait	Healthy	GRF	[72]
	Flora	CVD	Active gait	Healthy	Knee and hip angle	[73]
	Ikeuchi's research	CVD	Active gait	Healthy	GRF	[74]
			Active gait	Healthy	Unloading force	[75]
	BWS system	CVD	Active gait	Healthy	GRF	[76]
	KineAssist	CVD	Active gait	—		[77]
				—		[63]
	Where	CVD	Active gait	Healthy	Unloading force	[78]
				Healthy	Unloading force	[79]
				Healthy	Unloading force	[80]
	Mouri's research	Other	Active gait	—	GRF	[81]
	Franz's research	Other	Active gait	Healthy	GRF Unloading force	[82]
				Healthy	GRF unloading force	[83]
	LiteGait	Other	Active gait	—		[84]
	AID-1-M	CVD	Active gait	—		[85]

improved and that this method of rehabilitation was effective in reteaching walking patterns to the CNS [35]. In collaboration with Uhlenbrock, Hesse developed a gait Trainer (Figure 3) with an added mechanism to control leg position, thus reducing the physical effort needed to guide both of the legs and to ensure reproducibility of instructions during rehabilitation. With this machine, the feet of the patient are fixed onto footplates, one of which is fixed to the center of a planet gear on a planetary gear system allowing the footplate to move back and forth. The ratio of stance phase to swing phase is set at 6 : 4 [36]. In order to verify whether this gait Trainer enables similar ambulatory rehabilitation to conventional methods, Hesse et al. compared EMG signals from the legs of a healthy subject and subjects with CVD-induced hemiparesis when walking with the gait Trainer and when walking with therapist assistance, but did not observe any significant difference in either group [37]. In a study by Werner et al. [38] comparing the effects of walking with a gait Trainer and walking with therapist assistance over 6 weeks of rehabilitation on CVD patients, no significant difference was observed between the two methods based on respective FAC scores.

Table 2: Reference about gait rehabilitation device number 2.

Type	Device name	Target	Rehabilitation method	Subject	Evaluation item	Reference
Lifting device with lower limb orthosis	Lokomat	SCI,CVD	Passive gait Active gait	Healthy	EMG of lower limbs	[86]
				Healthy	EMG of lower limbs	[87]
				Healthy	Knee and hip angle	[39]
				Healthy	EMG of lower limbs Knee and hip angle	[88]
				Healthy SCI	Knee and hip angle	[40]
				Healthy SCI	Knee and hip angle	[41]
				Healthy SCI	Knee and hip torque MAS scale	[89]
				Healthy	Hip torque	[42]
				Healthy	MAS scale	[90]
				Healthy SCI	Knee and hip torque Knee and hip angle EMG of lower limbs	[43]
	PAM with POGO	SCI,CVD	Passive gait	Healthy	Pelvic position	[44]
				Healthy	Pelvic position	[46]
				—		[47]
				Healthy CVD	Pelvic position EMG of lower limbs	[48]
				Healthy	Pelvic position	[91]
	Gait Trainer	SCI,CVD	Passive gait	CVD	EMG of lower limbs	[34]
				Healthy	EMG of lower limbs	[36]
				CP	Gait velocity, stride	[35]
				—		[92]
	ARTHuR	SCI,CVD	Passive gait	Healthy	FAC	[38]
				Healthy	Foot trajectory	[45]
				SCI	EMG of lower limbs Foot trajectory	[93]
				—		[55]
	GNU Gait Trainer	SCI,CVD	Passive gait	Healthy	Foot trajectory	[53]
				Healthy	Foot trajectory	[54]
				Healthy	Foot trajectory	[56]
				Healthy	Knee and hip angle	[94]
	HapticWalker	SCI,CVD	Passive gait	Healthy	Foot trajectory	[58]
				—		[59]
	Autoambulator	SCI,CVD	Passive gait	—		[95]
	Airgait	SCI,CVD	Passive gait	Healthy	Knee and hip angle	[96]
Walker	i-walker	Other	Active gait	Elder	Movement trajectory	[26]
	RT-walker	Other	Active gait	—		[27]
	Wang's research	Other	Active gait	—		[28]
	Ishida's research	Other	Active gait	Elder	Muscle power	[29]

Colombo et al. [39] developed a "driven gait orthosis" (DGO) that guides the hip and knee joints using a two-link robot arm to achieve more normal locomotion of these joints during gait rehabilitation. The DGO comprises a BWS system attached to a treadmill, and motorized devices attached from the hip to the foot. The patient is suspended over the treadmill by a harness attached to the BWS system and is assisted in extending and flexing the knee/hip joints by the attached motors. The angle of each joint is measured by joint potentiometers. The length of the upper and lower leg

Figure 3: Gait Trainer.

Figure 4: Lokomat.

segments of the orthosis can be adjusted to suit the length of the patient's thigh and lower leg. Joint angle position of the DGO and speed of the treadmill can be controlled in accordance with the gait pattern objectives designated by the therapist. Jezernik et al. [40] subsequently developed the Lokomat (Figure 4) as the successor to the DGO and created an adaptive control algorithm using an impedance controller, adopting the hip and joint angles of healthy subjects as default reference values as a way of controlling the leg motors. However, leg joint angles differ for each individual, so using hip and knee joint angles of another person as reference values forces the human user to compete with the machine and inhibits spontaneous movement of the user. The reference values provided by Lokomat can therefore be adjusted to reduce the estimated interactive torque of the robotic arms and patient's legs. Locomotion experiments were conducted using healthy subjects, with reference values compared against actual measured values, position control

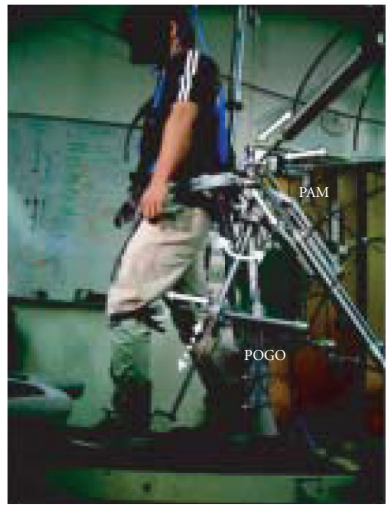

Figure 5: PAM, POGO.

precision was confirmed, and good results were obtained [41]. Interactive torque when using the Lokomat to walk was estimated based on the motor torque produced by automatic movement at each joint using the Lokomat and the torque at each joint produced without using the orthosis. As a result, interactive torque was estimated to increase during the swing phase [42]. Comparison with control based on visual feedback and impedance control indicated the latter method is more effective. A force sensor was attached to the Lokomat and leg maximal muscle strength and leg spasticity evaluation systems were proposed and assessed in patients with neurological disease, and were consequently found to be effective. Four training modes were then integrated with biofeedback and evaluation systems [43]. Ichinose et al. [44] pointed out that the Lokomat and gait Trainer are capable of guiding the legs without restriction, but inhibit the important gait movements of rotating, inclining, and horizontally moving the pelvis and developed the pelvic assist manipulator (PAM) (Figure 5) to address these shortcomings. The PAM comprises a BWS system, a treadmill, and six pneumatic cylinders fixed to a support column positioned behind the patient's pelvis. Force sensors are attached at either end of the pneumatic cylinders, while the ends of the left and right cylinders are attached to the left and right sides of the patient's pelvis. The pneumatic cylinders are used to actuate the pelvis, providing more degrees of freedom (DOF) of pelvic movement and being relatively cheaper per DOF than other actuators. This system can control five DOF, comprising pelvic rotation and obliquity as well as up-down, forward-back, and left-right movements. The PAM controls patient gait by recording the pelvic trajectory of a healthy subject during walking based on the length of the left and right cylinders and then reproducing the trajectory sequence on the patient. Based on an experiment carried out on healthy subjects both with and without the use of the PAM, the precision of pelvic position control with the PAM was found to be good. However, the PAM is unable to guide patient pelvic

Figure 6: LOPES.

movements, so Ichinose et al. developed a new gait training robot known as the Ambulation-assisting Robotic Tool for Human Rehabilitation (ARTHuR) [45], which is capable of guiding pelvic and leg movements. The team also performed pneumatic cylinder modeling and constructed a system that monitors the force generated by the pneumatic cylinders during position control in real time to prevent excessive force from being applied to the patient's body [46]. However, the feed-forward control system that measures and applies the pelvic position of a healthy individual to a patient as reference values sometimes causes considerable force to be applied to the body of the patient, due to differences in individual gait patterns. Such force can result in inhibition of pelvic movement. The researchers therefore came up with a position control method using impedance control to address the need for real-time monitoring of changes in inputs to the patient [47]. Comparing the use and non-use of impedance control in SCI patients revealed that impedance control did not yield a considerable range of pelvic movement. The team also developed the Pneumatically Operated Gait Orthosis (POGO), which guides leg movements using two pneumatic cylinders on each leg, and built a system to integrate this device with the PAM. The first of POGO's pneumatic cylinders is positioned between the pelvis and ankle joint, and the second is set up between the first cylinder and the knee joint [48].

Ekkelenkamp et al. [49] developed the Lower-extremity powered exoSkeleton (LOPES) (Figure 6) to meet the need for ambulatory rehabilitation in various environments so as to acquire practical gait patterns, rather than only in certain external environments such as on a treadmill. LOPES is a gait rehabilitation orthosis with a two-link robot arm applied to the hip and knee joints, with the robot arm attached to a treadmill. A virtual external environment is set up on the treadmill and reaction force applied to the leg is measured based on the angle of leg joints, with the acquired data then used to control the robot arm torque. The LOPES research team validated the responsiveness of torque control and

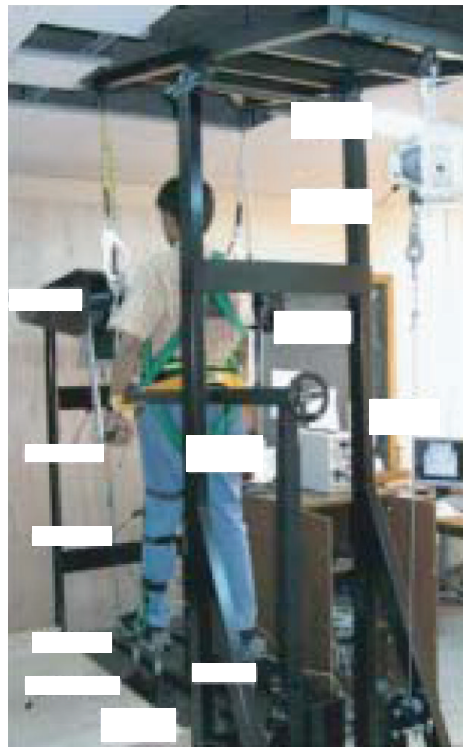

Figure 7: GNU Trainer.

confirmed that the reaction force can be communicated to the subject. There is a risk of considerable force being applied to the patient in simple position control mode, so the team developed an impedance controller using the leg joint angles of a healthy subject during gait as reference values. However, comparison of gait patterns of a healthy subject in terms of leg EMG signals and leg joint angles with and without the use of LOPES did not reveal any significant differences [50]. Comparison of leg joint angles in healthy subjects in multiple virtual external environments revealed that angles varied according to the environment [51]. Gait patterns of healthy subjects were compared in terms of leg EMG signals and joint angles using a treadmill and the LOPES device with the aim of reducing impedance parameters and confirming the impact of the device. As a result, use of the LOPES device was found to increase pelvic inclination and alter leg muscular activity, and these outcomes were attributed to the inertia of the device itself [52]. The GNU Trainer (Figure 7) is a gait rehabilitation orthosis utilizing a BWS system without a treadmill [53, 54]. Gait rehabilitation can be effective when conducted in various environments, so we have developed a gait rehabilitation system for use in virtual external environments. The BWS mechanism comprises wires attached to both shoulders and suspended by a winch via springs. A motorized single-axis pendulum is mounted on the shoulders of the patient to assist with swinging motions of the arms. Footplates control the foot angle and position, while a bilateral base portion is moved backwards and forward by a single motor via a belt. The footplates attached to the base are controlled by two cylinders and one

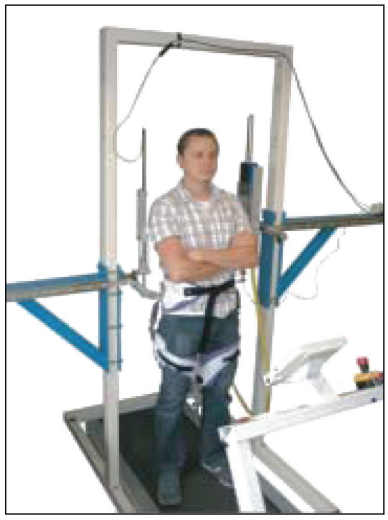

Figure 8: RGR Trainer.

linear slider, with the cylinders mounted to the heel and toe portions to control heel and toe heights, and the linear slider is attached to the plantar portion to control forward and backward movements of the footplates. A device for fixing pelvic position of the patient is secured to the BWS unit and prohibits pelvic movement during gait rehabilitation.

A liquid crystal display (LCD) is set up in front of the patient's line of sight and displays images of virtual external environments during rehabilitation. A basic gait pattern is designated based on the gait data of a healthy subject and the walking speed; step size and maximum plantar angle are set while the arm link cycle; base cycle and cylinder orbit are determined before commencing rehabilitation. A target value is then designated for the virtual external environment and the patient is induced to walk. Following testing on healthy subjects to confirm the setting precision of the walking route according to the virtual external environment, the ability of the orthosis to induce walking was demonstrated. We proposed a footplate mechanism with four DOF based on the notion that a more realistic feedback system could be constructed by controlling not only ankle joint angle and foot position, but also inward and outward ankle joint rotations and metatarsophalangeal (MTP) articulations [55]. Conventional methods have controlled the base portion symmetrically using a single motor, but the gait of CVD patients is asymmetrical, so we proposed a mechanism with independent left and right bases and conducted a locomotion experiment to validate this method [56]. Pietrusinski et al. [57] developed the Robotic Gait Rehabilitation (RGR) Trainer (Figure 8) to guide the pelvic movements of CVD patients during gait rehabilitation. Although pelvic motions of CVD patients are already restricted during walking, the Lokomat orthosis further limits movement of the pelvis. The PAM enables passive mechanical movement of the pelvis, but spontaneous pelvic movement by the patient has proven to be difficult. The RGR Trainer was therefore developed to provide assistance to the patient without inhibiting spontaneous pelvic movements. The system comprises left and right support portions attached to a treadmill. The support portions comprise a load cell, encoder, and cylinder. Pelvic positions of a healthy subject during a gait cycle are used as reference values and force is controlled relative to position error in the vertical direction by feedback of load cell values. Maciej et al. confirmed the frequency response of this system and the fact that the RGR Trainer does not inhibit pelvic movements. After measuring the gait patterns of a healthy subject with and without use of the RGR Trainer, the inventors also established that no significant differences exist in respective pelvic position data.

Figure 9: HapticWalker.

Schmidt et al. [58, 59] developed the HapticWalker (Figure 9) with the aim of providing tactile feedback to patients during gait rehabilitation. Providing feedback on the force exerted on the foot is crucial in gait rehabilitation of CVD patients. Conducting rehabilitation in various environments is also important to acquire a practical gait pattern. Schmidt et al. therefore developed a gait rehabilitation system for use in simulated external environments. The HapticWalker comprises three DOF footplates attached to a BWS system. The footplates control ankle joint flexion and extension, as well as sagittal and vertical foot positions. The patient walks in the simulated external environment wearing a head-mounted display and force exerted on the foot is controlled based on feedback from six DOF force sensors attached to the footplates. Agrawal and Fattah [60] proposed a passive gait rehabilitation system without the use of motive energy, based on the assumption that mechanical gait rehabilitation systems that use motive energy to automatically move the legs may actually inhibit spontaneous movements by the patient. The proposed system targets patients with CVD, Guillain-Barre syndrome, multiple sclerosis, and severe muscle weakness. It comprises a device attached to the pelvic and knee joints and a brace for securing this device. The device is a two-link arm employing a parallelogram linkage mechanism at the knee joint portion, while springs from the upper lumbar and lower thigh regions assist hip joint flexion and extension, in addition to knee joint flexion. Agrawal et al. demonstrated the efficacy of the system after conducting kinematic analysis and estimating assisted hip/knee joint torque. To demonstrate the efficacy of the prototype, the inventors measured the gait patterns of a healthy subject in terms of EMG signals and knee

Figure 10: GBO.

Figure 11: ALEX.

joint angles both with and without use of the device, and subsequently found that hip/knee joint movements were similar, but that muscle activity was reduced when using the prototype. Furthermore, measurement of knee and hip joint angles during gait of stroke patients with and without the prototype device revealed that using the device did not yield considerable ranges of knee/hip joint movement.

Based on those research findings, Agrawal et al. developed a gravity-balancing orthosis (GBO) (Figure 10). Banala et al. measured the changes in hip/knee joint angle torque during gait after altering the rate of leg motion assistance provided by the orthosis using a two-link model [62]. Choon-Young and Ju-Jang [63] developed a mobile gait rehabilitation orthosis with a BWS unit. The orthosis is capable of self-propulsion using two motorized drive wheels at the base portion. The motorized BWS unit is secured to the base. Lee et al. developed an orthosis movement algorithm and designated a reference trajectory, then performed a simulation. Constructing a BWS algorithm and modeling the human body as a spring-mass-damper system, the team also designated a reference BWS force and performed a BWS simulation [78]. Coming up with an optimal controller setting to control the BWS mechanism has proven difficulty in the past, as each subject is different. To overcome this issue, Lee et al. created a learning controller utilizing neural networks. The team successfully performed a BWS experiment on a subject while measuring the BWS force [79]. The BWS mechanism operates at a constant force using a simple control system, allowing the team to develop a mechanism linking a pneumatic cylinder in parallel with a motor. After designating reference BWS values and performing a BWS simulation, the team obtained good results [80]. Banala et al. [65] developed the Active Leg EXoskeleton (ALEX) (Figure 11) using a treadmill and motorized leg orthosis. The body of the patient is supported by a thigh device while linear actuators and load cells are attached to the hip and knee joints. The patient walks while looking at the reference foot trajectory appearing on the display placed in front of them. The display also shows the actual foot trajectory of the patient in real time. The orthosis is controlled by linear actuator force commands to the hip and knee joints, with commands generated by calculating the deviation in actual foot joint position and reference position based on feedback of hip and knee joint angles and gait speed. A healthy subject walked on the ALEX orthosis for 1 h to confirm the learning effects on patients. As a result, Banala et al. confirmed the efficacy of the system based on the error between the reference trajectory before and after the experiment. The efficacy of the ALEX was also confirmed on a stroke patient who underwent 15-day gait rehabilitation on the orthosis based on increases in gait speed and declines in reference trajectory error observed after the experiment [66]. Yoshiyuki et al. [96] developed the "airgait" gait rehabilitation orthosis using the motive power of McKibben pneumatic artificial muscles (PAMs). The actuators are PAMs, and so have the benefits of being lightweight and capable of generating substantial power. The airgate itself comprises a motorized orthosis, counterweight BWS unit, and treadmill. The motorized orthosis is secured to the treadmill by a parallel linkage with gas spring. The PAMs are arranged as antagonistic biarticular and monoarticular muscles modeled on the human musculoskeletal system. After setting the reference knee and hip joint angles and reference pressure levels for PAMs, pressure commands are issued to each of the PAMs based on feedback on the current values of knee and hip joint angles and respective pressure levels of PAMs. Shibata et al. tested the accuracy of the airgait's positional control by conducting a gait session on a healthy subject and comparing reference and actual measured values. The AutoAmbulator [95] is a gait rehabilitation orthosis with a BWS system developed by HealthSouth. This orthosis comprises a BWS system, treadmill, and hip and knee joint devices that are secured to the treadmill. The attached devices guide the legs of the patient according to the reference gait trajectory and speed set by the therapist. Tokioka and Watanabe [73] developed a weight-bearing BWS orthosis named Flora that lifts the user with a crane attached to a steel ceiling with a permanent magnet. The BWS portion employs a constant force spring and motor. The gait mode in Flora is activated by a therapist using the switch controller.

In an experiment using the Flora orthosis on a healthy subject, Tokioka et al. confirmed that raising the BWS lift force of the device increased gait cycle and reduced step size. Frey et al. [72] developed a BWS system called Lokolift using a spring and a motor. Lokolift comprises a lifting wire connected to a harness worn by the patient, a motor that controls the length of the wire, and a motor that controls the wire tension via a spring. Frey et al. tested the precision of the lifting force control from Lokolift by lifting a healthy subject during gait and obtained good results. Gazzani et al. [70] developed the walking assistance and rehabilitation device (WARD) BWS system using a pneumatic cylinder. After conducting a gait experiment on healthy subjects while varying the lifting force in order to demonstrate the effects of lifting force on gait action, Gazzani et al. found that increasing the lifting force reduced gait speed and that lifting the subject at a force equivalent to 70–80% of body weight makes walking difficult. Surdilovic et al. [71] developed a BWS system called STRING-MAN, which attaches multiple wires to the anterior and posterior trunk and controls the zero moment point (ZMP) of the patient. The aim of using this device is to reteach balance during gait by controlling the ZMP. Surdilovic et al. developed an algorithm to control the ZMP via a parallel wire mechanism and performed ZMP control simulation using a kinesiological model, then investigated the number of wires needed and built a prototype. Peshkin et al. [77] developed the KineAssist robotic device for gait and balance training. KineAssist comprises a mechanism to support the pelvis of the patient and a base to secure the mechanism and perform actuation. This device is intended for gait and balance rehabilitation in patients with CVD and cerebellar ataxia and is designed to facilitate therapist guidance of the patient's legs without the use of a leg-guiding robotic arm mechanism, based on the notion that orthoses such as the Lokomat that automate leg guidance fail to incorporate the techniques developed by therapists into rehabilitation. KineAssist allows left-right, forward-backwards, and inclined pelvic movements, as well as transverse rotations and movements. Watanabe et al. [76] developed a BWS system to alleviate leg burden during gait rehabilitation. The system comprises a pelvic support device attached to a treadmill. The device features a load cell to measure weight-bearing load, an encoder to measure transverse pelvic rotation angle, and a motorized mechanism that moves up and down. The system allows left-right, forward-backwards, and inclined movements as well as transverse rotation of the pelvis. The controller operates as follows. Values from the encoder are used to estimate heel-contact and toe-off and reference lift force values are designated accordingly. Device motor speed commands are then generated based on the error between load cell values and the reference lifting force. Fujie et al. tested the precision of lifting force control for the BWS system by lifting a healthy subject during gait. Lee and Sankai [61] developed a powered exoskeleton known as the Hybrid Assistive Limb (HAL) that drives motors positioned at each of the user's joints based on surface EMG signals. HAL is a wearable exoskeleton with motors attached to the hip and knee joints of the user. Electrodes are attached to the anterior and posterior lower and upper thighs to measure EMG signals. The measured signals are converted into absolute values, hip and knee joint torques are estimated, and the estimates are then used to generate torque commands. HAL is researched as a study device of gait pattern for CNS patients. Ikeuchi et al. [74] developed a gait support device that lifts the subject using a crane moving back and forth along an elliptical rail. They researched how to maintain constant leg burden by adjusting the weight-bearing load based on measurements from a floor reaction force gauge built into the walking surface. In an experiment on healthy subjects, a lift control simulation was performed after determining the transfer function from the BWS system to the floor reaction force gauge. While unrelated to gait rehabilitation, we introduce the MIT-MANUS as the motion teaching system for CVD patients. The MIT-MANUS is a therapeutic robotic arm developed by the Massachusetts Institute of Technology (MIT) to provide motion training to CVD patients. MIT-MANUS is a task-oriented device operated using a horizontal robotic training arm. The user manipulates this arm to move a cursor towards a target displayed on a screen. The device is equipped with a visual feedback unit and also features motorized passive actuation capability to allow users who lack sufficient autonomic movement to reach the target. Rehabilitation using the MIT-MANUS enhances proximal arm muscle strength with sustained, long-term effects [97, 98].

6. Summary

Gait rehabilitation devices designed for patients with CNS disorders use actuators and a treadmill to passively move patients with the aim of reteaching gait patterns to the CNS. While research has been conducted on passive actuator mechanisms targeting the pelvis, hip joints and knee joints, no proposals have been made for mechanisms that incorporate the ankle joints. Furthermore, a number of actuator control methods have been suggested. The first is position and impedance control of reference values obtained from the limb movements of a healthy subject. The second is adaptive control whereby the limb movements of a healthy subject are set as default reference values and subsequently adjusted to reduce competing forces between the patient and actuator. The third is model-based control estimating the necessary force using inverse kinematic modeling based on the patient's joints. These control methods should be determined according to the condition of the patient and the intended type of input stimuli and are targeted at patients with CNS disorders. However, no studies on control methods have yet been aimed at subjects with orthopedic disorders such as bone fracture. Given the state of research at present, there is currently a need for mechanical devices that passively actuate the pelvis and hip, knee and ankle joints. There is also a need for actuator control methods that target specific disorders.

Acknowledgments

The authors would like to give special thanks to Yoshifumi Yasuda, Professor in Toyohashi University of Technology's,

Head of Health Science Center, for his guidance and help. Some of our ideas and examples are from Dr. Yasuda.

References

[1] P. Langhorne, G. Taylor, G. Murray et al., "Early supported discharge services for stroke patients: a meta-analysis of individual patients' data," *The Lancet*, vol. 365, no. 9458, pp. 501–506, 2005.

[2] P. Langhorne, L. Widen-Holmqvist, G. Taylor et al., "Early supported discharge after stroke," *Journal of Rehabilitation Medicine*, vol. 39, no. 2, pp. 103–108, 2007.

[3] A. M. Thorsén, L. W. Holmqvist, J. De Pedro-Cuesta, and L. Von Koch, "A randomized controlled trial of early supported discharge and continued rehabilitation at home after stroke: five-year follow-up of patient outcome," *Stroke*, vol. 36, no. 2, pp. 297–302, 2005.

[4] Y. F. Kuo, G. V. Ostir, C. V. Granger, and K. J. Ottenbacher, "Examination of follow-up therapy in patients with stroke," *American Journal of Physical Medicine and Rehabilitation*, vol. 85, no. 3, pp. 192–200, 2006.

[5] T. Graham Brown, "The intrinsic factors in the act of progression in the mammal," *Proceedings of the Royal Society B*, vol. 84, pp. 308–319, 1911.

[6] S. Grillner, "Control of locomotion in bipeds, tetrapods, and fish," *Proceedings of the Royal Society B*, vol. 84, pp. 308–319, 1911.

[7] S. Grillner, T. Deliagina, O. Ekeberg et al., "Neural networks that co-ordinate locomotion and body orientation in lamprey," *Trends in Neurosciences*, vol. 18, no. 6, pp. 270–279, 1995.

[8] A. M. Laursen, P. Dyhre-Poulsen, A. Djorup, and H. Jahnsen, "Programmed pattern of muscular activity in monkeys landing from a leap," *Acta Physiologica Scandinavica*, vol. 102, pp. 492–494, 1978.

[9] B. Bussel, A. Roby-Brami, P. Azouvi, A. Biraben, A. Yakovleff, and J. P. Held, "Myoclonus in a patient with spinal cord transection. Possible involvement of the spinal stepping generator," *Brain*, vol. 111, no. 5, pp. 1235–1245, 1988.

[10] B. Bussel, A. Roby-Brami, O. R. Néris, and A. Yakovleff, "Evidence for a spinal stepping generator in man. Electrophysiological study," *Acta Neurobiologiae Experimentalis*, vol. 56, no. 1, pp. 465–468, 1996.

[11] B. Bussel, A. Roby-Brami, A. Yakovleff, and N. Bennis, "Late flexion reflex in parapletic patients. Evidence for a spinal stepping generator," *Brain Research Bulletin*, vol. 22, no. 4, pp. 53–56, 1989.

[12] B. Calancie, B. Needham-Shropshire, P. Jacobs, K. Willer, G. Zych, and B. A. Green, "Involuntary stepping after chronic spinal cord injury: evidence for a central rhythm generator for locomotion in man," *Brain*, vol. 117, no. 5, pp. 1143–1159, 1994.

[13] V. Dietz, "Human neuronal control of automatic functional movements: interaction between central programs and afferent input," *Physiological Reviews*, vol. 72, no. 1, pp. 33–69, 1992.

[14] D. P. Ferris, K. E. Gordon, J. A. Beres-Jones, and S. J. Harkema, "Muscle activation during unilateral stepping occurs in the nonstepping limb of humans with clinically complete spinal cord injury," *Spinal Cord*, vol. 42, no. 1, pp. 14–23, 2004.

[15] H. Barbeau and S. Rossignol, "Recovery of locomotion after chronic spinalization in the adult cat," *Brain Research*, vol. 412, no. 1, pp. 84–95, 1987.

[16] R. D. De Leon, J. A. Hodgson, R. R. Roy, and V. R. Edgerton, "Locomotor capacity attributable to step training versus spontaneous recovery after spinalization in adult cats," *Journal of Neurophysiology*, vol. 79, no. 3, pp. 1329–1340, 1998.

[17] A. Jaillard, C. D. Martin, K. Garambois, J. François Lebas, and M. Hommel, "Vicarious function within the human primary motor cortex? A longitudinal fMRI stroke study," *Brain*, vol. 128, no. 5, pp. 1122–1138, 2005.

[18] R. J. Nudo, B. M. Wise, F. SiFuentes, and G. W. Milliken, "Neural substrates for the effects of rehabilitative training on motor recovery after ischemic infarct," *Science*, vol. 272, no. 5269, pp. 1791–1794, 1996.

[19] R. J. Nudo, G. W. Milliken, W. M. Jenkins, and M. M. Merzenich, "Use-dependent alterations of movement representations in primary motor cortex of adult squirrel monkeys," *Journal of Neuroscience*, vol. 16, no. 2, pp. 785–807, 1996.

[20] M. Visintin, H. Barbeau, N. Korner-Bitensky, and N. E. Mayo, "A new approach to retrain gait in stroke patients through body weight support and treadmill stimulation," *Stroke*, vol. 29, no. 6, pp. 1122–1128, 1998.

[21] V. Dietz, "Body weight supported gait training: from laboratory to clinical setting," *Brain Research Bulletin*, vol. 78, no. 1, pp. 1–4, 2009.

[22] J. B. Dingwell, J. S. Ulbrecht, J. Boch, M. B. Becker, J. T. O'Gorman, and P. R. Cavanagh, "Neuropathic gait shows only trends towards increased variability of sagittal plane kinematics during treadmill locomotion," *Gait and Posture*, vol. 10, no. 1, pp. 21–29, 1999.

[23] M. D. Lewek, "The influence of body weight support on ankle mechanics during treadmill walking," *Journal of Biomechanics*, vol. 44, no. 1, pp. 128–133, 2011.

[24] M. K. Aaslund and R. Moe-Nilssen, "Treadmill walking with body weight support. Effect of treadmill, harness and body weight support systems," *Gait and Posture*, vol. 28, no. 2, pp. 303–308, 2008.

[25] V. Dietz, R. Müller, and G. Colombo, "Locomotor activity in spinal man: significance of afferent input from joint and load receptors," *Brain*, vol. 125, no. 12, pp. 2626–2634, 2002.

[26] K. Takehito and T. Sosuke, "Walking direction control of the i-walker: the intelligently controllable walker aimed to assist gaits of the elderly people," in *Proceedings of the JSME Symposium on Welfare Engineering*, pp. 522–525, 2010.

[27] A. Hara, Y. Hirata, and K. Kosuge, "Environment-adaptive motion control for passive type intelligent walking support system "RT walker"," in *Proceedings of the International Conference on Intelligent Robots and Systems (IROS '04)*, vol. 4, pp. 3871–3876, The Japan Society of Mechanical Engineers, September-October 2004.

[28] S. Wang, K. Ishida, and M. Fujie, "A new walk training machine for the severe patients," in *Proceedings of the 27th Annual Conference of the Robotics Society of Japan*, pp. 34–35, The Japan Society of Mechanical Engineers, 2009.

[29] K. Ishida, S. Wang, and T. Kishi, "Development of all-way mobile walker," in *Proceedings of the JSME Symposium on Welfare Engineering*, pp. 36–38, 2009.

[30] M. Goldfarb and W. K. Durfee, "Design of a controlled-brake orthosis for FES-aided gait," *IEEE Transactions on Rehabilitation Engineering*, vol. 4, no. 1, pp. 13–24, 1996.

[31] R. Williamson and B. J. Andrews, "Gait event detection for FES using accelerometers and supervised machine learning," *IEEE Transactions on Rehabilitation Engineering*, vol. 8, no. 3, pp. 312–319, 2000.

[32] M. Goldfarb, K. Korkowski, B. Harrold, and W. Durfee, "Preliminary evaluation of a controlled-brake orthosis for

FES-aided gait," *IEEE Transactions on Neural Systems and Rehabilitation Engineering*, vol. 11, no. 3, pp. 241–248, 2003.

[33] M. M. Skelly and H. J. Chizeck, "Real-time gait event detection for paraplegic FES walking," *IEEE Transactions on Neural Systems and Rehabilitation Engineering*, vol. 9, no. 1, pp. 59–68, 2001.

[34] S. Hesse, M. Konrad, and D. Uhlenbrock, "Treadmill walking with partial body weight support versus floor walking in hemiparetic subjects," *Archives of Physical Medicine and Rehabilitation*, vol. 80, no. 4, pp. 421–427, 1999.

[35] M. R. Schindl, C. Forstner, H. Kern, and S. Hesse, "Treadmill training with partial body weight support in nonambulatory patients with cerebral palsy," *Archives of Physical Medicine and Rehabilitation*, vol. 81, no. 3, pp. 301–306, 2000.

[36] S. Hesse and D. Uhlenbrock, "A mechanized gait trainer for restoration of gait," *Journal of Rehabilitation Research and Development*, vol. 37, no. 6, pp. 701–708, 2000.

[37] S. Hesse, "Treadmill training with partial body weight support after stroke: a review," *NeuroRehabilitation*, vol. 23, no. 1, pp. 55–65, 2008.

[38] C. Werner, S. Von Frankenberg, T. Treig, M. Konrad, and S. Hesse, "Treadmill training with partial body weight support and an electromechanical gait trainer for restoration of gait in subacute stroke patients: a randomized crossover study," *Stroke*, vol. 33, no. 12, pp. 2895–2901, 2002.

[39] G. Colombo, M. Joerg, R. Schreier, and V. Dietz, "Treadmill training of paraplegic patients using a robotic orthosis," *Journal of Rehabilitation Research and Development*, vol. 37, no. 6, pp. 693–700, 2000.

[40] S. Jezernik, G. Colombo, and M. Morari, "Automatic gait-pattern adaptation algorithms for rehabilitation with a 4-DOF robotic orthosis," *IEEE Transactions on Robotics and Automation*, vol. 20, no. 3, pp. 574–582, 2004.

[41] R. Riener, L. Lünenburger, S. Jezernik, M. Anderschitz, G. Colombo, and V. Dietz, "Patient-cooperative strategies for robot-aided treadmill training: first experimental results," *IEEE Transactions on Neural Systems and Rehabilitation Engineering*, vol. 13, no. 3, pp. 380–394, 2005.

[42] R. Banz, M. Bolliger, and G. Colombo, "Movement analysis with the driven gait orthosis lokomat," *Gait and Posture*, vol. 24, pp. S215–S216, 2006.

[43] A. Duschau-Wicke, J. Von Zitzewitz, A. Caprez, L. Lünenburger, and R. Riener, "Path control: a method for patient-cooperative robot-aided gait rehabilitation," *IEEE Transactions on Neural Systems and Rehabilitation Engineering*, vol. 18, no. 1, pp. 38–48, 2010.

[44] W. E. Ichinose, D. J. Reinkensmeyer, D. Aoyagi et al., "A robotic device for measuring and controlling pelvic motion during locomotor rehabilitation," in *Proceedings of the 25th Annual International Conference of the IEEE Engineering in Medicine and Biology Society*, vol. 2, pp. 1690–1693, September 2003.

[45] J. L. Emken, J. H. Wynne, S. J. Harkema, and D. J. Reinkensmeyer, "A robotic device for manipulating human stepping," *IEEE Transactions on Robotics*, vol. 22, no. 1, pp. 185–189, 2006.

[46] D. Aoyagi, W. Ichinose, D. J. Reinkensmeyer, and J. E. Bobrow, "Human step rehabilitation using a robot attached to the pelvis," in *Proceedings of the International Mechanical Engineering Congress and Exposition (IMECE '04)*, pp. 443–449, Anaheim, Calif, USA, November 2004.

[47] D. J. Reinkensmeyer, D. Aoyagi, J. L. Emken et al., "Tools for understanding and optimizing robotic gait training," *Journal of Rehabilitation Research and Development*, vol. 43, no. 5, pp. 657–670, 2006.

[48] D. Aoyagi, W. E. Ichinose, S. J. Harkema, D. J. Reinkensmeyer, and J. E. Bobrow, "A robot and control algorithm that can synchronously assist in naturalistic motion during body-weight-supported gait training following neurologic injury," *IEEE Transactions on Neural Systems and Rehabilitation Engineering*, vol. 15, no. 3, pp. 387–400, 2007.

[49] R. Ekkelenkamp, J. Veneman, and H. Van Der Kooij, "Lopes: selective control of gait functions during the gait rehabilitation of CVA patients," in *Proceedings of the 9th International Conference on Rehabilitation Robotics (ICORR '05)*, pp. 361–364, July 2005.

[50] E. H. F. Van Asseldonk, R. Ekkelenkamp, J. F. Veneman, F. C. T. Van Der Helm, and H. Van Der Kooij, "Selective control of a subtask of walking in a robotic gait trainer(LOPES)," in *2007 IEEE 10th International Conference on Rehabilitation Robotics (ICORR '07)*, pp. 841–848, June 2007.

[51] J. F. Veneman, R. Kruidhof, E. E. G. Hekman, R. Ekkelenkamp, E. H. F. Van Asseldonk, and H. Van Der Kooij, "Design and evaluation of the LOPES exoskeleton robot for interactive gait rehabilitation," *IEEE Transactions on Neural Systems and Rehabilitation Engineering*, vol. 15, no. 3, pp. 379–386, 2007.

[52] E. H. F. Van Asseldonk, J. F. Veneman, R. Ekkelenkamp, J. H. Buurke, F. C. T. Van Der Helm, and H. Van Der Kooij, "The effects on kinematics and muscle activity of walking in a robotic gait trainer during zero-force control," *IEEE Transactions on Neural Systems and Rehabilitation Engineering*, vol. 16, no. 4, pp. 360–370, 2008.

[53] B. Novandy, J. Yoon, and Y. Christiand, "A VR navigation of a 6-DOF gait rehabilitation robot with upper and lower limbs connections," in *Proceedings of the 8th IEEE-RAS International Conference on Humanoid Robots*, pp. 592–597, December 2008.

[54] Y. Jungwon, B. Novandy, C. H. Yoon, and K. J. Park, "A 6-DOF gait rehabilitation robot with upper and lower limb connections that allows walking velocity updates on various terrains," *IEEE/ASME Transactions on Mechatronics*, vol. 15, no. 2, Article ID 5424007, pp. 201–215, 2010.

[55] Y. Jungwon and R. Jeha, "A novel reconfigurable ankle/foot rehabilitation robot," in *Proceedings of the IEEE International Conference on Robotics and Automation (ICRA '05)*, pp. 2290–2295, April 2005.

[56] Y. Jungwon, R. Jeha, P. Jangwoo, and B. Novandy, "Walking analysis of a dual-track treadmill using a foot-platform locomotion interface," in *Proceedings of the International Conference on Rehabilitation Robotics (ICORR '09)*, pp. 851–856, June 2009.

[57] M. Pietrusinski, I. Cajigas, M. Goldsmith, P. Bonato, and C. Mavroidis, "Robotically generated force fields for stroke patient pelvic obliquity gait rehabilitation," in *Proceedings of the International Conference on Robotics and Automation (ICRA '10)*, pp. 569–575, May 2010.

[58] H. Schmidt, D. Sorowka, S. Hesse, and R. Bernhardt, "Design of a robotic walking simulator for neurological rehabilitation," in *Proceedings of the IEEE/RSJ International Conference on Intelligent Robots and Systems*, vol. 2, pp. 1487–1492, October 2002.

[59] S. Hesse, R. Bernhardt, and J. Kruger, "Hapticwalker-a novel haptic device for walking simulation," *ACM Transactions on Applied Perception*, vol. 2, no. 2, pp. 166–180, 2005.

[60] S. K. Agrawal and A. Fattah, "Theory and design of an orthotic device for full or partial gravity-balancing of a human leg during motion," *IEEE Transactions on Neural Systems and Rehabilitation Engineering*, vol. 12, no. 2, pp. 157–165, 2004.

[61] S. Lee and Y. Sankai, "Power assist control for walking aid with HAL-3 based on EMG and impedance adjustment around knee joint," in *Proceedings of the International Conference on Intelligent Robots and Systems*, pp. 1499–1504, October 2002.

[62] S. K. Banala, S. K. Agrawal, A. Fattah et al., "Gravity-balancing leg orthosis and its performance evaluation," *IEEE Transactions on Robotics*, vol. 22, no. 6, pp. 1228–1239, 2006.

[63] L. Choon-Young and L. Ju-Jang, "Walking-support robot system for walking rehabilitation: design and control," *Artificial Life and Robotics*, vol. 4, no. 4, pp. 206–211, 2000.

[64] S. K. Agrawal, S. K. Banala, A. Fattah et al., "Assessment of motion of a swing leg and gait rehabilitation with a gravity balancing exoskeleton," *IEEE Transactions on Neural Systems and Rehabilitation Engineering*, vol. 15, no. 3, pp. 410–420, 2007.

[65] S. K. Banala, S. K. Agrawal, and J. P. Scholz, "Active Leg Exoskeleton (ALEX) for gait rehabilitation of motor-impaired patients," in *Proceedings of the 10th International Conference on Rehabilitation Robotics (ICORR '07)*, pp. 401–407, June 2007.

[66] S. K. Banala, S. H. Kim, S. K. Agrawal, and J. P. Scholz, "Robot assisted gait training with active leg exoskeleton (ALEX)," *IEEE Transactions on Neural Systems and Rehabilitation Engineering*, vol. 17, no. 1, pp. 2–8, 2009.

[67] K. Maeda and J. Nango, "Design of walker with assist equipment translating suspected walking motion to rotational motion," in *Proceedings of the JSME Annual Meeting*, vol. 4, pp. 13–14, The Japan Society of Mechanical Engineers, 2007.

[68] J. Nango and R. Kato, "Static analysis of pedaling walker with assist equipment," in *Proceedings of the JSME Annual Meeting*, vol. 4, pp. 203–204, The Japan Society of Mechanical Engineers, 2008.

[69] J. Nango and R. Kato, "Design of walker with planar six-bar mechanisn involving prismatic pair," in *Proceedings of the JSME Annual Meeting*, vol. 4, The Japan Society of Mechanical Engineers, 2009.

[70] F. Gazzani, A. Fadda, M. Torre, and V. Macellari, "Ward: a pneumatic system for body weight relief in gait rehabilitation," *IEEE Transactions on Rehabilitation Engineering*, vol. 8, no. 4, pp. 506–513, 2000.

[71] D. Surdilovic, J. Zhang, and R. Bernhardt, "String-man: wire-robot technology for safe, flexible and human-friendly gait rehabilitation," in *Proceedings of the 10th International Conference on Rehabilitation Robotics (ICORR '07)*, pp. 446–453, June 2007.

[72] M. Frey, G. Colombo, M. Vaglio, R. Bucher, M. Jörg, and R. Riener, "A novel mechatronic body weight support system," *IEEE Transactions on Neural Systems and Rehabilitation Engineering*, vol. 14, no. 3, pp. 311–321, 2006.

[73] S. Tokioka and H. Watanabe, "Development of walk-support-system flora," *Kumagai Technical Research Report*, vol. 63, pp. 87–92, 2005.

[74] H. Ikeuchi, K. Onishi, K. Imado, H. Miyagawa, and Y. Saito, "Discussion about characteristics of sling system in gait training system," *Proceedings of the Symposium on Biological and Physiological Engineering*, vol. 21, pp. 25–28, 2006.

[75] H. Ikeuchi, S. Takiyama, I. Mamoru, and Y. Saito, "Discussion of sling control simulation in feedback type gait training system," in *Proceedings of the International Conference on Rehabilitation Robotics (ICORR '09)*, pp. 360–365, June 2009.

[76] T. Watanabe, E. Ohki, Y. Kobayashi, and M. G. Fujie, "Leg-dependent force control for body weight support by gait cycle estimation from pelvic movement," in *Proceedings of the International Conference on Robotics and Automation (ICRA '10)*, pp. 2235–2240, May 2010.

[77] M. Peshkin, D. A. Brown, J. J. Santos-Munné et al., "KineAssist: a robotic overground gait and balance training device," in *Proceedings of the 9th International Conference on Rehabilitation Robotics (ICORR '05)*, pp. 241–246, July 2005.

[78] L. Choon-Young, S. Kap-Ho, O. Changmok, and L. Ju-Jang, "A system for gait rehabilitation with body weight support: mobile manipulation approach," *International Journal of Human-Friendly Welfare Robotic Systems*, vol. 2, pp. 16–21, 2001.

[79] L. Choon-Young, J. Il-Kwon, L. In ho, K. H. Seo, and J. J. Lee, "Development of rehabilitation robot systems for walking-aid," in *Proceedings of the IEEE International Conference on Robotics and Automation (ICRA '04)*, pp. 2468–2473, May 2004.

[80] S. Kap-Ho and L. Ju-Jang, "The development of two mobile gait rehabilitation systems," *IEEE Transactions on Neural Systems and Rehabilitation Engineering*, vol. 17, no. 2, Article ID 4785182, pp. 156–166, 2009.

[81] K. Mohri, T. Kishi, J. Ueta, and Y. Tsuno, "Omni-directional walking rehabilitation machine with load support mechanism," in *Proceedings of the JSME Symposium on Welfare Engineering*, pp. 32–33, 2009.

[82] J. R. Franz, P. O. Riley, J. Dicharry, P. E. Allaire, and D. C. Kerrigan, "Gait synchronized force modulation during the stance period of one limb achieved by an active partial body weight support system," *Journal of Biomechanics*, vol. 41, no. 15, pp. 3116–3120, 2008.

[83] J. R. Franz, M. Glauser, P. O. Riley et al., "Physiological modulation of gait variables by an active partial body weight support system," *Journal of Biomechanics*, vol. 40, no. 14, pp. 3244–3250, 2007.

[84] http://www.litegait.com/.

[85] http://www.japanem.co.jp.

[86] T. Erni and G. Colombo, "Locomotor training in paraplegic patients: a new approach to assess changes in leg muscle EMG patterns," *Neurobiology Papers*, vol. 109, pp. 135–139, 1998.

[87] M. Pijnappels, B. M. H. Van Wezel, G. Colombo, V. Dietz, and J. Duysens, "Cortical facilitation of cutaneous reflexes in leg muscles during human gait," *Brain Research*, vol. 787, no. 1, pp. 149–153, 1998.

[88] S. Jezernik, G. Colombo, T. Keller, H. Frueh, and M. Morari, "Robotic orthosis lokomat: a rehabilitation and research tool," *Neuromodulation*, vol. 6, no. 2, pp. 108–115, 2003.

[89] L. Lunenburger, G. Colombo, R. Riener, and V. Dietz, "Clinical assessments performed during robotic rehabilitation by the gait training robot lokomat," in *Proceedings of the 9th International Conference Rehabilitation Robotics (ICORR '05)*, pp. 345–348, 2005.

[90] R. Riener, L. Lünenburger, and G. Colombo, "Human-centered robotics applied to gait training and assessment," *Journal of Rehabilitation Research and Development*, vol. 43, no. 5, pp. 679–694, 2006.

[91] D. Aoyagi, W. E. Ichinose, S. J. Harkema, D. J. Reinkensmeyer, and J. E. Bobrow, "An assistive robotic device that can synchronize to the pelvic motion during human gait training," in *Proceedings of the 9th International Conference on Rehabilitation Robotics (ICORR '05)*, pp. 565–568, July 2005.

[92] S. Hesse, H. Schmidt, C. Werner, and A. Bardeleben, "Upper and lower extremity robotic devices for rehabilitation and for studying motor control," *Current Opinion in Neurology*, vol. 16, no. 6, pp. 705–710, 2003.

[93] J. L. Emken, S. J. Harkema, J. A. Beres-Jones, C. K. Ferreira, and D. J. Reinkensmeyer, "Feasibility of manual teach-and-replay and continuous impedance shaping for robotic locomotor training following spinal cord injury," *IEEE Transactions on Biomedical Engineering*, vol. 55, no. 1, pp. 322–334, 2008.

[94] Y. Jungwon, "Auralius manurung kinematic and kinetic patterns during gait training on gnu gaittrainer rehabilitation robot," in *Proceedings of the International Conference on Management of Innovation and Technology (ICMIT '09)*, pp. 380–383, 2009.

[95] http://medgadget.com/.

[96] S. Yoshiyuki, I. Shingo, N. Tatsuya, and Y. Shinichiro, "Development of body weight support gait training system airgait," in *Proceedings of the JSME Symposium on Welfare Engineering*, pp. 540–543, 2010.

[97] N. Hogan and H. I. Krebs, "Interactive robots for neurorehabilitation," *Restorative Neurology and Neuroscience*, vol. 22, no. 3-4, pp. 349–358, 2004.

[98] H. I. Krebs, N. Hogan, M. L. Aisen, and B. T. Volpe, "Robot-aided neurorehabilitation," *IEEE Transactions on Rehabilitation Engineering*, vol. 6, no. 1, pp. 75–87, 1998.

Hindawi Publishing Corporation
Journal of Robotics
Volume 2011, Article ID 167516, 10 pages
doi:10.1155/2011/167516

Research Article

Finger Rehabilitation Support System Using a Multifingered Haptic Interface Controlled by a Surface Electromyogram

Masaaki Hioki,[1] Haruhisa Kawasaki,[1] Hirofumi Sakaeda,[2] Yutaka Nishimoto,[3] and Tetsuya Mouri[1]

[1] *Faculty of Engineering, Gifu University, Yanagido 1-1, Gifu 501-1193, Japan*
[2] *Gifu Red Cross Hospital, 3-36 Iwakuracho, Gifu 502-8511, Japan*
[3] *Gifu University School of Medicine, Yanagido 1-1, Gifu 501-1194, Japan*

Correspondence should be addressed to Masaaki Hioki, o3812204@edu.gifu-u.ac.jp

Received 31 May 2011; Accepted 18 October 2011

Academic Editor: Doyoung Jeon

This paper presents a new type of finger rehabilitation system using a multifingered haptic interface that is controlled by the patient though a surface electromyogram. We have developed the multifingered haptic interface robot: HIRO III that can give 3-directional forces to 5 fingertips. This robot can also be used as a rehabilitation device that can provide various fingertip exercises and measure various types of information. The sEMG works together with the HIRO III to consider the patient's intent. The proposed system is intended for patients having paralysis in the hand and fingers, and the motions will be provided as biofeedback to the fingertips with the device. In contrast to completely passive rehabilitation, the proposed system can provide active rehabilitation using sEMG. The experiment involved finger opening and closing with this system by ten able-bodied subjects. The results show that almost all subjects felt appropriate motion support from the device.

1. Introduction

Hand finger function is very important for daily life, and finger injury can be a very serious problem. These patients need timely and persistent rehabilitation to recover their lost abilities and to resume their normal daily lives. Long rehabilitation training sessions with therapists, who are in relative shortage, are not always available to patients. One solution to this problem could be a robotic rehabilitation system for hand fingers used by individual patients.

Recently, many robotic systems for rehabilitation have been studied. Many aspects of robotic arm rehabilitation therapy [1–3], including clinical tests [4, 5], have been reported. Arm rehabilitation therapy with the aid of a robot [6], which involves bimanual, mirror-image, patient-controlled therapeutic exercises, is one type of self-controlled rehabilitation. Kong and Jeon [7] have developed a tendon-driven exoskeletal power assistive device that uses an sEMG signal and fuzzy control. Saint-Bauzel et al. [8] have presented a reactive robotized interface for lower limb rehabilitation with clinical results.

Hand rehabilitation, however, is particularly difficult, because the hand possesses many degrees of freedom of motion, and the device must be relatively small in size. Connelly et al. [9] have developed a VR hand rehabilitation system with a pneumatic glove, and Oblak et al. [10] have developed a universal haptic device for arm and wrist rehabilitation. In the former, it is slightly difficult for a patient with hand paralysis to wear the glove, and the latter can provide exercise at the shoulder, arm, and wrist only, not the hand or fingers. Compact devices with a cable system to be used after a stroke [11, 12], and exoskeleton-type robotic devices [13, 14] have been presented. The former is a compact device but provides only limited exercises because of the cable actuate. The latter can assist not only with flexion/extension, but also with abduction/adduction and thumb opposition motions but can assist only with joint motion, not 3-directional fingertip motions.

The surface electromyogram (sEMG) records the electrical activity of muscles underlying the skin and is useful for rehabilitation robotic devices. Rehabilitation control strategies for a gait robot [15], upper limb rehabilitation [16], and

a trial of the recovery process for wrist rehabilitation [17] have been reported. However, the application of sEMG to finger rehabilitation has not been widely researched.

In Japan, there are many patients with finger paralysis; for example, carpal tunnel syndrome may lead to finger paralysis, as can long-term dialysis, and the population currently needing dialysis in Japan is approximately 280 thousand. Because hand and finger function is very important for daily life, this paper proposes a new type of finger rehabilitation system for providing more effective rehabilitation. In these cases, the robotic device should be able to provide various exercises including flexion or extension and should be with compact size. A solution to this problem would be a rehabilitation system that could provide 3-directional motions to the fingertips. Usually, it is easier for people to imagine "moving the fingertips" than "moving each finger joint." The proposed system therefore provides a haptic interface for hand finger rehabilitation. A multifingered haptic interface robot [18] has previously been developed, and this device can provide fingertip motion to the operator. In order to achieve more effective rehabilitation for patients, this system utilizes sEMG control. A finger joint angle estimation system from sEMG has been developed [19], and this system will be helpful for complex exercises. In the opinion of one practitioner, this research could result in a challenging clinical trial, and it is of great significance to integrate the sEMG into a rehabilitation robotics system for hand finger. The above system will be effective for patients with peripheral nerve injury of the arm.

As a pretest for the clinical trial, we present herein the experimental results from this system using able-bodied subjects. The purpose of this pretest was to confirm that the fingertips were moved based on a user's intentions in the case of a healthy body.

2. System

Figure 1 shows the outline of the proposed system.

This system uses a haptic device for the fingertips and sEMG information from the patient's forearm or hand. Since this haptic device is so small, it can be used on a desk while the patient is seated. First, this system decides the appreciate fingertips exercises from the sEMG; after that, the device provides exercises at the fingertips. For example, if the sEMG from muscles for finger extension (extensor digitorum muscle) activates and crosses over a certain threshold value, the haptic device exerts 3-axis forces at each fingertip in order to open the fingers. The following sections provide the details of the system.

2.1. Multifingered Haptic Interface HIRO III. Figure 2 shows the multifingered haptic interface robot, the HIRO III, that we have developed [18] (the specifications for the hand part are in Table 1).

This robot consists of a hand part and an arm part. The hand part has 5 haptic fingers, and each haptic finger has 3 joints and 3 degrees of freedom (DOF). The arm part has 6 joints and 6 DOF. Therefore, in total, the HIRO III has 21 DOF. This robot has the following features.

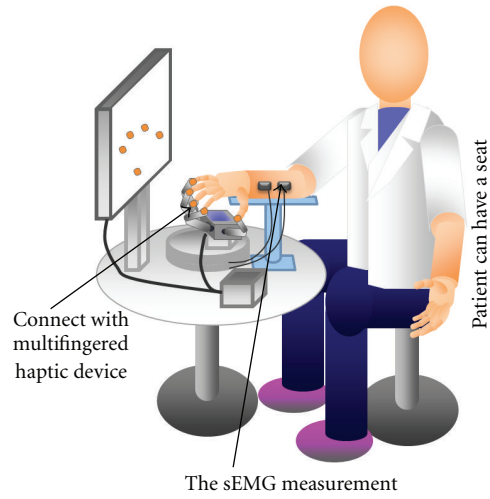

Figure 1: Outline of the system. The patient connects his/her fingertips to the multifingered haptic interface. Because this device is so small, it can be put on table and the patient can be seated during rehabilitation.

Table 1: Specifications of the HIRO III hand.

Component		Quantity
Hand	Number of fingers	5
	Degrees of freedom	15 DOF
	Weight [kg]	0.78
Finger	Degrees of freedom	3 DOF
	Weight [kg]	0.12
	Maximum output force [N]	3.6
	Maximum pulling force between the magnet and the metal ball [N]	4.3
	Volume of workspace [cm^3]	705 (thumb) 587 (other)

(i) The haptic finger has three DC motors in the frames and three active joints (Figures 2(e) and 2(f)). The first joint is for abduction-adduction of the middle phalanx (MP) joint of the haptic finger, and the second and third are for flexion extension of the MP and proximal interphalangeal (PIP) joint, respectively. Additionally, a haptic finger has a 3-axis force sensor at the tip (Figure 2(d)), and each motor has an encoder.

(ii) HIRO III has five haptic fingers and can simultaneously provide 3-directional forces on multiple fingertips.

(iii) Also, the haptic finger has a permanent magnet at the tip (Figure 2(d)). The operator puts up the finger folders at the fingertips, and this folder has a metal ball (Figure 2(c)). The folder and the metal ball together form a passive spherical joint (Figure 2(d)) that can change the posture of a user's finger against the haptic finger.

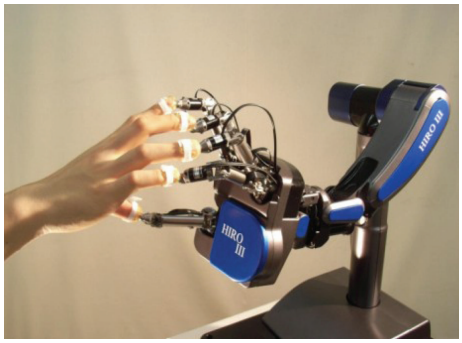

(a) The haptic interface: HIRO III overview with arm

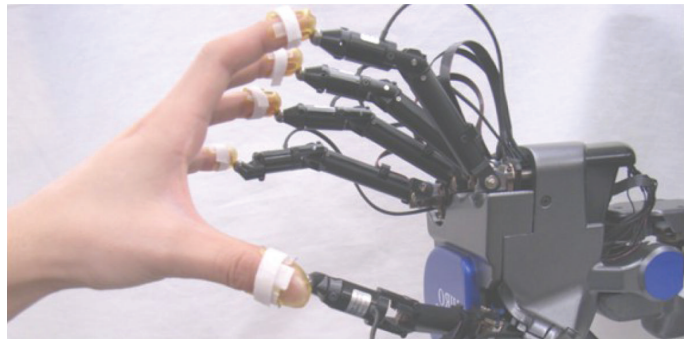

(b) Connect to hand part of HIRO III

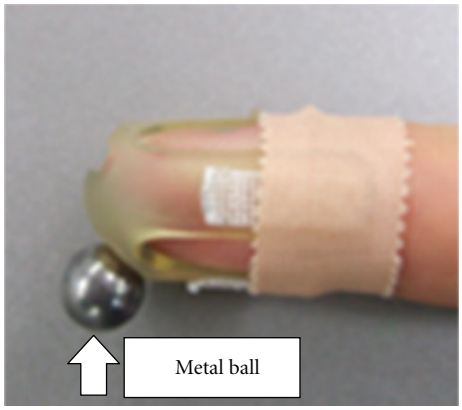

(c) Installation of finger folder at fingertip

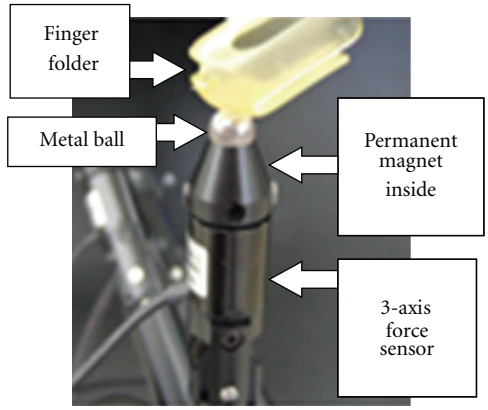

(d) Passive spherical joint at the top of haptic finger

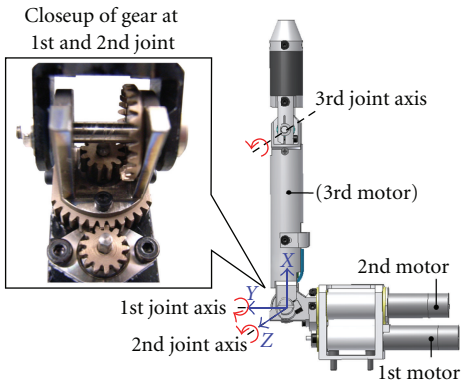

(e) Finger mechanism

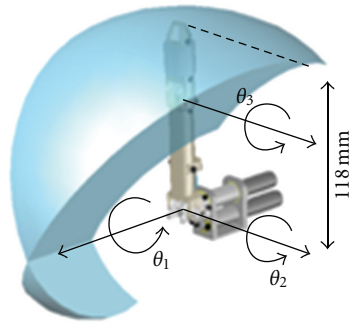

(f) Work space and joint axis of a haptic finger

FIGURE 2: The system of the multifingered haptic interface robot: HIRO III. This robot has five haptic fingers, and the fingers have 3 degree of freedom and a 3-axis force sensor. In (f) the blue volume shows the movable work space of the haptic fingertip.

(iv) The HIRO III system with the arm can realize the large work space. Meanwhile, the hand part can be use as a compact haptic device.

In the case that this device is used as a rehabilitation device, there are some advantages. Ordinary robotics devices for finger rehabilitation are generally an exoskeleton type [13, 14], or a tendon-driven type at the fingertip [11, 12]. The HIRO III has the following advantages over these device types.

(i) Three-directional motion at each fingertip: while a tendon-driven type device can only provide motion directed along the wire to the user's finger, the HIRO III allows for 3-directional motion. That is, various types of finger exercises are possible with the HIRO III. Because this robot has a 3-axis force sensor per finger, the system can limit applying force to user. It can realize safety control strategy. The value of maximum output force of one finger (3.6 N) can be considered as sufficient value from medical aspect for the case of biofeedback interface (described later sections). By comparison, an exoskeleton type [13] is designed in such a way as to apply about 0.3 Nm torque at finger joint.

(ii) Connecting to the device: an exoskeleton-type device must firmly connect the device's link to the user's finger link. In contrast, the user connects to the HIRO III with a finger folder and passive spherical magnet joints, allowing them to connect quickly and easily.

(iii) Compact size: a robot system that supports the motion of finger extension with a tendon-driven or exoskeleton type is generally quite large. While gear transfer mechanism has backlash, this system adopts the force depending control method not position control. In this aspect, this demerit of gear mechanism is not large problem. The HIRO III without the arm is comparatively compact in size and can support desktop rehabilitation.

(iv) Daily rehabilitation: thanks to the ease of connection and rehabilitation on the table, the HIRO III system provides rehabilitation that is easy to keep doing every day. Daily rehabilitation is very important to prevent joint contracture and provide early recovery.

2.2. The Electromyogram for Finger Rehabilitation. The sEMG measures bioelectrical signals from muscles in response to voluntary contractions. These signals provide various type of information about a person's intent. It is therefore hoped that the sEMG will function as a new type of human-machine interface, and it has been studied by many researchers [19, 20].

In the rehabilitation area, sEMG is used as a biofeedback tool. For instance, rehabilitation with sEMG is very efficient in the case of "nerve injury," because it is easy for the patient to identify the muscle that should be focused upon when using sEMG as biofeedback. In rehabilitation applications, the forms of sEMG as biofeedback to the patient are primarily waveforms on display or sound.

As another way of using the sEMG, this signal shows muscle activity and is therefore a barometer of recovery level. In the case of "peripheral" or "central nerve injury," the degree of recovery can be determined by measuring the sEMG over long period.

The control methods for ordinary rehabilitation robotics systems can be divided into the following types: the simple teaching playback type [11], the symmetry master-slave type [12], and the telerehabilitation system [14]. The teaching playback type systems and telerehabilitation systems cannot reflect the patient's intent or thinking. It is a strictly passive rehabilitation, while effective rehabilitation should actually involve patient activity. Systems adopting the symmetry master-slave structure can provide exercises along to user's intent. But this type can be used only in limited injury cases, for example, hemiplegia or one-side paralysis of the brain in which case the patient can move the healthy side of the body. Furthermore, in these systems, patients tend to concentrate on moving only their healthy side, not the paralysis side.

In the present study, the haptic device was controlled by the sEMG. First, the motion intent of the user was extracted from the sEMG, and the fingertip exercises along with the intent were then provided to the user by the HIRO III. This biofeedback is very easy to image for the patient compared with waveforms or sounds. And as opposed to completely passive exercise, the proposed system can give the patient a rehabilitative experience that reflects the patient's intent.

2.3. Medical Aspects of the Proposed System. This section includes the feedback of 2 medical orthopedic doctors. Feedback from practitioners is clearly very important when carrying out research in the medical or rehabilitation area.

The opinions of doctors A and B are as follows.

Doctor B indicated that from a medical perspective, this research will lead to a challenging clinical trial. It is of great significance to integrate the sEMG into the rehabilitation robotics system for hands and fingers. This proposed system will be able to be applied to general cases of hand finger paralysis.

The above system will be effective for patients with "peripheral nerve injury" of the arm (note that this case is also one type of hand finger paralysis). In the forearm, muscles with similar function run parallel to each other. It will be important in this research to analyze the relationship between the sEMG and the muscle and finger function. According to the degree of paralysis or recovery of the patients, the fixation of the upper limb or elbow might be needed.

As pointed out above, the proposed system can be applied to the case of hand finger paralysis. While this condition has many different causes, two cases related to peripheral nervous are described below.

(i) Peripheral nerve injury: the peripheral nervous system resides or extends outside the central nervous system, which consists of the brain and spinal cord. The following three peripheral nerves are related to the fingers and hand: median nerve, ulnar nerve, and radial nerve. Injury of these nerves can be caused by external wounds such as those inflicted with a sharp knife.

(ii) Carpal tunnel syndrome: this case is caused by compressing the peripheral nerve running in the carpal tunnel for some reason. In particular, carpal tunnel syndrome may be caused by dialysis over a long term, and in 2010, the number of patients who need dialysis in Japan is approximately 280 thousand.

In this paper, a case of peripheral nerve injury is considered, as suggested by a medical doctor. In such cases, the patient have undergone surgery. After the operation, recovered neuraxons will reach end organs, again. This is the reinnervation. However, in this process, the neuraxons might reach different organs than those to which they were originally connected. If the neuraxons do reach different organs, the patients will not be able to move their muscles in the same way that they did previously. To solve this problem, rehabilitation for muscle reeducation is needed. During this reeducation period, the patients cannot do the desired motion. As such, a patient's motivation to continue with the rehabilitation will be reduced, and contracture of the joints will begin to occur due to the reduced movement of the muscle.

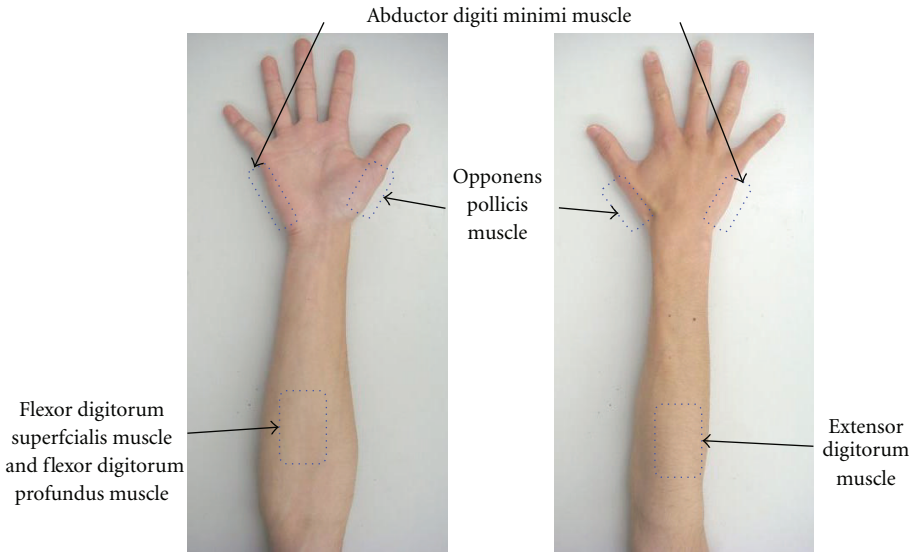

Figure 3: The muscles related to finger motion. The muscle functions are as follows: the flexor digitorum superficialis muscle is for PIP joint flexion of the 2–5th fingers and is innervated by the median nerve. The flexor digitorum profundus muscle is for DIP joint flexion of the 2-5th fingers and is innervated by median nerve. The extensor digitorum muscle is for MP, PIP, and DIP extension of the 2–5th fingers and is innervated by the radial nerve. The above 3 muscles are located at the forearm. The abductor digiti minimi muscle is for abduction of the pinkie and is innervated by the ulnar nerve. The opponens pollicis muscle is for thumb opposition motion and is innervated by the median nerve. These two muscles are in the hand.

Rehabilitation exercises will differ according to the injured nerves or the degree of recovery, so the therapist should determine the appropriate exercise for each case. Examples of the rehabilitation fingertip exercise are shown below, and Figure 3 shows the relationship of the muscle and the work in the forearm and hand.

(i) Median nerve injury: thumb opposability, lunge motion (MP flexion and PIP, DIP extension) of the index or middle finger, and independent flexion of the thumb, index, and middle fingers.

(ii) Ulnar nerve injury: ring finger and pinkie flexion.

(iii) Radial nerve injury: finger extension, curl up (MP extension and PIP, DIP flexion) motion of fingers.

In the case of nerve injury, these exercises are important for muscle reeducation for reinnervation.

2.4. Advantage of the Proposed System. As mentioned above, the proposed system can provide "daily" and "active" rehabilitation.

The former is realized due to the compactness of the HIRO III device, the ease of connecting the device to various sensors (for fingertip forces, fingertip positions, and sEMG signals at certain muscles). Daily rehabilitation is very important to prevent joint contracture and early recovery. Furthermore, recording the above information at every rehabilitation time is efficient for evaluating the degree of recovery over the long term.

Active rehabilitation is then achieved by using the sEMG to make fingertip motions. Because the sEMG is closely related to voluntary motion, it helps to reflect the intent of the patient, allowing the patient to do active rehabilitation without assistance. This system requires a positive intent of the patient for successful rehabilitation and recovery.

2.5. The Control Strategy Outline. The general control strategy for the proposed system will be described in this section, while the details of the experiment will be presented in a later section.

First, the sEMG is helpful for understanding the patient's intent. But raw sEMG data also provide undesired information (e.g., typical biological noise or personal difference, etc.), so signal processing will be needed. As for signal processing of the sEMG, the system adopts an extracting feature value method, determining the mean absolute value (MAV) or root means square (RMS) with segmentation and normalizing [21]. For these processes, it will be useful to use feature values rather than raw sEMG data.

Second, a patient's motion intent should be extracted from the sEMG information. While the relationship between the sEMG and finger motion is quite complex, by focusing on certain finger functions, many methods are available. For example, if MAV from the sEMG around common digital extensor muscle is over a certain threshold, then the intent of the user is "to open the fingers." Of course, this rule must be determined depending on the case of injury or the patient. For almost all cases, this rule or extracting method should be simple. However, if it is necessary or effective to utilize a more complex finger exercise, a system to estimate the finger joint angles [21] will be helpful.

After obtaining the desired fingertip exercise by the above method, the system must transform from the exercise into a continuous fingertip trajectory. The haptic device HIRO III provides fingertip forces depending on the desired fingertip trajectory. For rehabilitation, force control is appropriate rather than position control in that the force can be adjusted. As a simple example, one switches the target positions by the intent. It is necessary to measure these positions beforehand. When the joints of a patient do not have contraction, the target positions can be measured with the help of a therapist or by the patient. When the joints have contraction, the length of the patient's finger link and range of motion are measured, and solving the kinematics with these parameters will identify the target positions. The simplest method to generate the desired fingertip forces is to use the virtual spring model (Figure 4).

This method requires only the target position and the current position. The desired force vector $\mathbf{F}_d$ of one finger is calculated with

$$\mathbf{F}_d = \mathbf{k}(\mathbf{x}_d - \mathbf{x}_c), \tag{1}$$

where $\mathbf{k}$ is the spring coefficient diagonal matrix, $\mathbf{x}_c$ is the current fingertip position of a certain finger, and $\mathbf{x}_d$ shows the target or the desired fingertip position. These motors inside the haptic device have an encoder, and all kinematical parameters are available so the current fingertip positions can be calculated by forward kinematics. Furthermore, in order to adjust the forces to the fingertip, the desired forces should be applied with a low-pass filter (LPF), limiting to the appropriate range.

Finally, the haptic finger of HIRO III will be controlled by the PI control law for fingertip forces [18]. First, the error of torque vector $\boldsymbol{\tau}_e$ is defined as follows:

$$\boldsymbol{\tau}_e = \mathbf{J}^T(\mathbf{F}_d - \mathbf{F}) \in \mathbf{R}^3, \tag{2}$$

where $\mathbf{J}$ is the kinematical Jacobian matrix of a haptic finger, $\mathbf{F}_d$ is the desired fingertip force vector calculated by the virtual spring method, as explained in the previous section, and $\mathbf{F}$ is the measured fingertip force vector from a 3-axis force sensor located at the top of the haptic finger. The HIRO III system adopts the following PI control law:

$$\boldsymbol{\tau} = \mathbf{K}_P\boldsymbol{\tau}_e + \mathbf{K}_I \int \boldsymbol{\tau}_e dt, \tag{3}$$

where $\boldsymbol{\tau}$ is the applied torque vector onto a haptic finger and $\mathbf{K}_P$ and $\mathbf{K}_I$ are the proposed and integral component gain matrix, respectively. The equation shows the PI control law. The gains or parameters are calibrated in advance. Figure 5 shows the entire block diagram of this system.

3. Experiment

As a pretest for the clinical trial, the proposed system was tested with ten able-bodied persons (ten adult males, ages 22–24). In this pretest, the target exercises were to "open the hand" and "pinch with all fingers". These are simple but basic hand functions and important exercises for rehabilitation for peripheral nerve injury (the former is for the radial nerve and the latter for the median and radial nerves). To measure how the sEMG relates to these motions, two terminals will be placed around the common digital extensor muscle and the flexor digitorum profundus muscle, respectively. The subject applies five finger folders to each fingertip and connects with the device. In this experiment, five fingers will be used (Figure 6).

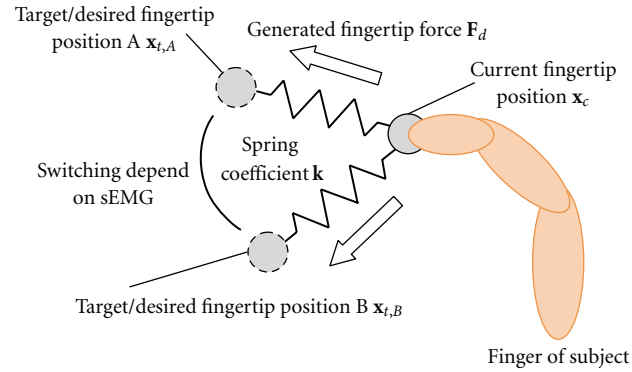

Figure 4: Virtual spring model. This method needs current and target fingertip positions. The current position can be obtained from the haptic device. It is necessary to measure the target positions beforehand or to calculate them with solving kinematics.

The purpose of this pretest was to confirm that fingertips in response to the user's intention extracted from the sEMG by a simple strategy in the case of a healthy body. Note that in the doctor's opinion, the sEMG can be measured from the patient with peripheral nerve injury. To make it easier to concentrate, two sEMG terminal are used and the strategy adopt simple switching method for deciding the exercise mode from the sEMG.

3.1. Acquisition and Signal Processing for the sEMG. Sampling was carried out with a gain of 1000, 1 ms, and 12 bits. In this experiment, the system used 2 sEMG electro nodes, one for the common digital extensor muscle and the other for the flexor digitorum profundus muscle. The raw sEMG data were first filtered with a band pass filter (10–350 Hz) and then segmented (length of segment is 256, and the length of the shift is 32). Finally, MAV of the sEMG was extracted from the segmented sEMG. In the following sections, the "MAV1" refers to the value of MAV extracted from the common digital extensor muscle, and the "MAV2" to that from the flexor digitorum profundus muscle. Similarly, "Thre1" refers to the threshold value for MAV1 and "Thre2" to the threshold value for MAV2. When the MAV value crosses over the corresponding threshold, it can be assumed that the muscle is activated.

3.2. Extracting the Motion Intent. In this pretest, the system selects the following mode as the subject's intention with the if-then rule. This rule will decide the following fingertip exercise mode: the Mode 0 means that the haptic device does not provide any force, and the patient's hand will maintain

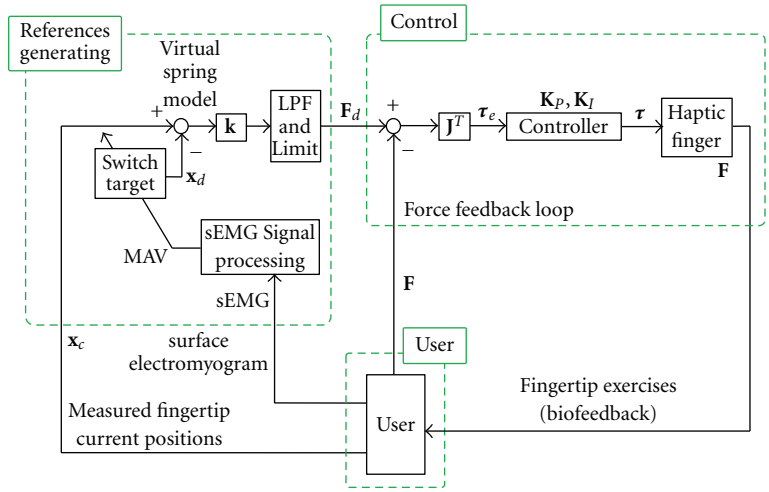

Figure 5: The control block diagram. This system can be divided into three parts: user, robot system including controller, and desired force generator from sEMG and fingertip positions. The details of the robot control method are given in Section 2.5.

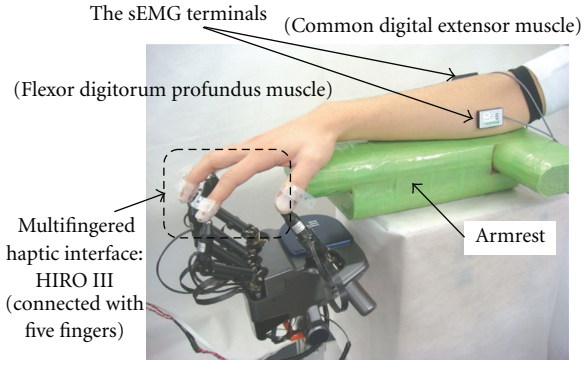

Figure 6: Experimental appearance. The subject can use the armrest for rejecting the effect on the sEMG from certain muscles that relate to wrist movement. Since the proposed system is focused on fingertip movement, in order not to move the wrist, the subject puts the palm on the armrest.

```
if ((MAV1 < Thre1) and (MAV2 < Thre2)) then
    Mode 0; (applying zero forces)
else if (MAV1 >= Thre1) then
    Mode 1; (opening the fingertips)
else then
    Mode 2; (closing the fingertips)
```

Algorithm 1

a relaxed state. In the case of Mode 1, the desired fingertip exercise is opening the hand. Finally, with Mode 2, the desired exercise is pinching or closing all the fingers. The detail of the if-then rule is shown in Algorithm 1.

Note that when MAV1 > Thre1 and MAV2 > Thre2, then the mode is 2. This rule is determined through a trial-and-error process.

3.3. Generating the Fingertip Motion Corresponding to the Intention. As a simple method to determine the fingertip motion, in this pretest, the fingertip position data measured beforehand is selected according to the mode every 32 milliseconds. It is necessary to determine these data (the fingertip positions at the state of "open the hand" and "pinch with all fingers") in advance.

3.4. Generating the Desired Forces Sent to the Haptic Device. The virtual spring model generates the desired forces from the selected target fingertip positions (Figure 4). The spring coefficient k is 150 N/m, the maximum force limit at one axis is 3 N, and the cutoff frequency of the low-pass (first order) filter is 0.2 Hz (Figure 5). These parameters are determined so that the generated forces may not cause rapid change. The cutoff frequency presents system response character, because this experiment targets able-bodied subject, the value is determined as above by try and error. When this system is applied to people has failure at hand, the value should be started from small value. Similarly, spring coefficient and maximum force limit are also must be determined in a careful way. In the case with user who has spasticity of the fingers, the value of spring coefficient and maximum force limit are should be small.

3.5. Experimental Procedure. The experimental procedure included the following steps.

First, the system and the experiment were explained to the subject. After the subject understood the method and purpose, the experiment was carried out.

Secondary, two sEMG terminals were attached to the subject's forearm (common digital extensor muscle and flexor digitorum profundus muscle), and the five fingertips were connected to the HIRO III with a finger folder.

Next, the fingertip positions of the opened and closed hand were measured.

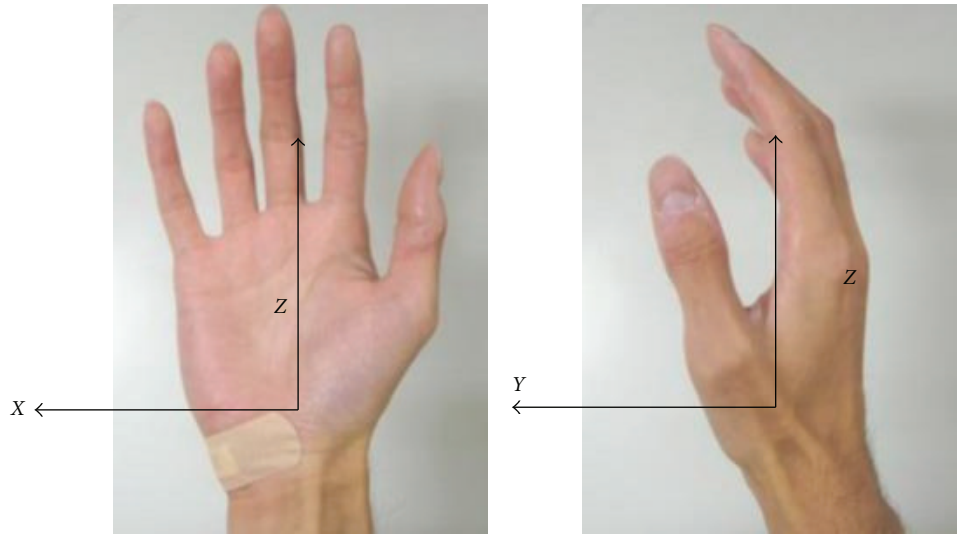

(a) (b)

Figure 7: The system coordinate and origin.

After that, it was necessary to calibrate the two MAV thresholds. These were adjusted so that the subject could switch the exercise mode as subject's thought.

Finally, the experiment and data acquisition were carried out (Figure 6). Subject used the armrest for resting the forearm and wrist and connected each fingertip into the haptic device on the opposite side.

After the experiment, the subject responded to the questionnaire described below.

3.6. Subjective Evaluation. After the experiment, the subject responded to the following questionnaire. The scores corresponding to each question items ranged from 1 to 5. In this questionnaire, 5 corresponds to good/desirable and 1 to bad/undesirable.

(i): "Was the considered movement supported by the device?" Point: 1 (Not at all.)–5 (I think so.)

(ii): "Was the support natural?" Point: 1 (I think it's not natural.)–5 (I think very natural.)

(iii): "Was there anxiety?" Point: 1 (I felt fear.)–5 (I relaxed.)

4. Results and Discussion

Table 2 shows the responses of the subjects to the questionnaire.

Almost all items have high point totals, indicating that the proposed system may be useful as a rehabilitation device. In particular, items (i) and (iii) have very high points. This point is very important for a rehabilitation device controlled by sEMG, and this fact points out that the proposed system may be effective.

Figure 7 shows the system coordinates and the origin, and example graphs of experimental results corresponding to the x axis of thumb and the y axis of the middle finger

Table 2: Questionnaire scores from subjects.

	Subject										Average	Standard deviation
Item	A	B	C	D	E	F	G	H	I	J		
(i)	5	4	3	4	4	5	4	4	4	4	4.1	0.57
(ii)	4	3	4	4	4	4	3	3	3	4	3.6	0.52
(iii)	4	3	5	5	5	4	4	5	4	5	4.4	0.70

are shown in Figure 8. In this graph case, Thre1 is 0.024 and Thre2 is 0.003.

The table and the graph show that the fingertip motions corresponding to the intention of the subject are generated to some extent. However, in the graph that shows mode switching, the switching may have an error at the transition of the mode, for example at approximately 2 or 7 seconds. This type of error sometimes exists at the other subject, and almost all cases are caused at the mode transition from the other mode to mode 0. The reason for this error is thought to be that the sEMG can increase corresponding to the subject's intentions but that it is difficult for the person to quickly decrease the sEMG. Generally, a small amount of time is necessary to decrease the sEMG through oscillations. It is therefore necessary to modify the system so that the operator can switch the mode corresponding to the operator's intent. For example, to improve this error, one solution is to use a hysteresis threshold method, that is, using two threshold values (one is for exceeding and the other for falling below). While this should be considered, this experiment shows that an able-bodied subject can control the exercise mode by sEMG and switch from a relaxed to a motion state.

5. Conclusion and Future Works

This paper proposes a new type of finger rehabilitation system with a multifingered haptic interface controlled by sEMG. The system can therefore provide the patient with

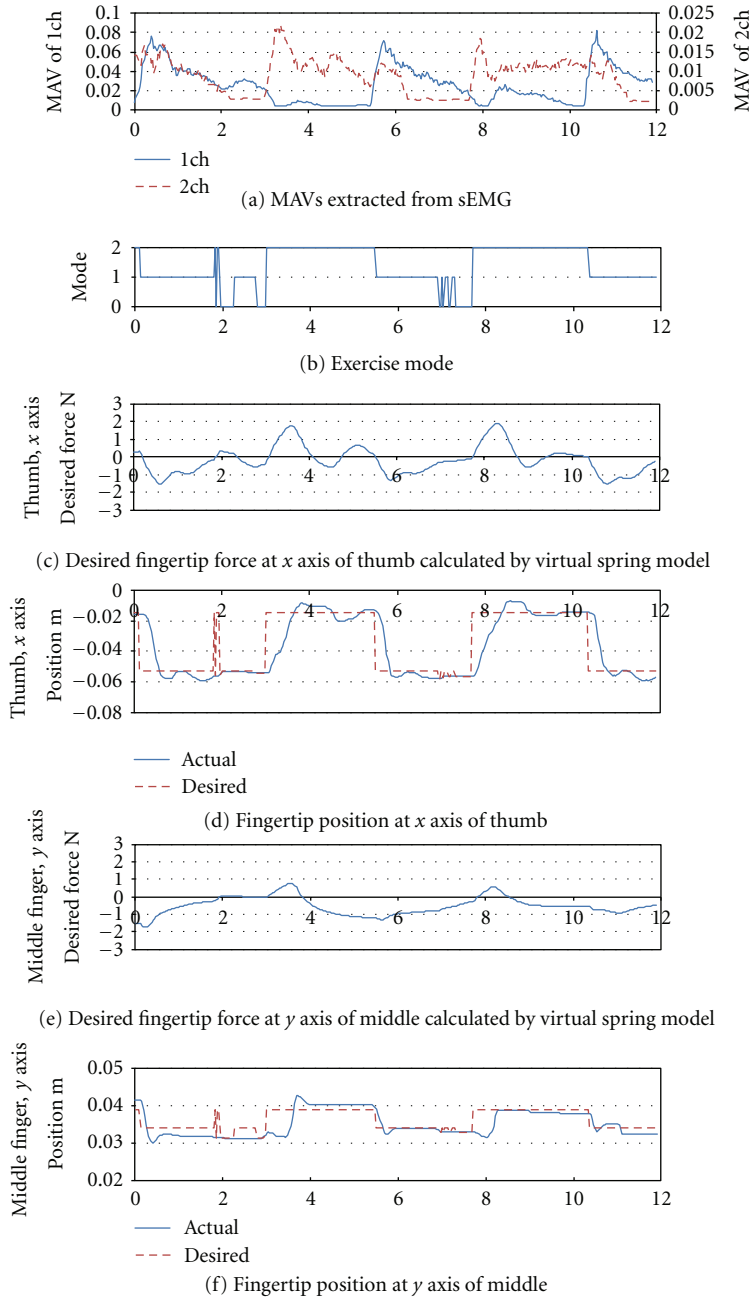

Figure 8: Example of the experiment. The horizontal axis of each subfigure shows the time history. Note that in the subfigure (a) the left side vertical axis shows MAV1 (MAV extracted from 1 ch sEMG) and the right shows MAV2. In this case, Thre1 is 0.024 and Thre2 is 0.003.

effective finger rehabilitation. According to the doctor's opinion, it seems that this research will lead to a challenging clinical trial.

As a pretest for the clinical trial, experimental results obtained with the system for able-bodied subjects are presented. This study targeted two types of movements with two sEMG terminals. Our results show that the system provided 3-directional forces at each fingertip corresponding to the subject's sEMG, and that the subjects felt natural movement support. The results did show that the system had a switching error at the transition of the mode. This problem must be solved so that the patient can switch the mode corresponding to their intent.

In the future, it will be necessary to modify the system so that the system can provide a greater variety of movements. For example, the pinch exercise with thumb and index finger is very important and is also a barometer for recovery. Paralysis related to this motion can be caused by carpal canal syndrome or injury of the medial nerve. Of particular concern is that Japanese use chopsticks in daily life, and this tool requires a pinch motion. Our intent is to carry out a clinical trial with the proposed system.

References

[1] C. Carignan, M. Liszka, and S. Roderick, "Design of an arm exoskeleton with scapula motion for shoulder rehabilitation," in *Proceedings of the 12th International Conference on Advanced Robotics (ICAR '05)*, pp. 524–531, July 2005.

[2] A. Gupta and M. K. O'Malley, "Design of a haptic arm exoskeleton for training and rehabilitation," *IEEE/ASME Transactions on Mechatronics*, vol. 11, no. 3, pp. 280–289, 2006.

[3] D. J. Reinkensmeyer, C. T. Pang, J. A. Nessler, and C. C. Painter, "Web-based telerehabilitation for the upper extremity after stroke," *IEEE Transactions on Neural Systems and Rehabilitation Engineering*, vol. 10, no. 2, pp. 102–108, 2002.

[4] L. E. Kahn, M. L. Zygman, W. Z. Rymer, and D. J. Reinkensmeyer, "Effect of robot-assisted and unassisted exercise on functional reaching in chronic hemiparesis," in *Proceedings of the 23rd Annual International Conference of the IEEE Engineering in Medicine and Biology Society*, pp. 1344–1347, October 2001.

[5] R. M. Mahoney, H. F. M. van der Loos, P. S. Lum, and C. Burgar, "Robotic stroke therapy assistant," *Robotica*, vol. 21, no. 1, pp. 33–44, 2003.

[6] C. G. Burgar, P. S. Lum, P. C. Shor, and H. F. M. van der Loos, "Development of robots for rehabilitation therapy: the Palo Alto VA/Stanford experience," *Journal of Rehabilitation Research and Development*, vol. 37, no. 6, pp. 663–673, 2000.

[7] K. Kong and D. Jeon, "Fuzzy control of a new tendon-driven exoskeletal power assistive device," in *Proceedings of the IEEE/ASME International Conference on Advanced Intelligent Mechatronics (AIM '05)*, pp. 146–151, July 2005.

[8] L. Saint-Bauzel, V. Pasqui, and I. Monteil, "A reactive robotized interface for lower limb rehabilitation: clinical results," *IEEE Transactions on Robotics*, vol. 25, no. 3, pp. 583–592, 2009.

[9] L. Connelly, Y. Jia, M. L. Toro, M. E. Stoykov, R. V. Kenyon, and D. G. Kamper, "A pneumatic glove and immersive virtual reality environment for hand rehabilitative training after stroke," *IEEE Transactions on Neural Systems and Rehabilitation Engineering*, vol. 18, no. 5, pp. 551–559, 2010.

[10] J. Oblak, I. Cikajlo, and Z. Matjačić, "Universal haptic drive: a robot for arm and wrist rehabilitation," *IEEE Transactions on Neural Systems and Rehabilitation Engineering*, vol. 18, no. 3, pp. 293–302, 2010.

[11] L. Dovat, O. Lambercy, R. Gassert et al., "HandCARE: a cable-actuated rehabilitation system to train hand function after stroke," *IEEE Transactions on Neural Systems and Rehabilitation Engineering*, vol. 16, no. 6, pp. 582–591, 2008.

[12] L. Dovat, O. Lambercy, V. Johnson et al., "A cable driven robotic system to train finger function after stroke," in *Proceedings of the 10th IEEE International Conference on Rehabilitation Robotics (ICORR '07)*, pp. 222–227, June 2007.

[13] H. Kawasaki, S. Ito, Y. Ishigure et al., "Development of a hand motion assist robot for rehabilitation therapy by patient self-motion control," in *Proceedings of the 10th IEEE International Conference on Rehabilitation Robotics (ICORR '07)*, pp. 234–240, June 2007.

[14] T. Mouri, H. Kawasaki, T. Aoki, Y. Nishimoto, S. Ito, and S. Ueki, "Telerehabilitation for fingers and wrist using a hand rehabilitation support system and robot hand," in *Proceedings of the 9th International Symposium on Robot Control*, pp. 751–756, September 2009.

[15] P. Wang, A. H. McGregor, A. Tow, H. B. Lim, L. S. Khang, and K. H. Low, "Rehabilitation control strategies for a gait robot via EMG evaluation," in *Proceedings of the IEEE International Conference on Rehabilitation Robotics (ICORR '09)*, pp. 86–91, June 2009.

[16] A. M. Hughes, C. Freeman, J. Burridge, P. Chappell, P. Lewin, and E. Rogers, "Upper limb rehabilitation of stroke participants using electrical stimulation: changes in tracking and EMG timing," in *Proceedings of the IEEE International Conference on Rehabilitation Robotics (ICORR '09)*, pp. 59–65, June 2009.

[17] X. L. Hu, K. Y. Tong, R. Song, X. J. Zheng, and W. W. F. Leung, "A randomized controlled trial on the recovery process of wrist rehabilitation assisted by electromyography (EMG)-driven robot for chronic stroke," in *Proceedings of the IEEE International Conference on Rehabilitation Robotics (ICORR '09)*, pp. 28–33, June 2009.

[18] T. Endo, H. Kawasaki, T. Mouri et al., "Five-fingered haptic interface robot: HIRO III," *IEEE Transactions on Haptics*, vol. 4, no. 1, pp. 14–27, 2011.

[19] M. Hioki and H. Kawasaki, "Estimation of finger joint angles from sEMG using a recurrent neural network with time-delayed input vectors," in *Proceedings of the IEEE International Conference on Rehabilitation Robotics (ICORR '09)*, pp. 289–294, June 2009.

[20] N. Bu, M. Okamoto, and T. Tsuji, "A hybrid motion classification approach for EMG-based human—robot interfaces using bayesian and neural networks," *IEEE Transactions on Robotics*, vol. 25, no. 3, pp. 502–511, 2009.

[21] M. Asghari Oskoei and H. Hu, "Myoelectric control systems—a survey," *Biomedical Signal Processing and Control*, vol. 2, no. 4, pp. 275–294, 2007.

Hindawi Publishing Corporation
Journal of Robotics
Volume 2011, Article ID 543060, 10 pages
doi:10.1155/2011/543060

Research Article

Stroke Rehabilitation in Frail Elderly with the Robotic Training Device ACRE: A Randomized Controlled Trial and Cost-Effectiveness Study

M. Schoone,[1] E. Dusseldorp,[2] M. E. van den Akker-van Marle,[3] A. J. Doornebosch,[4] R. Bal,[5] A. Meems,[4] M. P. Oderwald,[6] and R. van Balen[5,7]

[1] *Department of Sustainable Productivity, TNO, P.O. Box 718, 2130 AS Hoofddorp, The Netherlands*
[2] *Department of Life Style, TNO, P.O. Box 2215, 2301 CE Leiden, The Netherlands*
[3] *Department of Medical Decision Making, Leiden University Medical Centre, P.O. Box 9600, 2300 RC Leiden, The Netherlands*
[4] *Pieter van Foreest-De Bieslandhof, Nursing Home and Rehabilitation Centre, Beukenlaan 2, 2612 VC Delft, The Netherlands*
[5] *Laurens-Antonius Binnenweg, Nursing Home and Rehabilitation Centre, Nieuwe Binnenweg 33, 3014 GC Rotterdam, The Netherlands*
[6] *Department of Technical Sciences, TNO, P.O. Box 155, 2600 AD Delft, The Netherlands*
[7] *Department of Public Health and Primary Care, Leiden University Medical Centre, P.O. Box 9600, 2300 RC Leiden, The Netherlands*

Correspondence should be addressed to M. Schoone, marian.schoone@tno.nl

Received 31 May 2011; Accepted 20 September 2011

Academic Editor: Ludovic Saint-Bauzel

The ACRE (ACtive REhabilitation) robotic device is developed to enhance therapeutic treatment of upper limbs after stroke. The aim of this study is to assess effects and costs of ACRE training for frail elderly patients and to establish if ACRE can be a valuable addition to standard therapy in nursing home rehabilitation. The study was designed as randomized controlled trial, one group receiving therapy as usual and the other receiving additional ACRE training. Changes in motor abilities, stroke impact, quality of life and emotional well-being were assessed. In total, 24 patients were included. In this small number no significant effects of the ACRE training were found. A large number of 136 patients were excluded. Main reasons for exclusion were lack of physiological or cognitive abilities. Further improvement of the ACRE can best be focused on making the system suitable for self-training and development of training software for activities of daily living.

1. Introduction

Stroke is the leading cause of long-term disability in the elderly in Western societies [1–3]. In The Netherlands, each year 41,000 people suffer a stroke for the first time, 19,000 of those are men and 22,000 are women. Twenty to twenty-five percent of these patients die within four weeks. At this moment, about 190,000 people in the Netherlands have suffered one or more strokes [4]. A large part of the patients who survive meet permanent disabilities and participation problems. Main physical consequences of a stroke are one-sided paralyses/paresis of upper and lower limbs, loss of sensibility, (partial) loss of speech or sight, and coordination problems. Also cognitive problems are reported like problems with orientation, attention, memory, concentration, information, and communication, still influencing the quality of life of the patients two years after stroke [5] and often the rest of their lives. No significant differences in the consequences of stroke are known related to age or gender of the patients. Right- and left-sided paralysis however relate to specific co-disorders. Right-handed paralysis relates to left hemisphere functions and may be accompanied by problems like communication, while left-handed paralysis may be accompanied by right hemisphere problems in the area of spatial awareness. Rehabilitation after stroke starts in the first week (acute phase) and ends in the chronic phase. Best practice in the Netherlands, as well as internationally, is the Stroke Service [6]. After a short stay of 7–10 days in the hospital,

60% of the stroke patients return home and, if necessary, receive day treatment in a rehabilitation centre. Around 10% of the patients die in hospital, 5% are discharged to a specialist rehabilitation centre, and 25%, mostly elderly people who are not able to return home, are discharged to a nursing home for a rehabilitation period up to 70 days average. This study focuses on this latter group. At this moment, standard treatment aiming at motor recovery of stroke patients in the nursing home consists of exercises under supervision of a physiotherapist or occupational therapist during their stay. A normal therapy session involves individual treatment by a therapist. It is evidence-based practice that a more intensive therapeutic treatment during the first period after stroke leads to earlier and better recovery [7]. However, economic reasons are limiting the number of therapy sessions of elderly people in a rehabilitation setting of the nursing home to two or three sessions of 30 minutes each week.

The ACRE (ACtive REhabilitation) device is developed to enhance therapeutic treatment of the upper limbs. A manipulator is attached to the user's forearm and provides a large 6 degrees of freedom motion range. In this study, one degree of freedom was limited by the arm/hand support (hand rotation around the forearm axis). The weight of the user's arm is balanced at all positions by an adjustable spring-based gravity compensation mechanism. This allows the user to move the arm through the whole motion range with very low muscle power (Figure 1).

An intrinsically safe impedance controller operates the back-driveable motorized joints to actively support the movements of the user's arm. It feels as a gentle force that helps you to go to the correct position. The level of support is adjustable from 0 to 100%. The system can be reversibly adapted from right- to left-handed use.

The position of the hand is shown on a computer screen in front of the user and is used to do training exercises or play games for rehabilitation purposes. Especially by the use of the games the patients are stimulated to train their affected arm more frequently and repetitively [7, 8]. The device is complementary to traditional arm-hand therapy and designed as an instrument for self-training. Eventually, a future version of the ACRE could even be placed at home for further rehabilitation and activation after stroke. A more detailed description of the current ACRE robot can be found in an article on the early pilot study with the ACRE prototype [8].

The conclusion of a first user pilot study from 2005 was that both the patient and the therapist found the ACRE suitable for rehabilitation after stroke [8].

The aim of the current study is to assess the effects and costs of the assisted use of an active rehabilitation self-training system (i.e., ACRE) for frail elderly stroke patients and to establish whether it can be a valuable addition to standard therapy within a nursing home rehabilitation program. The effect of additional ACRE training to standard therapy during rehabilitation was measured and related to the costs of adding ACRE training, with help of a therapist or in self-training, to standard therapy.

2. Method

2.1. Design. This study was designed as a two-arm pretest posttest randomized controlled trial in the nursing home setting. For this study with frail elderly persons, a review of medical-ethical aspects is mandatory, and permission of the Medical Ethical Trial Committee of the Leiden University was obtained before starting the inclusion of patients.

At the two participating nursing and rehabilitation centres, Pieter van Foreest (location De Bieslandhof) and Laurens (location Antonius Binnenweg), all consecutively admitted patients with main diagnosis stroke were asked to participate after meeting a set of inclusion criteria (see Section 2.2). Thereafter, they were assigned randomly to the ACRE training group or the control group, by drawing a closed envelope containing a participant number with a colour coding, indicating training or control group. The order of the colour coding was determined by a random number sequence generated using the software environment R version 2.12 [9]. To maintain good balance of the total number of patients assigned to each condition, permuted block randomization was used. The size of each block was set at 10. The randomization was stratified by training centre. Before treatment, a baseline measurement (pretest T0) was performed on functioning and emotional well-being. The control group received usual care including individual exercises and group physical therapy. Participants in the ACRE training group received usual care (including individual exercises and group physical therapy) plus 3 additional training sessions with ACRE per week for 6 weeks. The ACRE training varied from 10 to 30 minutes per session and consisted of various exercises chosen by the therapists according to progress and abilities of the patient. After this period of 6 weeks, the measurements were repeated for both ACRE training group and control group (posttest T1).

2.2. Participants. Patients arrived at the nursing and rehabilitation centre after a stay of approximately one week at the hospital. Patients were assessed and selected by the therapists taking into account the following inclusion criteria:

(i) adequate *physiological abilities* to endure the additional ACRE training, that is, being able to sit in a (wheel) chair for 30 minutes;

(ii) adequate *cognitive abilities* to comprehend and accomplish ACRE training, that is, being able to understand and perform a simple task;

(iii) impaired *motor function of upper limb* (right or left) as a result of the recent stroke as perceived by the physiotherapists as basis for the need for therapy;

(iv) no *other illnesses* impairing the ability to comply with ACRE training, such as aphasic disorder, delirium, low vision, pain, and tumor cerebri;

(v) *moment of stroke* less than 60 days prior to moment of inclusion, either first stroke or recurrence with no resulting impairments to the upper limbs from antecedent strokes;

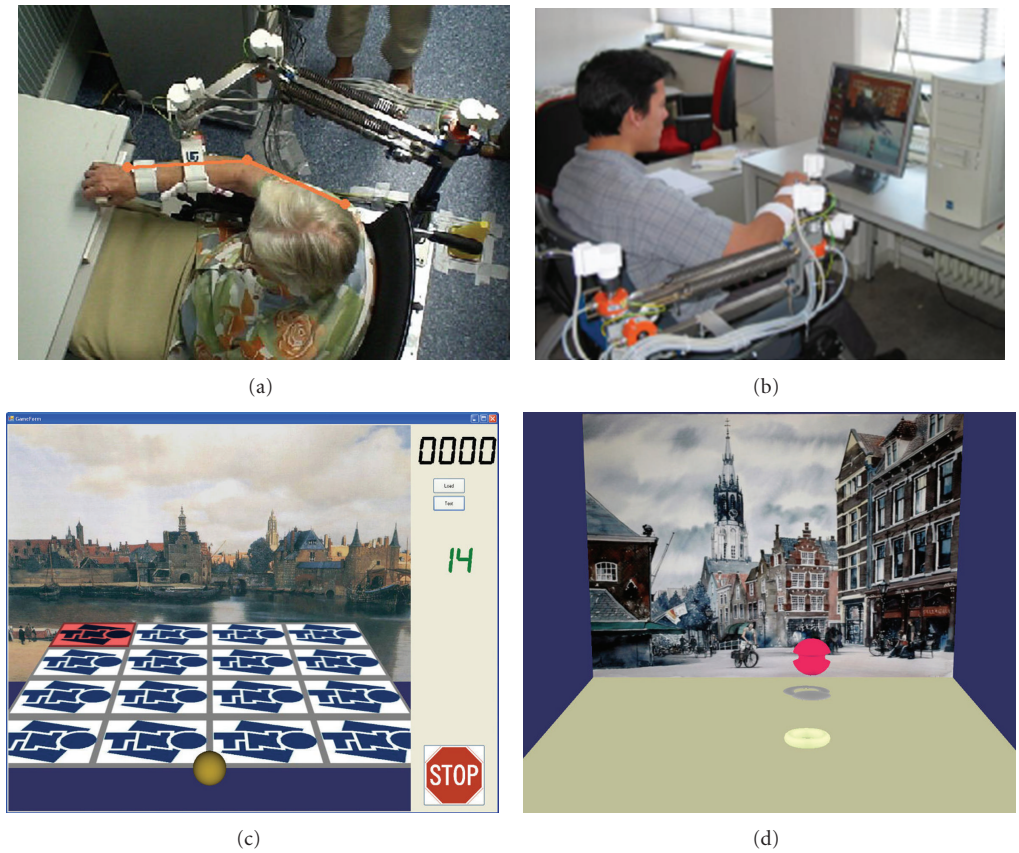

(a) (b)

(c) (d)

Figure 1: (a) The ACRE rehabilitation robot (top view). (b) Impedance controlled actuators help the patient to reach the desired positions. (c) "Go to the red tile" game. The ball represents the patients hand position. (d) "Follow the ball" game allows therapist to create custom movement for training. The red ball must stay close to the (moving) white ring.

A number of 64 patients for both the intervention group (receiving ACRE training) as well as the control group was aimed at, assuming a 6-point difference in the mean change on the Action Research Arm Test (ARAT) total score between the two groups to be clinically relevant. The power calculation was based on a two-sided α of .05, a power (1-β) of .80 and a correlation of 0.60 between the ARAT scores at T0 and T1. Standard deviations were derived from Van der Lee et al. [10].

2.3. Assessments and Outcome Parameters. At inclusion, patient characteristics were registered such as age, gender, preferred hand, and medical history. Primary and secondary outcomes were measured at base-line (T0) and at 6 weeks (T1) for all included patients in the ACRE training group and the control group. These assessments were made by two independent physiotherapists in training who were blind to the intervention.

2.3.1. Outcome Parameters. Primary outcome was motor recovery of the upper limb. Two tests with validated motor assessment instruments were used: The Action Research Arm Test (ARAT) and the Fugl-Meyer assessment for the arm. Although the Fugl-Meyer is widely used, the ARAT is considered to be more change-sensitive and related to functional recovery. The ARAT was used as a primary outcome measure in this study. The ARAT score is used to measure performance of movements and the ability to grasp, move, and release objects of different size, weight, and shape and will serve as a primary outcome measure in this study. The test consists of 19 items, rated on a 4-point ordinal scale (0 to 3). The ARAT has been shown to be valid, reliable, and responsive [11]. The ARAT-19 total score was computed as a sum score of the 19 items (range 0–57, 0 for no motor function and 57 for normal motor function). The minimal clinical importance difference is set at about 10% of the range of the total score, that is, 6 points [11]. In addition, an ARAT-15 total score was computed as a sum score of the 15 items recommended by Van der Lee et al. [12]. The Fugl-Meyer score for the upper extremities is a reliable and validated test of motor function in stroke patients [13]. This scale is a disease-specific objective impairment index designed specifically as an evaluative measure for assessment of recovery in the post stroke hemiplegic patient. The abilities (33 in total) are scored 0 for low, 1 for medium, and 2 for high. For upper limb functions, a maximum of 66 points can be reached, which means optimal function or no impairment. In the field of stroke rehabilitation, the Fugl-Meyer assessment is considered to be one of the most comprehensive quantitative

measures of motor function following stroke, and its use has been recommended for clinical trials of stroke rehabilitation [14]. This test is widely used in intervention studies.

A set of secondary outcomes were measured to add insight into the patients' functionality both senso-motoric as well as psychological and social. To assess health-related quality of life, the generally applicable EuroQol-5 Dimensions (EQ-5D) was used [15], from which we calculated utilities using the Dutch tariff as assessed by Lamers et al. [16]. The utilities range from −.33 (worse than death) to 1 (completely healthy). We expected the quality of life to improve and the recovery to be faster, if patients have an active role in their recovery. The functionality of the paretic arm, as perceived by the patient, was scored with the Stroke Impact Scale version 3 in Dutch [17]. The Stroke Impact Scale consists of 8 subscales, and a Visual Analogue Scale measuring general recovery from stroke. A difference of 10% of the range is considered clinically relevant [17]. Disease specific aspects of emotional well-being, for example, depression, for patients with stroke were measured using the questionnaire Geriatric Depression Scale for mental state [18]. The assessment of the secondary outcomes was done per interview because most of the patients were not able to complete these questionnaires autonomously.

For the excluded patients age, gender and Barthel Index were registered at T0.

2.4. Analyses. In initial analyses, baseline characteristics were checked on significant differences by means of independent t-test. These t-test tells us if the two treatment groups (with or without ACRE) are comparable with respect to motor function, quality of life, daily functioning, depression and demographic variables, such as age, gender, and stroke characteristics before the start of the treatment. Also, the normality of the distribution of the outcome measures was checked.

Because of missing data at the posttest (T1), we performed multiple imputation with the method Multivariate Imputation via Chained Equations (MICE) [19, 20] to obtain 10 complete data sets. Several imputation models were used, because of the strong correlations between the functional measures (i.e., 0.86 between ARAT-19 and Fugl-Meyer total score); each imputation model included a functional measure and a quality of life measure (measured at both time points) and all background variables. The (cost-) effectiveness analyses were performed for these 10 sets, and the pooled results are reported.

To assess the short-term effectiveness of the ACRE treatment, an independent t-test was performed using as outcome variable the change scores on the ARAT from T0 to T1. The t-test indicates whether the mean change in the intervention group is significantly different from that of the control group. This type of analysis was repeated for the other outcome measures.

In the economic evaluation the cost of the additional effects of the ACRE on quality of life compared to standard treatment was assessed. In a cost utility analysis differences in costs at T1 were compared to differences in QALY (quality-adjusted life year) gain during the six week follow-up period. The cost analysis was performed from the perspective of the rehabilitation centre, therefore in this cost analysis only costs incurred by the rehabilitation centre are included. Costs were converted into 2011 price levels using the general Dutch consumer price index [21]. The costs included are the costs of activities aiming at the motor recovery. These are sessions with physiotherapists and occupational therapists, costs of volunteers taking patients to therapy sessions and the costs of ACRE. The costs of the ACRE consist of both the expected purchase price and the operating costs of the ACRE. Cost information was gathered during the six-week period of training. Information on the activities of the physiotherapists, occupational therapists, and volunteers was obtained from the patient logbook kept by the caregivers. Time spent by physiotherapists, occupational therapists, and volunteers was translated into costs by using standard costs [22]. Costs of ACRE were estimated at €30.000. Using a deprivation period of 10 years at 4.3% interest, 6.4% overhead costs and yearly cost of maintenance of 8.0% of the initial costs [22] result in yearly costs of €6394 for the ACRE. Assuming a yearly number of 2.000 ACRE sessions, results in a cost per ACRE session of €3.20. Depending on the willingness to pay for obtained effectiveness, a strategy is cost-effective compared with an alternative strategy if it has a better average net benefit (willingness to pay $*$ QALYs − costs). Given the statistical uncertainty of differences between costs and QALYs, cost-effectiveness acceptability curves graph the probability that a strategy is cost effective, as a function of willingness to pay. Group differences in QALY and costs were statistically analysed using standard t-tests for unequal variance.

In all analyses, a two-sided α of .05 was used as significance level. The analyses were performed using SPSS (version 17), R (version 2.12), and STATA (version 9.2).

3. Results

3.1. Participants. During the inclusion period of one year, a total of 24 persons were included and 136 exclusions were registered from the inflow of stroke patients. The 24 patients all gave their informed consent and complied with the baseline (T0) assessments. Six persons did not complete the training period of 6 weeks because of early leave of the nursing home or relapse and were not assessed at T1. They did not differ significantly from the patients who did not drop out on the background characteristics.

The baseline measurements showed no significant differences in patient characteristics between the ACRE training group and the control group (Table 1).

3.1.1. Characteristics of Exclusions. The total of 136 excluded patients consisted of 67 men and 66 women (gender of 3 patients unknown). The excluded patients varied in age from 35 to 98 years, with an average of 71.3 (age of 17 patients unknown). The Barthel Index of the excluded patients varied from 0 to 20 (Barthel Index of 19 patients unknown). Between the group of participants and the group of exclusions, no significant differences on age and gender

Table 1: Patient characteristics at baseline.

Variable	ACRE training group		Control group	
	n	mean (SD) or %	*n*	mean (SD) or %
Demographics				
Age (years)	10	73.4 (8.0)	14	76.5 (8.3)
Sex (female (%))	10	30.0	14	35.7
Right handed (%)	10	80.0	14	100.0
Barthel Index[a]	9	8.7 (4.4)	13	8.9 (6.0)
Characteristics of the stroke				
First stroke (%)	10	70.0	14	78.6
Ischemic cerebral vascular accident(%)	10	100.0	14	92.9
Consequences of the stroke				
Affected part of the brain	10		14	
Right hemisphere (%)		70.0		64.3
Left hemisphere (%)		30.0		35.7
Stroke-affected dominant arm (%)	10	30.0	14	35.7
Legs affected	10		14	
Left leg affected (%)		70.0		57.1
Right leg affected (%)		30.0		35.7
Legs not affected (%)		0.0		7.1
Swallow disorder (%)	10	30.0	14	64.3
Phatic disorder (%)	10	20.0	14	35.7
Neglect (%)	10	20.0	14	7.1
Apraxia (%)	10	0.0	14	28.6
Planning (%)	10	30.0	14	28.6
Attention (%)	10	30.0	14	21.4
Other neurological disorder (%)	10	57.2	14	50.0
Motor function[b]				
ARAT total score 19 items [0–57]	10	31.2 (27.0)	14	15.9 (14.6)
ARAT total score 15 items [0–45]	10	25.3 (21.6)	14	14.9 (13.3)
Fugl-Meyer total score [0–66]	10	40.7 (21.4)	14	37.2 (19.4)
Stroke impact score (SIS)[b]				
Strength [4–20]	9	11.0 (3.5)	13	11.5 (2.8)
Memory and thinking [7–35]	9	29.9 (6.7)	13	28.7 (3.4)
Emotion [9–45]	9	37.5 (5.5)	13	35.8 (5.8)
Communication [7–35]	9	32.7 (4.5)	13	31.1 (4.6)
Daily Activities (ADL) [10–50]	9	28.7 (7.2)	13	27.4 (8.3)
Mobility [9–45]	9	17.1 (4.1)	13	23.2 (10.2)
Hand function [5–45]	9	8.3 (2.9)	13	7.5 (3.5)
Participation [8–40]	9	32.2 (6.2)	13	28.4 (7.5)
Stoke recovery [0–100]	9	48.3 (26.5)	13	43.4 (27.7)
Quality of Life[b]				
EQ-5D [−0.33–1]	9	0.57 (0.25)	13	0.67 (0.19)
General health status [0–100]	9	59.6 (29.9)	13	61.9 (20.5)
Depression[b]				
Geriatric Depression Scale total score [0–15]	8	3.8 (2.6)	13	3.3 (2.5)

Note. None of the differences between groups were statistically significant ($P < 0.05$).
[a]Barthel Index is a standard assessment of the impact of an impairment on daily functioning (ADL).
[b]These assessments were part of the measurements of the effect study. Range is given between square brackets: [].

Table 2: Patient characteristics at baseline for included and excluded patients.

Variable	Participants (ACRE and control group)		Exclusions	
	n[b]	mean (SD) or %	n[c]	mean (SD) or %
Age (years)	24	75.2 (8.2)	119	71.3 (14.2)
Sex (female (%))	24	33.3	133	49.6
Barthel Index[a]	21	9.2 (5.0)	77	9.4 (6.7)

[a]Zero values were excluded.
[b]Total 24 participants, lower numbers for variable indicate missing values.
[c]Total 136 exclusions, lower numbers for variables indicate missing values.

were found (Table 2). Also no significant differences in mean Barthel Index were found, when zero values were excluded (Table 2). However, 39 (34%) of the excluded patients had a Barthel Index of zero, whereas 1 (5%) of the participants ($P < 0.01$), implying that all but one of the most impaired patients were excluded.

Because of the large number of exclusions a qualitative analyses was made of the reasons for exclusion (Table 3). The reasons for exclusion were categorized into six groups:

(i) insufficient *physiological abilities*: low endurance, fatigue, condition problems, and balance problems;

(ii) insufficient *cognitive abilities*: low cognition, insufficient learning abilities, insufficient understanding, dementia, and neuropsychological impairments;

(iii) no *impaired functioning* to upper limbs: no arm/hand problems, that is, no rehabilitation for upper limbs needed;

(iv) *speech/communication problems*: aphasiac disorder, language barrier;

(v) *other illnesses* or medical reasons: fall incident, low vision, delirium, away for dialyses, bedridden, non stroke, subarachnoid haemorrhage, subdural hematoma, pain, subcomatose, tumor cerebri, deceased, and lower arm amputation;

(vi) *other reasons*: refused therapy, social problems, non cooperation, stroke over 60 days ago, and short stay only.

3.2. Effects. With regard to the motor recovery of the upper limb, our results were more favourable for the control group compared to the ACRE group. In the ACRE group an average decline in ARAT scores was found from T0 to T1, whereas an increase was found for the control group (Table 4). The same pattern was found for the Fugl Meyer and for the Stroke Impact Subscale Hand function. However, the differences in change scores between the groups were not statistically significant, due to the small sample size. Also, due the small sample size, the amount of uncertainty about the size of the effect was very large (see the confidence intervals given in the last column of Table 4). With regard to general health-related quality of life, our results were more favourable for the ACRE group compared to the control group. According to the EQ-5D, the improvement in quality of life from T0 to T1 in the ACRE group was larger than in the control group. Both groups showed an average decline on the general health status scale, but this decline was less in the ACRE group than in the control group. Again, the differences in change scores between groups were not significant, and the confidence intervals were large (Table 4).

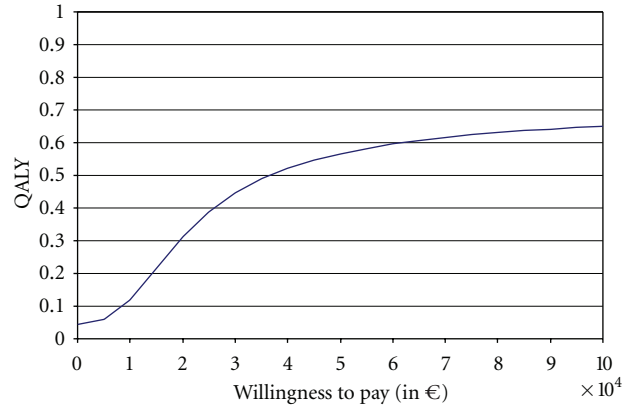

Figure 2: Cost-effectiveness acceptability curves for ACRE group in comparison with control group.

3.3. Economic Evaluation

3.3.1. QALYs. According to the EQ-5D, an increase of 0.006 QALY (2.2 days) per patient in the ACRE group compared to the control group was found in the first six weeks after randomization. This difference between the groups was not significant ($P = 0.56$).

3.3.2. Costs. The average costs per patient in the intervention group were €220 (95% confidence interval €−33 to €474) higher than the average costs in the control group. This is mainly due to the costs of the additional ACRE training consisting of therapist cost and cost of the ACRE (Table 5).

3.3.3. Cost Utility Analysis. The combination of higher costs and more favourable QALY outcomes in the intervention group result in probability that the intervention is cost effective compared to the control group dependent of the willingness to pay (Figure 2). For values of the willingness to pay up to €40.0000 per QALY, the current Dutch threshold, usual care is preferred. For a willingness to pay higher than €40.000 per QALY, the intervention is preferred.

4. Discussion

4.1. Participants. Inclusion of participants from the target group of frail elderly turned out to be far more difficult than we expected. With an inclusion rate of 15% average the inclusion during one year only leveled approximately 20% of the number needed for statistical power of the results.

Analysis of the reasons for exclusion showed a wide variety of reasons for noncompliance, multiple reasons apparent

Table 3: Reasons for exclusion (♂/♀/total).

Location	Physical reasons			Cognitive reasons			No arm/hand problems			Communication problems			Other medical reasons			Other reasons		
	♂	♀	total	♂	♀	total	♂	♀	total	♂	♀	total	♂	♀	total	♂	♀	total
(1)	9	11	20	5	5	10	4	3	8	1	3	4	3	6	9	1	2	3
(2)	17	13	31	12	11	24	15	16	31	7	0	7	13	10	23	15	12	29
Total	26	24	51	17	16	34	19	19	39	8	3	11	16	16	32	16	14	32

Table 4: Means at baseline (T0) and posttest (T1) and change scores (T1-T0) for Motor function (ARAT/Fugl Meyer), Stroke Impact Scale, Quality of Life (EQ-5D), and Geriatric Depression Scale; results of independent t-test (change score was used as dependent variable) and the differences between the groups on the change scores.

Variable	Mean (SD)[1]				Change score (SD)[1]		Difference between groups[2] [95% CI]
	Acre group ($n = 10$)		Control group ($n = 14$)		Acre group ($n = 10$)	Control group ($n = 14$)	
	T0	T1	T0	T1			
ARAT-19	31.2 (27.0)	27.3 (24.9)	15.9 (14.6)	24.4 (20.7)	−4.0 (13.5)	8.4 (13.9)	−12.4 [−25.5, 0.8]
ARAT-15	25.3 (21.6)	24.8 (20.1)	14.9 (13.3)	22.8 (17.6)	−0.5 (8.4)	7.8 (9.8)	−8.3 [−17.6, 1.1]
Fugl-Meyer total score	40.7 (21.4)	36.8 (19.7)	37.2 (19.4)	39.1 (15.5)	−3.9 (13.1)	1.9 (18.1)	−5.8 [−20.3, 8.6]
Stroke impact Scale strength	10.8 (3.4)	12.4 (1.8)	11.4 (2.9)	13.1 (3.0)	1.6 (3.9)	1.7 (2.9)	−0.1 [−3.1, 2.9]
Stroke Impact Scale Memory/thinking	29.9 (6.4)	30.4 (3.2)	28.7 (3.4)	30.5 (2.7)	0.4 (6.7)	1.7 (3.7)	−1.3 [−5.9, 3.4]
Stroke impact Scale emotion	36.8 (5.6)	35.4 (3.9)	35.5 (5.8)	35.9 (5.4)	−1.5 (6.0)	0.4 (6.2)	−1.9 [−7.3, 3.5]
Stroke Impact Scale Communication	32.7 (4.3)	32.5 (4.2)	31.2 (4.4)	32.1 (3.9)	−0.2 (1.4)	0.9 (2.7)	−1.1 [−3.2, 1.0]
Stroke Impact Scale daily activities	28.2 (7.1)	28.4 (7.5)	27.2 (8.1)	31.4 (8.5)	0.2 (6.5)	4.3 (7.9)	−4.1 [−11.8, 3.6]
Stroke Impact Scale mobility	17.3 (3.9)	27.5 (9.6)	22.9 (9.9)	30.1 (10.0)	10.1 (7.1)	7.3 (7.5)	2.8 [−4.3, 10.0]
Stroke Impact Scale hand function	8.1 (2.9)	7.9 (4.0)	7.4 (3.5)	9.4 (5.8)	−0.2 (5.0)	2.0 (3.8)	−2.2 [−6.1, 1.8]
Stroke Impact Scale participation	32.4 (6.0)	27.3 (5.2)	28.7 (7.4)	30.8 (7.3)	−5.2 (8.7)	2.2 (11.7)	−7.3 [−16.6, 2.0]
Stroke Impact Scale stroke recovery	48.2 (25.0)	50.7 (18.2)	43.9 (26.7)	58.0 (22.7)	2.5 (22.9)	14.1 (18.2)	−11.7 [−29.7, 6.3]
EQ5-D-utilities	0.55 (0.26)	0.66 (0.16)	0.66 (0.20)	0.66 (0.25)	0.11 (0.32)	0.00 (0.30)	0.11 [−0.22, 0.44]
General health status	60.8 (29.5)	57.5 (20.4)	61.6 (20.9)	53.5 (21.4)	−3.3 (27.5)	−8.1 (30.2)	4.8 [−26.5, 36.2]
Geriatric Depression Scale Total score	3.5 (2.7)	4.7 (3.7)	3.4 (2.6)	5.1 (3.5)	1.2 (4.4)	1.7 (3.4)	−0.5 [−4.6, 3.6]

[1] Mean values are given of the statistic computed for the 10 imputed datasets.
[2] Pooled results are given of independent t-test for the 10 imputed datasets; CI: Confidence Interval.
None of the differences between the groups were significant (two-sided $P < 0.05$).

in half of the cases, the most important being insufficient physiological or cognitive abilities. Apparently, a large part of the patients who come to a nursing home, after their first week in hospital following the stroke, are not able to sit up for 30 minutes at a time or are not able to understand and perform a simple task. Also in almost a fourth part of the cases the stroke had not affected the upper limbs in such a way that arm-hand therapy was necessary. The most significant difference between the included and excluded patients was a 2-point lower Barthel Index, indicating a

Table 5: Mean cost per patient in the ACRE and control group in the first six weeks after randomization.

Cost item	ACRE group $N = 10$ Costs (€)	Control group $N = 14$ Costs (€)	Difference Costs (€)	P value*
Therapist	591.74 (346.21)	420.08 (208.21)	171.67	0.17
Volunteer	11.75 (21.30)	2.92 (9.36)	8.84	0.22
ACRE	40.64 (13.58)	0.75 (2.82)	39.89	0.00
Total costs	644.14 (361.01)	423.74 (204.75)	220.39	0.09

general lower state of ability in the excluded group. Due to early discharge from the hospital, the incoming patients in nursing homes are more impaired and frail than a few years ago [23, 24]. Because of evidence of motor-recovery ability being best at (and even limited to) the first period after the stroke [8, 11], guidelines for rehabilitation aim at starting rehabilitation training as soon as possible after the incident. This standpoint has led to our criterion for the moment of stroke being less than 60 days prior to the moment of inclusion. However, these frail elderly may benefit from ACRE training at a later stage of the rehabilitation, when they have regained a better physical condition.

4.2. Effects. Our results showed on the one hand a negative difference in the mean change scores (from pretest to posttest) between the ACRE training group and the control group for the primary outcome measures on motor recovery. On the other hand, our results showed a positive difference in change scores for general health-related quality of life. However, because of the low number of inclusions, no significant effects could be demonstrated for any of the variables.

Our negative result for motor recovery needs more reflection. The ACRE group showed a decline in motor functioning from T0 to T1, whereas the control group showed an improvement. In the ACRE group, four patients were included with an Action Research Arm Test (ARAT) baseline score at the upper extreme (i.e., 50 or higher). The physiotherapists had included these patients in the study, because they perceived that the patients still could improve the quality of their performance (i.e., speed, flexibility, reach). When we excluded these patients from the analysis, an improvement of the mean ARAT score from T0 to T1 was found for the remaining patients, but this improvement was still smaller than that of the control group. This result could be interpreted in two ways. Firstly, the result suggests a negative effect of the ACRE on motor recovery; however, the effect could be based merely on chance due to the small sample size. Alternatively, this result suggests that the ARAT was not sensitive enough to measure the effect of the ACRE training. Therefore, we recommend for future research that the quality of the performance should also be part of the assessment to gain a more complete representation of motor recovery.

Besides, the patients at the upper extreme of baseline ARAT scale, also three ACRE patients at the lower extreme were included, that is, an ARAT score of zero. Also, three control patients with a zero baseline score were included. All of these six patients scored zero on ARAT at the posttest. This result is in line with the conclusions of Kwakkel et al. [11] who found that highly impaired patients (ARAT scores less than ten) were not likely to benefit from intensive training aiming at motor recovery.

From the qualitative evaluation of the use of the ACRE in the study, it appeared that the training with ACRE using the games was fun and the robot training, as addition to standard therapy, was met by hardly any aversion from patients or therapists.

4.3. Economic Evaluation. The costs of ACRE therapy are currently primarily determined by the costs of the supervising therapists. The cost-utility analyses showed that for acceptable values for a QALY usual care is preferred if only the study period of six weeks is considered. However, if after the six weeks of the intervention the improvement in quality of life in the ACRE patients compared to usual care will be maintained, the additional costs per QALY will decrease, which will result in the ACRE being already preferred for values of the willingness to pay below €40.000 per QALY. Within this respect, further study with a longer follow-up period to prove its effectiveness. The attempt for a third assessment moment three months after inclusion within this study was met with too many practical problems.

4.4. Future Possibilities. To turn ACRE training for frail elderly after stroke to good account, use of ACRE at a later stage of the rehabilitation may be considered, when the patient has regained a better physical condition. Careful consideration must be given as to the subgroup benefitting from this kind of training, that is, patients with impairment of the upper limb, with a reasonable physical condition. Maybe the average nursing home patient may not fit this profile and beneficiaries of ACRE training will primarily be found in a polyclinical setting. Also the aim of ACRE training has to be reconsidered. ACRE training at a later stage may be aiming less at motor recovery as such, but more at improving general functioning of the patient in daily life, leading to greater independence of the patient and improvement of quality of life.

In a more structural use of ACRE in the nursing home setting, ACRE training is depicted with little or no therapist supervision at all, resulting in a low-cost alternative additional training possibility. Further development of the ACRE system is needed to make it suitable for autonomous use, with respect to functionality, adaptability to the patient, ease of use, feedback of training results, safety, and so forth, A more simplified ACRE could even be placed at the home for further training after discharge from the nursing home.

We still think that the use of additional ACRE training may be worthwhile for a select group of patients or at a later stage of the rehabilitation process. To prove (cost-) effectiveness for this select group additional research with a larger number of participants during a longer follow-up period is needed.

5. Conclusion

This study showed that for various reasons patients were not able to participate in the ACRE training. Based on this experience, expectations for the applicability of ACRE in regular stroke rehabilitation in frail elderly early in the rehabilitation process should be on the conservative side. Especially the target group recovering in the nursing home setting consists of fragile elderly with comorbidity who may have problems of physical or cognitive nature in early stages of recovery. In total, 24 patients were included. For this small sample no significant effects of the ACRE training were found. Because of the low inclusion numbers, caution in relation to the outcomes is justified. Further improvement of the ACRE can best be focused on making the system suitable for self-training and on development of training software for activities of daily living.

Acknowledgments

The authors thank Professor H. J. M. Cools, M.D., Ph.D., for making this study happen, because of his believe that also the frail elderly in nursing homes have the right to state-of-the art rehabilitation including robotic equipment. He retired from his function as a Medical Director of De Bieslandhof and Professor at Leiden University Medical Centre halfway this study. We also thank the staff involved at the two Dutch nursing homes and rehabilitation centres: De Bieslandhof, Pieter van Foreest at Delft and Antonius Binnenweg, Laurens at Rotterdam for their time. The study was partially funded by ZonMw, The Netherlands organisations for health research and development (Grant no. 17099109).

References

[1] American Heart Association, *Heart and Stroke Statistical Update*, American Heart Association, Dallas, Tex, USA, 2000.

[2] H. L. Koek and M. L. Bots, *Cijfers en Feiten van Hart en Vaatziekten*, Nederlandse Hartstichting Den Haag, 2004.

[3] J. Van Exel, M. A. Koopmanschap, J. D. H. van Wijngaarden, and W. J. M. Scholte op Reimer, "Costs of stroke and stroke services: determinants of patients costs and a comparision of costs of regular care and care organised in stroke services," *Cost Effectiveness and Resource Allocation*, vol. 1, article 2, 2003.

[4] Beroerte, cijfers en feiten. Uitgave van de Nederlandse Hartstichting, augustus 2006.

[5] S. Coote and E. K. Stokes, "Robot mediated therapy: attitudes of patients and therapists towards the first prototype of teh GENTLE/s system," *Technology and Disability*, vol. 15, no. 1, pp. 27–34, 2003.

[6] J. van Exel, M. A. Koopmanschap, J. D. H. van Wijngaarden, and W. J. M. Scholte op Reimer, "Costs of stroke and stroke services: determinants of patient costs and a comparison of costs of regular care and care organised in stroke services," *Cost Effectiveness and Resource Allocation*, vol. 1, article 2, 2003.

[7] M. Schoone, P. Van Os, and A. Campagne, "Robot-mediated Active Rehabilitation (ACRE) A user trial," in *Proceedings of the 10th IEEE International Conference on Rehabilitation Robotics (ICORR '07)*, pp. 477–481, Noordwijk, The Netherlands, June 2007.

[8] A. J. Doornebosch, H. J. M. Cools, M. E. C. Slee-Turkenburg, M. G. van Elk, and M. Schoone-Harmsen, "Robot-mediated ACtive REhabilitation (ACRE2) for the hemiplegic upper limb after a stroke: a pilot study," *Technology and Disability*, vol. 19, no. 4, pp. 199–203, 2007.

[9] R Development Core Team, *R: A Language and Environment for Statistical Computing*, R Foundation for Statistical Computing, Vienna, Austria, 2011.

[10] J. H. Van der Lee, R. C. Wagenaar, G. J. Lankhorst, T. W. Vogelaar, W. L. Devillé, and L. M. Bouter, "Forced use of the upper extremity in chronic stroke patients: results from a single-blind randomized clinical trial," *Stroke*, vol. 30, no. 11, pp. 2369–2375, 1999.

[11] G. Kwakkel, B. J. Kollen, J. V. Van der Grond, and A. J. H. Prevo, "Probability of regaining dexterity in the flaccid upper limb: impact of severity of paresis and time since onset in acute stroke," *Stroke*, vol. 34, no. 9, pp. 2181–2186, 2003.

[12] J. H. Van der Lee, L. D. Roorda, H. Beckerman, G. J. Lankhorst, and L. M. Bouter, "Improving the action research arm test: a unidimensional hierarchical scale," *Clinical Rehabilitation*, vol. 16, no. 6, pp. 646–653, 2002.

[13] P. W. Duncan, L. B. Goldstein, D. Matchar, G. W. Divine, and J. Feussner, "Measurement of motor recovery after stroke: outcome assessment and sample size requirements," *Stroke*, vol. 23, no. 8, pp. 1084–1089, 1992.

[14] D. J. Gladstone, C. J. Danells, and S. E. Black, "The Fugl-meyer assessment of motor recovery after stroke: a critical review of its measurement properties," *Neurorehabilitation and Neural Repair*, vol. 16, no. 3, pp. 232–240, 2002.

[15] R. Brooks and F. De Charro, "EuroQol: the current state of play," *Health Policy*, vol. 37, no. 1, pp. 53–72, 1996.

[16] L. M. Lamers, P. F. M. Stalmeier, J. McDonnell, P. F. M. Krabbe, and J. J. Van Busschbach, "Measuring the quality of life in cost-utility analyses: the Dutch EQ-5D tariff," *Nederlands Tijdschrift voor Geneeskunde*, vol. 149, no. 28, pp. 1574–1578, 2005.

[17] I. G. L. Van de Port, K. Leenes, D. Sellmeijer, A. Zuidgeest, and G. Kwakkel, "Betrouwbaarheid en concurrente validiteit van de Nederlandse Stroke Impact Scale 2.0 bij patienten met een CVA," *Nederlands Tijdschrift voor Fysiotherapie*, vol. 118, no. 1, pp. 12–18, 2008.

[18] T. Burgler, L. J. Tiesinga, K. Wynia, and B. Middel, "Zorg voor mensen met een cerebraal vasculair accident; inventarisatie van meetinstrumenten naar psychosociale gezondheidsproblemen bij CVA en de rol van de verpleegkundige daarbij," in *State-of-the-Art Studie Verpleging en Verzorging*, I. Jongerden and Y. Heijnen-Kaales, Eds., pp. 92–109, Elsevier, Gezondheidszorg, The Netherlands, 2003.

[19] S. Van Buuren and K. Groothuis-Oudshoorn, "MICE: multivariate imputation by chained equations in R," *Journal of Statistical Software*, vol. 45, no. 3, pp. 1–67, 2011.

[20] S. Van Buuren, H. C. Boshuizen, and D. L. Knook, "Multiple imputation of missing blood pressure covariates in survival analysis," *Statistics in Medicine*, vol. 18, no. 6, pp. 681–694, 1999.

[21] Statistics Netherlands, Consumer price index, 2011 http://www.cbs.nl.

[22] L. Hakkaart-van Roijen, S. S. Tan, and C. A. M. Bouwmans, *Manual for Costing Research, Methods and Standard Costs for Economic Evaluations in Health Care*, Dutch Health Care Insurance Board, Amstelveen, The Netherlands, 2010.
[23] ETC Tangram: Peerenboom P. B. G., Spek J., Zekveld G. and Leiden University Medical Centre: Cools H. J. M., van Balen R., Hoogenboom M. J. Revalidatie in de AWBZ. Omvang aard en intensiteit, 2008, http://www.tangram.info/.
[24] ETC Tangram, *Aard en Omvang Geriatrische Revalidatie Anno 2009/2010*, Leusden, The Netherlands, 2010.

Hindawi Publishing Corporation
Journal of Robotics
Volume 2011, Article ID 650415, 7 pages
doi:10.1155/2011/650415

Research Article

Mechanical Performance of Actuators in an Active Orthosis for the Upper Extremities

Roland Wiegand, Bastian Schmitz, Christian Pylatiuk, and Stefan Schulz

Institute for Applied Computer Science, Karlsruhe Institute of Technology, 76344 Karlsruhe, Germany

Correspondence should be addressed to Roland Wiegand, roland.wiegand@kit.edu

Received 31 May 2011; Revised 25 August 2011; Accepted 30 September 2011

Academic Editor: Tetsuya Mouri

The aim of the project OrthoJacket is to develop a lightweight, portable, and active orthosis for the upper limps. The system consists of two special designed fluidic actuators which are used for supporting the elbow function and the internal rotation of the shoulder. A new design of flexible fluid actuator (FFA) is presented that enables more design options of attaching parts, as it is allowed by conventional actuators with a stationary centre of rotation. This advantage and the inherent flexibility and the low weight of this kind of actuator predestined them for the use in exoskeletons, orthoses, and prostheses. The actuator for the elbow generates a maximum torque of 32 Nm; the internal rotation is supported with 7 Nm. Both actuators support the movement with up to 100% of the necessary power. The shells for the arm and forearm are made of carbon reinforced structures in combination with inflatable cushions.

1. Introduction

Most of the 300,000 persons in Europe who suffer from a spinal cord injury have a lesion between the fourth and the fifth vertebra [European Multicenter Study of Spinal Cord Injury; http://www.emsci.org/]. These patients often have limited remaining functions of the shoulder and elbow [1] but cannot use them in everyday life, as the strength is insufficient to autonomously execute activities. For the assistance of people with a tetraparesis or tetraplegia, various systems exist [2, 3]. They focus on stationary rehabilitation and therapy with the assistance of medical staff [4–6]. The OrthoJacket project is aimed at developing a lightweight, wearable, inconspicuous, and mobile support system for the upper extremities. The system was built to support the patients and to give them more autonomy and independence in everyday life. For this purpose, the movements of the upper extremities are supported actively, and the joints are protected by an orthosis. This system is not only developed for training purposes, but it also has to be usable in everyday life. Therefore, it must be a mobile system, contrary to other rehabilitation systems [7, 8]. The orthosis will be more accepted and used by the patients, if it is uncomplicated and reliable in operation. Moreover, wearing and use of the system should be possible without attracting attention. As the resulting functional restrictions vary for every patient, the system consists of different self-sufficient functional parts. Consequently, it can be adapted easily to the individual needs of different patients. OrthoJacket consists of three parts that can be used alone and in combination with the other parts (see Figure 1) [9–11].

(i) The movement of the wrist and the grasping function of the hand are achieved by functional electrical stimulation (FES).

(ii) At the elbow, the system consists of a lightweight active orthosis that is partly integrated in a jacket and a flexible fluidic actuator [12, 13]. The shells of the orthosis are made of an inflatable cushion, and a support structure is made of carbon fiber.

(iii) The shoulder function is supported by a linear axle system. It is attached to the wheelchair and actuated by two stepper motors.

The orthosis will be controlled by electromyography measurements [14, 15] at different, voluntarily contractible muscles, or by a joystick which is attached to the shoulder

Figure 1: CAD model of the OrthoJacket.

or the neck. These two types of control mechanisms do not provide a nominal value, only a direction of movement and perhaps a speed can be obtained from these signals [16]. This paper focuses on the actuators for the support of the elbow function and the internal rotation, adduction, and anteversion of the shoulder and the inflatable shell structure.

2. Methods

The first tests of the system were made with healthy subjects. In these tests, it was determined how large the range of movement is for persons of different sizes. The effect of limbs of varying weight on system operation was also evaluated. The three individuals were able to move their upper extremities unrestrictedly. Their weights ranged from 63 to 95 kg, and their size varied between 1.84 and 1.92 m. The age was between 24 and 29. For comparison, the measure of the 50% male person from the Man-Systems Integration Standards NASA-STD-3000 [17] is also given in Table 1.

In a multibody simulation, the moments required for the movement of the patient's upper extremities were determined. This simulation consisted of two different actions. One was putting a glass to the mouth and drinking, the other action consisted in eating with a fork. In the simulation, weights and inertia of each segment of the upper extremities were considered. The friction of the joints depends on physical conditions of the patients and, hence, was not considered in the simulation. Instead, the weight of the fork and glass was multiplied by a safety factor, so that the items had a higher weight in this case than in reality (fork 0, 15 kg, glass 0, 75 kg) [18]. Based on the multibody simulation results, a minimum torque was defined, which is necessary for the movement of the arm. This minimum torque amounts to 7 Nm in the range from 0 to 90° and 5 Nm from 90 to 120°. In the article "A study of the external forces and moments at the shoulder and elbow while performing everyday tasks" [19], the joint moments of healthy individuals in ten different everyday tasks were determined. In this paper, a maximum torque of 5 Nm for the elbow is indicated. Due to the uncertainty in the weight of the patient and the joint friction, our maximum has a higher value. For the shoulder, torques in the range of 30 Nm are required. (Adduction, anteversion about 30 Nm and for the internal rotation about 3.5 Nm)

Table 1: Data of the three subjects.

Patient	Weight [kg]	Size [m]	Arm weight [kg]	Upper arm circumference [m]
1	63	1.84	2.2	0.23
2	84	1.88	3.8	0.32
3	95	1.92	5.2	0.33
50%	82.2	1.697	4.48	0.312

Table 2: Data sheet of the elbow actuator.

Weight	33.2	g
Air volume	$16 \times 1286 = 20576$	mm^3
Air volume	0.020576	L
Thickness at 0 kPa	17	mm
Thickness at 100 kPa	180 (mechanical stop)	mm
Angle	130 (mechanical stop)	°
Operating pressure	200 to 300	kPa
Maximum pressure	400	kPa
Burst pressure	960	kPa
Assembly	16 Chambers	
Area per chamber	1737	mm^2

These values are higher than in [19], because the additional weight of the orthosis must be moved, too.

2.1. Design of the Elbow Actuator. As a drive, a flexible fluid actuator is used, because these actuators have a high power density, a small weight, inherent compliance, and they ensure safety [20]. The elbow orthosis is moved by an FFA which will be integrated in the orthosis. As the actuator is built of several chambers made of film, the geometry can be adapted easily to the space available. The newly designed fluidic actuator consists of 16 arched and interconnected chambers (see Table 2). It assumes the shape of a hemisphere under pressure. At each end of a chamber, a strap is attached for mechanical guiding of the actuator. The straps are connected with each other and with the joint axle. Hence, the actuator can be integrated easily in a piece of clothing and hardly interferes with the natural aspect. In order to minimize additional loading of the joint by the actuator, the rotation axis of the orthosis should be positioned at the same point and with the orientation corresponding to the rotation axis of the human elbow joint. The actuator is made of a fabric-reinforced polyurethane film. The cloth is a tightly woven fabric made of polyamide with plain weave (235 dtex), which is laminated on both sides with a layer of thermoplastic polyurethane. This fabric-reinforced plastic film has a tensile strength of about 200 N and a thickness of 400 micron. From this tissue, individual foil segments are punched and connected in a multistage high-frequency welding process. For flexion, the actuator is pressurized with an overpressure of up to 400 kPa. Extension requires a smaller torque, because it is not necessary to overcome gravity. Consequently, 90 kPa partial vacuum is sufficient to move the forearm back to the 0° position. Exact

Figure 2: Elbow orthosis with shells made of ABS.

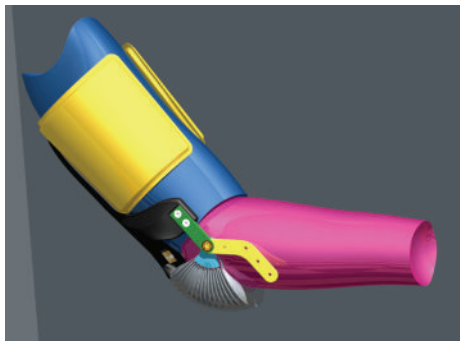

Figure 3: Inflatable shell structure.

pressure adjustment between −90 and 400 kPa is accomplished by a proportional valve (modified Festo MPPE 3-1 1/8-6-010-B). Together with the pump and the storage tank for compressed air, it is located in a sound-proof container below the seat of the wheelchair. For the first prototype, the shells were made of ABS plastic, which was shaped as desired by a rapid prototyping process (see Figure 2). The structure of the heavily loaded segments was reinforced with carbon fiber. For the measurement of the elbow joint angle, a digital angle sensor based on the Hall effect is used. It determines the current angle with a resolution of 12 bit.

2.2. Inflatable Shell Structure. In conventional, passive orthoses, the arm of the user is fixed in a half shell of a thermoplastic or fiber-composite material. The fasteners for the arm are made of a combination of a Velcro fastener and elastic straps. Depending on how strong the orthosis should be attached to the body of the patient, the tapes are prestressed. In the case of an active orthosis, the elbow and shoulder actuators support the patient with up to 30 Nm, as a result of which the shell must be attached securely to the upper extremity. If an active orthosis attached firmly to the arm with straps, the blood flow is obstructed and also the skin is severely squeezed. The disturbed blood circulation [21] of the upper extremities from quadriplegics will be further complicated by this attachment method. To avoid this effect, an inflatable shell structure has been developed. It distributes the force over a larger area than conventional

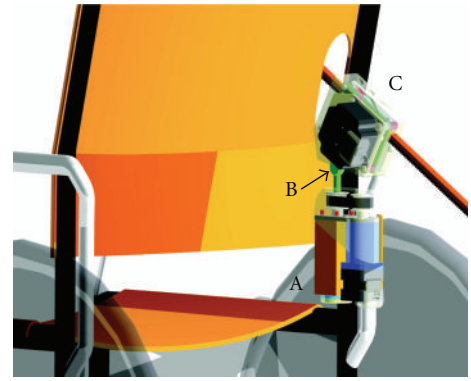

Figure 4: Shoulder supports structure mounted on the wheelchair A: vertical axle, B: passive joint, C: linear unit.

tapes. Additionally, its rigidity and thickness are adjustable via the air pressure (see Figure 3, yellow part in the CAD model). Consequently, the air pressure in the OrthoJacket can be reduced at recovery time, and, thus, the skin is given time to relax. This new shell structure consists of a rugged composite material structure that connects the two supporting points of the elbow joint and the support points of the actuators. Additionally, this structure extends along the longitudinal axis of the upper or lower arm and is used for constant application of force into the body (see Figure 3, black stripe in the CAD model). When pressurized, the inflatable support structure assumes a semicircular shape and surrounds the arm independently. It is composed of two 300 or 325 by 100 mm large rectangles which are welded together at the perimeter. The surfaces of the two rectangles are connected by 27 stripes. This prevents the structure from deforming. Inside, the shell is lined by thin-layer upholstery. Outside, the orthosis is covered by two layers of fabric. An important point in the development of the shell structure was to create the possibility to dress and undress the orthosis easily. As the user of the system cannot participate actively in the dressing process, the system has to be easy to attach to the upper extremities. This is achieved by a zipper that runs along the longitudinal axis of the arm. Thus, the arm can be positioned on the unfolded orthosis, and the zipper can be closed. Then, the elbow is bent to make sure that the elbow joint is at the same place as the axle of the elbow support structure. Only then will the support structure be inflated and connect the OrthoJacket with the patients arm.

2.3. Shoulder Support Structure. The system to support the shoulder consists of a vertically oriented axis of rotation that allows for the rotation of the shoulder. Adduction and anteversion are achieved by an actively driven linear axle which acts in the middle of the upper arm, thus, lifting the arm (see Figure 4). The angle between the linear axle and the horizontal axle is located above a passive rotational degree of freedom. By using a kinematic unit with a linear axle, the problem of the nonstationary pivot point of the shoulder joint is solved. With this solution, it is possible to support the full shoulder function with only two drivers, with the control of the system being facilitated for the patient.

According to the simulation, the maximum torque required for adduction, anteversion, and rotation is about 30 Nm (adduction, anteversion) and about 3.5 Nm for the rotation. With this stepper motor/gearbox combination, movements in the angle range of 0 to 80° for adduction and anteversion and −30 to +30° for rotation are possible. Restrictions may be due to the anatomy of the user and must be considered. Small inaccuracies (up to 10 mm) in the positioning of the patient relative to the shoulder system are no problem. When using a shoulder support system (S^3) with three actuators arranged around the shoulder, it must always be ensured that the center of rotation of the shoulder and the support structure are exactly at the same position.

The vertical axle of the S^3 consists of a stepper motor. It drives a planetary gear with a reduction ratio of 1 : 49. This combination generates about 4.5 Nm of torque. Using a belt with a slip clutch in the driven gear, the vertical axle is moved. At the end of the vertical axle (see Figure 4, A), the linear unit (see Figure 4, C) is mounted with a passive degree of freedom (see Figure 4, B). The linear unit consists of a stepper motor with 0.65 Nm torque and a two-stage spur gear unit with a reduction ratio of 1 : 4. The linear axle consists of an aluminum profile onto which a rack made of steel is mounted. The linear axle of the stressed segments is guided by ball bearings. Lateral guiding is achieved by Teflon journal bearings. The active and passive rotational degrees of freedom are monitored by absolute position encoders. The linear axle has to perform a reference run at the beginning. The current position is identified by counting the steps of the stepper motor. Internal rotation is achieved by another fluid actuator (Figure 5). It is mounted at the top of the linear axle and allows bending of ±45°. By an optimized mounting position, an angle from 0 to 90° between the linear axle and the forearm can be set.

The actuator also supports the anteversion movement. It consists of six stacked, circular segments; each of them is divided into eight separate chambers (see Table 3). The chambers of stacked segments are connected with each other, such that the actuator consists of eight independent controllable subactuators. At the top and bottom segment, a connecting plate is mounted. These two plates are connected with a string of high-strength yarn that allows for lateral tilting but limits the maximum height of the actuator. By varying the air pressure in the individual subactuators, it is possible to generate movements to the left, right, top, and bottom. With a special sequence of pressure rises, even rotational motions are possible. The actuator has a diameter of 65 mm; the single chambers are circular sectors with an opening angle of 45°. The height of the actuator is limited to 35 mm. As the actuator has no fixed rotation axles, the two tilt angles are determined by two geomagnetic field sensors. These sensors deliver a vector with three components, one for each spatial direction. The value corresponds to the strength of the magnetic field which is parallel to the direction of the vector components. It is possible to determine the angular position of the sensor relative to the Earth's magnetic field. Such a sensor is attached to each of the two connecting plates. From the difference of the two vectors, the angle between the two connection plates can be determined. Due to the small distance between the two sensors, possible variations of the geomagnetic field will always affect both sensors, as a result of which the relative position to each other is determined correctly. The actuator is controlled by a proportional valve (Festo MPPE 1/8-6-010-B 3-1) which is connected in series with eight shift valves (Bürkert 6104). The shift valves are used as a switch connecting the proportional valve to one of the eight chambers. This actuator is controlled directly by the patient. The pressure in the chamber is increased or decreased until the desired angle of the support structure is reached. With the two geomagnetic field sensors, the position of the orthosis is monitored. In addition, the two angles needed to adjust the position of the hand are controlled. Furthermore, a pressure limit is implemented to detect a locked drive.

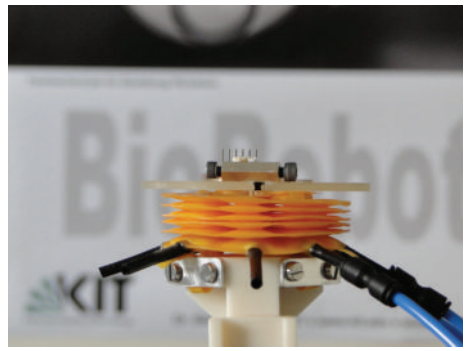

Figure 5: Actuator for internal rotation without pressure.

Table 3: Data sheet of the 2D actuator.

Weight	22	g
Volume	8 × 4.5	mL
Nominal area of a chamber	295	mm^2
Diameter	65	mm
Nominal height	10	mm
Max. height	45	mm
Operating pressure	600	kPa
Max. pressure	1100	kPa
Assembly	6 segments, each with 8 individual chambers	

3. Results

3.1. Elbow Actuator. The newly designed elbow actuator is able to support the elbow with up to 32 Nm. The burst pressure of one actuator chamber is 970 kPa. Figure 7 shows the actuator providing the torques required for a safe operation of the orthosis. The required pressure range for operation is between 200 and 300 kPa (Figure 6). In this range, the torque curve is approximately linear. Using the first prototype of this active orthosis, the step response of the control path consisting of valve, elbow actuator, and orthosis was determined. To make the test as real as possible, the brace was loaded with a cast resin forearm with hand

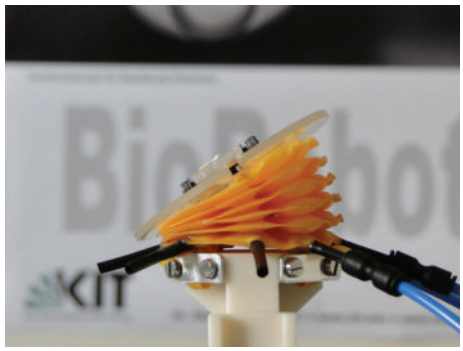

Figure 6: Actuator for internal rotation, 3 chambers with a pressure of 300 kPa.

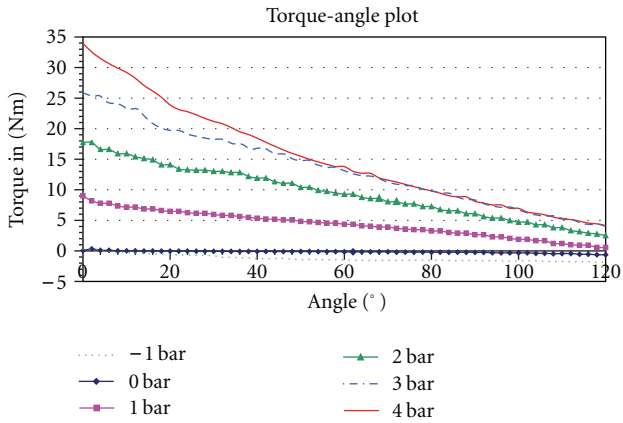

Figure 7: Torque plot of the elbow actuator.

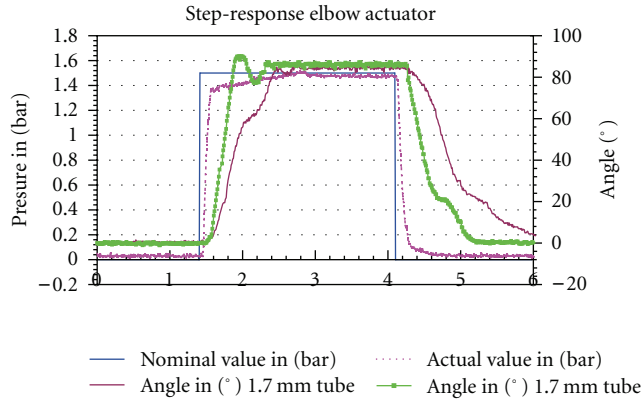

Figure 8: Step response of the elbow actuator with a 1.7 and a 2.7 mm tube and 150 kPa pressure.

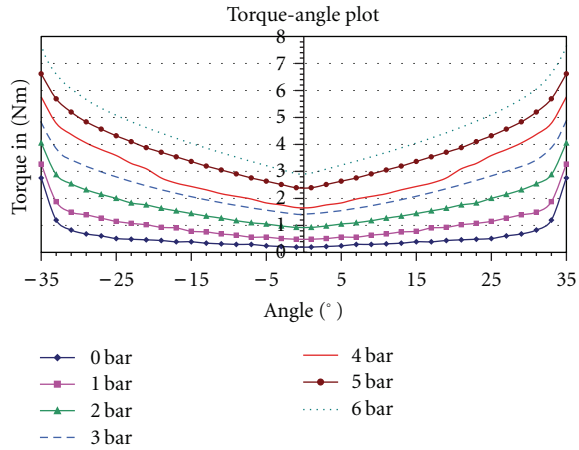

Figure 9: Torque plot of the actuator for internal rotation.

(1.61 kg). Compressed air is supplied via a polyurethane tubing with an inner diameter of 4.2 mm, followed by a tube which has an inner diameter of 1.7 or 2.7 mm. The tubing of 1.7 mm is flexible and can be integrated inconspicuously in the jacket. The higher flow resistance of the 1.7 mm tube causes lifting of the forearm in 0.9 seconds. For the tube with the internal diameter of 2.7 mm, the lifting time only is about half a second (see Figure 8). The step response (0–150 kPa) of the actuator/valve combination has a reaction time of 0.1 seconds. Then, it almost behaves similarly to a PT1 element. The slight decline of the 1.7 mm tube in the upper part of the plot results from a kink in the tube. The control of the valve and the recording of the sensor data are performed with a USB-connected card from National Instruments on a Windows PC with LabVIEW.

3.2. Shoulder Support Structure. The rotation axle and the linear axle produce a torque of 4.5 Nm and a maximum force of 210 N. The maximum torque of the FFA at the top of the linear axle is 7 Nm. Other data of the FFA actuator can be found in Table 3. With this fluid actuator, an angle torque plot was recorded (see Figure 9). These curves are linear over a wide area, only for large angles are they significantly increased. The discontinuity at 0° is caused by the exchange of the chambers. Using this actuator, step response was recorded as it was done for the elbow actuator. The test assembly of the system corresponds to the mounting position in the wheelchair. The proportional valve is linked to a tube of 4.2 mm internal diameter. After 150 mm of 2.7 mm tubing, one of the shift valves controlling the individual chambers is connected. These are directly connected to the actuator. Measured values are recorded with the same hardware as used for the step response of the elbow actuator. The response time of the proportional valve is 0.1 seconds; the switching time of the shift valve is in the range of 14 or 18 ms (open and close, value from the data sheet). The time necessary to inflate one of the eight chambers of the actuator with 300 kPa is about 0.25 seconds (see Figure 10), and a complete filling process (open shift valve, set pressure with the proportional valve, close shift valve) requires 0.37 seconds to reach the proper air pressure. The time until all eight chambers have the desired air pressure is 2.96 seconds.

3.3. Evaluation of the Movement Space. The real ranges of movement of the OrthoJacket were determined for five subjects of different sizes and weights (see Table 4). The maximum angle of every joint reached by the orthosis was identified. Several different stopping criteria were specified, some were set by the mechanics, others by the subject

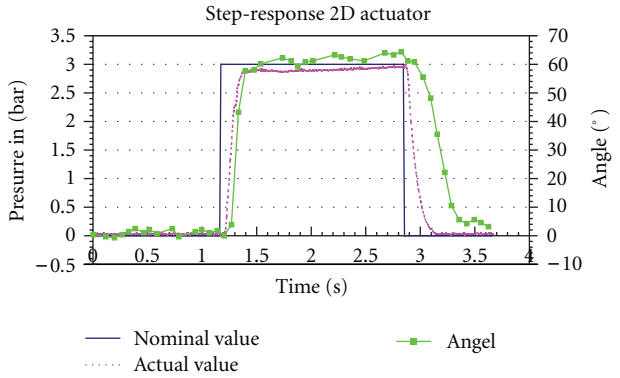

Figure 10: Step response of the actuator for internal rotation with 300 kPa pressure.

Table 4: Body dimensions of the subjects.

Subject	Weight in [kg]	Size in [mm]	Weight of the upper extremity in [kg]	Circumference of the upper arm in [mm]
1	63	1840	2200	230
2	84	1880	3800	320
3	95	1920	5200	360
4	77	1640	3500	280
5	68	1780	3400	275

Table 5: Description of the stopping criteria.

Stopping criteria	Description
1	Drive is mechanically blocked
2	Drive has not enough power
3	Subject does not feel comfortable
4	Subjects and mechanics collide
5	Enough for everyday tasks

(see Table 5). The angle of the elbow was limited to 90°. In this test, only the elbow orthosis and the two electrically driven axles of the shoulder system were used.

The first tests of the mechanical parts of the system were made with healthy subjects. Healthy people are able to give better feedback about the function and comfort of the system. The angular ranges for anteversion and adduction of about 75 and 45° are in the expected range. The system works as expected (see Table 6). None of the three subjects felt uncomfortable when using the orthosis. For patient three, the traverse path of the linear axle was not sufficient to further lift the arm. The collision of the system and the arm rest of the wheelchair can be prevented by choosing another wheelchair or by some modifications of the current one.

A second test was made with a tetraplegic patient. The patient was paralyzed below C4, and random movement of the biceps was very difficult. Controlled activation of the triceps was impossible. In this test, only the elbow orthosis was used. With the orthosis, the patient was able to move his arm from about 10 to 90°. The elbow orthosis was controlled

Table 6: Results of the test.

Patient	Anteversion in [°] (Stopping criteria)	Adduction in [°] (Stopping criteria)	Elbow in [°] (Stopping criteria)
1	0 (5) to 76 (5)	−20 (4) to 29 (1)	0 (3)–90
2	0 (5) to 71 (5)	−18 (4) to 30 (1)	0 (3)–90
3	0 (5) to 51 (3)	−12 (4) to 29 (1)	0 (3)–90
4	0 (5) to 79 (3)	−10 (4) to 28 (1)	0 (3)–90
5	0 (5) to 77 (3)	−18 (4) to 29 (1)	0 (3)–90

by a shoulder joystick. In the patient test, it was checked how well the orthosis works on a tetraplegic patient and how reliably it can be moved. When the joystick signal exceeded a certain threshold value, the pressure in the actuator was increased slowly. When the signal dropped below the value, the movement stopped. The forearm was lowered according to the same principle, but with another threshold value. The results were satisfactory but also show that the patient first requires a training phase to eliminate acampsia of the joint and reduce the shortening of the sinews before the system can be used correctly.

4. Conclusion

The elbow orthosis and the shoulder system without the fluid actuator for internal rotation were evaluated on volunteers, and it was found that they are able to support the shoulder and elbow function in healthy persons with 100% of the required force. The torque plots indicate that patients with restricted motor functions can be supported with up to 100%. Thanks to the flexibility of the fluidic actuators, the system is yielding and, in the case of spasticity, prevents high forces from being generated and decreases the risk of injury. The next steps are the integration of the FES system in the OrthoJacket and the installation of the control system. Additional tests with three tetraplegics will be performed. Grasping and release tests like those of [22, 23] will be carried out with some modifications for our patient group (C4, C5, and maybe C6). These tests will take place in autumn 2011 at our project partner, the Orthopaedic University Hospital in Heidelberg, Germany.

Acknowledgment

This work was supported by the Federal Ministry of Education and Research (BMBF) within the funding program "Innovative aids," grant no. 01EZ-0774. The project Orthojacket is a health research cooperation between science and industry. The authors acknowledge support by Deutsche Forschungsgemeinschaft and the Open Access Publishing Fund of Karlsruhe Institute of Technology.

References

[1] A. Curt, M. E. Schwab, and V. Dietz, "Providing the clinical basis for new interventional therapies: refined diagnosis and assessment of recovery after spinal cord injury," *Spinal Cord*, vol. 42, no. 1, pp. 1–6, 2004.

[2] A. Gupta and M. K. O'Malley, "Design of a haptic arm exoskeleton for training and rehabilitation," *IEEE/ASME Transactions on Mechatronics*, vol. 11, no. 3, pp. 280–289, 2006.

[3] R. J. Sanchez Jr., E. Wolbrecht, R. Smith et al., "A pneumatic robot for re-training arm movement after stroke: rationale and mechanical design," *Proceedings of the 9th IEEE International Conference on Rehabilitation Robotics (ICORR '05)*, pp. 500–504, 2005.

[4] T. J. Engen, "Recent advances in upper-extremity orthotics," in *The Advance in Orthotics*, Edward Arnold, 1976.

[5] S. Balasubramanian, W. Ruihua, and M. Perez, "Rupert: an exoskeleton robot for assisting rehabilitation of arm functions," in *Proceedings of Virtual Rehabilitation*, pp. 163–167, 2008.

[6] K. Kadota, M. Akai, K. Kawashima, and T. Kagawa, "Development of power-assist robot arm using pneumatic rubbermuscles with a balloon sensor," in *Proceedings of the 18th IEEE International Symposium on Robot and Human Interactive Communication (RO-MAN '09)*, pp. 546–551, 2009.

[7] J. Klein, S. J. Spencer, J. Allington et al., "Biomimetic orthosis for the neurorehabilitation of the elbow and shoulder (BONES)," *Proceedings of the 2nd Biennial IEEE/RAS-EMBS International Conference on Biomedical Robotics and Biomechatronics (BioRob '08)*, pp. 535–541, 2008.

[8] I. Vanderniepen, R. Van Ham, M. Van Damme, R. Versluys, and D. Lefeber, "Orthopaedic rehabilitation: a powered elbow orthosis using compliant actuation," *Proceedings of the IEEE International Conference on Rehabilitation Robotics (ICORR '09)*, pp. 172–177, 2009.

[9] S. Schulz, C. Pylatiuk, A. Kargov et al., "Design of a hybrid powered upper limb orthosis," in *Proceedings of the World Congress on Medical Physics and Biomedical Engineering: Neuroengineering, Neural Systems, Rehabilitation and Prosthetics*, pp. 468–471, September 2009.

[10] R. Rupp, U. Eck, O. Schill, M. Reischl, and S. Schulz, "Orthojacket an active fes-hybrid orthosis for the paralyzed upper extremity," in *Proceedings of the Technically Assisted Rehabilitation (TAR '09)*, pp. 18–19, Berlin, Germany, 2009.

[11] C. Pylatiuk, A. Kargov, I. Gaiser, T. Werner, S. Schulz, and G. Bretthauer, "Design of a flexible fluidic actuation system for a hybrid elbow orthosis," in *Proceedings of the IEEE International Conference on Rehabilitation Robotics (ICORR '09)*, pp. 167–171, June 2009.

[12] A. Kargov, I. Gaiser, H. Klosek et al., "Design and evaluation of a pneumatically driven anthropomorphic gripper for service robotics," in *Proceedings of the International Scientific-and-Technological Exhibition-Congress Mechatronics and Robotics*, St. Petersburg, Russia, October 2007.

[13] I. Gaiser, A. Kargov, S. Schulz, and G. Bretthauer, "Enhanced flexible fluidic actuators for biologically inspired lightweight robots with inherent compliance," in *Proceedings of the Workshop on Actuation & Sensing in Robotics*, Saarbrcken, Germany, October 2010.

[14] D. S. Andreasen, S. K. Allen, and D. A. Backus, "Exoskeleton with EMG based active assistance for rehabilitation," in *Proceedings of the 9th IEEE International Conference on Rehabilitation Robotics (ICORR '05)*, vol. 2005, pp. 333–336, 2005.

[15] O. Schill, R. Rupp, C. Pylatiuk, S. Schulz, and M. Reischl, "Automatic adaptation of a self-adhesive multi-electrode array for active wrist joint stabilization in tetraplegic SCI individuals," in *Proceedings of the IEEE Toronto International Conference on Science and Technology for Humanity (TIC-STH '09)*, pp. 708–713, 2009.

[16] J. Rosen, M. Brand, M. B. Fuchs, and M. Arcan, "A myosignal-based powered exoskeleton system," *IEEE Transactions on Systems, Man, and Cybernetics Part A*, vol. 31, no. 3, pp. 210–222, 2001.

[17] DC 20546-0001 Washington, *Man-Systems Integration Standards NASASTD-3000*, vol. I, Public Communications Office NASA Headquarters Suite 5K39 Washington, DC 20546-0001, 1995.

[18] O. Schill, R. Wiegand, B. Schmitz et al., "OrthoJacket: an active FES-hybrid orthosis for the paralysed upper extremity," *Biomedizinische Technik*, vol. 56, no. 1, pp. 35–44, 2011.

[19] I. A. Murray and G. R. Johnson, "A study of the external forces and moments at the shoulder and elbow while performing every day tasks," *Clinical Biomechanics*, vol. 19, no. 6, pp. 586–594, 2004.

[20] R. Wiegand, B. Schmitz, C. Pylatiuk, S. Schulz, and R. Rupp, "Fluidic actuation and sensors of the elbow joint in the hybrid orthosis othojacket," *Biomedizinische Technik*, vol. 55, no. s1, 2010.

[21] G. A. Zaech, *Paraplegie—Ganzheitliche Rehabilitation*, Karger, 2005.

[22] W. Michael, M. D. Keith, B. S. Kathryn Stroh Wuolle et al., "Development of a quantitative hand grasp and release test for patients with tetraplegia using a hand neuroprosthesis," *Journal of Hand Surgery*, vol. 19, no. 2, pp. 209–218, 1994.

[23] B. T. Smith, M. J. Mulcahey, and R. R. Betz, "Quantitative comparison of grasp and release abilities with and without functional neuromuscular stimulation in adolescents with tetraplegia," *Paraplegia*, vol. 34, no. 1, pp. 16–23, 1996.

Hindawi Publishing Corporation
Journal of Robotics
Volume 2011, Article ID 419465, 8 pages
doi:10.1155/2011/419465

Research Article

Two-Fingered Haptic Device for Robot Hand Teleoperation

Futoshi Kobayashi, George Ikai, Wataru Fukui, and Fumio Kojima

Department of Systems Science, Kobe University, 1-1 Rokkodai-cho, Nada-ku, Kobe 657-8501, Japan

Correspondence should be addressed to Futoshi Kobayashi, futoshi.kobayashi@port.kobe-u.ac.jp

Received 31 May 2011; Revised 23 August 2011; Accepted 27 September 2011

Academic Editor: Tetsuya Mouri

A haptic feedback system is required to assist telerehabilitation with robot hand. The system should provide the reaction force measured in the robot hand to an operator. In this paper, we have developed a force feedback device that presents a reaction force to the distal segment of the operator's thumb, middle finger, and basipodite of the middle finger when the robot hand grasps an object. The device uses a shape memory alloy as an actuator, which affords a very compact, lightweight, and accurate device.

1. Introduction

Various humanoid robot hands have been developed so far. The Utah/MIT dexterous hand has four fingers with four joints driven by tendon cables and tactile sensors over the entire surface [1, 2]. The Gifu hand has five fingers and 20 joints with 16 degrees of freedom (DOF) [3], and the KH hand type S has five fingers and 20 joints with 15 DOF [4]. More recently manufactured, robot hands incorporate multiaxis/force torque sensors and tactile sensors with conductive ink and are relatively lightweight. The TWENDY-ONE hand has four fingers and 16 joints with 13 DOF [5]. This robot hand is equipped with the six-axis force sensors and array-type tactile sensors. Honda Motor Co., Ltd., has developed a multifingered robot hand, which has five fingers and 20 joints with 13 DOF [6]. Each DOF is hydraulically actuated, and the robot hand has tactile sensors on the entire surface. AIST also developed a multifingered robot hand with 4 fingers and 17 joints with 13 DOF that are actuated by an electrical servomotor [7]. The AIST robot hand also employed multi-axis force/torque sensors in the fingertips. Many other robot hands have been developed and researched [8, 9]. We have also reported the universal robot hands I [10] and II [11].

A tele-rehabilitation system receives attention for medical care because of a shortage of rehabilitation therapists [12]. The tele-rehabilitation system with a robot hand allows a rehabilitation therapist to care intuitively. However, typically a tele-operation system is unable to give tactile and haptic information to the human operator because conventional teleoperation systems lack a feedback system. It is difficult to complete tasks or control various operations without dexterous tactile and haptic information; thus human operators make errors because there is no tactile feedback. Therefore, many haptic devices were developed to enable the human operator to feel the force. The haptic devices are classified into three types according to their mechanical grounding configuration [13] including the grounded type [14–19], the nongrounded type [20–24], and the body-grounded type [25, 26]. The grounded haptic device easily provides weight sensation or 3-Dimensional (3D) forces, but is limited because it is fixed to a static object like a table or the floor. The nongrounded haptic device includes an internal ground mechanism. The internal ground acts as counteractive base to create linear or angular momentum, and therefore, the device is easily repositioned because it is mechanically ungrounded. However, the ungrounded device cannot generate a large force in multiple directions or maintain continuous stimuli. The body-grounded haptic device is a wearable. These devices are worn and mounted on the human operator, which is used as a counteractive base or a point to impress a force or torque on the human operator. The wearable haptic devices provide a wide range of motion and force. However, for such devices to be usable, they must be small and lightweight. When a human opens a door or picks up an object, the hand and the arm

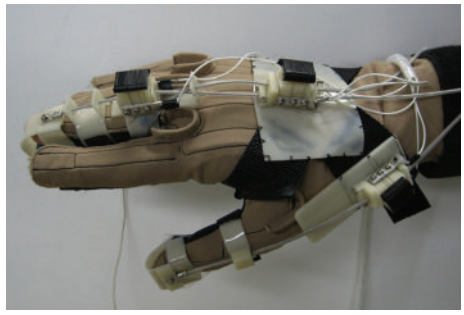

Figure 1: ExoPhalanx mounted on CyberGlove.

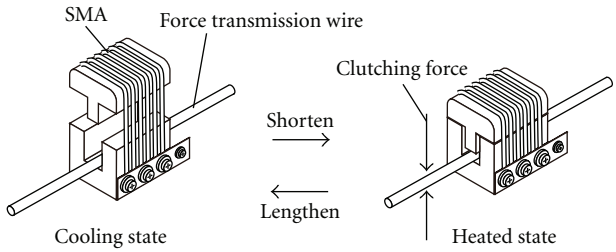

Figure 2: Schematic of SMA clutch brake showing cooled and heated states.

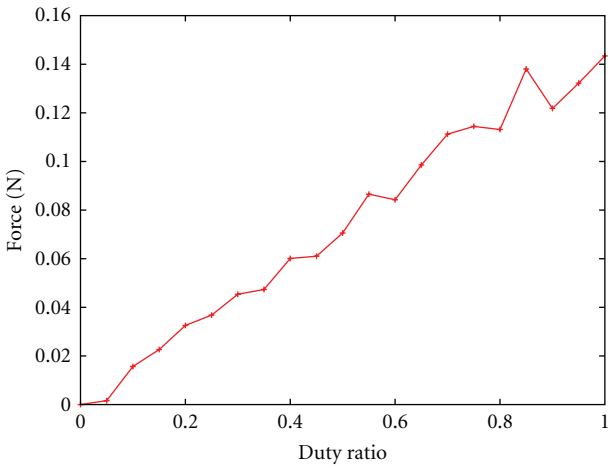

Figure 3: Clutching force by clutch brake against duty ratio.

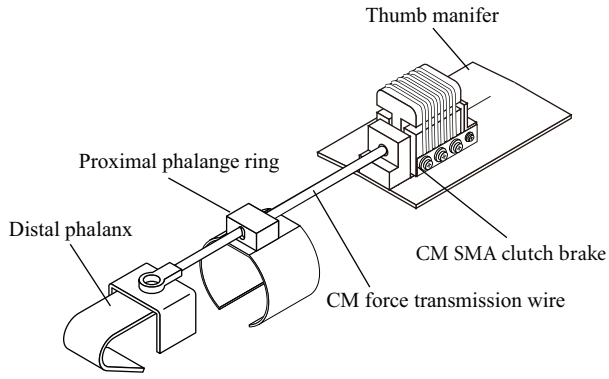

Figure 4: Thumb exoskeleton with CM SMA clutch brake.

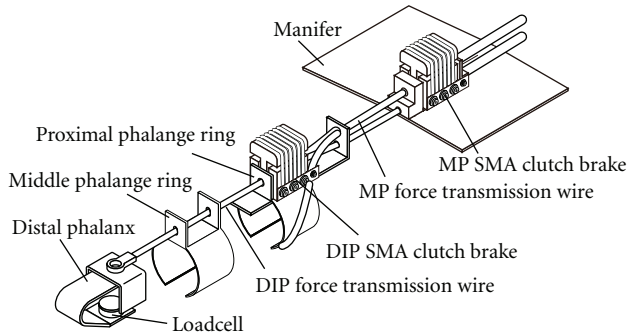

Figure 5: Middle finger exoskeleton showing DIP and MP wires and clutch brakes.

move simultaneously allowing for a wide working space and range of motion. A human also demands a greater force when a solid object like a glass is grasped. Therefore, the body-grounded haptic device is a preferred in applications involving grasping objects while maintaining feeling using tele-operation because it provides a wide workspace and considerable force in many directions.

In this paper, we have developed a two-fingered body-grounded haptic device called ExoPhalanx. The ExoPhalanx provides force to the distal segment of the human operator's thumb and middle finger, and the basipodite of the middle finger. Here, the ExoPhalanx presents only one-directional force to the human operator because the haptic device becomes small and lightweight in order to mount on the human hand. The performance of the haptic device was measured using a two-finger grasping tele-operation experiment with the Universal Robot Hand II and the haptic device ExoPhalanx.

The remainder of the paper is arranged as follows. The haptic device is introduced in Section 2. The robot hand tele-operation system with the developed haptic device is described in Section 3. The preliminary experiment showing the basic performance of the SMA clutch brake of the ExoPhalanx and the results of the grasping experiment with two fingers are presented in Section 4. Finally, the conclusions of this study are presented in Section 5.

2. Haptic Device

The developed haptic device ExoPhalanx is shown in Figure 1. The ExoPhalanx is used as a passive force feedback

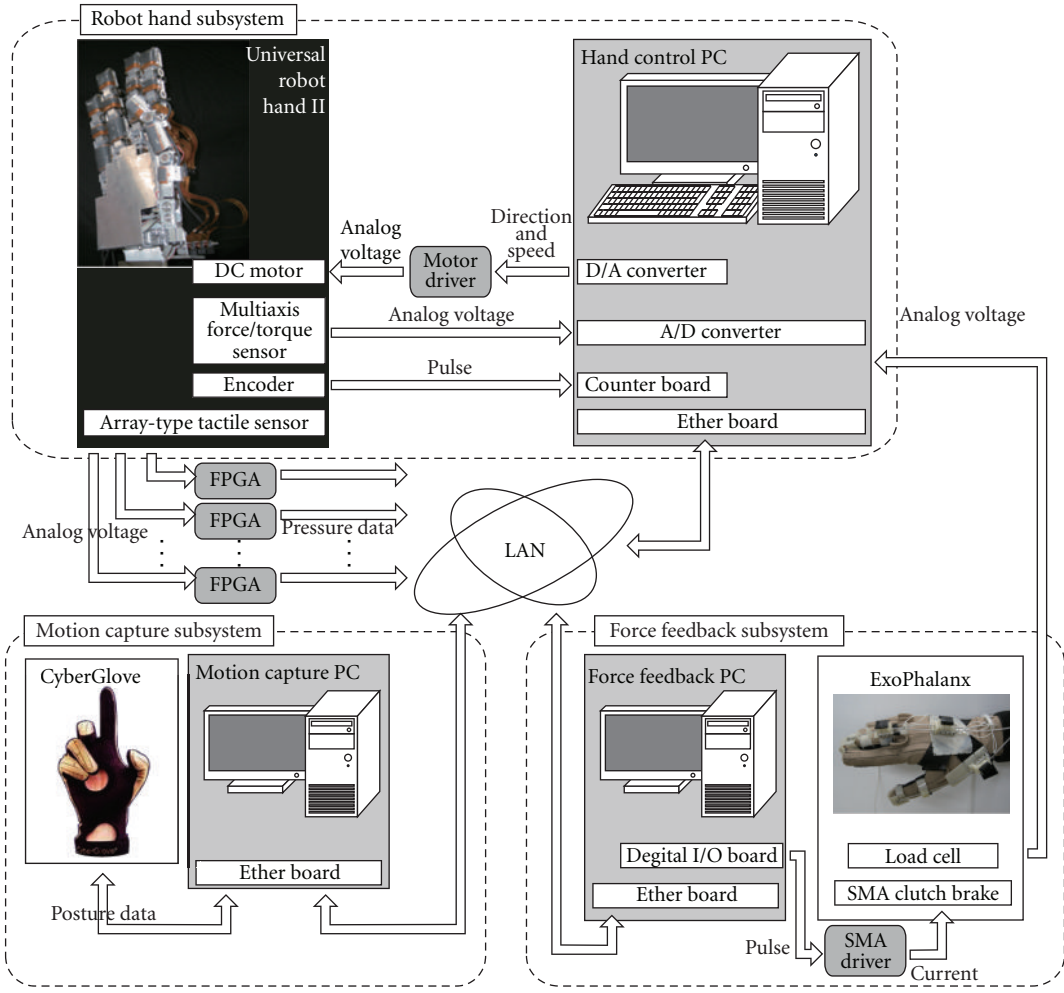

Figure 6: Robot hand teleoperation system with haptic device mounted on CyberGlove.

device. This device is wearable and mounted above the motion capture data glove CyberGlove using a tightening belt. Here, the body-grounded haptic device can create the illusion of directed forces by adequate positioning and distributing of grounding forces [27]. The ExoPhalanx consists of a thumb exoskeleton, a middle finger exoskeleton, and a manifer exoskeleton. The thumb exoskeleton consists of a distal phalanx and a proximal phalange ring. The middle finger exoskeleton consists of a distal phalanx, a middle phalange ring, and a proximal phalange ring. The proximal phalange ring of the thumb exoskeleton and the middle finger exoskeleton are belted on the proximal phalanx of the operator's finger. The manifer exoskeleton is belted on the operator's palm and forearm. This design takes advantage of the fact that fingertip mechanoreceptors are significantly more sensitive than those of the proximal phalanx, the forearm and the palm [28].

2.1. SMA Clutch Brake. An SMA clutch brake is installed in the ExoPhalanx, which is made into a string-like SMA. When the string-like SMA is heated over the transforming temperature, it is shortened. Alternatively, when it is cooled under the transforming temperature, it is lengthened to the original size. The SMA is flexible and the diameter is 150 μm. Here, the SMA is used as a clutch brake as shown in Figure 2. The heated SMA tightens a force transmission wire causing frictional force in the wire. The frictional force is presented as a force to the human operator. The SMA is heated using electricity because the SMA has electrical resistance of ~300 Ω/m. The cooling state of the SMA is based on the natural cooling process.

The driver circuit is simplified for the SMA clutch brake by using the Pulse Width Modulation (PWM) as the heating method. The PWM applies a square wave voltage with the duty ratio D. The heat quantity per unit time is as follows,

$$\int_0^1 \frac{dQ}{dt}dt = \frac{IV}{T}\int_0^\tau dt = D \cdot IV, \tag{1}$$

where Q, I, and V are the heat quantity, the applied current, and the applied voltage, respectively. In (1), T represents the cycle time of the square wave, τ is the time of the applied voltage in one wave, and the duty ratio, D, is defined as $D = \tau/T$.

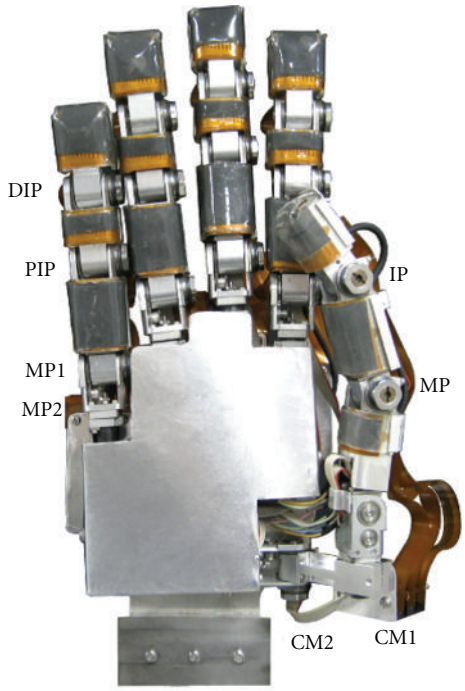

Figure 7: Universal robot hand I.

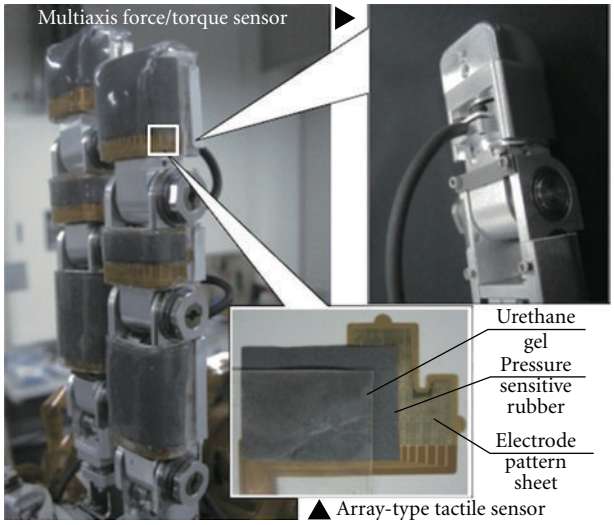

Figure 8: Tactile sensor and multi-axis force/torque sensor.

The size and weight of the SMA clutch brake are 1 mm^3 and 11 g, respectively. Figure 3 shows the clutching force of the clutch brake measured using the force gage FGP-0.2 (Nidec-SHIMPO Corporation) at various duty ratios. According to the graph, the clutching force is almost in proportional relation with the duty ratio.

2.2. Thumb Exoskeleton. The thumb exoskeleton is composed of a distal phalanx, a proximal phalange ring, and a thumb manifer as shown in Figure 4. A CM force transmission wire was used in the exoskeleton. One end of this wire is fixed to the distal phalanx and the other is free. The wire traces the tendon of the operator's thumb and passes the proximal phalange ring. A CM SMA clutch brake is placed on the thumb manifer. The wire slides normally and bends with IP, MP, CM joints of human thumb, unless it is engaged in which case the wire stops and restrains bending of the thumb.

2.3. Middle Finger Exoskeleton. The middle finger exoskeleton is composed of the distal phalanx, a middle phalanx ring, and a proximal phalange ring as shown in Figure 5. The middle finger exoskeleton consists of two force transmission wires, which were used for restricting the bend in the DIP joint of the human middle finger and for the MP joint or the DIP force transmission wire and MP force transmission wire, respectively. One end of the DIP force transmission wire is fixed to the distal phalanx part and the other is free. Similarly, one end of the MP force transmission wire is fixed to the proximal phalange ring and the other is free end.

The DIP and MP force transmission wires follows the tendons of the human middle finger. The DIP force transmission wire passes the DIP SMA clutch brake on the proximal phalange ring and under the MP SMA clutch brake. The MP force transmission wire passes into the MP SMA clutch brake on the manifer. The DIP wire slides with DIP and PIP joint rotation. The MP wire slides with bend-stretch rotation of the MP joint. When the DIP SMA clutch brake is driven, the operator DIP-PIP joint bending is locked. When the MP SMA clutch brake clutches the MP wire, the operator MP joint bending is locked. A loadcell mounted on the distal phalanx exoskeleton measures fingertip force of the operator's middle finger. The operator bends their middle finger and pushes the loadcell, which measures the force on the middle fingertip.

3. Robot Hand Teleoperation System with Haptic Device

Figure 6 shows the robot hand tele-operation system with the developed ExoPhalanx device. The tele-operation system consists of the robot hand subsystem with the universal robot hand II, the motion capture subsystem with the CyberGlove which is a well-knows motion capture data glove, and the force feedback subsystem with the developed ExoPhalanx device. In the robot hand tele-operation system, the universal robot hand II is controlled according to the motion of the operator's hand measured in the motion capture subsystem. Then, the ExoPhalanx gives a reaction force to the operator in the force feedback subsystem.

3.1. The Robot Hand Subsystem with Universal Robot Hand II. This subsystem controls the motion of the universal robot hand by the PID control and acquires the force and the tactile measurements. The universal robot hand II has five movable fingers and a palm as shown in Figure 7. The thumb is 195 mm long and the other fingers are 230 mm long with four joints. Each joint is driven using a miniaturized DC motor with a rotary encoder and reduction gears

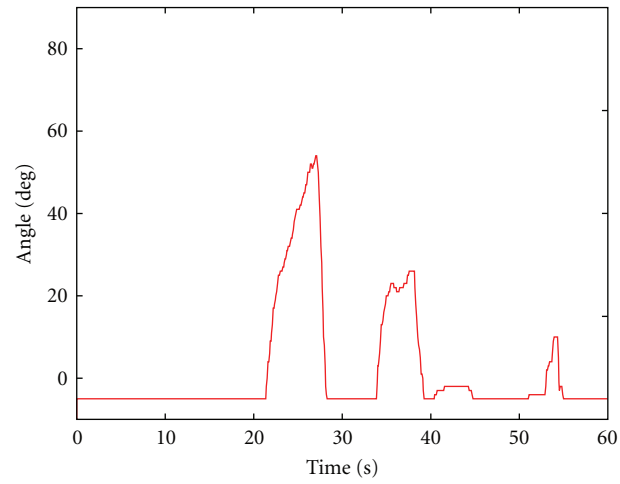

Figure 9: DIP joint angle against time.

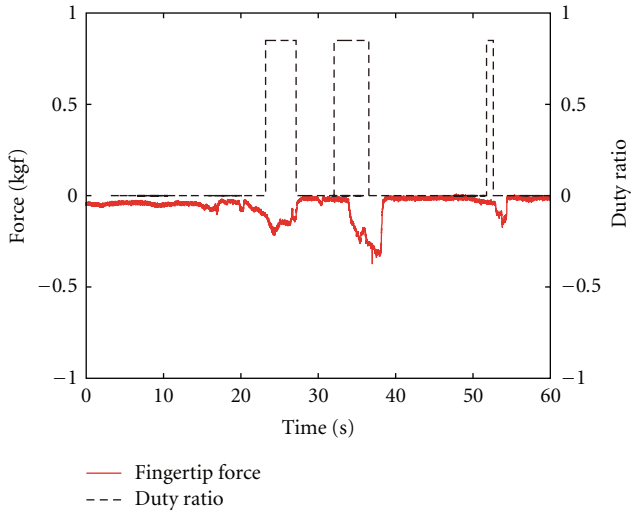

Figure 10: Force and duty ratio against time.

(manufactured by Harmonic Drive Systems. co.) built into each link. In addition, two fingertip joints, joints 3 and 4, drive at equal ratios as a human finger, so each finger has three degrees of freedom. Each finger has multi-axis force/torque sensors (manufactured by BL AUTOTEC, Ltd.) in the distal link of the finger and array-type tactile sensors on the palmar surface of the fingers as shown in Figure 8. Here, the multi-axis force/torque sensor is used in detection of the distal phalange link contact object and the array-type tactile sensor is used in detection of the proximal phalange link contact object.

3.2. Motion Capture SubSystem with CyberGlove. This subsystem measures the posture of the operator by using the CyberGlove. The measured operator's posture is sent to the robot hand subsystem through the network. The CyberGlove has three flexion sensors per finger, four abduction sensors, a palm-arch sensor, and sensors to measure wrist flexion and abduction. Here, this subsystem utilizes the sensor values except the DIP joints because the DIP joints and the PIP joints of the universal robot hand synchronize like a human finger.

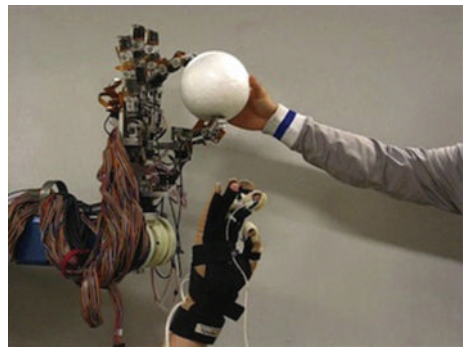

Figure 11: Two finger grasping experiment.

3.3. Force Feedback Subsystem with ExoPhalanx. A human operator wears the ExoPhalanx, which is mounted on the CyberGlove. The ExoPhalanx works in order to restrain the human fingers according to the contact force measured by the multi-axis force/torque sensors and the array-type tactile sensors in the universal robot hand. Here, the multi-axis force/torque sensor measures the contact force on the fingertips, and the tactile sensor measures the contact force on the palmar surface of the proximal phalange. If the thumb and/or the middle fingertip of the robot hand contacts the object, then the ExoPhalanx control PC drives the CM and/or the DIP SMA clutch brake. Similarly, if the proximal phalange of the middle robot finger contacts the object, then the ExoPhalanx control PC drives the MP SMA clutch brake. Consequently, the human operator cannot bend his thumb and/or the middle finger.

4. Experiments

The performance of the ExoPhalanx is verified through two experiments. The first is the clutch brake experiment used to confirm the performance of the SMA clutch brake. The second is the two finger grasping experiment used to evaluate the haptic feedback performance. Here, the duty ratio for controlling the SMA clutch brake is fixed in these experiments because it is difficult to control the force presented to the operator by changing the duty ratio.

4.1. Clutch Brake Experiment. To confirm the haptic performance of the SMA clutch brake, a preliminary experiment is executed. In this experiment, we confirm whether the SMA clutch brake can restrain the human operator from bending his/her finger.

The human operator wears the CyberGlove and the ExoPhalanx and bends the DIP and PIP joints of their middle finger. The CyberGlove captures the operator's postures. In this experiment, the operator bends the DIP joint over 20°, theoretically resulting in the ExoPhalanx stopping the corresponding force transmission wire. If the operator feels

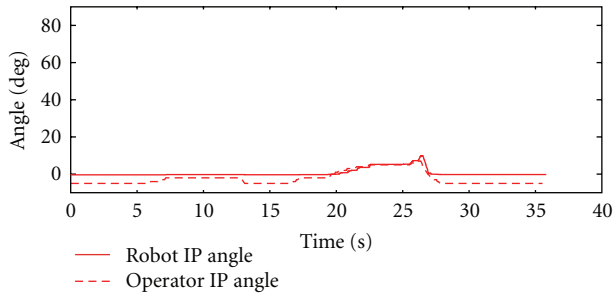

(a) IP joint angle

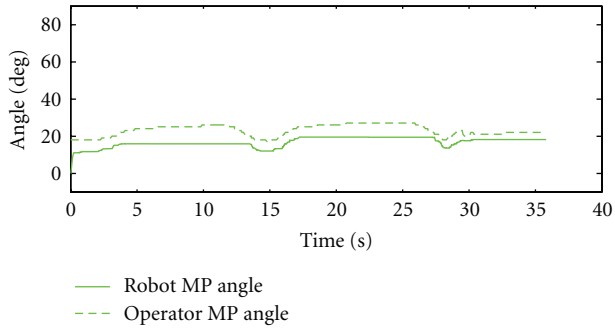

(b) MP joint angle

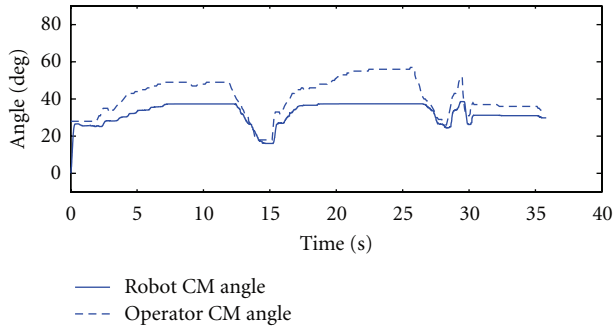

(c) CM joint angle

Figure 12: Joint angles of thumb for robot and operator.

sufficient force at the specified joints, then the operator stretches the middle finger. The change of the DIP joint angle and force presented to the human operator are shown in Figures 9 and 10, respectively. Figure 10 includes the change of the duty ratio in the experiment. From the clutch brake experiment, the operator recognizes that their DIP joint is locked by the ExoPhalanx and stretches their middle finger. However, if the operator bends the DIP joint over 20°, the SMA clutch brake stops the DIP force transmission wire because the force transmission wire loosens.

4.2. Two-Finger Grasping Experiment. A two-finger grasping experiment is used to evaluate the haptic feedback performance by the ExoPhalanx as shown in Figure 11. The grasped object is a polystyrene ball of 150 mm in diameter similar to the size of a baseball.

The duty ratio is constant for driving the SMA clutch brake. The operator then manipulates the universal robot hand II using the following protocol:

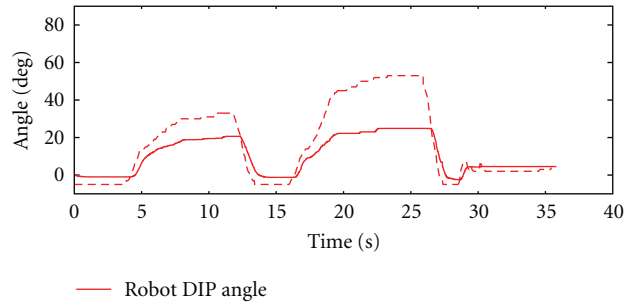

(a) DIP Joint Angle

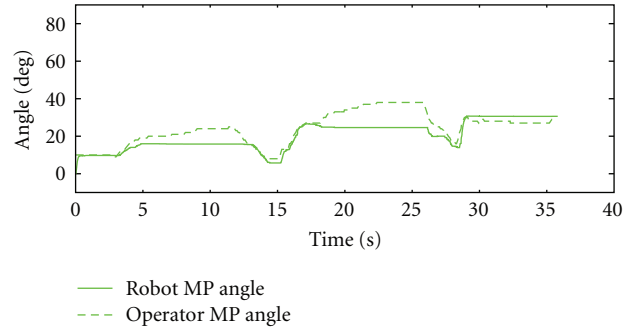

(b) MP joint angle

Figure 13: Joint angles of middle finger for robot and operator.

(1) The operator stretches all fingers.

(2) The ball is set in front of the universal robot hand II.

(3) The operator remotely manipulates the robot hand with the thumb and middle finger to grasp the ball with the fingertips of the robot hand.

(4) The operator continues bending their fingers until a reaction force on their fingertip from the ExoPhalanx is felt.

(5) If the operator feels sufficient force, they release the ball.

This experiment is implemented twice with the experiments being soft and strong grasping.

Figures 12 and 13 show the results of the two-finger grasping experiment. The IP, MP, and CM joint angles of the thumb for the robot hand and the operator are shown in Figures 12(a), 12(b), and 12(c), respectively. The DIP and MP joint angles of the middle finger for the robot and operator are shown in Figures 13(a) and 13(b), respectively. From these figures, the robot hand grasps the ball with the CM joint at 37° of the robot thumb and the DIP joint at 20° of the robot middle finger. Although the robot hand grasps the ball, the operator's CM joint of the thumb and DIP joint of the middle finger are over the joint angles of the robot hand. This is because the force transmission wire loosens similarly to the clutch brake experiment. Figures 14 and 15 show the force measured in the robot hand and the operator's hand, respectively. Here, the force of the operator's hand is measured by the loadcell equipped in ExoPhalanx. In Figures 14 and 15, the maximum forces of the robot hand

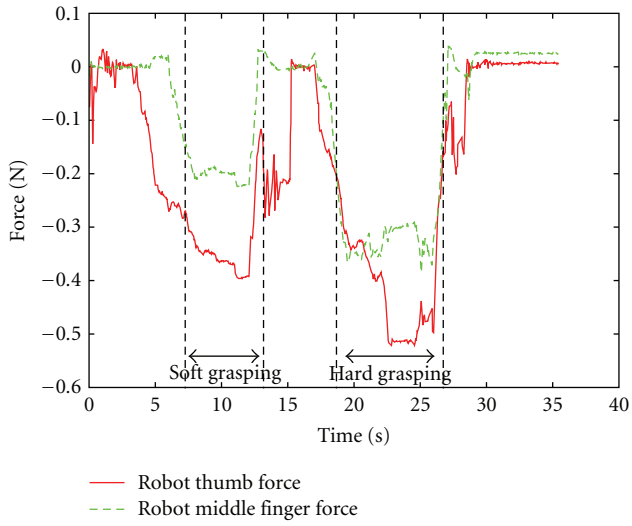

Figure 14: Force measured in robot hand.

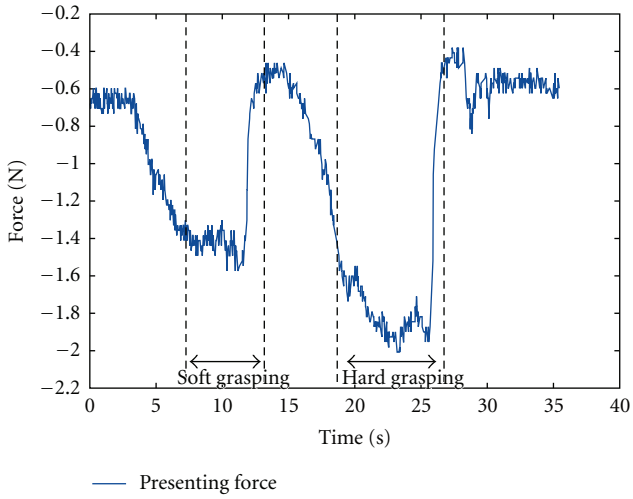

Figure 15: Force measured in operator hand.

and the operator's hand are about 0.2 N and 1.5 N in the soft grasping experiment, and those maximum force are about 0.4 N and 2.0 N in the hard grasping.

5. Conclusions and Future Works

5.1. Conclusions. Presented herein was the reaction force using a haptic feedback device allowing for important scientific advancement in the operation of a robot hand remotely and dexterously. We developed the passive force feedback device ExoPhalanx. ExoPhalanx is a small and lightweight device that uses an SMA-fitted clutch brake. The developed ExoPhalanx provides reaction force on the distal phalange and proximal phalange to the remote operator. Moreover, in the tele-operation system, ExoPhalanx was mounted to the motion capture data glove, CyberGlove. The effectiveness of the ExoPhalanx system for tele-operation applications was verified through preliminary experiments.

5.2. Future Works. The future work involves improvement of the SMA clutch brake so that it is proportionally controlled and reduces the backlash between each link of the exoskeletons. Moreover, we will develop a control method of the fingertip force presented to the operator and present the force according to the measured force in the universal robot hand II by the ExoPhalanx. Finally, it is proposed that the ExoPhalanx system will be extended to five fingers.

References

[1] J. M. Hollerbach and S. C. Jacobsen, "Anthropomorphic robots and human interactions," in *Proceedings of the 1st International Symposium on Humanoid Robots*, pp. 83–91, 1996.

[2] D. Johnston, P. Zhang, J. Hollerbach, and S. Jacobsen, "Full tactile sensing suite for dextrous robot hands and use in contact force control," in *Proceedings of the IEEE International Conference on Robotics and Automation*, pp. 661–666, 1996.

[3] T. Mouri, H. Kawasaki, K. Yoshikawa, J. Takai, and S. Ito, "Anthropomorphic robot hand: gifu hand III," in *Proceedings of the International Conference on Control, Automation and Systems*, pp. 1288–1293, 2002.

[4] T. Mouri, H. Kawasaki, and K. Umebayashi, "Developments of new anthropomorphic robot hand and its master slave system," in *Proceedings of the IEEE/RSJ International Conference on Intelligent Robots and Systems*, pp. 3474–3479, 2005.

[5] H. Iwata and S. Sugano, "Design of anthropomorphic dexterous hand with passive joints and sensitive soft skins," in *Proceedings of the 2nd IEEE International Symposium on System Integration (SII '09)*, pp. 129–134, 2009.

[6] K. Takahashi, H. Waita, M. Kokusho, and M. Hayakawa, "Development of dexterous and powerful multi-fingered hand for humanoid robots," in *Proceedings of the 27th Annual Conference of the Robotic Society of Japan*, vol. AC1A1-01, 2009.

[7] K. Kaneko, K. Harada, and F. Kanehiro, "Development of multi-fingered hand for life-size humanoid robots," in *Proceedings of the IEEE International Conference on Robotics and Automation (ICRA '07)*, pp. 913–920, Roma, Italy, April 2007.

[8] S. Schulz, C. Pylatiuk, and G. Bretthauer, "A new ultralight anthropomorphic hand," in *Proceedings of the IEEE International Conference on Robotics and Automation (ICRA '01)*, pp. 2437–2441, May 2001.

[9] J. Jockusch, J. Walter, and H. Ritter, "A tactile sensor system for a three-fingered robot manipulator," in *Proceedings of the IEEE International Conference on Robotics and Automation (ICRA '97)*, pp. 3080–3086, April 1997.

[10] H. Nakamoto, F. Kobayashi, and F. Kojima, "Shape classification using tactile information in rotation manipulation by universal robot hand," *Robotics 2010 Current and Future Challenges*, pp. 123–132, 2010.

[11] W. Fukui, F. Kobayashi, F. Kojima et al., "Development of multi-fingered universal robot Hand with torque limiter mechanism," in *Proceedings of the 35th Annual Conference of the IEEE Industrial Electronics Society*, pp. 2225–2230, 2009.

[12] M. D. Duong, K. Terashima, T. Miyoshi, and T. Okada, "Rehabilitation system using teleoperation with force-feedback-based impedance adjustment and EMG-moment model for arm muscle strength assessment," *Journal of Robotics and Mechatronics*, vol. 22, no. 1, pp. 10–20, 2010.

[13] S. J. Biggs and M. A. Srinivasan, "Haptic interfaces," in *Handbook of Virtual Environments: Design, Implementation,*

and Applications, Human Factors and Ergonomics, K. Stanney, Ed., chapter 5, pp. 93–115, Lawrence Erlbaum Associates, 2002.

[14] T. Endo, H. Kawasaki, T. Mouri et al., "Five-fingered haptic interface robot: HIRO III," in *Proceedings of the 3rd Joint EuroHaptics Conference and Symposium on Haptic Interfaces for Virtual Environment and Teleoperator Systems*, pp. 458–463, Salt Lake City, Utah, USA, March 2009.

[15] T. Endo, T. Kanno, M. Kobayashi, and H. Kawasaki, "Human perception test of discontinuous force and a trial of skill transfer using a five-fingered haptic interface," *Journal of Robotics*, vol. 2010, Article ID 542360, 14 pages, 2010.

[16] P. Berkelman and M. Dzadovsky, "Extending the motion ranges of magnetic levitation for haptic interaction," in *Proceedings of the 3rd Joint EuroHaptics Conference and Symposium on Haptic Interfaces for Virtual Environment and Teleoperator Systems*, pp. 517–522, Salt Lake City, Utah, USA, March 2009.

[17] A. Gupta, M. K. O'Malley, V. Patoglu, and C. Burgar, "Design, control and performance of ricewrist: a force feedback wrist exoskeleton for rehabilitation and training," *International Journal of Robotics Research*, vol. 27, no. 2, pp. 233–251, 2008.

[18] W. Park and S. Park, "Haptic mouse interface actuated by an electromagnet," in *Proceedings of the International Conference on Complex, Intelligent, and Software Intensive Systems*, L. Kim and S. Shin, Eds., pp. 643–646, Seoul, Korea, June 2011.

[19] Z. Zhang and T. Chen, "Study on the control of 6-DOF manipulators system with force feedback," in *Proceedings of the International Conference on Intelligent Computation Technology and Automation (ICICTA '08)*, vol. 1, pp. 498–502, Hunan, China, October 2008.

[20] T. Amemiya, T. Maeda, and H. Ando, "Location-free haptic interaction for large-area social applications," *Personal and Ubiquitous Computing*, vol. 13, no. 5, pp. 379–386, 2009.

[21] K. N. Winfree, J. Gewirtz, T. Mather, J. Fiene, and K. J. Kuchenbecker, "A high fidelity ungrounded torque feedback device: the iTorqU 2.0," in *Proceedings of the 3rd Joint EuroHaptics Conference and Symposium on Haptic Interfaces for Virtual Environment and Teleoperator Systems, World Haptics 2009*, pp. 261–266, Salt Lake City, Utah, USA, March 2009.

[22] H. Gurocak, S. Jayaram, B. Parrish, and U. Jayaram, "Weight sensation in virtual environments using a haptic device with air jets," *Journal of Computing and Information Science in Engineering*, vol. 3, no. 2, pp. 130–135, 2003.

[23] A. Chang and C. O'Sullivan, "Audio-haptic feedback in mobile phones," in *Proceedings of the International Conference for Human-Computer Interaction (CHI '05)*, pp. 1264–1267, Portland, Ore, USA, 2005.

[24] H. Yano, Y. Miyamoto, and H. Iwata, "Haptic interface for perceiving remote object using a laser range finder," in *Proceedings of the 3rd Joint EuroHaptics Conference and Symposium on Haptic Interfaces for Virtual Environment and Teleoperator Systems, World Haptics 2009*, pp. 196–201, Salt Lake City, Utah, USA, March 2009.

[25] M. J. Lelieveld, T. Maeno, and T. Tomiyama, "Design and development of two concepts for a 4 DOF portable haptic interface with active and passive multi-point force feedback for the index finger," in *Proceedings of the ASME International Design Engineering Technical Conferences and Computers and Information In Engineering Conference (DETC '06)*, September 2006.

[26] K. Koyanagi, Y. Fujii, and J. Furusho, "Development of VR-STEF system with force display glove system," in *Proceedings of the International Conference on Augmented Tele-Existence (ICAT '05)*, pp. 91–97, Christchurch, New Zealand, December 2005.

[27] H. Z. Tan, M. A. Srinivasan, B. Eberman, and B. Cheng, "Human factors for the design of force-reflecting haptic interfaces," *American Society of Mechanical Engineers, Dynamic Systems and Control Division*, vol. 55, pp. 353–359, 1994.

[28] R. L. Klatzky and S. J. Lederman, "*Touch*", *Handbook of Psychology*, vol. 4 of *Experimental Psychology*, John Wiley and Sons, New York, NY, USA, 2003.

Hindawi Publishing Corporation
Journal of Robotics
Volume 2011, Article ID 284352, 8 pages
doi:10.1155/2011/284352

Research Article

Mina: A Sensorimotor Robotic Orthosis for Mobility Assistance

Anil K. Raj, Peter D. Neuhaus, Adrien M. Moucheboeuf, Jerryll H. Noorden, and David V. Lecoutre

Florida Institute for Human and Machine Cognition, 40 South Alcaniz Street, Pensacola, FL 32502, USA

Correspondence should be addressed to Anil K. Raj, araj@ihmc.us

Received 2 June 2011; Revised 10 September 2011; Accepted 15 October 2011

Academic Editor: Tetsuya Mouri

While most mobility options for persons with paraplegia or paraparesis employ wheeled solutions, significant adverse health, psychological, and social consequences result from wheelchair confinement. Modern robotic exoskeleton devices for gait assistance and rehabilitation, however, can support legged locomotion systems for those with lower extremity weakness or paralysis. The Florida Institute for Human and Machine Cognition (IHMC) has developed the Mina, a prototype sensorimotor robotic orthosis for mobility assistance that provides mobility capability for paraplegic and paraparetic users. This paper describes the initial concept, design goals, and methods of this wearable overground robotic mobility device, which uses compliant actuation to power the hip and knee joints. Paralyzed users can balance and walk using the device over level terrain with the assistance of forearm crutches employing a quadrupedal gait. We have initiated sensory substitution feedback mechanisms to augment user sensory perception of his or her lower extremities. Using this sensory feedback, we hypothesize that users will ambulate with a more natural, upright gait and will be able to directly control the gait parameters and respond to perturbations. This may allow bipedal (with minimal support) gait in future prototypes.

1. Introduction

The limited mobility assistance options for those suffering from paraplegia or paraparesis typically utilize wheeled devices, which require infrastructure (ramps, roads, smooth surfaces, etc.), and 69.8% of spinal cord injured (SCI) paraplegics use a manual wheelchair as their primary means of locomotion, which limits range and terrain options [1]. Wheeled conveyances allow access to only a small fraction of the locations accessible to pedestrians. Wheelchairs have trouble on curbs, stairs, irregular terrain such as hiking trails and narrow corridors. Even with advances in powered wheelchairs, such as the iBot (http://www.ibotnow.com/), mobility remains limited to relatively smooth terrain, precluding access to much of the natural outdoors. Additionally, being confined to a wheelchair has significant consequences on physiological and psychological health, quality of life, and social interactions. Health-related issues include pressure sores, poor circulation, loss of bone density muscle mass, and changes in body fat distribution [2–4]. Robotic lower extremity orthosis designs can offer new mobility options for those currently limited to a wheelchair, enabling such individuals to regain access to areas that require legged locomotion and to restore the health benefits associated with an upright posture. In addition to improving quality of life as orthotic devices, exoskeletons could also bridge the gap to future regenerative medicine approaches for this population. For example, a paraplegic user of a robotic orthosis could maintain healthy bone and muscle mass and range of joint motion that could reduce rehabilitation time following stem cell therapy.

1.1. Robotic Orthoses. Current robotic assistance devices such as the body-worn ReWalk from Argo Medical Technologies (http://www.argomedtec.com/) and the eLegs from Berkely Bionics (http://berkeleybionics.com/) have motors at the hips and knees to move the legs and provide powered gait. The user provides balance with the aid of forearm crutches and uses torso motions, arm movements, and/or a push button interface. Both devices can operate untethered for several hours on a single charge. Users have demonstrated stair climbing with the ReWalk; however, neither device has demonstrated operations over rough and irregular terrain. Both

devices target paraplegic users who cannot initiate any motion of their legs and thus must operate in a rigid position control mode. Use by paraparetics, however, requires a more compliant mode of operation. Both devices are undergoing clinical trials, and neither device is currently available for personal use.

The commercially available hybrid assistive limb (HAL) device, which has significant operational experience with able-bodied users [5], augments user-initiated movement by detecting electromyographic (EMG) signals in the user's lower extremity muscles. A new version of this device, HAL-5 LB (Type C), specifically targets paraplegic users [6], but has only demonstrated transition from sitting to standing, not overground mobility. This design, however, does include an actuator at the ankle, a feature lacking from the ReWalk and the eLegs. The wearable power assist leg (WPAL) [7, 8], another paraplegic gait assist device, relies on a walker rather than crutches for the required balance stabilization. The walker provides a significant support polygon for the user and requires a different, less natural gait. Similarly, the EXoskeleton for Patients and the Old by Sogang University (EXPOS) [9], designed as a walking assist device for the elderly and for patients with muscle or nerve damage in the lower body, uses a wheeled-caster walker to carry the actuators and computer system. It transfers actuator forces to the exoskeleton joint via cables and employs position control of the exoskeleton joints, but it lacks force sensing in the actuators. Force sensors on the leg braces are used to detect the user intent, but the integral caster walker limits operation and utility of this device to smooth floors. Zabaleta et al. [10] also propose to track EMG and utilize compliant actuation for a robotic exoskeleton for rehabilitation.

A number of robotic orthoses developed for treadmill-based operation face some of the same challenges, share some of the same technologies, and they are strictly limited to rehabilitation activities. The Powered Gait Orthosis (PGO) [11] and LOwer-extremity Powered ExoSkeleton (LOPES) [12] utilize force sensors on each actuator, which allows for torque control of the joints. One of the most utilized and studied treadmill-based robotic orthotic devices, the Lokomat [13, 14], has demonstrated the advantages of compliant control strategies [15, 16].

At the Florida Institute for Human and Machine Cognition (IHMC), we have designed and built a robotic orthosis called Mina (Figure 1) to provide overground mobility for paraplegic and paraparetic users. Mina utilizes compliant control actuators and can provide both rigid position control for paraplegic users and assistive force control for paraparetic users. In its current state of development, the prototype Mina offers operates similarly to the ReWalk and eLegs for paraplegic mobility with hip and knee actuation for powered execution of recorded gait. All three devices move the legs through predetermined joint trajectories with strict position control of the exoskeleton joint. However, the compliant control actuators that Mina utilizes facilitate operation over rough terrain.

In addition, Mina provides the user with sensory feedback from the exoskeleton. Sensory feedback provides a key element for motor-control missing from other paraplegic mobility assist devices. SCI users lack body awareness below the level of injury, which makes user control of orthotic devices cumbersome. Reinstating sensory feedback should facilitate the integration of the orthosis into the user's posture and ambulation strategy and, potentially, restoration of bipedal gait for this population.

Figure 1: The IHMC Mina sensorimotor robotic orthosis for mobility assistance prototype. Mina adjusts to fit users ranging from ~1.6 m to 1.9 m tall.

1.2. The Sensory Substitution Paradigm. Because perception occurs in the brain and not at the sensory end organ [17], sensory substitution interfaces can provide an alternative pathway for sensory perception. A sensory substitution system consists of three parts: a sensor, a coupling system, and a stimulator. Sensory substitution can occur across sensory systems such as touch-to-sight or within a sensory system such as touch-to-touch. The human brain, in fact, can reinterpret signals from specific nerves (e.g., from tactile receptors) given appropriate, veridical, and timely sensory feedback. This forms the basis for sensory substitution interfaces that can noninvasively and unobtrusively use alternative, intact sensory pathways. This plasticity inherent to the brain and nervous system supports both long-term and short-term anatomical and functional remapping of sensory data [18, 19] and will assist brain reorganization despite losses in muscle, bone, reflexes and will assist a user's ability to perform activities of daily living [20]. Tactile and proprioceptive feedback sensory substitution technologies have been developed for use with lower limb prostheses [21–24] to provide foot sole pressure information, joint angle, and other forces. Because paralyzed individuals lack proprio- and exteroception from the lower limbs, they must use their vision to monitor "what's going on" below their level of injury. Compensating for the loss of tactile information from the soles, as well as proprioceptive information (i.e., muscle

stretch and joint position) visually requires significant cognitive effort that could be redistributed through other sensory modalities. Mina provides similar input for users with intact but paralyzed legs by providing ground reaction forces and proprioceptive signal analogs from the insensate feet. The fundamental challenges for sensory augmentation in an exoskeleton relate to identification of the optimal information for the user when walking and intuitive presentation of that information without increasing cognitive workload or competing with vision or hearing.

1.3. Human Machine Interface (HMI) Considerations. The human motor control system relies on sensory information (feedback) in order to respond to perturbations and stabilize errors. Sensory feedback, for example, enables the brain to maintain the body's posture and helps it to determine the positions of the limbs in space and the amount of force required to execute a movement. Several sensory systems (i.e., the vestibular, visual, and somatosensory systems) contribute to the control of balance and offer an important channel of information that help to coordinate human interaction with the world. The vestibular system gives the sense of whole body orientation and motion in collaboration with the visual system. For both posture and gait, motor control mechanisms seek to hold the body's center of gravity (CG) over the polygon of support (defined by the position of the individual's feet). While determining position of the center of mass under dynamic conditions is hard to compute, the central nervous system can infer its position by using the information provided by the muscle-tendon stretch receptors and the cutaneous pressure receptors of the foot sole. Paraplegia deprives the user of both the motor and sensory functions; restoring mobility requires reinstatement of movement and sensation. The IHMC Mina system displays ground reaction forces and center of pressure, as well as joint positions and torque estimations, using noninvasive tactile interfaces, specifically a BrainPort intra-oral display (Wicab, Inc., Middleton, WI) and a VideoTact abdominal display (ForeThought Development, LLC, Blue Mounds, WI). These displays (Figure 2) interface to the relatively underutilized, with respect to hearing and vision, tactile channel and provide sufficient resolution for the data represented by Mina.

The BrainPort electrotactile transducer array is held in the mouth and connected to battery powered electronics that generate highly controlled electrical pulses that produce patterns of tactile sensations when the electrodes are in contact with the top surface of the tongue. The tongue's sensitivity, excellent spatial resolution, mobility, and distance to the brainstem make it an ideal site for a practical electrotactile HMI. An electrolytic solution (saliva) assures good electrical contact. Perception with electrical stimulation of the tongue appears to be better than with fingertip electrotactile stimulation, and the tongue requires only about 3% (5–15 V) of the voltage, and much less current (0.4–2.0 mA) than the fingertip for electrotactile stimulation [25]. Current BrainPort arrays can provide a 100 to 600 pixel resolution via the intraoral display (IOD) tongue array.

The VideoTact is also an electrotactile interface; however, it is placed on the abdomen. It can exploit the larger surface area of the abdomen to improve spatial separation. While the density of torso sensory receptors is not as high as the tongue, placing a high-resolution display (e.g., 24×32) on the abdomen allows for rapid perception of motion of objects [26] and can be worn discretely under the users clothing. The keratinized layer of dead skin cells of the epidermis on the torso requires the VideoTact to use higher voltage (15–40 VDC) and current (8–32 mA) than the BrainPort; however, it is battery driven and further electrically isolated by storing the stimulus charge in an array of capacitors that are disconnected from the power source prior to stimulus delivery.

Integrating these two displays to provide sensory substitution of proprioception and somatosensation to Mina users should lead to shorter training requirements, improved sense of balance, and sensorimotor reorganization that integrates both perception and control of the exoskeleton. Both devices have intensity control via software with user override for intensity and shut-off. IHMC has used these general-purpose sensory substitution displays previously for augmentation of individuals with balance disorders, as well as for vision and hearing substitution systems. IHMC is currently investigating the effectiveness of various sensory substitution symbologies to provide the user with an effective, intuitive understanding of the state of the exoskeleton with low cognitive demand.

2. Exoskeleton Design

Mina is a second-generation [27] lower extremity robotic gait orthosis with two actuated degrees of freedom per leg, hip flexion/extension, and knee flexion/extension, for a total of four actuators. Mina does not provide hip ab-/adduction or medial/lateral rotation of the leg and employs rigid ankle joint with a compliant carbon fiber footplate. Mina users connect to a rigid back plate, which has a curvature to match that of the human spine, via shoulder and pelvic straps. The system can accommodate a range of body sizes by using nested aluminum tubing as the structural links to attach to the user's thigh, leg, and foot. A tether provides the prototype with power for the computer and motors, as well as Ethernet communication; later versions will integrate battery power and wireless communications technologies for untethered operations. A fall prevention tether connected to an overhead trolley system supports the user and Mina only in the event that the user loses balance or missteps.

2.1. Actuators. Mina uses four identical rotary actuators (Figure 3) capable of both position and torque control. Each actuator consists of a DC brushless motor (Moog BN34-25EU-02) and a 160 : 1 harmonic drive (SHD-20 from HD Systems) gear reduction. The actuators are instrumented with two incremental encoders. One encoder measures the relative position between the motor shaft and the base of the actuator. This encoder (HEDL-5640#A13, Avago Technologies, Inc. San Jose, CA) has a resolution of 2000 counts per revolution, resolving to $1.96e-5$ rad/count at the output. The second encoder (RGH-24, Renishaw, PLC, Gloucestershire, England) measures the relative position between

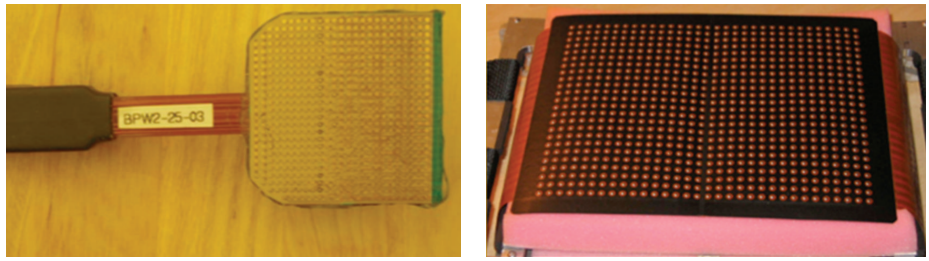

(a) (b)

Figure 2: Tactile sensory substitution electrotactile displays used by Mina. (a) Wicab BrainPort 600 pixel tongue array; (b) a 768 titanium electrode abdominal array (ForeThought VideoTact).

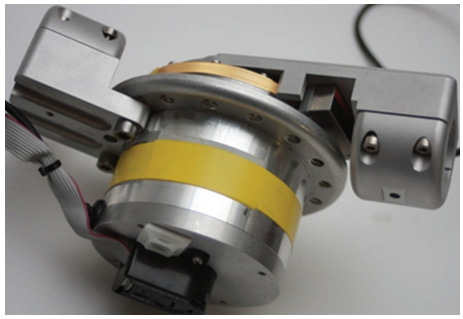

Figure 3: Actuator showing two encoders, golden read strip that is wrapped around the base of the harmonic drive gear reduction.

the output of the actuator and the base of the actuator using a linear encoder with the read-head mounted onto the output of the actuator and the linear encoding strip wrapped around the surface of the harmonic drive input (which is securely fixed onto the base of the actuator). This encoder has a resolution of 1 mm at a radius of 0.45 m, which resolves $2.22e-5$ rad/count.

The motion of the output encoder matches the motion of the motor encoder, minus any elastic deformation of the harmonic drive due to torque applied to the output shaft. By applying a known torque and measuring the deflection using the difference between the two encoders, we characterized the elasticity of each actuator. With a peak torque of about 60 Nm, the elastic deflection is about 0.0025 rad, indicating a stiffness of approximately 24 kNm/rad. In operation, an empirically determined look-up table is used to indicate the torque of the actuator based on harmonic drive deflection.

The Mina operates in position, or high impedance, control using only the motor shaft encoder (Avago HEDL-5640#A13) instead of the output encoder (Renishaw RGH-24) due to occasional loss of counts of the output encoder. Because the deflection of the harmonic drive is considered negligible with regard to the tolerance required on the output position, the simple proportional plus derivative feedback control algorithm only needs the output position to control the motor input current.

A series elastic actuator (SEA) was used in order to achieve torque control. In designing the SEA, the major design element to select is the spring rate, which is dependent on a number of factors, including the resolution of the spring deflection sensor, the maximum speed of the motor, the amount of impact isolation allowed to the gear train, the acceptable reflected inertia at the output, the bandwidth requirements on position and torque control, and complexity of the design. Our application can tolerate a stiff spring due to the inherent impact protection from the connection to the user and requires a stiff spring due to tight positioning requirements. By utilizing high-resolution encoders (approximately $2.0e-5$ radians/count) the design is able to function with a very stiff series spring. We determined that the inherent compliance of the harmonic drive was sufficient for this application and would result in a compact, low part count design. For torque control, Mina uses a simple proportional plus derivative controller (see Figure 4) where the error signal equals desired torque minus the applied torque and is used to determine the input current to the motor. The feedback gains were tuned empirically. The value for K_p was 2.0, and the value for K_d was 0.0002.

2.2. Computer and Electronics. An embedded PC-104 computer system mounted on the back plate, running a Real-Time Java under Solaris (Oracle, Corp., Redwood Shores, CA) and the control software, written in Real-Time Java provides closed-loop control of the actuators via Accelnet digital servo modules (ACM-180-20, Copley Controls, Peabody, MA) and communicates with a desktop host computer via a tethered Ethernet cable. The embedded computer runs the control code, stores the trajectories used for the paraplegic walking-mode and transmits relevant state variables to a host computer in real time (50 Hz) for display and monitoring.

Mina uses F-Scan (Tekscan, Inc., Boston, MA) insoles placed between the footplate and the shoe with up to 960 pressure sensors to detect ground reaction forces and determine center of pressure on each foot (smaller insoles are cut form the standard size, resulting in fewer total sensors). Figure 5 shows the normalized pressure map from the insoles (black = zero pressure, white = normalized maximum recorded during calibration). This map is resampled to match the 600 pixel array of the BrainPort IOD and presented as intensity (a tingling sensation) on the tongue. With a few minutes of training, a user can learn to interpret this signal as pressure on his or her feet.

Similarly, joint position from the actuator encoders and torque estimated from actuator current draw can be used to estimate the position of the Mina-user system CG over

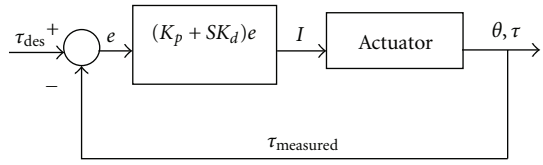

Figure 4: Diagram showing the feedback loop used to control the output torque of the actuator.

the stability polygon defined by the current stance as well as the relative "effort" exerted by Mina to maintain the current posture or execute a step. When presented on the VideoTact as a moving CG icon and a dynamic stability polygon, we believe that users will be able to effectively maintain awareness of their limits of stability during ambulation.

3. Gait Generation and Operation

Mina operates as a motion capture system that records trajectories from an able-bodied individual, which can then be "played back" in the paraplegic assistance mode. This method allows for generation of a natural gait with a quick development cycle.

3.1. Generating Walking Trajectories. Walking trajectories were generated from joint position recordings made while an able-bodied person wearing Mina walked over level terrain in the laboratory. This method of gait trajectory generation was selected because it allows for relatively natural gaits and the ability to develop new gaits in a short period of time. During this process, the actuators were set to torque control mode. For the hip joints, the desired torque was set to zero so that Mina would follow the user's motions without affecting them. Compliance in the user's flesh and the braces of Mina can result in a few degrees of offset between the user's joints and the device's joints. For example, full knee extension may occur before the knee joint of Mina extends fully. However, in paraplegic assistance mode, stable stance requires that the Mina knee joint extend fully. In order to assist the knee joint to the fully extended position while recording the gait, the desired torque was set to be 10 Nm in extension. This torque, generated by the actuators, ensured that the knee was fully extended during stance phase while allowing the able-bodied user to overcome it during swing.

Toe-off provides a significant component of natural gait [28] and people minimize the ground clearance of the foot as part of a muscle energy conservation strategy. However, for a robotic orthosis, electrical energy conservation does not equal muscle energy conservation. Because Mina lacks an ankle actuator, the able-bodied user walked with an exaggerated ground clearance in swing phase during gait recording to guarantee that the toe does not stub on the ground. The resulting gait mimicked walking on a slippery surface (i.e., with minimal the ground reaction shear forces). Because Mina does not have the same actuated degrees of freedom as a healthy person, the resultant gait cannot match that of a healthy person. In human walking, there is complex feedback loop between terrain sensing, joint position, and body position. Replicating this complex loop, especially the terrain sensing, will be studied in future work.

Table 1

Leg length (dist. from hip joint to ankle)	Actual step size	Step period	Walking speed
0.840 m	0.24 m	1.4 s	0.18 m/s
0.785 m	0.28 m	1.4 s	0.20 m/s

After the recording phase, the trajectories were played back in paraplegic assistance mode with an able-bodied user with relaxed lower limb muscles. From this playback, the best single gait cycle (stance and swing phase) was selected to use as a basis for the final walk. The joint angles at the end of this gait cycle were adjusted to match the starting joint angles, allowing the step to be played back in a smooth, endless loop. The joint angles were then copied to the other leg with a half cycle phase shift. This ensured that the left leg and the right leg executed the exact same step with the appropriate phase shift.

Three different walks were recorded, with step sizes ranging from zero (stepping in place) to what will be referred to as a large step. The precise value of the step size for a given walk depends on the leg length of the user. The quickest step period we have used to date with Mina is 1.4 seconds per step. The resulting walking speeds are presented in Table 1. Note that the recorded gait consists of a sequence of desired joint angles. The resulting walking speed is a function of how fast this sequence of desired joint angles is played and of the leg length of the user. The longer the user leg length the larger the actual step, and thus the faster the resulting walking speed. The fastest walk speed recorded was 0.2 m/s (see Table 1), which was limited by actuator performance rather than user capability.

The joint angles at the end of the best single recorded gait cycle (stance and swing phase) were adjusted to match the starting joint angles, allowing the step to be played back in a smooth, endless loop, and the joint angles were then copied to the other leg with a half cycle phase shift.

3.2. Operation. The Mina currently requires an external control operator in paraplegic assistance mode to activate/deactivate the system, trigger a single step or continuous steps, stop walking, and change gait speed between 50% and 130% of the recorded speed. In addition, the operator can adjust the time the controller pauses between left and right steps and responds to verbal and gesture cues from the user. For effective real-world mobility assistance, the user must have full control of the exoskeleton, which requires sensory perception of the orthosis dynamics. Sensory substitution interfaces provide this functionality in the updated Mina device.

4. Results from Initial Evaluations

Following IHMC Institutional Review Board (IRB) approval, two evaluators tested the initial Mina prototype. We required the evaluators to have an American Spinal Injury Association

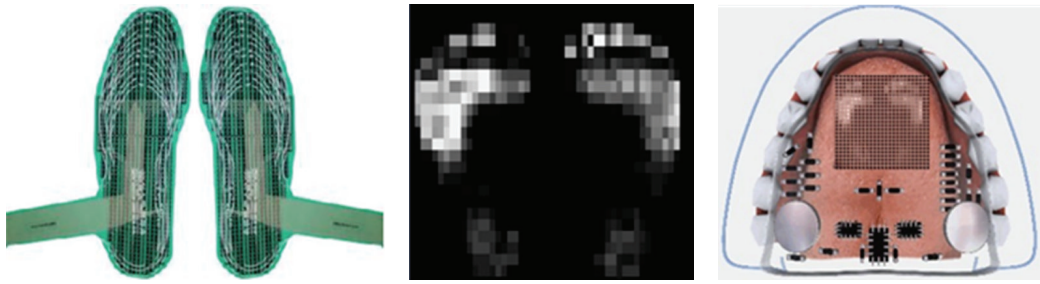

(a) (b) (c)

Figure 5: (a) Insole pressure sensory arrays (F-Scan); (b) visual representation of ground reaction force; (c) Mina representation of contact forces on Wicab BrainPort IOD.

(ASIA) Impairment Scale [29]. A (Complete) and a Walking Index for Spinal Cord Injury (WISCI) level 9 (Ambulates with walker, with braces and no physical assistance, 10 m) or higher [30]. Although the evaluators were able to walk prior to their SCI, walking in Mina differs significantly from able-bodied walking. As mentioned before, complete paraplegics lack feedback of the ground reaction force and center of pressure on their feet. Additionally, they do not use their remaining proprioception feedback loop for balance as frequently as able-bodied persons because they spend most of their awake hours seated. Finally, when walking in Mina, their arms become an integral part of balance and ambulation as they ambulate with a quadrupedal crawl consisting of a hind foot, ipsilateral front crutch, contralateral hind foot, and contralateral front crutch sequence. Because of the lack of integrated sensory feedback in the initial prototype, we placed a video monitor in front of the evaluator during initial training, which provided a real-time side view but forced the user to choose between watching the monitor and watching his or her legs directly. The user must learn how to position his or her body at the point of heel strike. If the user leans too far backward, then the upcoming swing leg will still be loaded at the time of swing, causing a backward fall. If the user leans too far forward, the foot will contact the ground before the swing completes, resulting in significantly reduced step size. Large step sizes with this prototype often caused the evaluator's center of mass to remain between the two feet during double support, leaving the trailing leg loaded as it initiated the next swing phase and triggering a fall. Using smaller steps mitigates this problem; however, this accentuates the need to provide appropriate sensory feedback for a more dynamic gait that could control a passively (spring loaded) or actively actuated ankle for toe-off. While both evaluators could easily walk with forearm crutches (Figure 6) as a quadruped with low cognitive effort [31], we believe that the next iterations with sensory augmentation will result in a more upright gait.

Figure 6: The Mina during evaluation.

5. Discussion

We evaluated Mina with two paraplegic evaluators and demonstrated that Mina is currently capable of providing mobility for paraplegic users on flat ground at slow walking speed. Even though Mina currently operates in a high impedance trajectory-tracking mode, able-bodied users tend to actively try to walk and balance using sensory feedback, such as ground reaction forces. The addition of sensory substitution interfaces to Mina will allow paraplegic users to receive similar information and should allow similar control behaviors. In evaluating Mina, we observed that all users required some amount of training and practice and that more training and practice was required for paraplegic users than able-bodied users. As with any new activity that requires coordinated motion, proficiency requires practice. The addition of proprioception analogs for the lower extremities in paraplegic users should reduce the cognitive effort and time to learn the task of coordinating arm motion with leg motion.

6. Future Work

Feedback systems integrated to Mina will seek to convey sensory information related to these characteristics of human balance during stance and dynamic gait. IHMC is evaluating the effects on balance of various tactile display symbologies by determining the *user's control stability* (maintenance of his

or her balance and the deviation of his/her center of mass) as well as the *user's perception* accuracy by asking him or her to estimate how much he/she deviates from a desired body posture. It will also be interesting to measure the participants' accuracy to estimate their body deviation when using the tactile feedback. These subjective estimations will guide design of the sensory feedback system and the symbology needed for user control of the Mina hardware. We are incorporating a video game interface using a WiiFit balance board (Nintendo Co, Ltd., Kyoto, Japan) as a stability measurement device for static posture with and without sensory substitution feedback and forearm crutches. The game element improved participant engagement as they learn to control their balance [32]. The data analysis will guide improvements that will ultimately lead to direct, dynamic control of Mina by the user. Lastly, we are integrating functional electrical stimulation (FES) to manage toe-off and toe-lift to allow Mina to use less exaggerated gait trajectories.

7. Conclusions

In this paper we introduced the Mina exoskeleton concept that can play back prerecorded joint trajectories using compliant control rather than rigid joint trajectory tracking to allow for robustness to unmodeled terrain variations and perturbation. Two device evaluators with spinal cord injury paraplegia maintained balance with forearm crutches to walk with a quadrupedal gait. This demonstrated the need to integrate sensory feedback systems with powered actuator mobility assistance robotics even for walking at relatively low speed on flat ground in a laboratory setting. We are currently developing various improvements to give the user operational control of the device using gestures provided by upper body motion. We will also investigate tracking user gaze as a control mechanism when navigating complex environments to, for example, adjust step height and step plant when walking on rough ground. Further development will continue to reestablish the sensorimotor loop by restoring sensory feedback and will improve user/orthosis coupling to form an integral sociotechnical team. This should enable increasing the speed of walking, walking over rough terrain, on hiking trails, and in urban environments with stairs and narrow passageways as well as a more natural upright, assisted bipedal gait.

Conflict of Interests

The authors have no financial conflicts of interest with respect to the work described. Any opinions, findings, and conclusions or recommendations expressed in this material are those of the authors and do not necessarily reflect the views of the Office of Naval Research.

Acknowledgments

The authors would like to thank their two evaluators for their invaluable feedback in testing Mina. They would also like to thank the team of medical professionals that volunteered their time to monitor the evaluation sessions. The Florida Institute for Human and Machine Cognition is a not-for-profit research institute of the State of Florida University System. This material is based on research sponsored by the Office of Naval Research under agreement numbers N00014-07-1-0790, N00014-09-1-0800 and N00014-10-1-0847.

References

[1] M. Berkowitz, P. O'Leary, D. Kruse, and C. Harvey, *Spinal Cord Injury: An Analysis of Medical and Social Costs*, Demos Medical Publishing, New York, NY, USA, 1998.

[2] S. Goemaere, M. Van Laere, P. De Neve, and J. M. Kaufman, "Bone mineral status in paraplegic patients who do or do not perform standing," *Osteoporosis International*, vol. 4, no. 3, pp. 138–143, 1994.

[3] T. Sumiya, K. Kawamura, A. Tokuhiro, H. Takechi, and H. Ogata, "A survey of wheelchair use by paraplegic individuals in Japan. Part 2: prevalence of pressure sores," *Spinal Cord*, vol. 35, no. 9, pp. 595–598, 1997.

[4] R. L. Ruff, S. S. Ruff, and X. Wang, "Persistent benefits of rehabilitation on pain and life quality for nonambulatory patients with spinal epidural metastasis," *Journal of Rehabilitation Research and Development*, vol. 44, no. 2, pp. 271–278, 2007.

[5] T. Hayashi, H. Kawamoto, and Y. Sankai, "Control method of robot suit HAL working as operator's muscle using biological and dynamical information," in *IEEE/RSJ International Conference on Intelligent Robots and Systems (IROS '05)*, pp. 3063–3068, August 2005.

[6] A. Tsukahara, Y. Hasegawa, and Y. Sankai, "Standing-up motion support for paraplegic patient with robot suit HAL," in *IEEE International Conference on Rehabilitation Robotics (ICORR '09)*, pp. 211–217, June 2009.

[7] T. Kagawa and Y. Uno, "A human interface for stride control on a wearable robot," in *IEEE/RSJ International Conference on Intelligent Robots and Systems (IROS '09)*, pp. 4067–4072, St. Louis, Mo, USA, October 2009.

[8] T. Kagawa and Y. Uno, "Gait pattern generation for a power-assist device of paraplegic gait," in *Proceedings of IEEE International Workshop on Robot and Human Interactive Communication*, pp. 633–638, Toyama, Japan, September 2009.

[9] K. Kong and D. Jeon, "Design and control of an exoskeleton for the elderly and patients," *IEEE/ASME Transactions on Mechatronics*, vol. 11, no. 4, pp. 428–432, 2006.

[10] H. Zabaleta, M. Bureau, G. Eizmendi, E. Olaiz, J. Medina, and M. Perez, "Exoskeleton design for functional rehabilitation in patients with neurological disorders and stroke," in *the 10th IEEE International Conference on Rehabilitation Robotics (ICORR '07)*, pp. 112–118, Noordwijk, The Netherlands, June 2007.

[11] Z. Feng, J. Qian, Y. Zhang, L. Shen, Z. Zhang, and Q. Wang, "Biomechanical design of the powered gait orthosis," in *IEEE International Conference on Robotics and Biomimetics (ROBIO '07)*, pp. 1698–1702, Sanya, China, December 2007.

[12] R. Ekkelenkamp, J. Veneman, and H. Van Der Kooij, "LOPES: selective control of gait functions during the gait rehabilitation of CVA patients," in *the 9th IEEE International Conference on Rehabilitation Robotics (ICORR '05)*, pp. 361–364, Chicago, Ill, USA, July 2005.

[13] G. Colombo, M. Joerg, R. Schreier, and V. Dietz, "Treadmill training of paraplegic patients using a robotic orthosis," *Journal of Rehabilitation Research and Development*, vol. 37, no. 6, pp. 693–700, 2000.

[14] G. Colombo, M. Jörg, and V. Dietz, "Driven gait orthosis to do locomotor training of paraplegic patients," in *the 22nd Annual International Conference of the IEEE Engineering in Medicine and Biology Society*, vol. 4, pp. 3159–3163, Chicago, Ill, USA, July 2000.

[15] R. Riener, L. Lünenburger, S. Jezernik, M. Anderschitz, G. Colombo, and V. Dietz, "Patient-cooperative strategies for robot-aided treadmill training: first experimental results," *IEEE Transactions on Neural Systems and Rehabilitation Engineering*, vol. 13, no. 3, pp. 380–394, 2005.

[16] A. Duschau-Wicke, A. Caprez, and R. Riener, "Patient-cooperative control increases active participation of individuals with SCI during robot-aided gait training," *Journal of Neuroengineering and Rehabilitation*, vol. 7, no. 1, article no. 43, 2010.

[17] P. Bach-y-Rita, *Brain Mechanisms in Sensory Substitution*, Academic Press, New York, NY, USA, 1972.

[18] L. H. Finkel, "A model of receptive field plasticity and topographic map reorganization in the somatosensory cortex," in *Connectionist Modeling and Brain Function: The Developing Interface*, S. J. Hanson and C. R. Olsen, Eds., pp. 164–192, MIT Press, Cambridge, Mass, USA, 1990.

[19] E. C. Walcott and R. B. Langdon, "Short-term plasticity of extrinsic excitatory inputs to neocortical layer 1," *Experimental Brain Research*, vol. 136, no. 1, pp. 143–151, 2001.

[20] P. Bach-y-Rita, "Theoretical aspects of sensory substitution and of neurotransmission-related reorganization in spinal cord injury," *Spinal Cord*, vol. 37, no. 7, pp. 465–474, 1999.

[21] J. Kawamura, O. Sweda, H. Kazutaka, N. Kazuyoshi, and S. Isobe, "Sensory feedback systems for the lower-limb prosthesis," *Journal of the Osaka Rosai Hospital*, vol. 5, pp. 102–109, 1981.

[22] D. Zambarbieri et al., "Biofeedback techniques for rehabilitation of the lower limb amputee subjects," in *Proceedings of the 8th Mediterranean Conference on Medical and Biological Engineering and Computing (MEDICON '98)*, Lemesos, Cyprus, June 1998.

[23] F. W. Clippinger, A. V. Seaber, and J. H. McElhaney, "Afferent sensory feedback for lower extremity prosthesis," *Clinical Orthopaedics and Related Research*, vol. 169, pp. 202–208, 1982.

[24] J. A. Sabolich and G. M. Ortega, "Sense of feel for lower-limb amputees: a phase-one study," *Journal of Prosthetics & Orthotics*, vol. 6, pp. 36–41, 1994.

[25] P. Bach-y-Rita, K. A. Kaczmarek, M. E. Tyler, and J. Garcia-Lara, "Form perception with a 49-point electrotactile stimulus array on the tongue: a technical note," *Journal of Rehabilitation Research and Development*, vol. 35, no. 4, pp. 427–430, 1998.

[26] P. Bach-Y-Rita, C. C. Collins, F. A. Saunders, B. White, and L. Scadden, "Vision substitution by tactile image projection," *Nature*, vol. 221, no. 5184, pp. 963–964, 1969.

[27] H. K. Kwa, J. H. Noorden, M. Missel, T. Craig, J. E. Pratt, and P. D. Neuhaus, "Development of the IHMC mobility assist exoskeleton," in *IEEE International Conference on Robotics and Automation (ICRA '09)*, pp. 2556–2562, Kobe, Japan, May 2009.

[28] D. A. Winter, *Biomechanics and motor control of human movement*, Wiley, New York, NY, USA, 2nd edition, 1990.

[29] F. M. Maynard Jr., M. B. Bracken, G. Creasey et al., "International standards for neurological and functional classification of spinal cord injury," *Spinal Cord*, vol. 35, no. 5, pp. 266–274, 1997.

[30] B. Morganti, G. Scivoletto, P. Ditunno, J. F. Ditunno, and M. Molinari, "Walking index for spinal cord injury (WISCI): criterion validation," *Spinal Cord*, vol. 43, no. 1, pp. 27–33, 2005.

[31] P. D. Neuhaus et al., "Design and evaluation of Mina, a robotic orthosis for paraplegics," in *Proceedings of the International Conference on Rehabilitation Robotics*, Zurich, Switzerland, 2011.

[32] P. Bach-y-Rita, S. Wood, R. Leder et al., "Computer-assisted motivating rehabilitation (CAMR) for institutional, home, and educational late stroke programs," *Topics in Stroke Rehabilitation*, vol. 8, no. 4, pp. 1–10, 2002.

Hindawi Publishing Corporation
Journal of Robotics
Volume 2011, Article ID 759764, 11 pages
doi:10.1155/2011/759764

Review Article

Lower-Limb Robotic Rehabilitation: Literature Review and Challenges

Iñaki Díaz, Jorge Juan Gil, and Emilio Sánchez

Applied Mechanics Department, CEIT, Paseo Manuel Lardizábal 15, 20018 San Sebastián, Spain

Correspondence should be addressed to Iñaki Díaz, idiaz@ceit.es

Received 20 April 2011; Revised 11 August 2011; Accepted 5 September 2011

Academic Editor: Doyoung Jeon

This paper presents a survey of existing robotic systems for lower-limb rehabilitation. It is a general assumption that robotics will play an important role in therapy activities within rehabilitation treatment. In the last decade, the interest in the field has grown exponentially mainly due to the initial success of the early systems and the growing demand caused by increasing numbers of stroke patients and their associate rehabilitation costs. As a result, robot therapy systems have been developed worldwide for training of both the upper and lower extremities. This work reviews all current robotic systems to date for lower-limb rehabilitation, as well as main clinical tests performed with them, with the aim of showing a clear starting point in the field. It also remarks some challenges that current systems still have to meet in order to obtain a broad clinical and market acceptance.

1. Introduction

Stroke is the third most frequent cause of death worldwide and the leading cause of permanent disability in the USA and Europe [1]. Neurological impairment after stroke frequently leads to hemiparesis or partial paralysis of one side of the body that affects the patient's ability to perform activities of daily living (ADL) such as walking and eating. Physical therapy, involving rehabilitation, helps improve the lost functions [2, 3].

The goal of rehabilitation exercises is to perform specific movements that provoke motor plasticity to the patient and therefore improve motor recovery and minimize functional deficits. Movement rehabilitation is limb dependent, thus the affected limb has to be exercised [4].

This paper focuses on lower-limb rehabilitation. One-third of surviving patients from stroke do not regain independent walking ability and those ambulatory, walk in a typical asymmetric manner [1]. Rehabilitation therapies are critical to recover, and therefore many research is ongoing on the field.

The rehabilitation process toward regaining a meaningful mobility can be divided into three phases [4–6]: (1) the bedridden patient is mobilized into the chair as soon as possible, (2) restoration of gait, and (3) improvement of gait (i.e., training of free walking if possible).

Traditional rehabilitation therapies are very labor intensive especially for gait rehabilitation, often requiring more than three therapists together to assist manually the legs and torso of the patient to perform training. This fact imposes an enormous economic burden to any country's health care system thus limiting its clinical acceptance. Furthermore, demographic change (aging), expected shortages of health care personnel, and the need for even higher quality care predict an increase in the average cost from first stroke to death in the future. All these factors stimulate innovation in the domain of rehabilitation [7] in such way it becomes more affordable and available for more patients and for a longer period of time.

Robotics for rehabilitation treatment is an emerging field which is expected to grow as a solution to automate training. Robotic rehabilitation can (i) replace the physical training effort of a therapist, allowing more intensive repetitive motions and delivering therapy at a reasonable cost, and (ii) assess quantitatively the level of motor recovery by measuring force and movement patterns.

In the recent literature many works deal with robotic lower-extremity rehabilitation. The purpose of this paper is

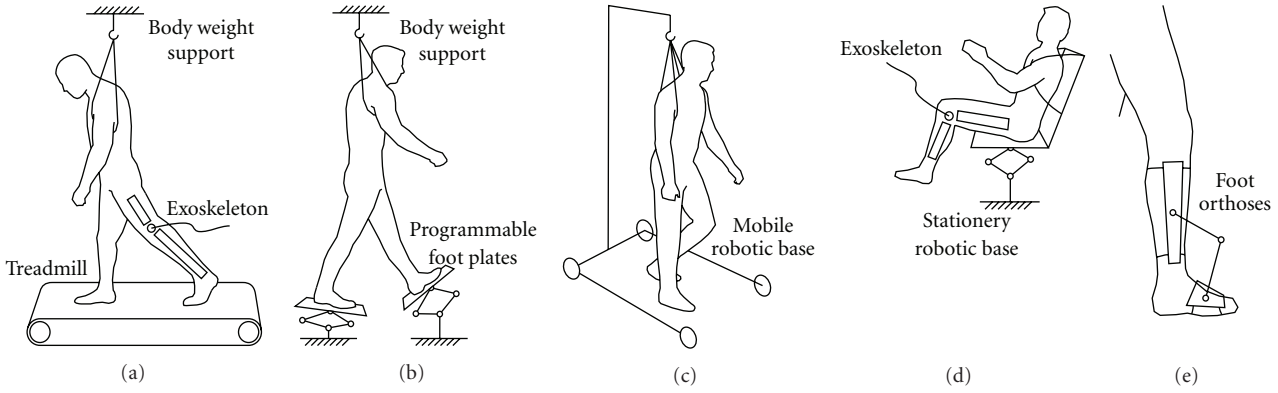

Figure 1: Robotic system types for lower-limb rehabilitation: (a) treadmill gait trainers, (b) foot-plate-based gait trainers, (c) overground gait trainers, (d) stationary gait and ankle trainers, and (e) active foot orthoses.

to review existing interfaces, as well as ongoing work, to show researchers current state of the art and roadmap in the field. Passive robotic rehabilitation devices, although less complex and cheaper, cannot supply energy to the affected limbs, hence are limited compared to active devices and are out of the scope of this work. Finally, current challenges in the field are also pointed out in the last section.

2. Robotic Systems for Lower-Limb Rehabilitation

Over the last decade, several lower-limb rehabilitation robots have been developed to restore mobility of the affected limbs. These systems can be grouped according to the rehabilitation principle they follow (Figure 1):

(i) treadmill gait trainers,
(ii) foot-plate-based gait trainers,
(iii) overground gait trainers,
(iv) stationary gait trainers,
(v) ankle rehabilitation systems,
  (a) stationary systems,
  (b) active foot orthoses.

Following subsections describe the working principle of each group and review all existing devices to date (to the best of our knowledge). Clinical tests performed with patients using such systems are also reported (test with healthy patients are excluded).

2.1. Treadmill Gait Trainers. Traditional therapies usually focus on treadmill training to improve functional mobility [8]. This rehabilitation technique is known as partial body-weight support treadmill training (PBWSTT). Three therapists assist the legs and hip of the patient walking on a treadmill while part of the patient's body weight is supported by an overhead harness.

Many robotic systems have been developed with the aim to automate and improve this training technique as a means for reducing therapist labor [9]. Usually these systems are based on exoskeleton type robots in combination with a treadmill (Figure 1(a)). Table 1 summarizes the systems available in literature.

Table 1: Robotic systems for treadmill gait training.

Robotic system	Company	Clinical tests
Lokomat [10]	Hocoma	[11–15]
LokoHelp [16]	LokoHelp Group	[16, 17]
ReoAmbulator [18]	Motorika	—
ARTHuR [19]	—	[21]
POGO and PAM [20]	—	—
ALEX [22]	—	[23]
LOPES [24]	—	[25]
ALTRACO [26]	—	—
RGR [27]	—	—
String-Man [28]	—	—

Of the 10 systems that compose the group, only three of them are on the market: the Lokomat, the LokoHelp, and the ReoAmbulator. The Lokomat (Hocoma AG) consists of a robotic gait orthosis and an advanced body weight support system, combined with a treadmill [10]. It uses computer-controlled motors (drives) which are integrated in the gait orthosis at each hip and knee joint (Figure 2). The drives are precisely synchronized with the speed of the treadmill to assure a precise match between the speed of the gait orthosis and the treadmill. Till date, it is the most clinically evaluated system [11–15] and one of the firsts of its type.

The LokoHelp (LokoHelp Group) is an electromechanical device developed for improving gait after brain injury [16]. The LokoHelp (Figure 3) is placed in the middle of the treadmill surface parallel to the walking direction and fixed to the front of the treadmill with a simple clamp. It also provides a body weight support system for the patient. Clinical trials have been conducted to analyze its feasibility and efficacy [16, 17]. The results show that the system improves the gait ability of the patient in the same way as the manual locomotor training; however, using the LokoHelp less therapeutic assistance is required and therapist

Figure 2: Lokomat system (picture courtesy of Hocoma).

Figure 3: LokoHelp gait trainer "Pedago" (picture courtesy of LokoHelp Group).

discomfort is reduced. This fact is a general conclusion for almost all robotic systems to date.

ReoAmbulator (Motorika Ltd., marketed in the USA as the "AutoAmbulator") is another body-weight-supported treadmill robotic system [18]. Robotic arms are strapped to the patient's legs at the thigh and ankle, driving them through a stepping pattern (Figure 4). A single-blind, randomized clinical trial to assess its effectiveness in stroke patients is currently underway. ReoAmbulator was developed in cooperation with the HealthSouth network of rehabilitation hospitals.

Other robotic systems are at a research state or under development, but have been already used to conduct some clinical testing. For example, the Biomechatronics Lab at the University of California has developed several robotic devices for locomotor training after spinal cord injury: the Ambulation-assisting Robotic Tool for Human Rehabilitation (ARTHuR), a device designed to measure and manipulate human stepping on a treadmill [19]; the Pneumatically

Figure 4: ReoAmbulator robotic system (picture courtesy of Motorika Ltd.).

Operated Gait Orthosis (POGO), an improved leg-robot design; the Pelvic Assist Manipulator (PAM), a device that can accommodate and control naturalistic pelvic motion [20]. The former, ARTHuR, has been tested in a clinical trial [21] showing its reliability to perform subject-specific assisted stepping, thus reducing the effort required by the trainer during manual assistance.

The Active Leg Exoskeleton (ALEX) is a powered leg orthosis with linear actuators at the hip and knee joints, and with a force-field controller developed to provide assistance to the patient by using the assist-as-needed approach [22]. It has been tested with two chronic stroke survivors, whose gait patterns were substantially improved after the training [23]. Improvement was measured as an increase in the size of the patients' gait pattern and in their walking speeds on the treadmill.

The gait rehabilitation robot LOPES (LOwer-extremity Powered ExoSkeleton) can move in parallel with the legs of a person walking on a treadmill, at pelvis height flexibly connected to the fixed world [24]. A first clinical trial is already completed that tests the efficacy of LOPES in improving the walking ability and quality of chronic stroke survivors [25].

Finally, there are three robotic systems under research: ALTRACO, RGR, and String-Man. The Automated Locomotion Training using an Actuated Compliant Robotic Orthosis (ALTACRO) project aims to develop a novel step rehabilitation robot using a lightweight, compliant, pneumatic actuator [26]. The device consists of a unilateral exoskeleton and a supportive arm to passively gravity-balance the device.

The Robotic Gait Rehabilitation (RGR) Trainer was built to target secondary gait deviations in patients after stroke. While patients ambulate on a treadmill, force fields are applied to the pelvis, that generate corrective forces as

Table 2: Foot-plate-based robotic systems.

Robotic system	Company	Clinical tests
Gangtrainer GT I [29]	Reha-Stim	[29–32]
HapticWalker [33]	—	[34]
GM5 [35]	—	[35]
LLRR [36]	—	—
Univ. Gyeongsang [37]	—	[37]

a response to deviations from normal pelvic motion [27]. The device is coupled to the patient via an orthopedic brace.

The String-Man [28], developed at Fraunhofer IPK, Berlin, is a robotic system for supporting the gait rehabilitation and restoration of motor functions. It has a particular kinematic structure with 7 wires attached to the trunk of the patient.

2.2. Foot-Plate-Based Gait Trainers. Some rehabilitation machines are based on programmable foot plates. That is, the feet of the patient are positioned on separate foot plates, whose movements are controlled by the robotic system to simulate different gait patterns (Figure 1(b)). Table 2 shows the review of such systems. It can be seen that only one system is on the market, although many others have done some clinical testing.

The Gangtrainer GT I (Figure 5), commercialized by Reha-Stim, can assist the patient in the recovery of his freedom of movement by relieving the body of its own weight and adapting speed from the individual ability of the patient [29]. Harness-secured patients are positioned on two foot plates, whose movements simulate stance and swing, and ropes attached to the patient can control the vertical and lateral movements of the center of mass. Many clinical studies have been conducted worldwide with this device [30–32], and it is considered as one of the pioneering robotic systems for rehabilitation. Similarly as for treadmill gait trainers, the Gangtrainer GT I is at least as effective as the manual treadmill therapy but requiring less input from the therapist.

The HapticWalker is a haptic locomotion interface able to simulate not only slow and smooth trajectories (like walking on an even floor and up/down staircases), but also foot motions like walking on rough ground or even stumbling or sliding, which require high-order system dynamics [33]. It is a major redesign of GT I with foot plate trajectories fully programmable, and it is currently being clinically evaluated in several trials with stroke patients and spinal cord injury patients [34].

The GaitMaster5 (GM5) is a recently developed gait rehabilitation system at the University of Tsukuba [35]. The patient straps his/her feet into pads that are lined with sensors (Figure 6). These pads are connected to motion platforms that can move the user's foot forward (simulating walking) or up and down (like climbing).

The Lower-Limb Rehabilitation Robot (LLRR) can assist patients in simulating normal people's footsteps and exercising leg muscles [36]. It is comprised with steps posture controlling system and weight alleviation controlling mechanism.

Figure 5: The Gangtrainer GT I (picture courtesy of Reha-Stim).

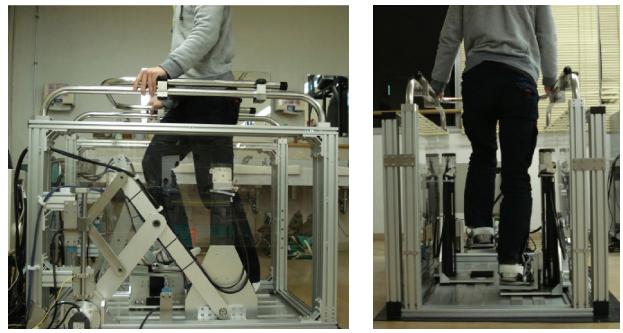

(a) (b)

Figure 6: The GaitMaster5 gait rehabilitation system (picture courtesy of Dr. Hiroaki Yano).

A 6-degree-of-freedom (DOF) gait rehabilitation robot has been developed at the Gyeongsang National University with upper and lower limb connections that allow walking velocity updates on various terrains. It is composed of an upper limb device, a sliding device, two footpad devices, and a body support system. A pilot clinical test has been conducted with a hemiplegic patient [37].

2.3. Overground Gait Trainers. Systems reported in Table 3 consist of robots that servo-follow the patient's walking motions overground. They allow patients move under their own control rather than moving them through predetermined movement patterns (Figure 1(c)). It is very noticeable that almost all systems reviewed have been commercialized.

The KineAssist is a robotic device (Figure 7), commercialized by Kinea Design, LLC, for gait and balance training [38]. It consists of a custom designed torso and pelvis harness attached to a mobile robotic base. The robot is controlled

Figure 7: KineAssist robotic device (picture courtesy of Kinea Design, LLC).

Figure 8: ReWalk wearable system (picture courtesy of ARGO Medical Technologies Ltd.).

Table 3: Overground gait trainers.

Robotic System	Company	Clinical Tests
KineAssist [38]	Kinea Design LLC	[39]
WalkTrainer [40]	Swortec SA	[41]
ReWalk [42]	ARGO Medical	—
HAL [43]	CYBERDYNE Inc.	[44, 45]
WHERE I-II [46]	—	[46]

according to the forces detected from the subject by the load cells located in the pelvic harness. A recent clinical trial has been conducted [39] in order to evaluate overground walking speed changes when using the KineAssist system.

The WalkTrainer (Swortec SA) is a robotic rehabilitation system composed by a deambulator, a pelvis orthosis, a body weight support, two leg orthoses, and a real-time controlled electrostimulator [40]. It is an overground walking reeducation deambulator with the association of pelvic and leg orthoses. First clinical trials have been carried out with the system [41].

ReWalk is a wearable, motorized quasi-robotic suit from ARGO Medical Technologies Ltd., (Figure 8) that can be used for therapeutic activities [42]. ReWalk comprises light wearable brace support suit, which integrates DC motors at the joints, rechargeable batteries, an array of sensors, and a computer-based control system. Upper-body movements of the user are detected and used to initiate and maintain walking processes. The device is undergoing clinical trial testing at the Moss Rehabilitation Hospital in Philadelphia.

Hybrid Assistive Limb (HAL) is a wearable robot designed for a wide range of applications, from rehabilitation to heavy works support, and built in several versions (full body version and two-leg version) [43]. Current version 5 has been used to conduct clinical tests [44]. A single-leg version of HAL has also been developed to support the walking of persons with hemiplegia (Figure 9). The walking support was assessed with one hemiplegic subject who was not able to bend his right knee [45].

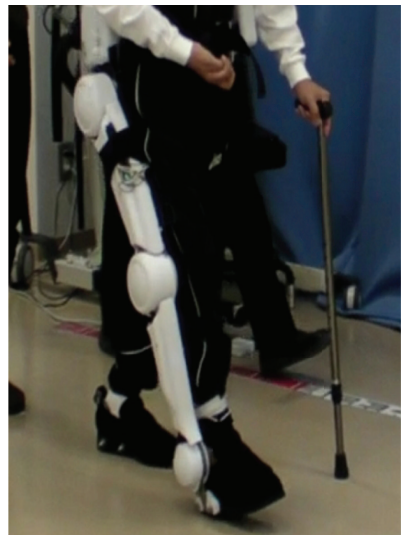

Figure 9: Single-leg version of HAL robot (picture courtesy of Professon Sankai, CYBERDYNE Inc./Univeristy of Tsukuba).

WHERE I and II are two mobile gait rehabilitation systems that enable overground gait training. Pilot clinical trials have been carried out to demonstrate the effectiveness of both systems (patients were in the stage of gait rehabilitation after suffering minor leg injuries) [46].

2.4. Stationary Gait Trainers. Table 4 presents robotic systems that are focused on guided movements of limbs in order to have an optimal effect from a therapeutic and functional perspective (Figure 1(d)). The objective of these systems is to obtain efficient strengthening of the muscles and the development of endurance, as well as joint mobility and movement coordination.

Table 4: Stationary robotic gait trainers.

Robotic system	Company	Clinical tests
MotionMaker [47]	Swortec SA	[40, 47]
Lambda [48]	—	—
AIST Tsukuba [49]	—	—

Figure 10: The MotionMaker rehabilitation system (Picture courtesy of Swortec SA).

The MotionMaker (Swortec SA) is a stationary training system which allows to carry out fitness exercises with active participation of the paralyzed limbs [47]. The limbs are only attached to the orthoses at the foot level to simulate natural ground reaction forces (Figure 10). The advantage of the MotionMaker is its real-time sensor-controlled exercises, combined with the controlled electrostimulation, adapted to the patients efforts. First clinical trials have been carried out with the system [40], showing an improvement of the patient's ability to develop a higher voluntary force during a leg-press movement.

Two other robotic systems that have been developed with a similar working principle: the Lambda, a rehabilitation and fitness robot used for mobilization of lower extremities [48] that provides the movement of the lower extremities in the sagittal plane, including an additional rotation for the ankle mobilization; and a wire-driven leg rehabilitation system [49] developed by the National Institute of Advanced Industrial Science and Technology (AIST) of Tsukuba.

2.5. Ankle and Knee Rehabilitation Systems. Neurological impairment after stroke can lead to reduced or no muscle activity around the ankle and knee causing the inability of an individual to lift their foot (drop foot). Ankle motion is very complicated due to its complex bone structures [50]. The overall motions of the ankle can be arranged as dorsiflexion/plantarflexion, inversion/eversion, abduction/adduction, and pronation/supination.

Many systems have been developed to enforce or restore these ankle and knee motions specifically. These systems can be grouped into stationary or active foot orthoses.

2.5.1. Stationery Systems. Stationary systems (Table 5) are those robotic mechanism designed to exercise the human ankle and knee motions without walking. The patient is positioned always in the same place, and only the target limb is exercised (Figure 1(d)).

Table 5: Stationery robotic systems for ankle rehabilitation.

Robotic System	Company	Clinical Tests
Rutgers Ankle [51]	—	[52–54]
IIT-HPARR [56]	—	—
AKROD [57]	—	—
Leg-Robot [58]	—	—
GIST [59]	—	—
NUVABAT [60]	—	—
Univ. London [61]	—	—
Univ. Auckland [62]	—	—
Univ. Cheng Kung [63]	—	—
Univ. Fuzhou [50]	—	—
AIST Tsukuba [64]	—	—

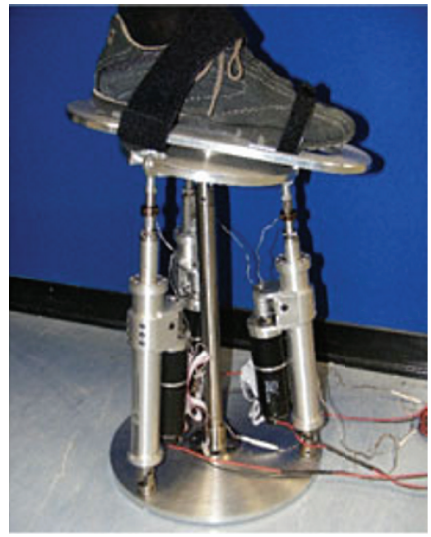

Figure 11: High Performance Ankle Rehabilitation Robot developed at the Istituto Italiano di Tecnologia.

The Rutgers Ankle was the first of this kind. It is a Stewart platform-type haptic interface that supplies 6 DOF resistive forces on the patient's foot, in response to virtual reality-based exercises [51]. Many clinical trials have been conducted with this system [52–54], showing the improvement of the patient on clinical measures of strength and endurance. In [55], the system was extended to a dual Stewart platform configuration to be used for gait simulation and rehabilitation.

The Istituto Italiano di Tecnologia (IIT) has developed a High Performance Ankle Rehabilitation Robot [56]. The proposed device allows plantar/dorsiflexion and inversion/eversion using an improved performance parallel mechanism that makes use of actuation redundancy to eliminate singularity and greatly enhance the workspace dexterity (Figure 11).

A more recent system, the Active Knee Rehabilitation Orthotic Devices (AKROD), provides variable damping at the knee joint, controlled in ways that can facilitate motor recovery in poststroke and other neurological disease patients and to accelerate recovery in knee injury patients [57]. Although it has been grouped as a stationary system, future work is focused on an actuated AKROD during walking.

The Osaka University has developed a leg-shaped robot (Leg-Robot) with a compact magnetorheological fluid clutch to demonstrate several kinds of haptic control of abnormal movements of brain-injured patients [58]. This system can be used in the practical training for students of physical therapy.

The Gwangju Institute of Science and Technology (GIST) has developed a reconfigurable ankle/foot rehabilitation robot to cover various rehabilitation exercise modes [59]. The robot can allow desired ankle and foot motions, including toe and heel raising as well as traditional ankle rotations. The system was designed to perform strengthening and balance exercises.

The so-called Northeastern University Virtual Ankle and Balance Trainer (NUVABAT) rehabilitation system is a low-cost, compact, mechatronic rehabilitation device for training of ankle range of motion (ROM) exercise in sitting and standing positions and also weight shifting and balance training in standing position [60].

The Department of Mechanical Engineering at the King's College has proposed an ankle rehabilitation robot based on a parallel mechanism with a central strut [61]. The University of Auckland has also developed a parallel robot to perform ankle rehabilitation exercises [62]. In this last system, the human ankle is secured to the end effector in such a way that it forms part of the kinematic constraint of the robot.

The Man-Machine Systems Laboratory (MML) at the National Cheng Kung University (NCKU) has developed a robot for assisting rehabilitation of patients with ankle dysfunction [63], and the School of Mechanical Engineering and Automation at the University of Fuzhou has performed an in-depth motion analysis of the ankle and has proposed two different kinds of rehabilitation robots [50]. The AIST of Tsukuba has developed a robotic device for ankle dorsiflexion/plantarflexion that can be applied to patients with complicated ankle joint deformity [64].

2.5.2. Active Foot Orthoses. On the contrary to stationary systems, active foot orthoses (Table 6) are actuated exoskeletons that the user wears while walking overground or in a treadmill (Figure 1(e)). They are intended to control position and motion of the ankle, compensate for weakness, or correct deformities. They are an evolution of traditional passive lower limb orthoses, with additional capabilities to promote appropriate gait dynamics for rehabilitation [65].

Two early attempts to develop such systems were the Powered Gait Orthosis (PGO) [66] and the Pneumatic Active Gait Orthosis (PAGO) [67]. Both devices underwent testing on human participants, but they were not commercialized.

Table 6: Active foot orthoses.

Robotic system	Company	Clinical tests
PGO [66]	—	[66]
PAGO [67]	—	[67]
Anklebot [68]	Interactive Motion	[69, 70]
MIT-AAFO [71]	—	[71]
AFOUD [72]	—	—
KAFO [73]	—	[81]
RGT [75]	—	[76]
Yonsei-AAFO [77]	—	[78]
SUkorpion AR [79]	—	—

Currently, the only commercialized system for rehabilitation is the Anklebot (Interactive Motion Technologies, Inc.), an ankle robot developed at the Massachusetts Institute of Technology (MIT) to rehabilitate the ankle after stroke [68]. It allows normal range of motion in all 3 DOF of the foot relative to the shank while walking overground or on a treadmill. Pilot controlled trials with such device were presented in [69, 70], showing a carry over to characteristics of gait with a general improvement in the walking distance covered and time.

The MIT also developed an Active Ankle-Foot Orthosis (AAFO) where the impedance of the orthotic joint is modulated throughout the walking cycle to treat drop-foot gait [71].

Another system is the Ankle Foot Orthosis at the University of Delaware (AFOUD) with 2 DOF. The two motions incorporated are dorsiflexion/plantarflexion and inversion/eversion motion [72].

Knee-Ankle-Foot-Orthosis (KAFO) is an orthosis powered by artificial pneumatic muscles during human walking [73]. The authors had previously built a powered Ankle-Foot-Orthosis (AFO) and used it effectively in studies on human motor adaptation and gait rehabilitation [74].

The Robotic Gait Trainer (RGT) developed in the Human Machine Integration Laboratory at the Arizona State University is a walking device (Figure 12) meant to be used on a treadmill [75]. It is naturally compliant due to the spring in muscle actuators and has the ability to achieve a more natural gait by allowing the patient's ankle joint to move in eversion, inversion, plantarflexion, and dorsiflexion. A case study conducted with a female was reported to examine the performance of the system [76]. The patient suffered no disadvantage as a result of the RGT incorporated therapy, where performance indicators either improved or stayed the same.

The Yonsei University has developed an active ankle-foot orthosis (Yonsei-AAFO) that can control dorsiflexion/plantarflexion of the ankle joint to prevent foot drop and toe drag during walking [77]. Gait analyses were performed on a hemiplegic patient, and the results indicated that the developed AAFO might have more clinical benefits to treat foot drop and toe drag in hemiplegic patients, comparing with conventional AFOs [78].

In a recent work, The Sabanci University Kinetostatically Optimized Reconfigurable Parallel Interface on Ankle Rehabilitation (named SUkorpion AR) has been presented,

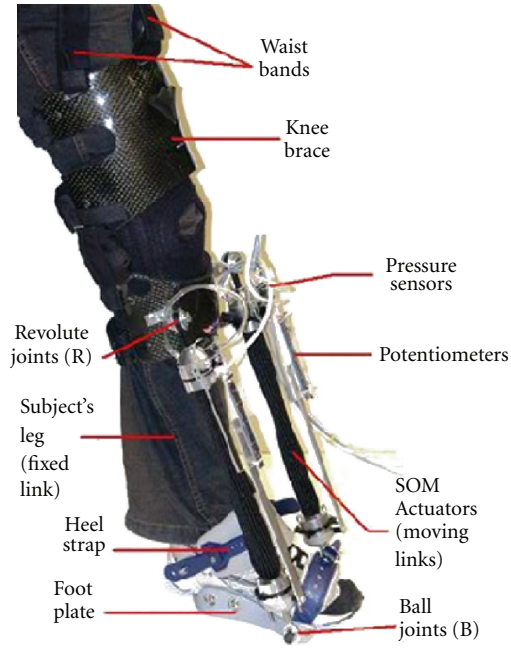

Figure 12: The Robotic Gait Trainer developed in the Human Machine Integration Laboratory at the Arizona State University.

which can be either employed as a balance/proprioception trainer or configured to accommodate range of motion and strengthening exercises [79].

3. Challenges

Robotic systems are believed to be used as standard rehabilitation tools in the near future. Furthermore, worldwide efforts are being made to automate locomotor training to reduce health care costs. The capacity of robots to deliver training with high intensity and repeatability make them very valuable assistant tools to provide high quality treatment at a lower cost and effort. These systems should also be used at home to allow patients to perform therapies independently, not replacing the therapist but supporting the therapy program.

This work has reviewed 43 robotic systems for lower-limb rehabilitation, of which more than half have not yet been marketed. Moreover, those systems available at the market are not developed as yet for application at home. Main reasons are elevated costs, lack of high clinical improvement evidence, and the need for a therapy protocol and assessment criteria. In addition, current systems are somewhat bulky and the mobile systems still lack long duration power supply solutions.

The usage of robotic systems allows precise measurement of movement kinematics and dynamics, which should be used for assessing patient recovery ability and progress. However, there is a need to develop standard protocols and procedures to obtain reliable assessment data. Currently, patient recovery of walking ability is usually quantified by employing clinical measures such as the Barthel index [80]. Regarding robotic systems, gait velocity and walking distance, ROM, and many other dynamic measures have been used for assessment. However, there is not an standardized and widely (and clinically) accepted method. Therefore, large clinical trials are needed to determine clinical criteria for its use.

Finally, clinical studies conducted still show little evidence for a superior effectiveness of the robotic therapy, although a clear benefit is shown in reduced therapist effort, time, and costs. It has been shown that robotic rehabilitation can be as effective as manually assisted training for recovery of locomotor capacity, but a higher benefit should be desirable to spread its use in clinics worldwide.

Conflict of Interests

The authors have declared that no conflict of interests exists.

References

[1] D. Lloyd-Jones, R. J. Adams, T. M. Brown et al., "Heart disease and stroke statistics—2010 update: a report from the American heart association," *Circulation*, vol. 121, no. 7, pp. e46–e215, 2010.

[2] D. S. Smith, E. Goldenberg, A. Ashburn et al., "Remedial therapy after stroke: a randomised controlled trial," *The British Medical Journal*, vol. 282, no. 6263, pp. 517–520, 1981.

[3] M. Dam, P. Tonin, S. Casson et al., "The effects of long-term rehabilitation therapy on poststroke hemiplegic patients," *Stroke*, vol. 24, no. 8, pp. 1186–1191, 1993.

[4] H. Schmidt, C. Werner, R. Bernhardt, S. Hesse, and J. Krüger, "Gait rehabilitation machines based on programmable footplates," *Journal of NeuroEngineering and Rehabilitation*, vol. 4, article 2, 2007.

[5] J. Carr and R. Shepherd, *A Motor Relearning Program for Stroke*, Aspen Publishers, 1987.

[6] D. Y. L. Chan, C. C. H. Chan, and D. K. S. Au, "Motor relearning programme for stroke patients: a randomized controlled trial," *Clinical Rehabilitation*, vol. 20, no. 3, pp. 191–200, 2006.

[7] G. J. Gelderblom, M. De Wilt, G. Cremers, and A. Rensma, "Rehabilitation robotics in robotics for healthcare; a roadmap study for the European Commission," in *Proceedings of the IEEE International Conference on Rehabilitation Robotics, (ICORR '09)*, pp. 834–838, Kyoto, Japan, June 2009.

[8] A. Wernig, S. Muller, A. Nanassy, and E. Cagol, "Laufband therapy based on "rules of spinal locomotion" is effective in spinal cord injured persons," *European Journal of Neuroscience*, vol. 7, no. 4, pp. 823–829, 1995.

[9] J. A. Galvez and D. J. Reinkensmeyer, "Robotics for gait training after spinal cord injury," *Topics in Spinal Cord Injury Rehabilitation*, vol. 11, no. 2, pp. 18–33, 2005.

[10] G. Colombo, M. Joerg, R. Schreier, and V. Dietz, "Treadmill training of paraplegic patients using a robotic orthosis," *Journal of Rehabilitation Research and Development*, vol. 37, no. 6, pp. 693–700, 2000.

[11] G. Colombo, M. Wirz, and V. Dietz, "Driven gait orthosis for improvement of locomotor training in paraplegic patients," *Spinal Cord*, vol. 39, no. 5, pp. 252–255, 2001.

[12] M. Wirz, D. H. Zemon, R. Rupp et al., "Effectiveness of automated locomotor training in patients with chronic incomplete spinal cord injury: a multicenter trial," *Archives of Physical Medicine and Rehabilitation*, vol. 86, no. 4, pp. 672–680, 2005.

[13] T. G. Hornby, D. H. Zemon, and D. Campbell, "Robotic-assisted, body-weight-supported treadmill training in individuals following motor incomplete spinal cord injury," *Physical Therapy*, vol. 85, no. 1, pp. 52–66, 2005.

[14] J. Hidler, D. Nichols, M. Pelliccio et al., "Multicenter randomized clinical trial evaluating the effectiveness of the Lokomat in subacute stroke," *Neurorehabilitation and Neural Repair*, vol. 23, no. 1, pp. 5–13, 2009.

[15] K. P. Westlake and C. Patten, "Pilot study of Lokomat versus manual-assisted treadmill training for locomotor recovery post-stroke," *Journal of NeuroEngineering and Rehabilitation*, vol. 6, no. 1, article 18, 2009.

[16] S. Freivogel, J. Mehrholz, T. Husak-Sotomayor, and D. Schmalohr, "Gait training with the newly developed "LokoHelp"-system is feasible for non-ambulatory patients after stroke, spinal cord and brain injury. A feasibility study," *Brain Injury*, vol. 22, no. 7-8, pp. 625–632, 2008.

[17] S. Freivogel, D. Schmalohr, and J. Mehrholz, "Improved walking ability and reduced therapeutic stress with an electromechanical gait device," *Journal of Rehabilitation Medicine*, vol. 41, no. 9, pp. 734–739, 2009.

[18] G. R. West, "Powered gait orthosis and method of utilizing same," Patent number 6 689 075, 2004.

[19] D. Reinkensmeyer, J. Wynne, and S. Harkema, "A robotic tool for studying locomotor adaptation and rehabilitation," in *Proceedings of the 2nd Joint Meeting of the IEEE Engineering in Medicine and Biology Society and the Biomedical Engineering Society*, vol. 3, pp. 2013–2353, October 2002.

[20] D. J. Reinkensmeyer, D. Aoyagi, J. L. Emken et al., "Tools for understanding and optimizing robotic gait training," *Journal of Rehabilitation Research and Development*, vol. 43, no. 5, pp. 657–670, 2006.

[21] J. L. Emken, S. J. Harkema, J. A. Beres-Jones, C. K. Ferreira, and D. J. Reinkensmeyer, "Feasibility of manual teach-and-replay and continuous impedance shaping for robotic locomotor training following spinal cord injury," *IEEE Transactions on Biomedical Engineering*, vol. 55, no. 1, pp. 322–334, 2008.

[22] S. K. Banala, S. K. Agrawal, and J. P. Scholz, "Active Leg Exoskeleton (ALEX) for gait rehabilitation of motor-impaired patients," in *Proceedings of the 10th IEEE International Conference on Rehabilitation Robotics, (ICORR '07)*, pp. 401–407, Noordwijk, The Netherlands, June 2007.

[23] S. K. Banala, S. H. Kim, S. K. Agrawal, and J. P. Scholz, "Robot assisted gait training with active leg exoskeleton (ALEX)," *IEEE Transactions on Neural Systems and Rehabilitation Engineering*, vol. 17, no. 1, pp. 2–8, 2009.

[24] J. F. Veneman, R. Kruidhof, E. E. G. Hekman, R. Ekkelenkamp, E. H. F. Van Asseldonk, and H. Van Der Kooij, "Design and evaluation of the Lopes exoskeleton robot for interactive gait rehabilitation," *IEEE Transactions on Neural Systems and Rehabilitation Engineering*, vol. 15, no. 3, pp. 379–386, 2007.

[25] E. van Asseldonk, C. Simons, M. Folkersman et al., "Robot aided gait training according to the assist-as-needed principle in chonic stroke survivors," in *Proceedings of the Annual Meeting of the Society for Neuroscience (Poster)*, Chicago, Ill, USA, October 2009.

[26] P. Beyl, M. van Damme, R. van Ham, R. Versluys, B. Vanderborght, and D. Lefeber, "An exoskeleton for gait rehabilitation: prototype design and control principle," in *Proceedings of the IEEE International Conference on Robotics and Automation, (ICRA '08)*, pp. 2037–2042, Pasadena, Calif, USA, May 2008.

[27] M. Pietrusinski, I. Cajigas, Y. Mizikacioglu, M. Goldsmith, P. Bonato, and C. Mavroidis, "Gait rehabilitation therapy using robot generated force fields applied at the pelvis," in *Proceedings of the IEEE Haptics Symposium, (HAPTICS '10)*, pp. 401–407, Waltham, Mass, USA, March 2010.

[28] D. Surdilovic and R. Bernhardt, "STRING-MAN: a new wire robot for gait rehabilitation," in *Proceedings of the IEEE International Conference on Robotics and Automation*, vol. 2, pp. 2031–2036, May 2004.

[29] S. Hesse and D. Uhlenbrock, "A mechanized gait trainer for restoration of gait," *Journal of Rehabilitation Research and Development*, vol. 37, no. 6, pp. 701–708, 2000.

[30] C. Werner, S. Von Frankenberg, T. Treig, M. Konrad, and S. Hesse, "Treadmill training with partial body weight support and an electromechanical gait trainer for restoration of gait in subacute stroke patients: a randomized crossover study," *Stroke*, vol. 33, no. 12, pp. 2895–2901, 2002.

[31] M. Pohl, C. Werner, M. Holzgraefe et al., "Repetitive locomotor training and physiotherapy improve walking and basic activities of daily living after stroke: a single-blind, randomized multicentre trial(deutsche gangtrainerstudie, degas)," *Clinical Rehabilitation*, vol. 21, no. 1, pp. 17–27, 2007.

[32] S. H. Peurala, O. Airaksinen, P. Huuskonen et al., "Effects of intensive therapy using gait trainer or floor walking exercises early after stroke," *Journal of Rehabilitation Medicine*, vol. 41, no. 3, pp. 166–173, 2009.

[33] H. Schmidt, "Hapticwalker—a novel haptic device for walking simulation," in *Proceedings of the EuroHaptics Conference*, pp. 60–67, Munich, Germany, June 2004.

[34] S. Hesse and C. Werner, "Connecting research to the needs of patients and clinicians," *Brain Research Bulletin*, vol. 78, no. 1, pp. 26–34, 2009.

[35] H. Yano, S. Tamefusa, N. Tanaka, H. Saitou, and H. Iwata, "Gait rehabilitation system for stair climbing and descending," in *Proceedings of the IEEE Haptics Symposium, (HAPTICS '10)*, pp. 393–400, Waltham, Mass, USA, March 2010.

[36] S. Chen, Y. Wang, S. Li, G. Wang, Y. Huang, and X. Mao, "Lower limb rehabilitation robot," in *Proceedings of the ASME/IFToMM International Conference on Reconfigurable Mechanisms and Robots, (ReMAR '09)*, pp. 439–443, London, UK, June 2009.

[37] J. Yoon, B. Novandy, C. H. Yoon, and K. J. Park, "A 6-DOF gait rehabilitation robot with upper and lower limb connections that allows walking velocity updates on various terrains," *IEEE/ASME Transactions on Mechatronics*, vol. 15, no. 2, Article ID 5424007, pp. 201–215, 2010.

[38] M. Peshkin, D. A. Brown, J. J. Santos-Munne et al., "KineAssist: a robotic overground gait and balance training device," in *Proceedings of the 9th IEEE International Conference on Rehabilitation Robotics, (ICORR '05)*, pp. 241–246, Evanston, Ill, USA, July 2005.

[39] J. K. Burgess, G. C. Weibel, and D. A. Brown, "Overground walking speed changes when subjected to body weight support conditions for nonimpaired and post stroke individuals," *Journal of NeuroEngineering and Rehabilitation*, vol. 7, no. 1, article 6, 2010.

[40] M. Bouri, Y. Stauffer, C. Schmitt et al., "The walktrainer: a robotic system for walking rehabilitation," in *Proceedings of the IEEE International Conference on Robotics and Biomimetics, (ROBIO '06)*, pp. 1616–1621, Kunming, China, December 2006.

[41] Y. Allemand and Y. Stauffer, "Overground gait rehabilitation: first clinical investigation with the walktrainer," in *Proceedings of the European Conference on Technically Assisted Rehabilitation, (TAR '09)*, Berlin, Germany, 2009.

[42] A. Goffer, "Gait-locomotor apparatus," US patent number 7 153 242, 2006.

[43] H. Kawamoto and Y. Sankai, "Power assist system hal-3 for gait disorder person," in *Proceedings of the 8th International Conference on Computers Helping People with Special Needs*, pp. 196–203, London, UK, 2002.

[44] K. Suzuki, Y. Kawamura, T. Hayashi, T. Sakurai, Y. Hasegawa, and Y. Sankai, "Intention-based walking support for paraplegia patient," in *Proceedings of the International Conference on Systems, Man and Cybernetics*, vol. 3, pp. 2707–2713, Hawaii, USA, October 2005.

[45] H. Kawamoto, T. Hayashi, T. Sakurai, K. Eguchi, and Y. Sankai, "Development of single leg version of HAL for hemiplegia," in *Proceedings of the 31st Annual International Conference of the IEEE Engineering in Medicine and Biology Society, (EMBC '09)*, pp. 5038–5043, Minneapolis, Minn, USA, September 2009.

[46] K. H. Seo and J. J. Lee, "The development of two mobile gait rehabilitation systems," *IEEE Transactions on Neural Systems and Rehabilitation Engineering*, vol. 17, no. 2, Article ID 4785182, pp. 156–166, 2009.

[47] C. Schmitt, P. Métrailler, A. Al-Khodairy et al., "The motion maker: a rehabilitation system combining an orthosis with closed-loop electrical muscle stimulation," in *Proceedings of the 8th Vienna International Workshop on Functional Electrical Stimulation*, pp. 117–120, Vienna, Austria, September 2004.

[48] M. Bouri, B. Le Gall, and R. Clavel, "A new concept of parallel robot for rehabilitation and fitness: the Lambda," in *Proceedings of the IEEE International Conference on Robotics and Biomimetics, (ROBIO '09)*, pp. 2503–2508, Guilin, China, December 2009.

[49] K. Homma, O. Fukuda, J. Sugawara, Y. Nagata, and M. Usuba, "A wire-driven leg rehabilitation system: development of a 4-dof experimental system," in *Proceedings of the International Conference on Advanced Intelligent Mechatronics, (IEEE/ASME '03)*, vol. 2, pp. 908–913, Piscataway, NJ, USA, July 2003.

[50] P. Sui, L. Yao, Z. Lin, H. Yan, and J. S. Dai, "Analysis and synthesis of ankle motion and rehabilitation robots," in *Proceedings of the IEEE International Conference on Robotics and Biomimetics, (ROBIO '09)*, pp. 2533–2538, Guilin, China, December 2009.

[51] M. Girone, G. Burdea, M. Bouzit, V. Popescu, and J. E. Deutsch, "Stewart platform-based system for ankle telerehabilitation," *Autonomous Robots*, vol. 10, no. 2, pp. 203–212, 2001.

[52] J. E. Deutsch, J. Latonio, G. C. Burdea, and R. Boian, "Post-stroke rehabilitation with the Rutgers Ankle system: a case study," *Presence: Teleoperators and Virtual Environments*, vol. 10, no. 4, pp. 416–430, 2001.

[53] R. Boian, C. Lee, J. Deutsch, G. Burdea, and J. Lewis, "Virtual realitybased system for ankle rehabilitation post stroke," in *Proceedings of the 1st International Workshop on Virtual Reality Rehabilitation, (VRMHR '02)*, pp. 77–86, Lausanne, Switzerland, November 2002.

[54] J. E. Deutsch, J. A. Lewis, and G. Burdea, "Technical and patient performance using a virtual reality-integrated telerehabilitation system: preliminary finding," *IEEE Transactions on Neural Systems and Rehabilitation Engineering*, vol. 15, no. 1, pp. 30–35, 2007.

[55] R. Boian, M. Bouzit, G. Burdea, and J. Deutsch, "Dual stewart platform mobility simulator," in *Proceedings of the 26th Annual International Conference of the IEEE Engineering in Medicine and Biology Society, (IEMBS '04)*, vol. 2, pp. 4848–4851, September 2004.

[56] J. A. Saglia, N. G. Tsagarakis, J. S. Dai, and D. G. Caldwell, "A high-performance redundantly actuated parallel mechanism for ankle rehabilitation," *International Journal of Robotics Research*, vol. 28, no. 9, pp. 1216–1227, 2009.

[57] J. Nikitczuk, B. Weinberg, P. K. Canavan, and C. Mavroidis, "Active knee rehabilitation orthotic device with variable damping characteristics implemented via an electrorheological fluid," *IEEE/ASME Transactions on Mechatronics*, vol. 15, no. 6, Article ID 5353649, pp. 952–960, 2010.

[58] T. Kikuchi, K. Oda, and J. Furusho, "Leg-robot for demonstration of spastic movements of brain-injured patients with compact magnetorheological fluid clutch," *Advanced Robotics*, vol. 24, no. 16, pp. 671–686, 2010.

[59] J. Yoon and J. Ryu, "A novel reconfigurable ankle/foot rehabilitation robot," in *Proceedings of the IEEE International Conference on Robotics and Automation, (ICRA '05)*, pp. 2290–2295, Barcelona, Span, April 2005.

[60] Y. Ding, M. Sivak, B. Weinberg, C. Mavroidis, and M. K. Holden, "NUVABAT: northeastern university virtual ankle and balance trainer," in *Proceedings of the IEEE Haptics Symposium, (HAPTICS '10)*, pp. 509–514, Waltham, Mass, USA, March 2010.

[61] J. S. Dai, T. Zhao, and C. Nester, "Sprained ankle physiotherapy based mechanism synthesis and stiffness analysis of a robotic rehabilitation device," *Autonomous Robots*, vol. 16, no. 2, pp. 207–218, 2004.

[62] Y. H. Tsoi and S. Q. Xie, "Impedance control of ankle rehabilitation robot," in *Proceedings of the IEEE International Conference on Robotics and Biomimetics, (ROBIO '08)*, pp. 840–845, Bangkok, Thailand, February 2009.

[63] C. C. K. Lin, M. S. Ju, S. M. Chen, and B. W. Pan, "A specialized robot for ankle rehabilitation and evaluation," *Journal of Medical and Biological Engineering*, vol. 28, no. 2, pp. 79–86, 2008.

[64] K. Homma and M. Usuba, "Development of ankle dorsiflexion/plantarflexion exercise device with passive mechanical joint," in *Proceedings of the 10th IEEE International Conference on Rehabilitation Robotics, (ICORR '07)*, pp. 292–297, Noordwijk, The Netherlands, June 2007.

[65] D. P. Ferris, G. S. Sawicki, and A. R. Domingo, "Powered lower limb orthoses for gait rehabilitation," *Topics in Spinal Cord Injury Rehabilitation*, vol. 11, no. 2, pp. 34–49, 2005.

[66] B. J. Ruthenberg, N. A. Wasylewski, and J. E. Beard, "An experimental device for investigating the force and power requirements of a powered gait orthosis," *Journal of Rehabilitation Research and Development*, vol. 34, no. 2, pp. 203–213, 1997.

[67] G. Belforte, L. Gastaldi, and M. Sorli, "Pneumatic active gait orthosis," *Mechatronics*, vol. 11, no. 3, pp. 301–323, 2001.

[68] A. Roy, H. I. Krebs, S. L. Patterson et al., "Measurement of human ankle stiffness using the anklebot," in *Proceedings of the 10th IEEE International Conference on Rehabilitation Robotics, (ICORR '07)*, pp. 356–363, Noordwijk, The Netherlands, June 2007.

[69] H. I. Krebs, L. Dipietro, S. Levy-Tzedek et al., "A paradigm shift for rehabilitation robotics," *IEEE Engineering in Medicine and Biology Magazine*, vol. 27, no. 4, pp. 61–70, 2008.

[70] I. Khanna, A. Roy, M. M. Rodgers, H. I. Krebs, R. M. MacKo, and L. W. Forrester, "Effects of unilateral robotic limb loading on gait characteristics in subjects with chronic stroke," *Journal of NeuroEngineering and Rehabilitation*, vol. 7, no. 1, article 23, 2010.

[71] J. A. Blaya and H. Herr, "Adaptive control of a variable-impedance ankle-foot orthosis to assist drop-foot gait," *IEEE*

Transactions on Neural Systems and Rehabilitation Engineering, vol. 12, no. 1, pp. 24–31, 2004.

[72] A. Agrawal, S. K. Banala, S. K. Agrawal, and S. A. Binder-Macleod, "Design of a two degree-of-freedom ankle-foot orthosis for robotic rehabilitation," in *Proceedings of the 9th IEEE International Conference on Rehabilitation Robotics, (ICORR '05)*, pp. 41–44, July 2005.

[73] G. S. Sawicki and D. P. Ferris, "A pneumatically powered knee-ankle-foot orthosis (kafo) with myoelectric activation and inhibition," *Journal of NeuroEngineering and Rehabilitation*, vol. 6, p. 23, 2009.

[74] D. P. Ferris, K. E. Gordon, G. S. Sawicki, and A. Peethambaran, "An improved powered ankle-foot orthosis using proportional myoelectric control," *Gait & Posture*, vol. 23, no. 4, pp. 425–428, 2006.

[75] K. Bharadwaj and T. G. Sugar, "Kinematics of a robotic gait trainer for stroke rehabilitation," in *Proceedings of the IEEE International Conference on Robotics and Automation, (ICRA '06)*, pp. 3492–3497, Orlando, Fla, USA, May 2006.

[76] J. A. Ward, S. Balasubramanian, T. Sugar, and J. He, "Robotic gait trainer reliability and stroke patient case study," in *Proceedings of the10th IEEE International Conference on Rehabilitation Robotics, (ICORR '07)*, pp. 554–561, Noordwijk, The Netherlands, June 2007.

[77] S. Hwang, J. Kim, J. Yi, K. Tae, K. Ryu, and Y. Kim, "Development of an active ankle foot orthosis for the prevention of foot drop and toe drag," in *Proceedings of the International Conference on Biomedical and Pharmaceutical Engineering, (ICBPE '06)*, pp. 418–423, Singapore, December 2006.

[78] J. Y. Kim, S. J. Hwang, and Y. H. Kim, "Development of an active ankle-foot orthosis for hemiplegic patients," in *Proceedings of the 1st International Convention on Rehabilitation Engineering and Assistive Technology, (i-CREATe '07)*, pp. 110–113, New York, NY, USA, April 2007.

[79] A. C. Satici, A. Erdogan, and V. Patoglu, "Design of a reconfigurable ankle rehabilitation robot and its use for the estimation of the ankle impedance," in *Proceedings of the IEEE International Conference on Rehabilitation Robotics, (ICORR '09)*, pp. 257–264, Kyoto, Japan, June 2009.

[80] G. Sulter, C. Steen, and J. De Keyser, "Use of the barthel index and modified rankin scale in acute stroke trials," *Stroke*, vol. 30, no. 8, pp. 1538–1541, 1999.

[81] G. S. Sawicki, K. E. Gordon, and D. P. Ferris, "Powered lower limb orthoses: applications in motor adaptation and rehabilitation," in *Proceedings of the 9th IEEE International Conference on Rehabilitation Robotics, (ICORR '05)*, pp. 206–211, July 2005.

Hindawi Publishing Corporation
Journal of Robotics
Volume 2011, Article ID 438514, 11 pages
doi:10.1155/2011/438514

Research Article

Toward Monitoring and Increasing Exercise Adherence in Older Adults by Robotic Intervention: A Proof of Concept Study

Prathik Gadde, Hadi Kharrazi, Himalaya Patel, and Karl F. MacDorman

School of Informatics, Indiana University, 535 West Michigan Street, Indianapolis, IN 46202, USA

Correspondence should be addressed to Karl F. MacDorman, kmacdorm@indiana.edu

Received 31 May 2011; Revised 17 August 2011; Accepted 18 August 2011

Academic Editor: Haruhisa Kawasaki

Socially assistive robots have the potential to improve the quality of life of older adults by encouraging and guiding their performance of rehabilitation exercises while offering cognitive stimulation and companionship. This study focuses on the early stages of developing and testing an interactive personal trainer robot to monitor and increase exercise adherence in older adults. The robot physically demonstrates exercises for the user to follow and monitors the user's progress using a vision-processing unit that detects face and hand movements. When the user successfully completes a move, the robot gives positive feedback and begins the next repetition. The results of usability testing with 10 participants support the feasibility of this approach. Further extensions are planned to evaluate a complete exercise program for improving older adults' physical range of motion in a controlled experiment with three conditions: a personal trainer robot, a personal trainer on-screen character, and a pencil-and-paper exercise plan.

1. Introduction

1.1. Benefits of Humanoid Robots to Older Adults. The proportion of adults aged 65 or older has been steadily increasing for more than a century in most developed countries. In the USA, it has increased from 4.1% (3.1 mil.) in 1900 to 8.1% (12.6 mil.) in 1950 to 12.4% (34.6 mil.) in 2000 and is projected to reach 20.6% (82 mil.) in 2050 [1]. This steep increase raises the concern of where older adults will live. A 1992 study found most of them prefer "aging in place," that is, remaining in their homes with little or no supervision [2, 3]. Although aging in place has some advantages, like increased autonomy and maintaining familiar surroundings, one potential disadvantage is fewer opportunities for receiving encouragement to engage in physical activity.

Physical activity may delay the onset of physical deficits contributing to frailty. These deficits include decreased skeletal muscle strength, gait speed, musculoskeletal flexibility, range of joint motion, postural stability (including balance, coordination, and reaction time), and cardiovascular responsiveness [4]. These conditions result in significant functional limitations. For example, 15% of people aged 75 to 84 are unable to climb stairs, and a substantial proportion of otherwise healthy older adults have limitations in gait speed that prevent them from crossing an intersection quickly enough to comply with traffic signals [4, 5]. Increased physical activity, such as through a daily exercise program, has been found to reduce physical ailments and improve strength and mobility [5–7]. However, exercise programs are beneficial only when followed regularly and consistently; living conditions and other factors may impede program adherence [8–11]. For instance, older adults living at home typically have reduced access to healthcare and health interventions as compared with those living under long-term care at a nursing home [12]. Furthermore, employing live-in-care staff can be expensive. Without the supervision and encouragement of nursing staff, stay-at-home older adults are at an increased risk of not adhering to an exercise program [13].

Another potential disadvantage of aging in place as compared with group living facilities is fewer opportunities for regular, meaningful interpersonal relationships. Companionship has important health benefits for older adults who age in place. For example, living together with another person significantly decreases feelings of loneliness in older

adults [14]. When human companionship is unavailable, an animal or robot companion can reduce feelings of isolation, in part by giving a sense of physical and social presence [15–17]. An animal companion positively impacts the health of socially isolated individuals and can produce long-term positive effects on the health and behavior of older adults [18, 19]. When a companion animal is not feasible, a robot may be substituted; this has the benefits of lower recurring costs, a lower burden of care and responsibility, and greater hygiene. Robots have elicited similar palliative outcomes when substituted for a companion animal [20–22].

However, few studies have been conducted on how to use robots or robot therapy to improve the mental and physical health or quality of life of older adults [20–24]. To close this research gap, the field of socially assistive robotics has emerged. Socially assistive robots have been used in certain contexts to aid recovery through social interactions [25]. The robot's interaction style may be informed by the human user's personality [26], movement, or physical orientation [27].

Socially assistive robots can be relatively inexpensive and simple to use. Paro [15, 28], for example, has been used in nursing homes in Japan, the United States, and Europe for companionship and to stimulate social interaction among patients [17, 20, 22]. Paro, which looks like a baby harp seal, is designed to provide therapy for older adults with dementia. Its sensors enable it to respond to both touch and speech in a manner resembling a domesticated animal companion.

Although Paro's cognitive capacities are extremely limited relative to those of people, animal pets, and even other robots, nonverbal cues such as looking toward the person speaking or responding to being petted can convey a sense of physical and social presence that in turn reduces loneliness and encourages the sharing of feelings [17]. Paro and other similar robots may provide comfort by giving the impression that "somebody is there." They succeed to the extent that they are able to "press our Darwinian buttons" by mimicking largely unconscious human and other animal behavior that elicits in their users prosocial behavior, such as the human desire to nurture and be nurtured [16]. Paro's success as a companion robot may result from its anthropomorphic appearance, and especially the inclusion of eyes, a conclusion supported by the findings of several unrelated experiments [29–31]. In particular, these findings support the theory that human beings have inherited an automatic, unconscious neural mechanism that conferred on their ancestors' selective advantage by increasing prosocial behavior when being observed. Thus, interactive technologies can be engineered to exploit unconscious mechanisms to promote adherence to a physical exercise program or to any other kind of activity supported by social expectations.

An advantage to humanoid robot companions is that not only can they be endowed with social intelligence but their appearance also affords the automatic perception of them as socially intelligent. Thus, when robots look, act, or are presented as humanlike, social entities, they are more likely to elicit in us the same responses that other human beings elicit [32]. This effect has been measured by the human interaction partner's conscious behavior, unconscious behavior (e.g., gaze) [33], attributions of thoughts, feelings, and intentions, and adherence to advice [34, 35]. The anthropomorphic physical embodiment of a humanoid robot could have a significant effect on patients' adherence to a physician-prescribed exercise program. Shinozawa et al. [34] found that participants are more likely to follow a robot's recommendation than that of an on-screen character. Kidd and Breazeal [35] found that participants track their exercise and calorie consumption for almost twice as long with a robot as with a computer or with paper and pencil. They also develop a closer relationship with the robot.

1.2. Affordable Interactive Exercise Systems. Despite the development of technologies for rapidly and robustly detecting human faces and hands, only recently have these technologies been applied to monitoring exercise performance and providing feedback [36]. Systems have been developed that demonstrate exercises [37] or provide feedback and encouragement for performing stroke rehabilitation exercises [38, 39] or completing mental and physical button-pressing tasks [40]. In 2011, Respondesign MayaFit Virtual Fitness Trainer [41], implemented on the PrimeSense OpenNI Framework, combines exercise adherence monitoring with an animated on-screen human-looking character to guide healthy individuals through a personalized sequence of exercise movements, monitor their progress, and provide feedback. (MayaFit uses the same three-dimensional motion capture technology as Microsoft's Kinect [42].) However, these are examples of specialized hardware and software. It should be possible to encourage exercise with more affordable, mass-produced devices [43].

In summary, older adults, especially those aging in place, are subject to physical and mental problems that drastically diminish their quality of life [44]. To reduce these problems, an interactive system could instruct, monitor, and encourage older adults during the performance of physician-prescribed exercises. Such a system would offer a combination of distinct advantages as compared with the usual paper-and-pencil-based materials or an automatic telephone reminder system. The interactive system performs the exercises in front of the participant; the system provides continuous instant feedback and encouragement during the exercises; the system provides a more affordable substitute for a human personal trainer; the system provides exercise guidance at flexible times; the system can increase adherence by presenting itself as a humanlike, social entity; the system can report the results back to the physician.

Interactive technologies can present their humanlike agency through the virtual embodiment of an on-screen character or through the physical embodiment of a humanoid robot. Each approach has its advantages. The advantages of an on-screen character, which requires only a computer, a video camera with a fixed focal length (i.e., a webcam), and software, are numerous: low purchase and maintenance costs, high portability (for notebook computer models), high reliability (as compared with robots, which are animated by motors that can jam and break), and the absence of safety risks related to physical contact (e.g., fingers pinched

by a robot joint) [45]. The advantages of an interactive robot are likewise numerous: the robot has heightened sociality because of its enduring anthropomorphic and physical presence, which is likely to increase adherence to treatment including exercise [34, 35]; even simple robots can provide a sense of companionship [16, 17]; robots often have mobility, which enables them to navigate their environments autonomously [23, 46], and thus can be designed to accompany their owners on walks; it is easier to see and understand exercises performed in three dimensions by a robot than in two dimensions by a character on a screen because the former affords depth perception by binocular disparity and movement parallax.

2. Prototype Interaction Design and System Design and Implementation

The long-term goal of this research is to increase adherence among adults aged 65 or older to a physician-prescribed exercise program through their interaction with a personal trainer robot in their own homes. This technology is intended for older adults who have a sedentary lifestyle. The fully developed system should be inexpensive, communicate with older adults in real time, and report the results to their physicians through a hospital webserver.

The humanoid robot in this study has been designed to start an exercise session with users and help them adhere to a predetermined schedule. When the user is ready, the robot demonstrates the first prescribed exercise by moving its body parts. If the user performs the exercise correctly, the robot praises the user and begins the next repetition. To communicate with the user, the robot uses synthesized speech in addition to the gestures that depict each exercise movement. The robot also recognizes hand and head movements to monitor the user's progress through the exercise set and to estimate the user's activity level (Figure 1).

2.1. Software Components of Personal Trainer Robot Prototype. The software is composed of a vision-processing unit and an exercise adherence unit, which communicate with each other to determine and carry out the next move of the robot. The interactive prototype detects the users' physical presence and recognizes the users' gestures (i.e., the exercise movements). It determines whether the user has successfully performed the exercise move as demonstrated by the robot. Next, the exercise adherence unit obtains the tracked head and upper arm positions from the vision-processing unit and delivers the appropriate voice commands accordingly (Figure 2).

2.1.1. Vision-Processing Unit. The vision-processing unit uses a wide-angle USB video camera. The camera captures the video, which is then processed in its native size. The system sets two different regions of interest (ROIs) to indicate the most likely location for features: one for the face and the other for the hands. The face and hand detection are then performed in their respective ROIs.

The user is encouraged to sit at a certain distance from the camera so as to be positioned at the center of the video

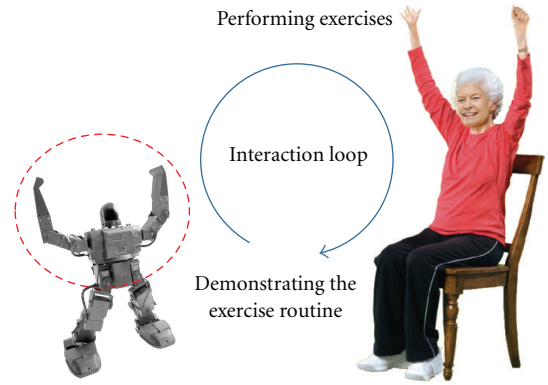

Figure 1: An interaction loop links the older adult user and the personal trainer robot. Within this loop, the robot leads the user through each exercise move by physically demonstrating it and giving encouragement and feedback on the user's adherence through synthesized speech.

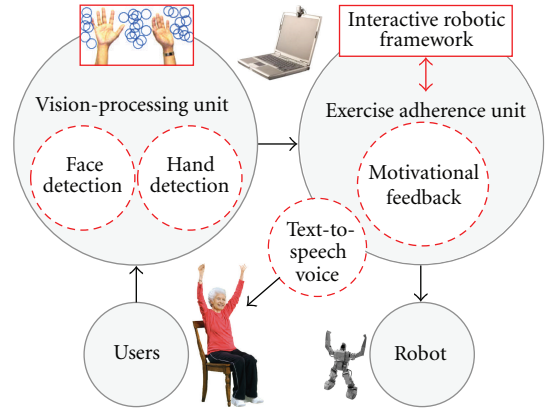

Figure 2: Information flows from the vision-processing unit, which monitors the user's movements, to the exercise adherence unit. The exercise adherence unit controls the robot's performance of each exercise move and, after the user completes (or fails to complete) the move, reports the adherence assessment. The interactive framework used in this study is shown in Figure 7.

frame. The optimal distance is determined by the user's height. Initially, the user is encouraged to perform trial exercise moves in front of the camera to check whether the user in the raised-hands position fits within the video frame. Lighting conditions consistent with a well-lit room should be maintained throughout the process so that enough light falls on the face and hands for accurate detection.

2.1.2. Face Detection and Tracking. Face detection is a part of object recognition research [47], and much work has been conducted on it since the inception of vision processing. Turk and Pentland [48] developed an automatic recognition system based on eigenfaces that compares the features of novel faces to already known faces. Liu [49] applied Bayesian discriminating features to frontal face detection, while Mohan et al. [50] devised an example-based algorithm. Viola and Jones [51] used machine-learning techniques and Haar-like features for rapid, accurate face detection and later added a set of tilted Haar-like features to enhance detection [52].

The current study builds on previous research by using classifiers with an extended set of Haar-like features, including edge, line, and center-surround features for rapid face detection and localization [51, 52]. The Haar-like features test for a face in the face ROI of each frame. A cascade of classifiers was employed to increase the detection rate. Once detected, the face is extracted within a bounded rectangular region, and the centroid of the rectangle is computed and continuously tracked.

Haar face and hand classifiers were created through a training process using the OpenCV library. Training a Haar classifier is a CPU time- and memory-intensive process that requires sample images of the object of interest (positive images) and of other objects (negative images). To improve classification accuracy, a 20-stage cascade of Haar classifiers was trained with the Gentle AdaBoost algorithm [53] using 5,000 positive and 6,500 negative images. The training required 18 days and was performed on a PC with an Intel Pentium 4 (2.2 GHz) processor and 2 GB of RAM.

To improve the system's classification accuracy, the user is positioned at the center of the video frame. Because users' heights in this study varied between 165 and 188 cm, they were first asked to sit in front of the camera so that the approximate regions of the face could be calculated and an ROI could be obtained. Based on these calculations, the face ROI origin point was set 200 pixels to the right and 100 pixels down from the top-left corner of the original frame (i.e., $x = 200$ and $y = 100$). An ROI 340 pixels wide by 300 pixels tall was then created with its top left corner at the face ROI origin point. Presetting the ROI increases the efficiency and the accuracy of the system because it provided a smaller area in which the face is likely to be found. The region was cropped and displayed in a separate window. The face detection system searched the entire region for a face by repeatedly applying the cascade of Haar classifiers in the Haar-like feature space. After locating a rectangular area containing a face, the system returns the coordinates of its centroid and four corners and tracks the face in that area. Thus, the movements of the face are continuously monitored, and the coordinates are stored in memory for future reference. The calculation of the centroid enabled the tracking of even small movements of the head, thereby increasing the sensitivity and effectiveness of the system.

2.1.3. Upper-Limb Motion Detection and Tracking. The Haar-like features and Haar classifiers that were used for face detection were initially applied to hand detection. However, because hand gestures are often more complex than those made by the head and face (i.e., because the hands can be twisted into more physically distinct configurations), the Haar classifiers were less effective for hand detection than for face detection and, subsequently, the results could not be used during real-time video streaming. A more feasible method of observing hand movements was using motion detection (Figure 3). The method was reused for detecting motion in the other parts of the upper limbs, including the forearms.

Motion Detection. The frames used for vision processing are captured from the camera. From each of these frames, the subframe defined by the ROIs is extracted and processed. An example of one such subframe on which the image processing is performed is shown in Figure 3(a). Subframes will contain some noise from the camera sensor, which should be reduced to avoid false positives (Figure 3(b)). Applying to the subframe a simple blur reduces this noise. Once noise is removed, the presence of motion is detected by calculating the absolute difference in corresponding pixel values from two consecutive subframes. A new image with the calculated difference is created, and the difference image is converted to 8-bit grayscale, so that it is easy to apply filters (Figure 3(c)). A binary threshold filter is then applied to the subframe (Figure 3(d)). The presence of motion is defined as a sufficient difference in pixel luminance values between two consecutive subframes [54]. In this difference image, white pixels indicate the presence of motion.

When the position of the object changes between subframes, it produces a shift in darker and lighter pixels: darker when an object at the location in the first frame disappears in the second frame, and lighter when an empty location in the first frame contains an object in the second frame. When the difference image is converted to grayscale, it becomes easier to find the differences between the two source images.

To provide visual feedback of upper-limb motion detection, the ROI is overlaid with equally sized circles, each of which is bounded by a square. The circles scatter away from areas where motion is present. For example, if motion occurs at the bottom of the ROI, the circles will scatter towards the middle and top. Whenever the total number of changed pixels in each bounding square exceeds the predefined value of 100, motion is considered present in the bounding square.

Upper-Limb Tracking. The absence of circles in two large areas of the ROI indicates the location of the upper limbs. The upper limbs are tracked by calculating the difference between the centroids of the two corresponding rectangular areas in consecutive frames.

Determining the Upper-Limb Region of Interest. For detecting motion in the upper limbs, an ROI was obtained by a method similar to the one used for calculating the ROI for face detection, namely, by observing several users making the motion, which in this case was raising their hands. An assumption was made that the location of the hands would provide sufficient information about the location of the corresponding forearms. On that assumption, the ROI for the hand region was obtained by observing the raised hands of several users. The hands ROI origin was set 100 pixels to the right of the top-left corner of the frame. An ROI subframe 400 pixels wide and 200 pixels tall was then created with its top left corner at the hands ROI origin point.

2.1.4. Exercise Adherence Unit. The exercise adherence unit monitors data from the vision-processing unit and plays the appropriate voice commands.

The communication of the robot is controlled by a program developed using the robot's software development kit

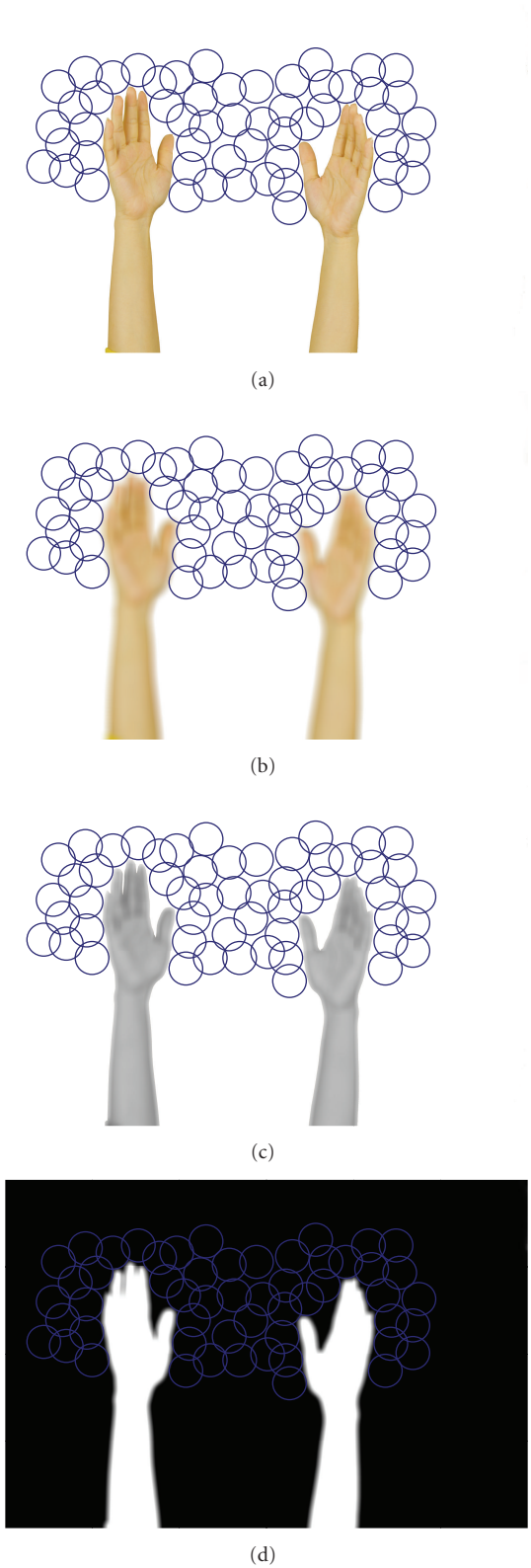

(a)

(b)

(c)

(d)

Figure 3: During motion detection, subframes within the region of interest are captured (a), blurred (b), and converted to shades of gray (c). In the areas of the subframe indicated by circles, the pixels changing between consecutive captures (d) comprise a direct measurement of motion. Such pixel changes are repeatedly summed and compared with a predefined threshold value. At a given time in a given area, if the threshold value is exceeded, motion is detected.

(SDK). The voice commands delivered by the robot during interaction were synthesized using AT & T Labs' Natural Voices text-to-speech software [55]. These voice commands are incorporated into the software system and synchronized with the exercise routines. A connection is made such that the exercise adherence unit communicates directly with the vision-processing unit to interact with the user. The exercise adherence unit receives information about the presence of a person from the vision-processing unit (Figure 4). If it detects a user, the robot greets the user and requests consent to start the exercise routine. The user indicates readiness by waving one hand overhead. The robot then starts the interaction cycle by demonstrating the first of the recommended physical exercise routines. The robot vocally announces the first exercise movement and then demonstrates it by moving its body parts. Next, the robot waits for the user to imitate the movement. The robot detects the movement, analyzes its timing and form, and judges whether the user's action is correct. After a successful attempt, the robot praises the user; otherwise, it repeats the movement and instructions. This continues until the user performs the exercise correctly. At the end of the interaction cycle, the robot gives verbal feedback on the user's performance during the exercise routines. The robot then provides a goodbye message and ends the session.

The exercise adherence unit demonstrates exercises by specifying parameters to the robot's servomotors for each exercise move: the desired angle for every joint and both the velocity and number of displacement steps with which the joint should move to that angle. Two exercise moves were used in this study: the overhead arm raise and the head turn.

Detecting an Overhead Arm Raise. To calibrate the system, the robot asks the user to raise the hands as far as possible. During the overhead arm raise, one repetition is counted if the user raises the hands at least 90% of that extent. The success rate is measured by the number of attempts divided by the number of trials. Range of motion is informally quantified as the percentage of the maximal arm raise averaged across all trials.

Detecting a Head Turn. The extent of a head turn is estimated from the deviation of the face's centroid from its head-on position divided by a constant and then taking the arcsine. The constant is determined empirically after setting up the system. The exercise adherence unit counts one head turn if the head is turned at least 45 degrees. If the user is unable to make a 45-degree head turn after three attempts, the threshold for a head turn is lowered to the mean of the maximal angle during the three attempts. The success rate is measured by the number of attempts divided by the number of trials. Range of motion is approximated as the mean degrees the head is turned across all trials, regardless of whether they were successful.

2.2. Hardware Components of Personal Trainer Robot Prototype. The interactive system has three hardware components: the robot, the webcam, and the controller computer.

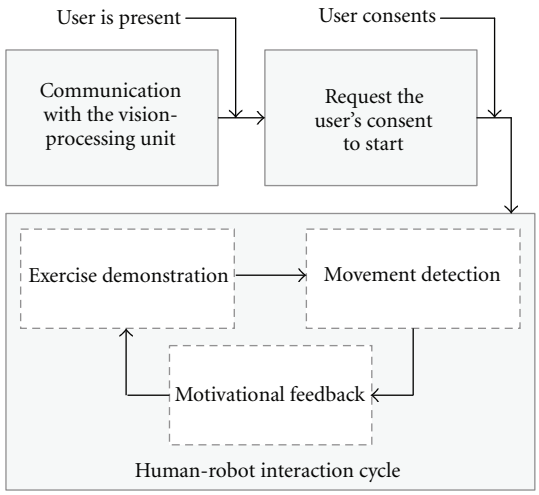

Figure 4: In the exercise adherence interaction framework, the interaction is controlled mainly by the user's consent to participate. Consent is requested both before the first exercise and after each completed exercise.

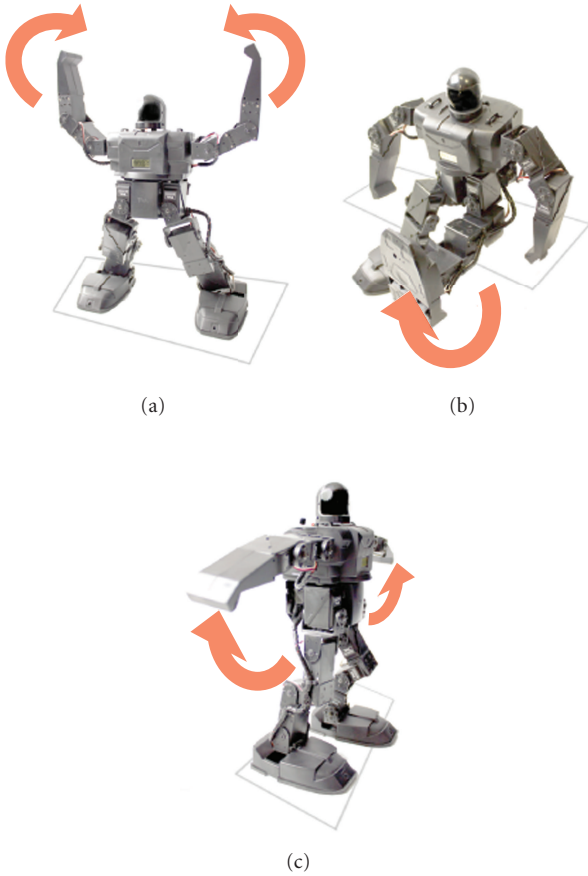

Figure 5: The set of possible exercises is determined by the physical capabilities of the humanoid robot. The robot's 20 servo motors enable the turning movements of the head, waist, and thighs and joint movements of the limbs.

2.2.1. Humanoid Robot. RoboPhilo, a programmable humanoid [56] robot, has been used in this study. It has 24 available servo channels with up to eight input-output interfaces. It has 20 servomotors that enable the turning movements of the head, waist, and thighs and joint movements of the limbs. It can be connected directly to a PC via an RS-232 serial connection and can be programmed using its SDK. It can be controlled directly by using the infrared remote or autonomously by using the SDK. The robot can be programmed with various exercise movements (e.g., Figure 5(a), 5(b), and 5(c)). At US$500, RoboPhilo is relatively inexpensive given the number and mobility of its joints. At the time of this writing, a complete system including computer, webcam, and SDK could be purchased for about US$900.

2.2.2. Webcam. The vision-processing unit can use a video camera that is either built in or externally attached to the PC. The testbed uses a Logitech Webcam Pro 9000 USB camera with a 72° diagonal field of view and a maximum resolution of 1600 × 1200 pixels. At that resolution, the video frame rate was 10 fps. The large field of view simultaneously captures both the head and hand regions, and the higher pixel count allows greater precision during motion tracking.

2.2.3. Controller PC. The vision-processing unit, exercise adherence unit, and robot were controlled by a PC running a 32-bit version of Microsoft Windows XP. The PC had an Intel Core 2 Duo processor, 4 GB of RAM, and a PCI-based RS-232 serial port. (A USB–RS-232 adapter could not be used because it increased the startup time to 15 s, which exceeds the 10 s interval during which RoboPhilo must receive its initial response from the PC to avoid halting.)

3. Methods

The quality of the human-robot interaction of the prototype system was assessed in a diagnostic usability test. The testing of the interaction was important at this initial stage to ascertain the participants' enthusiasm and interest when interacting with the robot and their perception of the robot as a potential trainer. This information is essential to assessing the system's user friendliness and commercial viability.

3.1. Procedure. The usability test was conducted in a room with large windows, overhead fluorescent lights, and lightly textured off-white walls. The setup conditions enabled the system to detect the face and hands of the participant easily. The testing equipment included the robot hardware unit, video camera, and computer. A chair was positioned against the wall and facing the robot and the camera. It was positioned so that the participant would always fit within the video frame (Figure 6). Other objects in the camera's field of view were removed to reduce false positives.

The participants were instructed to sit on the chair and were introduced to the purpose of the study, the capabilities

Figure 6: The first author demonstrates a typical position of a participant in the study.

and limitations of the robot, and the session's flow of interaction. They were cautioned about unexpected and out-of-sequence occurrences owing to the fact that the testbed was still in the development and testing stage. The participants were then asked to watch the robot and repeat its actions using only hand and head movements. The robot demonstrated two basic moves to the participants: the overhead arm raise and the head turn. The interactions were observed, and feedback was sought from the participants. The interactions were also video recorded for later analysis. Figure 7 details the step-by-step procedure of the interaction cycle.

4. Results and Discussion

4.1. Qualitative Results of the Usability Test. The interaction sequence for seven of the ten participants was conducted without any technical glitches (Table 1). However, for three of the participants, the sequence was interrupted. Two participants failed to comply with the instructions: they either moved their hands too quickly or did not turn their head in the same direction the robot turned its head. The robot failed to detect the raised hands of the third participant because the hands were outside of the captured frame. Although the interaction typically took seven to eight minutes, one interaction took 12 minutes.

Nine of the ten participants assumed that the robot could listen, understand, and process what they were saying and respond accordingly. They were reminded not to talk to the robot, but to communicate with it using hand or head movements. Their attempts at verbal communication indicate that most users expect an interactive robot to listen and reply to them in a way that is uniquely appropriate to the direction and nature of the conversation and situation [56]. The fulfillment of these user expectations is an area for future research.

4.2. Technical Refinements. As expected, the robot was unable to change its behavior and act according to the situation when the sequence was altered or disturbed. For example, in the case of the three participants with whom the interaction was not smooth, the robot either continued with its programmed responses regardless of the participants' reactions or it abruptly ended the sequence. This inconsistent behavior occurred because the robot has been programmed to detect threshold values for each of the exercise moves. The robot waits for the participant to reach before considering the participant's attempt as successful. However, in the case of an unsuccessful attempt by the participant, the vision-processing unit reported a random value, resulting either in the robot skipping essential steps in the sequence or in the termination of the entire sequence. These two errors were observed with the first two participants, but were fixed immediately thereafter. The errors did not occur with the remaining eight participants.

The trained Haar classifier detected multiple faces at the same time. This was problematic because in some cases, multiple faces were detected when there was only one face. Thus, enabling the detection of multiple faces resulted in more frequent false positives. This occurs because the classifier identifies as many sets of coordinates as the number of faces it detects, which results in the termination of the vision-processing unit. Although multiple face detection was intentionally implemented, we did not anticipate the problem of cycle termination. The bug was fixed by restricting the classifier to detect only one face in the frame and to reject all subsequent potential faces.

It was also observed that the robot terminated the interaction if the participants' response came too slowly after each exercise demonstration instead of waiting for the participant to respond. The bug was fixed after the usability test. Finally, the participants reported feeling that the robot terminated the program too abruptly after the exercise routines were completed. The participants reported that they would have preferred to receive more feedback about their performance before the robot conveyed the goodbye message. The exercise adherence unit was modified to report the percentage of repetitions completed and the average extent in percentages of the overhead arm raise and head turn.

5. Conclusion

By 2050, the number of Americans who are 65 or older is expected to more than double, reaching 82 millions. These older adults constitute the most sedentary segment of the US population, and they suffer from the most chronic conditions that are preventable through exercise. Although the most convenient and effective means of increasing exercise adherence among older adults living at home involve one-on-one monitoring and encouragement, the required human resources are in short supply and the costs are prohibitive. Medically, treating chronic conditions that are preventable through exercise incurs high economic costs for the afflicted individuals, their families, and for Medicare or their private health insurers. The loss of mobility can necessitate additional costs associated with nursing care, either at home or at a nursing facility. In addition, conditions preventable through exercise can incur high personal and social costs, including physical pain and suffering and social isolation caused by loss of mobility.

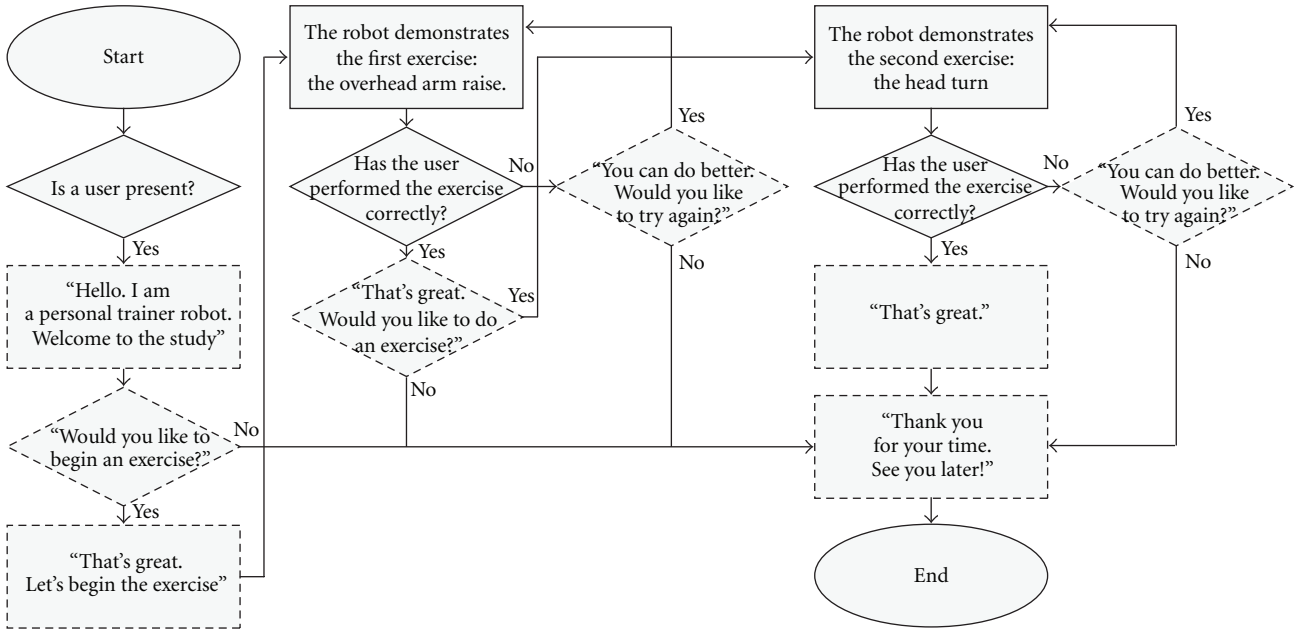

Figure 7: The initial interactive robotic framework is represented by a flowchart. When the vision-processing unit detects the presence of a user, it signals this information to the exercise adherence unit, which begins the interaction. If the user consents to begin an exercise, the robot first demonstrates it. Based on information from the vision-processing unit, the exercise adherence unit determines whether the user has completed an exercise correctly and, if the user has not, give the user an opportunity to be guided through the exercise again.

Table 1: Usability test.

Participants	Successful	User error	Tech. error
10	7	2	1

Presently, no widespread systems exist to measure and increase adherence to a physician-prescribed exercise program with the potential advantages of a humanoid robot, including enhanced sociality and companionship and the ability to lead or follow a person by their own locomotion. To address these issues and as a replacement for a human personal trainer, we have proposed an interactive framework for a personal trainer robot to remind users to perform their exercises, to demonstrate the exercises and provide instruction, to monitor performance progress in real time, and to provide feedback and encouragement. If an interaction framework embedded in a robot can increase exercise adherence, this could greatly reduce healthcare and nursing costs for the elderly and, by incorporating some of the abilities of a personal trainer, provide a high return on investment as compared with other interventions. It could also enable physicians to reliably and systematically monitor patients' adherence to a prescribed in-home exercise program by uploading data to a hospital webserver.

Using the robot as a personal trainer to empower patients in making a behavioral change is a relatively new area to explore. In this study, we conducted a usability test on an incomplete prototype system. The participants' initial response to the personal trainer robot was very positive. They were receptive and responded favorably to interacting with it. Valuable feedback was obtained through their interactions, which led to the implementation of changes to improve the functionality and usability of the robot.

5.1. Technical Limitations. One of the major limitations of the study is that the vision-processing software requires good lighting conditions to detect head and hand movements accurately. Poor lighting may result in false negatives, and excessive lighting may result in false positives. Another limitation is that to obtain accurate results, only one person can be in front of the camera during the detection process. A third limitation is that the vision-processing unit must be reset between users to adjust for differences in height. Finally, the software does not yet fully allow for tracking actions outside of the sequence.

5.2. Directions for Future Research. Because this is a proof of concept study, it has considerable scope for extension. To make the robot a feasible option to help older adults increase their physical activity, future research should include programming the robot to incorporate a complete exercise program, such as the moves recommended by the US National Institute of Aging [57]. To validate that this approach can increase both the exercise adherence and physical range of motion of older adults as compared with alternative interventions, an experiment is planned using this demographic with three conditions: a personal trainer robot, a personal trainer on-screen character, and a pencil-and-paper exercise plan.

During usability testing, users suggested an idea to improve the interaction: the incorporation of more realistic and timely feedback through voice commands or comments

after each step in the exercise routine and after both successful and unsuccessful attempts by the user. These voice messages could be tailored to the particular motivational needs of the user to increase adherence to physical activity. A validated methodology for determining what messages are appropriate for a particular individual is to apply a model of behavior change, such as the theory of planned behavior (TPB) [11, 58].

According to TPB, it is possible to change a person's behavior by changing that person's beliefs about behavioral outcomes, the normative expectations of others, and controlling factors, such as facilitating conditions or barriers [59]. These in turn elicit positive or negative attitudes toward the behavior and responses to social pressure. TPB has been found effective in changing the behavior of patients with diabetes, inflammatory bowel disease, and obesity in interactive games [60–62]. The behavior change model could be used by the personal trainer robot to give encouragement to a user that addresses that individual's particular concerns and priorities. This may prove critical to maintaining the user's motivation during long-term interventions. This interactive robot testbed can also be used in health games and by the health games community.

Another potential improvement is to train more efficient hand detection classifiers. For this version, the motion detection algorithm followed a low-level procedure. However, training Haar classifiers is a more robust method for detecting movement relative to motion detection, because it eliminates false positives from the motion of irrelevant objects. Using Haar classifiers is a high-level approach. The human hand can assume a number of positions and subsequently training classifiers for detecting hand movement are not straightforward. One solution, then, is to train multiple classifiers for the hand and to use them simultaneously [63]. Although using multiple classifiers might adversely affect processing speed, it may be suitable for use with older adults who have a restricted range of motion and slower hand movements, which will increase the detection rate and accuracy of motion tracking.

Another future direction is the development of an animated character for this system that will act as a trainer and substitute for the robot. This will enable the system to be distributed online rather than physically. An animated humanoid character, especially one with facial expressivity, may increase exercise adherence more than the paper-and-pencil method while costing less for the user than a humanoid robot. Whether the effectiveness of an animated character can rival that of a humanoid robot is a question for future research to address.

Acknowledgments

The authors would like to express their gratitude to Umesh K. Potti for help in developing the robot vision-processing and exercise adherence software. They would also like to thank Sirisha Peyyeti and Pratheek Karnati for technical assistance, Vincent Spruyt and Allesandro Ledda for supplying code for future work, and Amy Shirong Lu, Wade Mitchell, Preethi Srinivas, and the anonymous reviewers for constructive suggestions on improving an earlier version of this paper. This research was supported by an IUPUI Signature Center grant to the Android Science Center. There was no conflict of interests in the performance of this research. The trademarks and trade names used in this paper belong to their respective owners.

References

[1] W. He, M. Sengupta, V. A. Velkoff, and K. A. DeBarros, "U.S. Census Bureau," 2005, http://www.census.gov/prod/2006pubs/p23-209.pdf.

[2] J. J. Calahan, "Aging in place," *Generations*, vol. 16, no. 2, p. 5, 1992.

[3] K. D. Marek and M. J. Rantz, "Aging in place: a new model for long-term care," *Nursing Administration Quarterly*, vol. 24, no. 3, pp. 1–11, 2000.

[4] N. G. Kutner, M. G. Ory, D. I. Baker, K. B. Schechtman, M. C. Hornbrook, and C. D. Mulrow, "Measuring the quality of life of the elderly in health promotion intervention clinical trials," *Public Health Reports*, vol. 107, no. 5, pp. 530–539, 1992.

[5] C. Vallbona and S. B. Baker, "Physical fitness prospects in the elderly," *Archives of Physical Medicine and Rehabilitation*, vol. 65, no. 4, pp. 194–200, 1984.

[6] M. P. Buman, E. B. Hekler, W. L. Haskell et al., "Objective light-intensity physical activity associations with rated health in older adults," *American Journal of Epidemiology*, vol. 172, no. 10, pp. 1155–1165, 2010.

[7] D. E. R. Warburton, C. W. Nicol, and S. S. D. Bredin, "Health benefits of physical activity: the evidence," *Canadian Medical Association Journal*, vol. 174, no. 6, pp. 801–809, 2006.

[8] S. N. Culos-Reed, W. J. Rejeski, E. McAuley, J. K. Ockene, and D. L. Roter, "Predictors of adherence to behavior change interventions in the elderly," *Controlled Clinical Trials*, vol. 21, no. 5, pp. 200S–205S, 2000.

[9] A. C. King, W. J. Rejeski, and D. M. Buchner, "Physical activity interventions targeting older adults: a critical review and recommendations," *American Journal of Preventive Medicine*, vol. 15, no. 4, pp. 316–333, 1998.

[10] M. A. Napolitano, G. D. Papandonatos, B. A. Lewis et al., "Mediators of physical activity behavior change: a multivariate approach," *Health Psychology*, vol. 27, no. 4, pp. 409–418, 2008.

[11] M. S. Hagger, N. Chatzisarantis, and S. J. H. Biddle, "A meta-analytic review of theories of reasoned action and planned behavior in physical activity," *Journal of Sports and Exercise Psychology*, vol. 24, no. 1, pp. 3–32, 2002.

[12] W. D. Spector, J. Fleishman, L. Pezzin, and B. Spillman, "The characteristics of adult long-term care users: comparing the non-elderly and the elderly," *Association for Health Services Research Meeting*, vol. 16, p. 240, 1999.

[13] R. J. Nied and B. Franklin, "Promoting and prescribing exercise for the elderly," *American Family Physician*, vol. 65, no. 3, pp. 419–428, 2002.

[14] K. Holmén, K. Ericsson, and B. Winblad, "Social and emotional loneliness among non-demented and demented elderly people," *Archives of Gerontology and Geriatrics*, vol. 31, no. 3, pp. 177–192, 2000.

[15] Y. Tao, H. Wei, T. Wang, and D. Chen, "A multi-layered interaction architecture for elderly companion robot," *Lecture Notes in Artificial Intelligence*, vol. 5314, no. 1, pp. 538–546, 2008.

[16] S. Turkle, "Authenticity in the age of digital companions," *Interaction Studies*, vol. 8, no. 3, pp. 501–517, 2007.

[17] S. Turkle, W. Taggart, C. D. Kidd, and O. Dasté, "Relational artifacts with children and elders: the complexities of cybercompanionship," *Connection Science*, vol. 18, no. 4, pp. 347–361, 2006.

[18] E. Friedmann, A. H. Katcher, J. J. Lynch, and S. A. Thomas, "Animal companions and one-year survival of patients after discharge from a coronary care unit," *Public Health Reports*, vol. 95, no. 4, pp. 307–312, 1980.

[19] J. Serpell, "Beneficial effects of pet ownership on some aspects of human health and behaviour," *Journal of the Royal Society of Medicine*, vol. 84, no. 12, pp. 717–720, 1991.

[20] K. Wada, T. Shibatal, T. Musha, and S. Kimura, "Effects of robot therapy for demented patients evaluated by EEG," in *Proceedings of the IEEE International Conference on Intelligent Robots and Systems (IROS '05)*, pp. 1552–1557, 2005.

[21] K. Wada, T. Shibata, T. Saito, and K. Tanie, "Effects of robot-assisted activity for elderly people and nurses at a day service center," in *Proceedings of the IEEE*, pp. 1780–1788, November 2004.

[22] K. Wada, T. Shibata, T. Saito, K. Sakamoto, and K. Tanie, "Psychological and social effects of one year robot assisted activity on elderly people at a health service facility for the aged," in *Proceedings of the IEEE International Conference on Robotics and Automation*, pp. 2785–2790, April 2005.

[23] J. Pineau, M. Montemerlo, M. Pollack, N. Roy, and S. Thrun, "Towards robotic assistants in nursing homes: challenges and results," *Robotics and Autonomous Systems*, vol. 42, no. 3-4, pp. 271–281, 2003.

[24] J. Fasola and M. J. Matarić, "Robot exercise instructor: a socially assistive robot system to monitor and encourage physical exercise for the elderly," in *Proceedings of the 19th IEEE International Workshop on Robot and Human Interactive Communication*, Viareggio, Italy, 2010.

[25] D. Feil-Seifer, K. Skinner, and M. J. Matarić, "Benchmarks for evaluating socially assistive robotics," *Interaction Studies*, vol. 8, no. 3, pp. 423–439, 2007.

[26] A. Tapus, C. Tapus, and M. J. Mataric, "User—robot personality matching and assistive robot behavior adaptation for post-stroke rehabilition," *Intelligent Service Robotics*, vol. 1, pp. 169–183, 2008, Special issue on multidisciplinary collaboration for socially assistive robotics.

[27] A. Panangadan, M. Matarić, and G. S. Sukhatme, "Tracking and modeling of human activity using laser rangefinders," *International Journal of Social Robotics*, vol. 2, no. 1, pp. 95–107, 2010.

[28] C. Breazeal and B. Scassellati, "How to build robots that make friends and influence people," in *Proceedings of the IEEE/RSJ International Conference on Intelligent Robots and Systems (IROS '99)*, pp. 858–863, October 1999.

[29] M. Bateson, D. Nettle, and G. Roberts, "Cues of being watched enhance cooperation in a real-world setting," *Biology Letters*, vol. 2, no. 3, pp. 412–414, 2006.

[30] T. C. Burnham and B. Hare, "Engineering human cooperation," *Human Nature*, vol. 18, no. 2, pp. 88–108, 2007.

[31] K. J. Haley and D. M. T. Fessler, "Nobody's watching?" *Evolution and Human Behavior*, vol. 26, no. 3, pp. 245–256, 2005.

[32] K. F. MacDorman and H. Ishiguro, "The uncanny advantage of using androids in social and cognitive science research," *Interaction Studies*, vol. 7, no. 3, pp. 297–337, 2006.

[33] K. F. MacDorman, T. Minato, M. Shimada, S. Itakura, S. Cowley, and H. Ishiguro, "Assessing human likeness by eye contact in an android testbed," in *Proceedings of the 27th Annual Meeting of the Cognitive Science Society*, Stresa, Italy, 2005.

[34] K. Shinozawa, F. Naya, J. Yamato, and K. Kogure, "Differences in effect of robot and screen agent recommendations on human decision-making," *International Journal of Human Computer Studies*, vol. 62, no. 2, pp. 267–279, 2005.

[35] C. D. Kidd and C. Breazeal, "Robots at home: understanding long-term human-robot interaction," in *Proceedings of the IEEE/RSJ International Conference on Intelligent Robots and Systems (IROS '08)*, pp. 3230–3235, Nice, France, September 2008.

[36] L. E. Sucar, R. Luis, R. Leder, J. Hernandez, and I. Sanchez, "Gesture therapy: a vision-based system for upper extremity stroke rehabilitation," in *Biomedical Engineering Systems and Technologies*, A. Fred, F. Joaquim, and H. Gamboa, Eds., pp. 531–540, Springer, New York, NY, USA, 2009.

[37] M. B.-V. Kuren, "Robotic solutions in pediatric rehabilitation," in *Rehabilitation Robotics*, pp. 1–12, I-Tech, Vienna, Austria, 2007.

[38] R. Colombo, F. Pisano, A. Mazzone et al., "Design strategies to improve patient motivation during robot-aided rehabilitation," *Journal of NeuroEngineering and Rehabilitation*, vol. 4, no. 3, pp. 1–12, 2007.

[39] M. J. Matarić, J. Eriksson, D. J. Feil-Seifer, and C. J. Winstein, "Socially assistive robotics for post-stroke rehabilitation," *Journal of NeuroEngineering and Rehabilitation*, vol. 4, no. 5, pp. 1–9, 2007.

[40] J. Fasola and M. J. Mataric, "Robot motivator: improving user performance on a physical/mental task," in *Proceedings of the 4th ACM/IEEE International Conference on Human-Robot Interaction*, pp. 295–296, La Jolla, Calif, USA, 2009.

[41] P. A. Barnes, T. Spooner, J. L. Dhabolt, and J. Leighton, "Instructional gaming methods and apparatus," Patent A1 20090176581, 2009.

[42] J. Shotton, A. Fitzgibbon, M. Cook et al., "Real-time human pose recognition in parts from a single depth image," in *Proceedings of the International Conference on Computer Vision and Pattern Recognition*, June 2011.

[43] A. M. Okamura, M. J. Matarić, and H. I. Christensen, "Medical and health-care robotics," *IEEE Robotics and Automation Magazine*, vol. 17, no. 3, Article ID 5569021, pp. 27–37, 2010.

[44] M. P. Cutchin, "The process of mediated aging-in-place: a theoretically and empirically based model," *Social Science and Medicine*, vol. 57, no. 6, pp. 1077–1090, 2003.

[45] D. J. Feil-Seifer and M. J. Mataric, "Ethical principles for socially assistive robotics," *Robotics and Automation Magazine*, vol. 18, no. 1, pp. 24–31, 2011, Special issue on roboethics.

[46] H. Ishiguro, T. Ono, M. Imai, T. Maeda, T. Kanda, and R. Nakatsu, "Robovie: an interactive humanoid robot," *Industrial Robot*, vol. 28, no. 6, pp. 498–503, 2001.

[47] K. F. MacDorman, K. Tatani, Y. Miyazaki, and M. Koeda, "Proto-symbol emergence," in *Proceedings of the IEEE/RSJ International Conference on Intelligent Robots and Systems*, pp. 1619–1625, November 2000.

[48] M. Turk and A. Pentland, "Eigenfaces for recognition," *Journal of Cognitive Neuroscience*, vol. 3, no. 1, pp. 71–86, 1991.

[49] C. Liu, "A Bayesian discriminating features method for face detection," *IEEE Transactions on Pattern Analysis and Machine Intelligence*, vol. 25, no. 6, pp. 725–740, 2003.

[50] A. Mohan, C. Papageorgiou, and T. Poggio, "Example-based object detection in images by components," *IEEE Transactions on Pattern Analysis and Machine Intelligence*, vol. 23, no. 4, pp. 349–361, 2001.

[51] P. Viola and M. Jones, "Rapid object detection using a boosted cascade of simple features," in *Proceedings of the IEEE Computer Society Conference on Computer Vision and Pattern Recognition*, pp. 511–518, December 2001.

[52] R. Lienhart and J. Maydt, "An extended set of Haar-like features for rapid object detection," in *Proceedings of the IEEE International Conference on Image Processing (ICIP '02)*, pp. 900–903, September 2002.

[53] R. Lienhart, A. Kuranov, and V. Pisarevsky, "Empirical analysis of detection cascades of boosted classifiers for rapid object detection," in *Proceedings of the 25th DAGM Pattern Recognition Symposium*, vol. 2781, pp. 297–304, Magdeburg, Germany, 2003.

[54] P. Brox, I. Baturone, S. Sánchez-Solano, J. Gutiérrez-Ríos, and F. Fernández-Hernández, "Fuzzy motion adaptive algorithm for video de-interlacing," *Lecture Notes in Computer Science*, vol. 4252, pp. 363–370, 2006.

[55] AT&T Labs Inc. AT&T Labs Natural Voices Text-to-Speech Demo, 2010, http://www2.research.att.com/~ttsweb/tts/demo.php.

[56] P. Dourish, "What we talk about when we talk about context," *Personal and Ubiquitous Computing*, vol. 8, no. 1, pp. 19–30, 2004.

[57] National Institute of Aging. Go4Life, 2010, http://go4life.niapublications.org.

[58] I. Ajzen and M. Fishbein, *Understanding Attitudes and Predicting Social Behavior*, Prentice-Hall, Englewood Cliffs, NJ, USA, 1980.

[59] I. Ajzen, "The theory of planned behavior," *Organizational Behavior and Human Decision Processes*, vol. 50, no. 2, pp. 179–211, 1991.

[60] H. Kharrazi, C. Watters, and S. Oore, "Improving behavioral stages in children by adaptive applications," *Journal on Information Technology in Healthcare*, vol. 6, no. 1, pp. 322–326, 2008.

[61] H. Kharrazi, "Improving healthy behaviors in type 1 diabetic patients by interactive frameworks," in *Proceedings of the American Medical Informatics Association Symposium*, vol. 2009, pp. 322–326, San Francisco, Calif, USA, 2009.

[62] H. Kharrazi and L. Vincz, "Using health information technology and behavior change model to increase exercise adherence in obesity," in *Proceedings of the AMA-IEEE Medical Technology Conference on Individualized Healthcare*, Washington, DC, USA, 2010.

[63] V. Spruyt, A. Ledda, and S. Geerts, "Real-time multi-colourspace hand segmentation," in *Proceedings of the 17th International Conference on Image Processing (ICIP '10)*, pp. 3117–3120, Hong Kong, 2010.